

---

---

**Contract Nos. 94-33825-0383 and 98-38825-6063**

**10 August 2001**

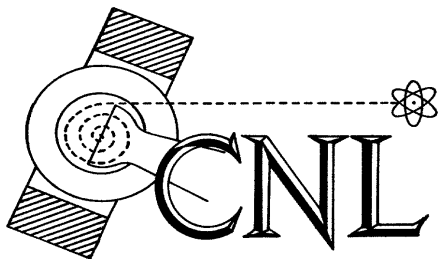
**INTERIM REPORT**  
**Sources and Sinks of PM<sub>10</sub> in the San Joaquin Valley**

A study for  
United States Department of Agriculture Special Research Grants Program

Robert G. Flocchini, Principal Investigator  
Crocker Nuclear Laboratory

Teresa A. James, Investigator  
Crocker Nuclear Laboratory

Lowell L. Ashbaugh, Michael S. Brown, Omar F. Carvacho, Britt A.  
Holmén, Robert T. Matsumura, Krystyna Trzepla-Nabaglo, Chris  
Tsubamoto, Investigators  
Crocker Nuclear Laboratory



**Air Quality  
Group  
Crocker  
Nuclear  
Laboratory  
University of  
California  
Davis, CA 95616-8569**

## Table of Contents

1	Background .....	1
1.1	Air Quality in the San Joaquin Valley .....	1
1.2	Agricultural Impacts on Air Quality .....	3
2	Overview .....	5
2.1	Objectives .....	5
2.2	Approach .....	8
2.3	Reporting .....	10
3	Methods .....	12
3.1	PM <sub>10</sub> Field Test Strategy and Array Design .....	12
3.1.1	Field Crops .....	12
3.1.2	Orchard Crops .....	12
3.1.3	Livestock .....	13
3.2	PM Point Samplers .....	13
3.3	Gravimetric and Reconstructed Mass (RCMA) Concentrations .....	15
3.4	Ammonia .....	16
3.4.1	Active Methods .....	16
3.4.2	Passive Methods .....	17
3.4.3	Facility Description .....	18
3.5	Quality Assurance .....	19
3.5.1	Filter Samples (PM <sub>2.5</sub> and PM <sub>10</sub> ) .....	19
3.5.2	Ammonia Samples (active and passive) .....	20
3.6	Soils .....	20
3.6.1	Soil Moisture .....	22
3.6.2	Dry Sieving .....	22
3.6.3	Wet Sieving .....	23
3.7	Light detection and ranging (lidar) .....	24
4	Emission Rate Calculations .....	25
4.1	PM from 1994 data .....	26
4.2	PM from 1995 data .....	27
4.3	PM from 1995 – 1998 data .....	27
4.3.1	Integration of lidar data .....	29
4.3.2	Plume Height and Uncertainty Calculations .....	31

4.3.3	Emission Factor Calculations .....	32
4.3.4	Emission Factor Confidence Rating.....	34
4.4	Ammonia from Measurements .....	35
5	Results from Field Measurements .....	39
5.1	Orchard Crops .....	41
5.1.1	1994 Field Tests .....	41
5.1.2	1995 Field Tests .....	45
5.1.3	1998 Field Tests .....	47
5.2	Cotton Harvest .....	51
5.2.1	1994 Field Tests .....	51
5.2.2	Assessment of simple box model emission factor calculations using 1995 Field Tests.....	52
5.2.3	1996-1998 Field Tests.....	56
5.3	Wheat Harvest.....	61
5.4	Land Preparation .....	62
5.5	PM from confined cattle facilities .....	67
5.6	Ammonia from confined cattle facilities.....	72
5.6.1	1996 Field Tests .....	72
5.6.2	1997 Field Tests .....	75
5.6.3	1999 Field Tests .....	76
6	Conclusions from field measurements.....	82
6.1	Orchard Crops .....	84
6.2	Cotton Harvest .....	86
6.2.1	Cotton Picking.....	86
6.2.2	Cotton Stalk Cutting.....	87
6.2.3	Cotton Root Cutting.....	89
6.3	Wheat Harvest.....	91
6.4	Land Preparation .....	93
6.4.1	Discing.....	93
6.4.2	Chiseling.....	94
6.4.3	Weeding.....	95
6.5	Confined Animal Facilities .....	97
6.5.1	Dairy .....	98
6.5.2	Beef Feedlot .....	99
6.6	Ammonia emission factors .....	100
6.6.1	Beef Feedlot .....	100
6.6.2	Dairies .....	101

6.7	Ongoing Research Directions.....	102
7	Associated Research: PM <sub>10</sub> Potential.....	104
7.1	Dust Collection Chamber:.....	106
7.2	PM <sub>10</sub> Inlet and the IMPROVE Sampler.....	106
8	Appendix A – Inventory of 1994 Field Tests .....	122
9	Appendix B – Inventory of 1995 Field Tests.....	127
10	Appendix C – Inventory of 1996 Field Tests .....	128
10	Appendix C – Inventory of 1996 Field Tests .....	129
11	Appendix D – Inventory of 1997 Field Tests .....	130
11	Appendix D – Inventory of 1997 Field Tests .....	131
12	Appendix E – Inventory of 1998 Field Tests.....	132
13	Appendix F – Text of Almond Harvester Report.....	133
14	Appendix G – Description of Database Structure.....	29
15	Appendix H – Text of Atmospheric Environment Papers.....	33

## List of Tables

Table 1.1 Value and Production of some major San Joaquin Valley crops, 1997 .....	1
Table 2.1 Summary of tests .....	7
Table 2.2 Summary of field equipment placement and year of introduction.....	11
Table 3.1 Description of the ammonia sampling arrays.....	16
Table 3.2 Nest of sieves used for particle size distribution analysis by dry sieving. ....	22
Table 3.3 Sieve sizes which define texture gradients of sand in wet sieving. ....	23
Table 4.1 Summary of exceptions to emission factor calculations for PM emissions from row crops and livestock.....	28
Table 4.2 Emission factor confidence ratings summary.....	35
Table 5.1 Comparison of fig harvest to almond harvest emission factors (kg/km <sup>4</sup> ) .....	44
Table 5.2 PM <sub>10</sub> emission factors (kg/km <sup>4</sup> ) by three calculation methods.....	46
Table 5.3 PM <sub>10</sub> emission factors for almond pick-up tests during which both PM <sub>10</sub> and wind speed were measured outside of the canopy.....	46
Table 5.4 Environmental conditions during almond pick-up tests.....	47
Table 5.5 PM <sub>10</sub> concentrations normalized to amount of windrow trash <2mm prior to harvest (µg/m <sup>4</sup> /g).....	50
Table 5.6 PM <sub>10</sub> emission rates from cotton operations, 1994.....	51
Table 5.7 Correlation statistics for models.....	55
Table 5.8 PM <sub>10</sub> Emission flux (kg/km <sup>4</sup> ) by three calculation methods .....	55
Table 5.9 Emission factors for cotton picking compiled from field data collected in 1995-1998.....	57
Table 5.10 Environmental conditions during cotton picking tests. ....	57
Table 5.11 Emission factors and uncertainties for cotton stalk cutting .....	59
Table 5.12 Environmental conditions during cotton stalk cutting tests. ....	60
Table 5.13 Emission factors and uncertainties for wheat harvest.....	61
Table 5.14 Environmental conditions during wheat harvest tests.....	62
Table 5.15 Emission factors and uncertainties for land preparation. ....	64
Table 5.16 Environmental conditions during land preparation tests.....	65
Table 5.17 Emission factors and uncertainties for cultivation .....	66
Table 5.18 Environmental conditions during cultivation tests.....	66
Table 5.19 Best fit PM <sub>10</sub> emission factors from open lot dairies .....	68
Table 5.20 Environmental conditions during dairy tests. ....	69
Table 5.21 Best fit PM <sub>10</sub> emission factors from feedlots.....	70
Table 5.22 Environmental conditions during feedlot tests. ....	71
Table 5.23 Results of ammonia emission factor calculation.....	76
Table 5.24 Ammonia concentration profiles and mass fluxes at downwind locations instrumented with active (bubbler) samplers.....	79
Table 6.1 Summary of average PM <sub>10</sub> emission factors.....	83
Table 6.2 Ammonia emission factors for open lot feedlots and dairies.....	100
Table 6.3 Completed measurements of PM <sub>10</sub> requiring further analysis and data reduction for the calculation of emission factors.....	102

Table 7.1 Averages of cumulative mass (mg/g) as a function of time for tested soils. ....	109
Table 7.2 Partial list of the USDA soil tested from San Joaquin Valley.....	110
Table 7.3 USDA soils tested for PM <sub>10</sub> index .....	112
Table 7.4 Results from soil samples collected in 1995 .....	115
Table 7.5 Results from soil samples collected in 1996 .....	115
Table 7.6 Results from soil samples collected in 1997 .....	115
Table 7.7 Results from soil samples collected in 1998 .....	116

## List of Figures

Figure 1.1 Primary PM <sub>10</sub> emissions inventory compiled by the California Air Resources Board (1993 Annual Average).....	3
Figure 3.1 Standard sampling array for measuring agricultural emissions of fugitive dust.....	14
Figure 3.2 Facility layout and sampler configuration for 1997 ammonia study.....	19
Figure 4.1 Lidar vertical profiles for PM tests 06 Nov 1998.....	30
Figure 4.2 Average plume heights: Lidar vs. point sampler estimates.....	31
Figure 5.1 Example of the PM <sub>10</sub> horizontal distribution downwind of an almond harvest tree shaking operation for silt and clay soil textures.....	42
Figure 5.2 Example of the PM <sub>10</sub> horizontal distribution downwind of an almond harvest sweeping (windrowing) operation for silt and clay soil textures.....	43
Figure 5.3 Example of the PM <sub>10</sub> horizontal distribution downwind of an almond harvest, nut pickup operation for silt and clay soil textures.....	43
Figure 5.4 Vertical distribution of aerosols from vertical profile tower.....	44
Figure 5.5 PM <sub>10</sub> emission factors for eight agricultural operations.....	45
Figure 5.6 PM <sub>2.5</sub> emission factors for eight agricultural operations.....	45
Figure 5.7 PM <sub>10</sub> concentrations downwind of harvester #1 and #2, (a) all tests, (b) solid-set irrigation, (c) micro-spray irrigation.....	49
Figure 5.8 PM <sub>10</sub> emission rates from cotton operations, 1994.....	52
Figure 5.9 PM <sub>10</sub> emission factor for 1995 cotton picking tests.....	53
Figure 5.10 PM <sub>10</sub> emission factor for 1995 cotton stalk shredding tests.....	53
Figure 5.11 PM <sub>10</sub> emission factor for 1995 cotton stalk incorporation tests.....	54
Figure 5.12 Ammonia emission factors for dairy and beef cattle derived from mass flux model.....	74
Figure 5.13 Comparison of ammonia emission rates derived from mass flux model of measurements made at two locations on the downwind fence line.....	75
Figure 5.14 Ammonia emission factors for day-time and night-time for dairy and beef cattle derived from mass flux model.....	75
Figure 5.15 Diurnal trend in ammonia emission factors from 1997 data.....	76
Figure 5.16 Average NH <sub>3</sub> fluxes calculated from measurements.....	78
Figure 5.17 Emission factors calculated from measurements.....	80
Figure 6.1 PM <sub>10</sub> emission factors (mg/m <sup>2</sup> ) and soil moisture (%) from 1995 tests of highest confidence for Almond pickup operations.....	85
Figure 6.2 PM <sub>10</sub> emission factors (mg/m <sup>2</sup> ) and relative humidity (%) for cotton picking tests with highest confidence ratings.....	87
Figure 6.3 PM <sub>10</sub> emission factors (mg/m <sup>2</sup> ) and relative humidity (%) for cotton stalk cutting tests with highest confidence ratings.....	89
Figure 6.4 PM <sub>10</sub> emission factors (mg/m <sup>2</sup> ) and relative humidity (%) for cotton root cutting tests with highest confidence ratings.....	90
Figure 6.5 PM <sub>10</sub> emission factors (mg/m <sup>2</sup> ) and relative humidity (%) for wheat harvesting tests with highest confidence ratings.....	92

Figure 6.6 PM <sub>10</sub> emission factors (mg/m <sup>2</sup> ) and soil moisture (%) for discing tests with highest confidence ratings.....	94
Figure 6.7 PM <sub>10</sub> emission factors (mg/m <sup>2</sup> ) and relative humidity (%) for chiseling tests with highest confidence ratings.....	95
Figure 6.8 PM <sub>10</sub> emission factors (mg/m <sup>2</sup> ) and soil moisture (%) for weeding tests with highest confidence ratings.....	96
Figure 6.9 Correlation of PM <sub>10</sub> emission factors (mg/m <sup>2</sup> ) and relative humidity (%) for confined cattle tests with highest confidence ratings.....	97
Figure 6.10 PM <sub>10</sub> emission factors (lbs/d*1000hd) and relative humidity (%) for dairy tests with highest confidence ratings.....	98
Figure 6.11 PM <sub>10</sub> emission factors (lbs/d*1000hd) and solar radiation (W/m <sup>2</sup> ) for feedlot tests with highest confidence ratings.....	99
Figure 7.1 Diagram of dust resuspension chamber.....	105
Figure 7.2 Diagram of CNL resuspension and collection chamber .....	106
Figure 7.3 PM <sub>10</sub> Index curve for the clay soils data in table 7.2.....	110
Figure 7.4 Cumulative mass for resuspension of select soils collected simultaneously with PM <sub>10</sub> emission factor measurements.....	111
Figure 7.5 Relationship between PM <sub>10</sub> Index calculated by the straight line and experimental PM <sub>10</sub> Index. ....	112
Figure 7.6 Distribution of soil texture for soils analyzed, based on wet sieving.....	113

# 1 BACKGROUND

California's San Joaquin Valley is one of the most productive agricultural regions in the United States. Over 350 crops are produced, including seeds, flowers and ornamentals. Over eight million acres were harvested in 1997, and a number of crops are produced exclusively, or nearly so, in California. In 1997 agriculture contributed \$26.8 billion to the state's economy. **Table 1.1** lists a few of the major crops in the San Joaquin Valley by dollar value, along with the percent of U.S. production and the number of acres harvested in 1997 (Johnston and Carter 2000).

**Table 1.1 Value and Production of some major San Joaquin Valley crops, 1997**

Crop	Value (Millions)	U.S. Ranking	Harvested acreage in 1993	Percent of U.S. Production
Grapes	\$2,819	1	497,100	91%
Cotton	\$984	2	1,036,316	14%
Almonds	\$1,127	1	410,000	100%
Walnuts	\$352	1	177,200	100%

The San Joaquin Valley is experiencing rapid population growth, especially in the northern and central regions. As home prices in the San Francisco Bay Area continue to rise, prospective homeowners increasingly turn to the northern San Joaquin Valley to find affordable housing. The central region of the valley also continues to grow as the economy of Fresno and surrounding areas continue to expand. The expansion of major employers in the area, such as the new University of California campus near Merced, will drive additional population growth.

The expansion of residential housing into agricultural areas can lead to conflicts between traditional practices and new expectations. These conflicts were minimal when the encroaching residential areas were associated with agricultural livelihoods and lifestyles. They are magnified, though, when a large percentage of the incoming residents lead lives separate from the agricultural community.

Air quality conflicts that develop between traditional agricultural uses of the land and encroaching urban development include odor and dust issues. Resolving these conflicts requires a concerted effort by affected parties to understand the characteristics of living in a rural setting and to take steps to reduce emissions where appropriate.

## 1.1 Air Quality in the San Joaquin Valley

The United States Environmental Protection Agency has designated the San Joaquin Valley a serious non-attainment area for PM<sub>10</sub>, particulate matter with an aerodynamic diameter less than 10 micrometers. This means the valley exceeds the National Ambient Air Quality Standards

(NAAQS) for PM<sub>10</sub> to such a degree that extreme actions may be required to meet them. PM<sub>10</sub> particles bypass the body's defense mechanisms and penetrate into the respiratory system. These particles have been linked to death by cardiac and respiratory disease. The valley also exceeds the NAAQS for ozone, a key component of photochemical smog. Ozone causes respiratory distress in some individuals, and also reduces crop yields.

The United States EPA recently enacted new standards for PM<sub>2.5</sub>, particles with an aerodynamic diameter less than 2.5 micrometers. These particles penetrate more deeply into the lung than PM<sub>10</sub>, and have been linked even more strongly to human deaths. The San Joaquin Valley is expected to exceed the new standards, although this will not be known for certain until a monitoring network has been established and operated for several years.

Particulate matter in the San Joaquin Valley typically peaks in the fall and winter, and exceeds the PM<sub>10</sub> standards during the early winter. During the spring and summer the concentrations are relatively low. Moreover, the nature of the particulate matter changes between early and late fall. From early September to mid-November, the PM<sub>10</sub> is composed primarily of soil dust in a size range greater than 1-2 micrometers. After the first winter rains fall, which normally happens in mid-November, the soil dust source is suppressed. At this same time, the soil surface cools and the atmospheric temperature inversion lowers from a few thousand meters to several hundred meters. Air temperature drops and humidity increases. Pollutants emitted into this atmosphere are trapped in a relatively small volume of cool, damp air. Thus, the particulate matter includes fewer soil dust particles and more particles from automotive tailpipes, burning of wood for heat, and particles formed in the atmosphere from gases such as ammonia, nitric acid, and sulfur dioxide. These particles differ from the earlier ones not only in their chemistry, but also in their size; they are primarily smaller than 2.5 micrometers in size.

The 1993 PM<sub>10</sub> annual average emissions inventory, compiled by the state Air Resources Board, is shown in Figure 1.1 (Chow, Watson et al. 1992). According to this inventory, the major sources of primary particulate matter in the San Joaquin Valley include farming operations, entrained road dust from paved and unpaved roads, and windblown dust. Smaller sources include fuel combustion, waste burning, industrial processes, and mobile sources. The inventory does not include residential wood combustion or secondary particles, though, and these are thought to make up much of the particulate matter in the winter. Although inventories are helpful tools for understanding the annual impact of various sources on air quality, seasonal variations in the relative importance of sources (as mentioned above) are not reflected in an annual inventory.

Secondary particles are formed in the atmosphere from ammonia, nitric acid, and sulfur dioxide, and from some organic gases as they condense from the vapor phase. Ammonia gas is produced largely from livestock operations, and to a lesser degree from sewage treatment facilities and fertilizer application. Nitric acid is a by-product of NO<sub>x</sub> emissions produced by motor vehicles and other combustion sources. Sulfur dioxide is produced from combustion and by numerous sources in the oil fields of the southern San Joaquin Valley. The formation of

ammonium nitrate particles is particularly important in the winter, as these particles form preferentially when the temperature is low and the humidity is high.

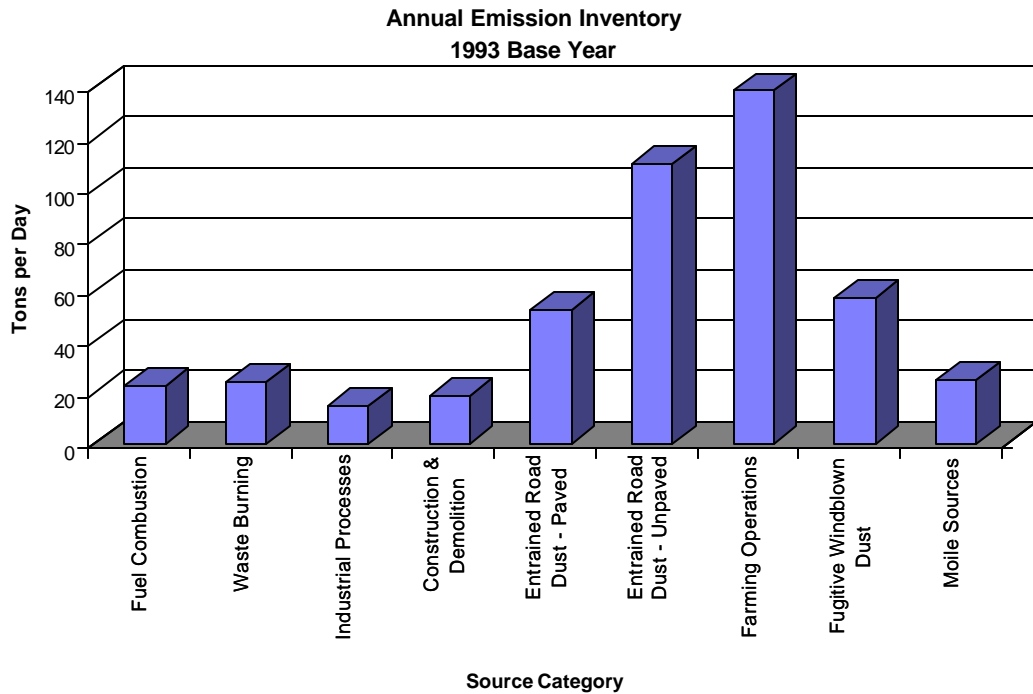


**Figure 1.1 Primary PM<sub>10</sub> emissions inventory compiled by the California Air Resources Board (1993 Annual Average)**

Source apportionment studies in the San Joaquin Valley indicate that soil dust is the major component of PM<sub>10</sub> annually and during the summer and fall months (Chow, Watson et al. 1992). During the winter months, though, the soil dust component is generally low while motor vehicle particles and secondary particles (ammonium nitrate and ammonium sulfate) are high. Smoke particles from residential and/or agricultural burning also make up a significant fraction of the PM<sub>10</sub>. It is important to note that the particles most prevalent during the winter months are also quite small, likely below 2.5 micrometers in aerodynamic diameter, while the particles most prevalent during the fall months are generally larger than 2.5 μm.

## 1.2 Agricultural Impacts on Air Quality

The most noticeable impacts of agriculture on air quality concern odors and dust. On windless summer days, dust plumes may extend upward above a tractor or harvester for hundreds of meters. During windy periods, the plumes may be blown horizontally across roads, impeding traffic, or may be blown into nearby residential areas. Odors develop on livestock facilities as anaerobic bacteria break down the organic byproducts of agricultural process water or livestock waste. Although ammonia is often thought to be the cause of odors, other malodorous amine compounds generally cause them.

The guidance provided in AP-42, *Compilation of Air Pollution Emission Factors* (U.S.E.P.A. 1995), for estimating the emissions of dust from agricultural activities is incomplete, though it represents the best data available for use by air pollution control districts in making regulatory decisions. The fugitive dust section of AP-42 is undergoing revision based on more recent scientific studies of dust emissions from paved and unpaved roads, agricultural tilling and harvesting, and windblown dust. Up to now, the emission estimates have been based largely on the soil silt content, the fraction of soil that passes through a 75 $\mu$ m sieve using a standard procedure. Research conducted as part of this study suggests that a different measure, the PM<sub>10</sub> Index of the soil, may be a more appropriate surrogate for estimating dust emissions.

Results of this study also indicate that there are meteorological and soil parameters of equal or greater importance than soil texture in determining PM<sub>10</sub> emission from agricultural sources. In an extreme example, primary PM<sub>10</sub> emitted from confined animal facilities (excluding emissions from unpaved service roads) originate in the animal pens which are composed (in the top 6 inches) of an organic material for which texture analysis is even valid. Yet emission rates vary greatly diurnally, seasonally, and as a result of animal activity. Similarly, it is evident to the casual observer that dust emission is reduced by rain, yet neither soil moisture, air humidity nor season are incorporated into the current emission factor guidance. In addition to the fact that soil texture may not be the most important variable determining PM<sub>10</sub> emission rates for agricultural sources under some conditions, soil texture is not a variable under control of the farmer. Thus, the emission factor provided for agricultural activities in the current AP-42 guidance document is not based on physically relevant parameters. An emission factor model based on controllable variables, however, would be applicable to facilities operating under varying levels of control and may even suggest mitigation techniques.

## 2 OVERVIEW

### 2.1 Objectives

The primary objectives of this study are:

- to measure the PM<sub>10</sub> emission factors from agricultural operations, including harvesting of both row and orchard crops, land preparation (discing, ripping, floating, planning), and livestock (dairy, feedlot).
- to measure ammonia emission factors from livestock operations (dairy, feedlot).

The study began in 1994 with measurements of PM<sub>10</sub> and PM<sub>2.5</sub> production from almond, fig, walnut, and cotton harvesting operations. The 1995 and 1996 work extended our 1994 studies by including additional soil types, harvesters, and harvesting practices. We extended the measurements to include some cotton stalk incorporation and wheat harvesting tests. Livestock as sources of PM<sub>10</sub> were also added in 1995 and 1996. The 1997 and 1998 work branched out to include various land preparation activities and a comparison of almond harvesting equipment. Both PM<sub>10</sub> and PM<sub>2.5</sub> have been collected using side by side samplers at 3 m during all phases of the project, though PM<sub>10</sub> has been used to calculate emission factors throughout due to higher frequency of analytical detection and the more complete profile measurements that were made. Particle size distributions have been evaluated for several operations (see section 5.1.1) and are an important component of filter sample quality assurance protocols (see section 3.5.1). We also measured ammonia emission from dairies and a feedlot, starting in 1996, with a comparison study in 1997, and culminating in a thorough study of wet season ammonia emission from dairies in 1999. Our most recent studies are focused on the comparison of land preparation operations following crops of characteristically different soil moisture and the integration of lidar data with PM<sub>10</sub> emission calculations. Table 2.1 summarizes the field tests analyzed in this study to date.

Beginning in June, 1997 use of (lidar) light detection and ranging has been incorporated with collection of PM<sub>10</sub> and PM<sub>2.5</sub> samples because the filter measurements cannot reasonably capture the entire PM plume generated across an agricultural source. Lidar applications have been developed in this project to address the limited ability of conventional point PM samplers to quantify PM emissions from these operations due to the following factors:

- The large spatial dimensions of agricultural sources, the spatial irregularity of dust plumes and the small number of point sampling locations results in under-sampling of the dust plume.
- The spatial variability in the PM source location (i.e., tractor) within the entire field as the operation traverses the field means the direction and distance from a point sampler to the PM source changes with time.
- The vertical extent of point sampling is limited to the height of portable towers.

The lidar technique offers high temporal (seconds) and spatial resolution (2.5 meters) and extensive analysis range (over 5 km) capabilities. It can currently provide important qualitative

data on agricultural PM<sub>10</sub> emissions and has been used to improve the point sampling methods used to estimate PM<sub>10</sub> emission factors from non-point agricultural sources [Holmén, 2000 #38; Holmén, 2000 #39].

The UCD studies are secondarily directed at improving information needed for estimating the emissions of dust from agricultural sources. Based on the current guidance provided in AP-42 (see section 1.2), soil properties have been examined by several methods since the initiation of this project. Both bulk and moisture samples of soils have been collected from each of the fields where PM<sub>10</sub> emissions were measured since 1994 (see section 3.6). Soil moisture has been measured throughout the study as a variable of potential importance in predicting PM<sub>10</sub> emissions. Dry sieving of soil samples to determine soil silt content as defined in the current guidance method for estimating PM<sub>10</sub> emissions has been performed in the lab of co-principal investigator Randy Southard. Wet sieving of soil samples has also been performed in Dr. Southard's lab to characterize the texture of the soils. This analysis has been performed on all samples collected in the project to obtain size fractions which complement the data obtained in the dry sieving analysis and which permit evaluation of the importance of aggregation in the soils studied. These procedures support the original research into PM<sub>10</sub> potential based on resuspension, which has been developed as part of this project since 1994.

The overall goal of soil resuspension is to provide a laboratory-based method of estimating the fugitive dust emission "potential" of soils. This will allow us to control, isolate, and vary environmental and agricultural factors that affect dust generation. The basic steps of the resuspension experiments include:

- Generating dust in an enclosed chamber. Bulk and size-fractionated soil samples are mechanically disturbed and/or entrained in turbulent airflow.
- Measuring the airborne dust by size and composition using the same techniques as in actual field tests.
- Varying specific environmental factors (e.g. soil moisture, energy input, soil texture, etc.) to isolate and quantify their impacts upon dust generation.

Measurements of the mass of dust generated in resuspension experiments have been used to define correlations between the dust potential as a function of soil texture (clay, silt, sand). These experiments provide an opportunity to measure the effect of mechanical energy input (for dust generation), soil moisture, and relative humidity on soil dust potential. Additionally, elemental analysis of resuspended dust samples provides a method for comparing soil elements and gravimetric mass from resuspended samples to obtain "soil factors" for the reconstruction of soils in PM<sub>2.5</sub> and PM<sub>10</sub> field samples. This analysis has been performed on samples collected since 1995.

**Table 2.1 Summary of tests**

**PM Tests Summary (1994-1998)** Seasons: (Nov-Apr) Winter; (May-Oct) Summer  
**1994**

County	Crop	Practice	Operation	# of Tests	Season/Yr.
Kern	Almond	Harvest	Sweeping	6	Summer 94
Kern	Almond	Harvest	Shaking	3	Summer 94
Kern	Almond	Harvest	Pickup	20	Summer 94
Merced	Figs	Harvest	Sweeping	6	Summer 94
Merced	Figs	Harvest	Pickup	3	Summer 94
Kings	Walnut	Harvest	Shaking	1	Summer 94
Kings	Walnut	Harvest	Sweeping	3	Summer 94
Hanford	Walnut	Harvest	Pickup	2	Summer 94
Hanford	Walnut	Harvest	Sweeping	1	Summer 94
Kern	Cotton	Harvest	Picking	5	Summer 94
Kern	Cotton	Harvest	Stalk cutting	3	Summer 94
Kern	Cotton	Harvest	Picking	3	Summer 94
Fresno	Cotton	Harvest	Picking	5	Summer 94
Kern	Cotton	Harvest	Picking	3	Summer 94
Kern	Cotton	Harvest	Stalk cutting	2	Summer 94
Kings	Cotton	Harvest	Picking	3	Winter 94 (10/30)
Kings	Cotton	Harvest	Stalk cutting	3	Winter 94 (11/1)
Fresno	Cotton	Harvest	Picking	2	Winter 94
Fresno	Cotton	Harvest	Stalk cutting	4	Winter 94
Kings	Cotton	Harvest	Picking	2	Winter 94

**1995**

Fresno	Raisins	Harvest	Tray burning	1	Summer 95
Kern	Almonds	Harvest	Pickup	14	Summer 95
Kern	Almonds	Harvest	Shaking	17	Summer 95
Kern	Almonds	Harvest	Sweeping	5	Summer 95
Kings	Cotton	Harvest	Picking	9	Summer 95
Kings	Cotton	Harvest	Stalk cutting	16	Summer 95
Kings	Cotton	Harvest	Stalk incorporati	4	Summer 95
Kings	Cotton	Harvest	Picking	4	Summer 95
Kings	Cotton	Harvest	Stalk incorporati	7	Winter 95
Kings	Cotton	Harvest	Picking	4	Winter 95
Kings	Cotton	Harvest	Stalk cutting	4	Winter 95
Kings	Cotton	Harvest	Picking	5	Winter 95
Kings	Cotton	Harvest	Stalk incorporati	2	Winter 95
Kings	Cotton	Harvest	Stalk cutting	2	Winter 95
Merced	Wheat	Harvest	Harvest	17	Summer 95
Yolo	Land	Land preparation	Land planning	5	Summer 95
Tulare	Milk	Dairy	Feeding	6	Summer 95
Tulare	Milk	Dairy	Activity	5	Summer 95
Tulare	Milk	Dairy	Sleeping	3	Summer 95
Tulare	Milk	Dairy	Loafing	3	Summer 95

**1996**

Kern	Beef	Feedlot	Loafing	2	Winter 96
Kern	Beef	Feedlot	Activity	3	Winter 96
Kern	Beef	Feedlot	Sleeping	3	Winter 96
Kern	Beef	Feedlot	Loafing	5	Summer 96
Kern	Beef	Feedlot	Activity	7	Summer 96
Kern	Beef	Feedlot	Sleeping	10	Summer 96
Kern	Beef	Feedlot	Feeding	1	Summer 96
Tulare	Milk	Dairy	Loafing	12	Winter 96
Tulare	Milk	Dairy	Activity	6	Winter 96
Tulare	Milk	Dairy	Sleeping	7	Winter 96
Kings	Wheat	Harvest	Harvest	15	Summer 96
Merced	Wheat	Harvest	Harvest	8	Summer 96
Kings	Cotton	Harvest	Picking	5	Winter 96
Kings	Cotton	Harvest	Stalk cutting	4	Winter 96
Kings	Cotton	Land preparation	Listing	4	Winter 96
Kings	Cotton	Land preparation	Root cutting	4	Winter 96
Kings	Cotton	Land preparation	Disking	8	Winter 96
Kings	Cotton	Land preparation	Chiseling	2	Winter 96

1997					
Kings	Wheat	Harvest	Harvest	7	Summer 97
Kings	Wheat	Land preparation	Disking	7	Summer 97
Kings	Wheat	Land preparation	Ripping	6	Summer 97

1998					
Kern	Almonds	Harvest	Pickup	31	Summer 98
Fresno	Cotton	Cultivation	Weeding	11	Summer 98
Fresno	Cotton	Harvest	Stalk cutting	2	Winter 98
Fresno	Cotton	Land preparation	Disking	6	Winter 98

#### NH3 Tests Summary (1994-1998)

1996					
Kern	Beef	Feedlot	Loafing	10	Winter 96
Kern	Beef	Feedlot	Activity	3	Winter 96
Kern	Beef	Feedlot	Sleeping	10	Winter 96
Kern	Beef	Feedlot	Loafing	4	Summer 96
Kern	Beef	Feedlot	Activity	5	Summer 96
Kern	Beef	Feedlot	Sleeping	9	Summer 96
Kern	Beef	Feedlot	Feeding	1	Summer 96
Tulare	Milk	Dairy	Loafing	12	Winter 96
Tulare	Milk	Dairy	Activity	6	Winter 96
Tulare	Milk	Dairy	Sleeping	7	Winter 96

1997					
Tulare	Milk	Dairy	Loafing	9	Winter 97
Tulare	Milk	Dairy	Sleeping	1	Winter 97

1999					
Tulare	Milk	Dairy	Feeding	2	Winter 99
Tulare	Milk	Dairy	Activity	1	Winter 99
Tulare	Milk	Dairy	Loafing	19	Winter 99
Tulare	Milk	Dairy	Sleeping	5	Winter 99

## 2.2 Approach

When work began on the project in 1994, few methods had been explored by others to quantify PM emission rates from agricultural operations. The first techniques used were pioneered by Cowherd et al. (Cowherd, Axetall et al. 1974; Cowherd and Kinsey 1986) using vertical profiles of TSP to characterize dust plumes and PM<sub>10</sub> measurements at a single height to quantify PM concentrations. In our application of this method we used a telescoping pole to support stacked filter units to monitor TSP concentrations at four heights up to 7 m above ground. Low flow rates (10 l min<sup>-1</sup>) and insufficient sensitivity of the method over the short (0.25 to 2 h) sampling duration used in plume characterization, however, made this sampler inappropriate for this purpose and very few (less than 10%) of the TSP mass profiles were interpretable. In 1995 we modified two 30-foot antenna towers to deploy IMPROVE PM<sub>10</sub> and PM<sub>2.5</sub> samplers at 7.5 m above ground. This provided the means for measurement of a three point vertical profile of size-selected aerosol concentrations and direct characterization of the PM<sub>10</sub> plume. These towers were also fitted with brackets to support anemometers and thermometers at 5 heights for more precise monitoring of wind speed and temperature gradients than had been possible with the tripod we used in 1994. However, each stationary tower required 3-4 man hours to construct and use was limited to areas accessible by road, since the components were heavy and the footprint (75 m<sup>2</sup>) was large.

Later in 1995 we obtained a pneumatic tower with a generator and air compressor and installed it in the bed of a pick-up truck with PM<sub>10</sub> and PM<sub>2.5</sub> samplers at 10 and 3 m and a PM<sub>10</sub> sampler to be set on the ground (1 m). This mobile array is effective in accessing most points within a field or orchard during harvesting activities and can be deployed by one person in as little as 10 minutes.

The addition of ammonia sampling equipment to the towers in 1996 required little technological development, since the acid-coated filtration method routinely used in our lab was modified for deployment on the towers by simply hanging the filter cassettes at the appropriate levels. This technique was adequate for sampling conducted in the winter of 1996, but the filters provided insufficient capacity for measuring ammonia concentrations downwind of a feedlot in summer. Thus, a sample collection method was developed based on a liquid bubbler and field tested in winter of 1997. While the bubbler sampler was shown to be accurate (compared to independent methods) and to have a high capacity (in laboratory testing), significant modifications were required to enable reliable, repetitive sampling at multiple heights. More importantly, the highly variable ammonia concentrations we had measured along the downwind edge of both dairies and feedlots indicated a need for at least three downwind profiles to adequately characterize the source.

We borrowed a pair of trailer mounted, semi-hydraulic towers from the UCD Engineering Department in 1998 for use in the almond harvester comparison study we conducted that summer. Used with the mobile array, these trailer towers gave us the ability to measure the PM<sub>10</sub> concentration profile at three locations downwind of the source simultaneously, and to relocate the samplers with the movement of the source. One person can deploy the trailer towers in less than half an hour. They also provided excellent platforms for the multi-height bubblers that had been developed for measuring ammonia profiles. The trailer towers were used at two dairies in the winter of 1999. Unfortunately, these towers are too heavy to be deployed within cropped fields when soil conditions are not firm and flat, as we found during disking and the harvest of wet crops such as melons and tomatoes in the summer of 1999. Nevertheless, this ability to measure the PM<sub>10</sub> and PM<sub>2.5</sub> concentration profiles at three locations downwind of a source simultaneously with an upwind concentration profile and a wind speed profile will be exploited to the fullest extent possible in our future research.

Protocols for the identification and tracking of individual samples in the data stream dictate how the data will be accessed, and to a large extent determine the interpretability of field-collected data. Aerosol samples collected from 1994 through 1999 underwent identical analyses using essentially the same instruments and data acquisition software. A database system for PM, meteorological, ammonia, and soil data has been created to include custom screens for data entry, error trapping, generation of sample labels, interface with data acquisition software, QA plotting, and flux and emission factor calculation. To the extent possible, all data generated during the project have been archived in a standardized format to enable all of the above listed functions. Exceptions are the 1994 data, which contain no usable PM profiles, and the 1995 data, which are archived in separate, but comparable, databases and cannot be accessed

directly by our most current QA plotting platform. The 1995 data were processed through Level II quality assurance using the same protocols as were used for all subsequent field samples, as described below.

### **2.3 Reporting**

This report is organized to provide easy reference to raw PM<sub>10</sub> concentrations and meteorological data as well as the estimated plume heights, emission factors, and associated errors and quality ratings, by source classification. Because sampling equipment was modified and introduced numerous times over the course of the reporting period (Table 2.2), the data available for the calculation of emission factors depends on the phase of the experiment in which those data were collected. Data collected in 1994 were analyzed using the simple box model (see section 4.1) only. These tests include all of our fig and walnut harvest data and our first year of almond harvest data. Emission factors were calculated from vertical profiles of wind speed and PM concentrations measured downwind of almond and cotton harvesting operations in 1995 using the block and logarithmic integration methods (see section 4.2) as well as the simple box model. These data provide a comparison by which to judge the 1994 results (see section 5.2.2). Emission factors were also calculated from the cotton harvesting data collected in 1995 using our most recently derived block, logarithmic, linear, and box modeling methods (see section 4.3). These results can be compared to the two previously reported methods results (see section 5.2). Emissions factors reported for wheat harvesting, land preparation operations and PM emissions from dairies and feedlots were calculated from data collected in 1995 - 1998 (Table 2.1) using slight modifications of this latest computational method (section 4.3). It is especially important to note that PM emission factors for dairies and feedlots are presented in the same units as those for row crop agriculture, mass per unit area, NOT on a per head basis (section 5.5). Ammonia emission factors were calculated from vertical profiles of wind speed and ammonia concentrations measured in 1996, 1997, and 1999 and from estimates of dietary nitrogen and animal population parameters (section 4.4). The ammonia emission factors are reported in mass of nitrogen per head per year.

**Table 2.2 Summary of field equipment placement and year of introduction**

<b>Variable</b>	<b>Sampler</b>	<b>Height (m)</b>	<b>Year</b>	<b>Analyses (METHOD)</b>
PM10 ( $\mu\text{g}/\text{m}^3$ )	IMPROVE Module D	1	1995	Gravimetric mass ( $\text{PM}_{10}$ concentration)
	PM10 inlet	3	1994	Optical absorption (LIPM, HIPS)
		(8.25, 9 or 10)	1995	Elemental analysis (PIXE, PESA, XRF) [Highest height nominally 9 m]
PM2.5 ( $\mu\text{g}/\text{m}^3$ )	IMPROVE Module A	3	1994	Gravimetric mass ( $\text{PM}_{2.5}$ concentration)
	AIHL Cyclone	(8.25, 9 or 10)	1995	Optical absorption (LIPM, HIPS) Elemental analysis (PIXE, PESA, XRF)
Temperature ( $^{\circ}\text{C}$ )	Fenwal UUT51J1 $\pm 0.4^{\circ}\text{C}$ radiation-shielded thermistor	2	1994	Vertical temperature profile Bulk Richardson number
		7.5	Early 1995	
		.5, 1, 4	1995	
Wind Speed (m/s)	Met One 014A cup anemometer 0.45m/s threshold $\pm 0.11\text{m/s}$	2	1994	vertical wind speed profile, $z_0, u^*$ used in PM flux calculation
		7.5, .5, 1, 4	1995	
Wind Direction (deg)	Met One 024A vane	2	1994-1996	used in PM flux calculation
		4	1997	
Relative Humidity (%)	HMP35C Vaisala capacitive	2	1994	atmospheric conditions
Solar Radiation ( $\text{W}/\text{m}^2$ )	pyranometer	4	1996	stability class
Qualitative measurement of dust plumes	CNL elastic lidar light source: Nd:YAG (1.064 $\mu\text{m}$ ) receiver: Cassegrain telescope (26 cm, f/10)		1997	Elastic backscattering is used to obtain information on the distribution and properties of atmospheric aerosols

## 3 METHODS

### 3.1 PM<sub>10</sub> Field Test Strategy and Array Design

All field measurements were made under actual field conditions. While sampling was coordinated with cooperative growers, special treatment of the fields to accommodate PM<sub>10</sub> sampling was not requested. No attempt was made to modify normal activities and great effort was taken to interview the staff and spend days in observation to ascertain what was “normal”. This policy lowered sampling efficiency and limited the range of conditions or implements that could be assessed but it assured that the conditions would be representative. All valid measurements (the only ones reported) were made under equally representative conditions. A combination of upwind/downwind source isolation and vertical profiling methods was used to quantify PM<sub>10</sub> emission factors (Cowherd, Axetall et al. 1974; Cuscino, Kinsey et al. 1984; Cowherd and Kinsey 1986; Flocchini, Cahill et al. 1994; James, Matsumura et al. 1996). As described above, field equipment was augmented from year to year to increase the number of vertical profiles collected and to improve the proximity of the samplers to the operations. In all cases for which data are presented in this report, with the exception of data collected in 1994, aerosol samples were collected using one upwind and at least one downwind vertical profile. Bulk soil and soil moisture samples were collected at locations representative of the source and conditions to correspond with each PM sampling period. Aerosol, ammonia, and soil samples were collected in the field using the methods described. Specific time periods are referred to as tests (Test ID), locations are referred to as (Loc) on a field or facility (Array). Along with a designation of the type of sample collected, referred to as the channel (Chan), these fields define each sample uniquely. Details regarding the use of these fields can be found in Appendix G.

#### 3.1.1 Field Crops

Aerosol samples and meteorological data were collected at the heights indicated in Table 2.2. Particulate matter measurements at the top of the tower are referred to by the nominal height of 9 m throughout this report. Both PM<sub>10</sub> and PM<sub>2.5</sub> were collected downwind of the agricultural operation in a sampling array (Figure 3.1) that was flexible enough to ensure downwind sampling relatively close to the moving source. When possible, two or three towers were used in different locations downwind of the source to better characterize the plume and provide analysis of sampling uncertainty. Soil samples were collected from the region of the field over which the tractor traveled whenever the operation or the soil conditions changed.

#### 3.1.2 Orchard Crops

Concentrations of PM<sub>10</sub> and PM<sub>2.5</sub> were measured in 1994 at one height, 3 m. Also, single height wind speed data was collected in 1994 (Table 2.2). Additionally, most of the 1994 PM and meteorological data were measured outside of the orchards. Appendix A includes a summary of all 1994 field tests. Almond harvesting was, chronologically, the first operation tested in 1995 and our profiling methods were developed during that field sampling campaign. Consequentially, many of those tests were conducted with vertical profiles of either wind speed or PM concentrations, but not both. Or, wind speed and PM concentrations were not both measured under the same conditions with regard to being either within or outside of the tree

canopy. Soil samples were collected as composites near the trees and in the lanes between the trees for both textural and moisture analyses.

A test was conducted in July 1998 to measure  $PM_{10}$  dust emissions under controlled conditions from older and newer models of the two major manufacturers of almond or “orchard crop” harvesting equipment. The overall test strategy was to sample  $PM_{10}$  dust concentrations upwind and downwind for each harvester under conditions that were as identical as possible. Three sampling towers were used to collect replicate test data simultaneously. The tests were conducted on two different orchards; one with solid-set and one with micro-spray irrigation. Three replicate measurements were made concurrently for each harvester/orchard combination, and the three replicate tests were repeated three times. The orchards were planted with two rows of Nonpareil trees, then a row of pollinator trees, followed by two more rows of Nonpareil trees. Each harvester was tested sequentially on three rows, once on the outside of the two Nonpareil rows near the towers, once on the middle row between the Nonpareil trees, and once on the outside of the two Nonpareil trees far from the towers. After these three tests, the sampling platforms were moved three rows and the tests were repeated using another harvester. Each harvester was tested in a configuration that had the fan blower pointing toward the particle samplers during operation so that the dust plume was carried over the samplers as the harvester passed them. Two meteorological towers were used to collect wind speed and direction data. One was located outside the orchard; the other was located inside. The meteorological data were examined to confirm valid test conditions. Soil samples were collected for this study as for previous orchard tests. Additionally, samples of the windrows on each row were collected and evaluated to determine the similarity of conditions tested by each harvester.

### 3.1.3 Livestock

Measurements of PM emission from dairies and feedlots were made at the same locations, using the same sampling strategies, as for active ammonia measurements (see section 3.4). In winter of 1996 vertical profiles of  $PM_{10}$  were measured at one location downwind of both the feedlot and the dairy (Table 3.1). In summer, 1996 vertical profiles of  $PM_{10}$  were measured at two locations downwind of the feedlot. No aerosol measurements were made at the dairy in 1997 and  $PM_{2.5}$  was collected at 3 m only in 1999. At the dairies in 1996 and 1999 PM samples were also collected using a calcium carbonate coated aluminum denuder upstream of a nylon filter and both Teflon and nylon filters were analyzed for the ions ammonium and nitrate to provide a measure of particulate ammonium concentrations and dissociation on the Teflon pre-filters. Soil samples collected within the animal confinement areas were not successfully analyzed for particle size characteristics due to the organic matter clogging the 50  $\mu\text{m}$  sieve during wet sieving. Soil moisture samples were collected from a representative area of mineral soil (outside the animal enclosures) for evaluation of relative soil moisture conditions.

## **3.2 PM Point Samplers**

The Interagency Monitoring of Protected Visual Environments (IMPROVE) aerosol samplers (Eldred, Cahill et al. 1988; Eldred, Cahill et al. 1990) were used to collect  $PM_{10}$  and  $PM_{2.5}$  on 25mm stretched Teflon filters (3  $\mu\text{m}$  pore-size Teflo®, Gelman R2P1025). These samplers have been used extensively in a nationwide monitoring program at remote sites (Malm, Sisler et al.

1994). Portable gasoline-powered generators placed downwind of the samplers provided power. EPA approved Sierra Anderson inlets (Model 246b) produced the 10  $\mu\text{m}$  size-cut, a cyclone was used for the  $\text{PM}_{2.5}$  size-cut (John and Reischl 1980). The IMPROVE samplers were modified to reduce their size and weight for placement atop the towers. The essential elements of the modified samplers from inlet to filter were identical to that of IMPROVE samplers, the differences were a shortened inlet stack (less than a meter long) and replacement of electronic solenoids with manual ones in some cases. Additionally, a calibration device used to audit flow rates directly was substituted for *in situ* flow measurement gauges for samples collected in 1998, and flow measurements for the samplers at the top of the towers were made using only vacuum gauges, rather than both magnehelic and vacuum gauges, for samples collected in 1996 and 1997. These modifications were shown in laboratory testing to have no effect on the integrity of the  $\text{PM}_{10}$  and  $\text{PM}_{2.5}$  samples collected or on the quality of the flow measurement (unpublished data).

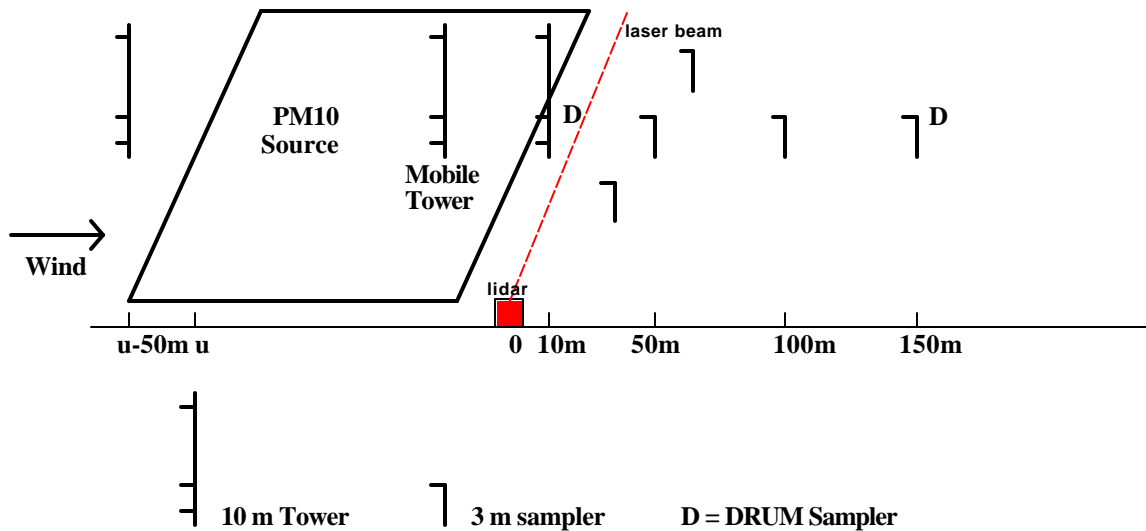


**Figure 3.1 Standard sampling array for measuring agricultural emissions of fugitive dust**

All PM samples were analyzed for gravimetric mass, light absorbing carbon, and elemental composition in accordance with IMPROVE protocols (Eldred, Cahill et al. 1989; Eldred, Cahill et al. 1990; Eldred, Cahill et al. 1997). The mass gain of dynamic field blanks (i.e., filters loaded into the samplers, subjected to flow measurement, but no air sampling) was used to calculate blank concentrations and minimum quantifiable limits (MQLs) for both  $\text{PM}_{10}$  and  $\text{PM}_{2.5}$  (Eldred, Cahill et al. 1990). The MQLs were calculated from the standard deviation of the average of the blanks and the sampled air volumes. Uncertainties in mass concentration were calculated by propagation of the analytical errors introduced in the measurements of mass and air volume.

The hybrid integrating plate and sphere laser analysis technique (Campbell, Copeland et al. 1995; Bond, Anderson et al. 1999) was used to provide an estimate of light absorbing carbon soot.

Particle induced x-ray emission (PIXE) and x-ray fluorescence (XRF) spectroscopy were used to determine the mass concentration of the elements of atomic mass between sodium and lead (Cahill 1995). There is considerable overlap in the range of elements analyzed by these two methods such that independent analyses of the transition metals facilitate quality control between them (Cahill 1995). Proton elastic scattering analysis (PESA), performed simultaneously with PIXE, provided a measure of the mass concentration of the bound hydrogen (as these analyses are performed under vacuum). Minimum detectable limits (MDLs) were defined as 3.3 times the square root of the background counts and analytical uncertainties were based on the propagation of counting errors and uncertainties in the measurement of the elemental mass (from reanalysis) and air volume.

### 3.3 Gravimetric and Reconstructed Mass (RCMA) Concentrations

The accumulation of a large database of measurements of PM<sub>10</sub> and PM<sub>2.5</sub> mass and elemental profiles through the operation of the IMPROVE particulate matter sampling and analysis network provides a series of composite variables that are defined by assumptions regarding the likely atomic mass ratio of the dominant elements of an aerosol constituent (Cahill, Eldred et al. 1977; Eldred, Cahill et al. 1997). These assumptions have been tested against independent analyses of related measurements for the database of IMPROVE samples (Cahill, Ashbaugh et al. 1981) and for agricultural source samples (James, Fan et al. 2000). For example, the gravimetric mass has been shown to be consistently well correlated with the composite variable “RCMA” which is the reconstructed mass obtained by summing factors of the common crustal elements (Al, Si, Ca, Ti, Fe), sulfur, light absorbing elemental carbon, hydrogen and non-soil potassium to emulate an average aerosol (Cahill, Eldred et al. 1989):

$$RCMA = 0.5 BABS + 2.5 Na + SOIL + 13.75 (H - 0.25 S) + 4.125 S + 1.4 (K - 0.6 Fe) \quad (3.1)$$

where  $SOIL = 2.2Al + 2.49Si + 1.63Ca + 1.94Ti + 2.42Fe$

BABS is an estimate of the mass concentration of light absorbing carbon (Campbell, Copeland et al. 1995; Bond, Anderson et al. 1999), and the elemental mass concentrations are represented by their atomic symbols. The uncertainty in this composite variable was calculated as a propagation of the uncertainties calculated for the mass concentrations of each constituent weighted by its coefficient.

Gravimetric PM<sub>10</sub> and RCMA were highly correlated for all of the sample sets collected during this project. An example is the set of concentration measurements made during land preparation activities between 1996-98. The 525 non-zero gravimetric and RCMA masses measured during these three analysis year sets were well correlated as indicated by the slope of the linear regression between these variables (0.77 with standard error = .0065). Therefore, either measure of PM<sub>10</sub> can be used to model the plume characteristics and estimate emission factors. The reconstructed mass was generally lower than gravimetric mass by an average of 13%, (stdev = 23%), due in part to the loss of volatile constituents in the vacuum of PIXE analysis.

Other mass losses sometimes occurred due to sample handling between the two analytical procedures and where the sequential mass loss from gravimetric to elemental analyses was atypically high, the samples were considered invalid. Because the elemental analyses were sufficiently more sensitive than the gravimetric mass measurements, the calculated RCMA was above detectable limits for 13 samples (of 90 in the example dataset) for which measured mass was not. Thus, RCMA was the parameter chosen for analysis of the PM<sub>10</sub> mass concentration profiles.

Data presented in this report for samples collected in 1994 and for the comparison of vertical profile-based and simple box model calculations of 1995 data are gravimetric masses (sections 5.1 and 5.2). Except where noted, RCMA is used for all other calculations of PM<sub>10</sub> emission factors. Where noted, gravimetric mass was substituted for RCMA where significant mass loss following weighing invalidated elemental analyses. Reconstructed mass was also calculated for all PM<sub>2.5</sub> samples collected for this project.

### 3.4 Ammonia

A combination of active and passive methods was used to measure NH<sub>3</sub> concentrations upwind and downwind of three commercial dairies and one feedlot. In 1996 we used a filter-based active method and in 1997 and 1999 changed to a bubbler active method. The passive method (see section 3.4.2) was unchanged throughout. The strategy for equipment placement was similar to that used for PM measurements, but was optimized for the stationary area source in the following manner. The meteorological tower was placed in a flat area as far as possible from any buildings or other obstructions. The active samplers were used at one, two, or three locations within 30 meters downwind of the animal enclosures. The passive filter packs were used at several cross-wind locations within 30 meters of the downwind fence line. A representative location was chosen upwind of the livestock, on the premises, for collection of a background sample using both sampling methods. The details of the sampler locations and the use of the data in the models are given in **Table 2.1**.

**Table 3.1 Description of the ammonia sampling arrays**

type of facility	# animals	Dates	# and type profile(s)	# profile heights	aerosols measured	type of active
feedlot	15147	3/96	None	0	PM <sub>10</sub>	filter
dairy	2000	4/96	1 active	2	PM <sub>10</sub>	filter
feedlot	30455	8/96	2 active	2	PM <sub>10</sub>	filter
dairy	4400	2/97	1 passive	5	None	bubbler
dairy	5720	2/99	3 active	3	PM <sub>2.5</sub>	bubbler
dairy	3060	3/99	3 active	3	PM <sub>2.5</sub>	bubbler

#### 3.4.1 Active Methods

Active filter packs used in 1996 were prepared using 2.5 cm glass fiber filters impregnated in a laminar flow hood with a solution of 1.5 g of citric acid and 1 ml of glycerol in 100 ml of methanol. The filters were dried in individual petri dishes in a vacuum desiccator and loaded into

25 mm Nuclepore plastic filter holders. Multiple holder adapters were used to position a 2  $\mu\text{m}$  pore Teflo® pre-filter upstream of the first impregnated filter and a secondary impregnated filter downstream. This filter pack was suspended upside-down at heights of either 2 or 7 meters from the ground with a vacuum line that attached it through a needle valve to a single diaphragm pump. Air flow rates of 10 L  $\text{min}^{-1}$  were set using an orifice cap inserted at the face of the filter holder and a magnehelic gauge. The impregnated filters were removed from the filter holders and stored in individual petri dishes until analysis. They were eluted with acidified water and the resulting eluent was analyzed conductimetrically for ammonium ion concentration.

An impinger-like bubbler was developed for the 1997 measurements because of problems experienced with the capacity of the active filter pack being exceeded in the previous year. The bubbler also used a teflon pre-filter to remove particulate matter from the air stream, but had two 250-ml bottles of boric acid in tandem to strip the ammonia from the drawn air. It was operated at 2 L  $\text{min}^{-1}$  using a battery powered pump, and flows were measured in the same way as for the filters. It was tested using a 495 ppmv compressed ammonia gas standard, which corresponded to about 350 times the highest concentration measured in the field. Comparison of the primary and secondary units in the bubbler showed the efficiency of each unit to be greater than 90%, over sampling durations of 30 to 240 minutes.

The lower flow rate and very large capacity of the bubblers built for the 1997 work resulted in a decreased sensitivity to lower concentrations and made them cumbersome for use in vertical profiles. So the bubblers were redesigned for the 1999 work with a total of 40 ml 3%  $\text{H}_3\text{BO}_3$  in two 60 ml glass vials with Teflon lined rubber septa connected in tandem by 1/8 inch Teflon tubing with plastic diffusion stones on the submersed end and a Teflon filter in a polypropylene holder at the inlet end. These were used at 2, 4, and 10 m above ground. Air flow rates between 1.5 and 3 L  $\text{min}^{-1}$  were recorded at the start and end of sampling using the same methods as before. In all cases, air concentrations were calculated by dividing the sample mass by the air volume.

#### 3.4.2 Passive Methods

The passive filter packs were adapted from Willems badges (Willems and Harssema 1995). Citric-acid coated Whatman filters were used in 37 mm Gelman filter holders with 2  $\mu\text{m}$  pore Teflo® pre-filters as described by Rabaud et al. (Rabaud, James et al. 2001). Field sampling with the passive samplers was initiated when the cap portion of the filter pack was removed, exposing the first spacer ring and most of the area of the pre-filter. The passive samplers were supported at 2 meters above the ground in all field trials, and 3, 6, 9, and 12 meter heights for the 1997 trial, at from 3 to 10 locations around the perimeter of the facility. Sampling was terminated by capping the cassette. When the filter packs were returned to the laboratory the spacer rings and the pre-filter were removed and the cap was replaced. The impregnated filters were eluted in the filter holders as described by Rabaud et al. (Rabaud, James et al. 2001). The eluent was analyzed conductimetrically for ammonium ion concentration.

### 3.4.3 Facility Description

The commercial feedlot where measurements were made in 1996 is located in the South San Joaquin Valley. In order to collect samples downwind of the facility during as many time periods as possible, two arrays of samplers were used. During the winter period (Table 3.1), when the wind was from the north-west an active filter pack was used near the south-east corner of the facility, co-located with a passive filter pack. Three additional passive filters were placed along the fence line to the west, at intervals of 50 to 100 m. For easterly winds, an active filter pack was centered on the western fence line along with a passive filter pack. Two additional filter packs were placed along the fence line to the north, at intervals of 150 m. All measurements were made 2 m above ground level. The feedlot covers an area of 705x880 m and there were 15,147 cattle on feed during this field trial. The same facility was revisited in the summer for the final field trial of 1996. Active filter packs were used at 2 and 7 m at two locations spaced 150 meters apart on the downwind fence line of the facility with 2 passive filters. The feedlot was operating at near capacity during this time, with 30,455 head of cattle on feed. The commercial dairy monitored in 1996 is located in the central San Joaquin Valley. Active filter packs were used at 2 and 7 m above ground centered on the southern fence line along with a passive filter pack. Five passive filter packs were located at 50 to 100 m intervals both east and west of the active samplers. The dairy covers an area 522x220 m and there were approximately 2000 cows and calves in residence at the time of sampling (1000 milking).

A dairy in central San Joaquin Valley was the site of a collaborative study at which ammonia concentrations were simultaneously monitored for 3 time periods of 2 hours each by an OP - FTIR instrument (Coe, Chinkin et al. 1998), with a path length of 400 m, 4 denuder samplers, (Fitz 1997), and two of our reference samplers with 7 passive filter packs on 14 February, 1997 (Figure 3.2). An additional 5 tests were conducted on 12 February. At that time the facility, which is 840 m on the east-west axis by 375 m on the north-south axis, housed approximately 2050 milking cows and approximately 2350 non-producing heifers. The milking cows were located on the eastern side of the dairy, the non-producing heifers were on the eastern side, and the waste management systems, including the wastewater lagoon, were located in the center. Samplers were strategically placed downwind of each source area, defined by the different animal populations in each area, or by the fact that there were no animals in an area (i.e. source area 2, Figure 3.2). A single profile of ammonia concentration measurements was collected using passive samplers at the tower labeled D1 (Figure 3.2). This dairy was revisited in 1999 when similar sampling locations were used but ammonia concentration profiles were measured at locations labeled L4, D1, and D2 (Figure 3.2) using active samplers. At this time there were 5720 head of cattle on the facility. Ammonia concentrations were measured on a second dairy in 1999. This facility, located in central San Joaquin Valley, is not rectangular but was modeled as a combination of 2 rectangles, one 375X395 m and one 371X176 m. Here 3 vertical profiles of ammonia concentration were also collected downwind of the milking cows, calves and heifers, and waste storage areas separately. Six passive samplers were interspersed between the vertical profilers with spacing of about 100 m.

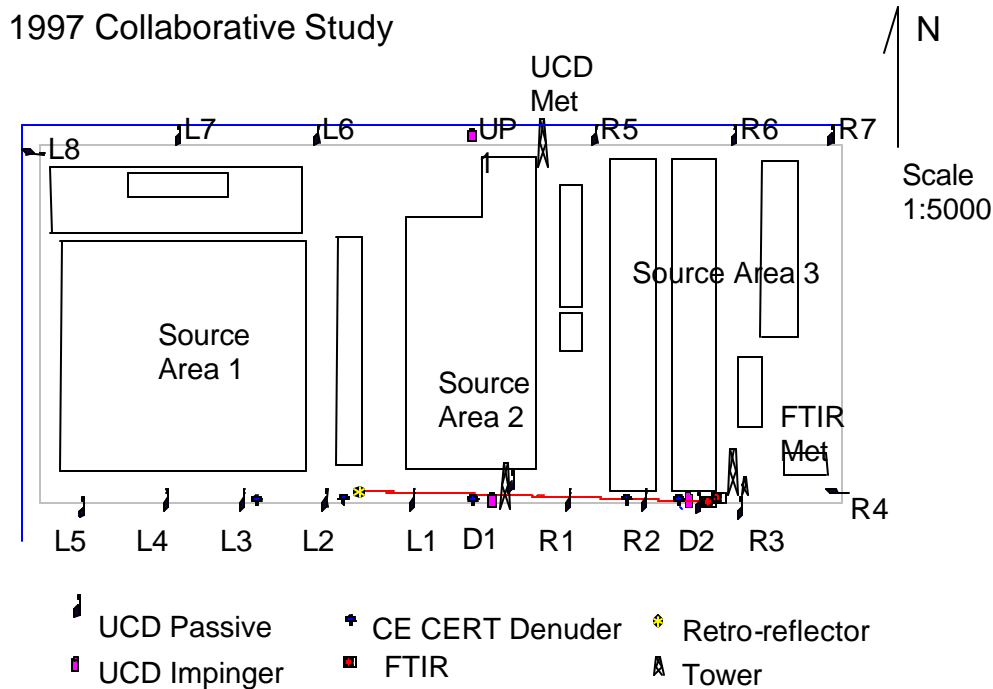


**Figure 3.2 Facility layout and sampler configuration for 1997 ammonia study**

The managers of the dairies and feedlot provided dietary, animal weight, and milk production data for each of the feeding groups on their facilities. Dry matter intake was provided by the producer or estimated from body weights provided by the producer and recommended standard tables (**National Research Council 1988**). Nitrogen intake was estimated as the product of dietary N concentration and average dry matter intake. Quantity and form of the excreted N was estimated using the regression models developed from the results of feeding trials and published results (Tomlinson, Powers et al. 1996) for each class of animals.

### 3.5 Quality Assurance

#### 3.5.1 Filter Samples ( $PM_{2.5}$ and $PM_{10}$ )

Collection of  $PM_{10}$  and  $PM_{2.5}$  in side by side sampling facilitates determination of the quality of analytical results through assessment of  $PM_{10}:PM_{2.5}$  ratios, which have been found to be consistent within a specific source. As the sampling arrays and protocols have been developed various crosschecks and error trapping procedures have been built into logsheets and data entry software to verify the essential elements of mass concentration calculations (elapsed time, flowrate, sample chain of custody). Elemental and optical absorption analyses also provide a great advantage in quality assurance of gravimetric data. The compilation of composite variables such as RCMA (see section 3.3) permit direct comparison of gravimetric mass with elemental data to identify samples that have either abnormally large artifacts in either analysis or have lost mass between analyses. Additionally, the concurrent administration of a large sample collection

network by this laboratory gives samples collected under this project the benefit of substrate acceptance testing, equipment development and testing, and general facilities maintenance performed by that group. Listed below are some of the major analytical validation checks made for filter samples that have undergone gravimetric mass, optical absorption, and elemental analysis:

- Elemental analysis of "clean" filters to check for elemental contamination of manufactured filters.
- Dynamic field blanks to determine gravimetric MQLs (section 3.1) for artifact subtraction.
- Reanalysis of previously analyzed samples to check the "precision" of elemental analysis measurements from different analytical sessions.
- Comparison of redundant measurements to check for consistency between separate and independent measurements.
- Comparison of "known" ratios of certain measured species (e.g. ratio of silicon to iron in soil-dominated aerosols, ratio of mass to hydrogen) to check for consistency between separate and independent measurements.

### 3.5.2 Ammonia Samples (active and passive)

Ammonia analyses were developed through application of the same philosophies and many of the crosschecks and data validation protocols are the same as for the aerosol samples. All ammonia sample solutions were analyzed by the DANR laboratory at Davis except for those collected in 1997, which were analyzed by CNL personnel using an identical instrument as the one used at DANR. Each instrument was tested with blind submission of standard solutions. Each analytical session included appropriate blanks and re-analyses, as mentioned below.

- Laboratory blanks to determine ammonia "background" from sample handling and storage only.
- Dynamic field blanks to determine ammonia "background" for actual samples. These samples also serve to check the precision of the ammonia measurements.

Additionally, the following sample collections protocols were developed over the course of the study to assure the quality of the ammonia concentrations data:

- Comparison of ammonia concentrations with concentrations of particulate ammonium to understand the dynamics of the gas-particle interactions near the source.
- Quantification of ammonium nitrate dissociation on Teflon pre-filters analogous to those used in the ammonia sampling protocol to determine the possible "artifact" caused by particulate ammonium.
- Collection and analysis of secondary filters and bubblers in the active method to quantify ammonia collection efficiency and capacity.
- Comparison of ammonia concentrations measured using co-located passive samplers to check for consistency between separate and independent measurements.

## **3.6 Soils**

Dust emissions that contribute to air pollution are caused by numerous processes, including wind erosion, construction activities, materials handling, and agricultural operations. Although these

activities are known to create fugitive dust emissions, the mechanisms that contribute to the suspension of soil dust into the atmosphere are not well understood. Nonetheless, the potential for exposed soil to release dust particles varies from place to place, and may depend on the soil type, soil moisture, and other factors. A method to quantify the PM<sub>10</sub> potential of a soil sample would provide useful information about how to predict PM<sub>10</sub> dust emissions, and may lead to cost-effective control measures.

The potential for natural soil to release dust into the atmosphere depends largely on the soil particle and aggregate size distributions. Suspendable particles exist in most natural soils, although particles in the PM<sub>10</sub> size range may be bonded to other particles because of their chemistry and/or other surface bonding forces. Energy is needed to break the bonds between small particles and generate fugitive dust. Particles smaller than 10 micrometers can be suspended and are potential PM<sub>10</sub> dust; particles greater than 80 micrometers rarely go into suspension because of their high settling velocity (Singh, Gregory et al. 1994).

The methods currently used to estimate dust emissions from soil sources rely on the silt content (defined as the fraction less than 75 µm physical size obtained by dry sieving) of the soil (U.S.E.P.A. 1995). These methods are coming under increasing scrutiny by both regulators and the regulated community, as plans are prepared to meet the National Ambient Air Quality Standard for PM<sub>10</sub>. The predictive equations to estimate dust emissions have been developed through empirical statistical relationships between measured emission rates and soil parameters. However, the equations developed in this way are not satisfying from a theoretical standpoint. The goal of our research is to extend our knowledge of PM<sub>10</sub> resuspension processes to improve predictions of PM<sub>10</sub> emissions from soils. Measurements of the moisture, silt content, and texture of soil samples collected simultaneously to the measurement of PM<sub>10</sub> emission factors for various agricultural activities furthers this end.

All soil samples were collected using standard methods as described in AP-42 (U.S.E.P.A. 1995). At the agricultural sites, 1-1.5 kg of soil was collected from the top 0.5 – 1.5 inches of soil using a spade or shovel. All samples were sealed in plastic bags for transport to the laboratory.

Soil samples have been analyzed for:

- a. Moisture Content (percentage)
- b. Particle Size distribution by: Wet Sieving (Soil Texture) and Dry Sieving (Silt Content)

Methods based on those described by the American Society for Testing and Materials (ASTM), and the methods described in AP-42 form the basis for our analysis tests. In addition the PM<sub>10</sub> Index was measured by resuspension from the 75 µm sieved (Silt Content) fraction (see section 7). This will help to elucidate the relationship between PM<sub>10</sub> emissions and soil texture.

### 3.6.1 Soil Moisture

Soil moisture was measured by determining the mass difference of tarred aluminum moisture cans, filled with the sample soil and sealed at the time of collection, before and after heating at 105°C for 12 hours or overnight to remove moisture. Soil moisture was calculated using the equation 3.2:

$$\text{Moisture}(\%) = \frac{\text{Mass of Water}}{\text{Mass of Dry Soil}} \times 100 \quad (3.2)$$

### 3.6.2 Dry Sieving

The easiest and most rapid method for obtaining soil aggregate particle size distribution is by sieving. A sieve consists of a pan with a bottom of wire cloth having defined space and uniform square openings. A weighed sample of dried aggregate is separated by size by passing the material through a series of nested (stacked) sieves with progressively smaller openings. Particles smaller than the openings in the wire mesh pass through each sieve. Dry sieving was performed to obtain Silt Content and erodability. Silt content is defined as the mass fraction of material that passed through the No. 200 sieve or 75 µm sieve openings. Erodability is defined as the mass fraction of material passed through the No. 20 sieve or 850 µm sieve openings.

Sieve sizes, both in diameter and openings, were modified between sampling years 1995 and 1998, as described in Table 3.2, to permit direct comparisons between aggregate sizing (dry sieving) and sizing of disaggregated samples (wet sieving). All sieves were cleaned with a brush and/or dry compressed air prior to and after use. Soil samples were first dried to a constant weight at a temperature of 105 ± 5 °C then 250 to 300 g (for the 8 inch diameter sieves) or 14 +/- 0.5 g (for the 3 inch diameter sieves) were introduced to the top sieve of a nest of sieves with a collection pan at the bottom. All of the sieves, including the pan were first preweighed. Sieves were agitated by hand or mechanical apparatus for 10 min (for 8 inch diameter sieves) or 4 min. (for 3 inch diameter sieves). Each sieve was then weighed and individual size fractions were removed and stored. The percent of the mass of the less than 75 µm fraction (No.200 mesh screen) was calculated as the Silt Content and the percentage of the total sample that passes through the 850 µm, (No. 20 mesh) was calculated as the erodibility using equations 3.3 and 3.4, below:

$$\text{Silt Content } \% = \frac{\sum \text{Dry Mass } < 75 \mu\text{m}}{\text{Total Dry Mass}} \times 100\% \quad (3.3)$$

$$\text{Erodability} = \frac{\sum \text{Dry Mass } < 850 \mu\text{m}}{\text{Total Dry Mass}} \times 100\% \quad (3.4)$$

**Table 3.2 Nest of sieves used for particle size distribution analysis by dry sieving.**

US Standard (ASTM) or	Nest of Sieves (µm) 1995	Nest of Sieves (µm) 1996	Nest of Sieves (µm) 1997	Nest of Sieves (µm) 1998

Alternate No,				
10				2000
18				1000
20	850	850	850	850
35				500
40	425			
50	300			
60		250	250	250
80	180			
100		150	150	
140	106	106	106	106
200	75	75	75	75
230	63			
270	53	53	53	53
400	38	38	38	
Pan	P	P	P	P

### 3.6.3 Wet Sieving

Particle size analysis (PSA) is used to define soil texture and the particle size distribution, these can be related to many other soil properties. In this procedure, two 15-g samples of soil aggregates < 2 mm are analyzed, one sample is dried in the oven to obtain the oven-dry weight. The other sample is dispersed with a sodium hexametaphosphate solution, and mechanically shaken overnight. For the first separation, the sand fraction is removed from the suspension by wet sieving using a 50 µm sieve and then the > 50 µm sand fraction is dried in an oven to be further fractionated by dry sieving according to Table 3.3. The clay fraction is determined using the suspension remaining from the wet sieving process. This suspension is diluted to 1 L in a sedimentation cylinder, stirred, and 25-mL aliquots removed with a pipette at calculated, predetermined intervals based on Stokes' law (Jackson 1956). The aliquots are dried at 105°C and weighed. The silt fraction is calculated as the difference between 100% and the sum of the percentages of sand and clay.

**Table 3.3 Sieve sizes which define texture gradients of sand in wet sieving.**

Sand Size	Opening (mm)	U. S. No.	Tyler Mesh Size
Very Coarse Sand (VCS)	1.0	18	16
Coarse Sand (CS)	0.5	35	32
Medium Sand (MS)	0.25	60	60
Fine Sand (FS)	0.105	140	150
Very Fine Sand (VFS)	0.047	300	300

### **3.7 Light detection and ranging (lidar)**

Tests conducted since June 1997 often had corresponding light detection and ranging (lidar) data. The lidar instrument, described previously (Holmén, Eichinger et al. 1998), records range-resolved elastic backscattering signals from PM produced by the agricultural operations with high temporal (sec) and spatial (5 m) resolution. The lidar 2D vertical scans were collected downwind of the tractor operation, just upwind of the downwind point sampler tower, as depicted in Figure 3.1. The lidar scan plane therefore approximated a cross-section of the downwind edge of the area source being sampled by the upwind/downwind point sampler profile array. The lidar scans are qualitative measures of relative PM backscatter, but provide useful information on PM plume variability over time in terms of spatial homogeneity, size, and shape.

Vertical profiles of lidar data were obtained by averaging the lidar signal collected at 2 m height intervals over a specified range (distance from the lidar) interval. The range interval was selected to correspond to the location of the point sampler tower. Background vertical profiles were similarly obtained from the lidar scans collected when the tractor was either stopped or downwind of the lidar vertical scan plane.

Maximum plume heights were recorded for each 2D vertical scan collected over a point sampler test period and averaged for comparison with the point sampler estimates. These average values of test period plume heights were based on plumes located at all locations across the field and, unlike the lidar vertical profiles, were not restricted to the ranges where the point sampler towers were located.

Although the lidar cannot distinguish between PM generated by different sources, the plume generated by the tractor and implement was usually easily distinguished from background PM because of the distinctive movement of the plume across the field from one lidar scan to the next. Possible sources of error in measuring the maximum extent of the plume from the lidar vertical scans include the fact that some plumes extended higher than the programmed vertical limits of the lidar scan; when plumes were very close to the lidar this problem was most severe. Another source of measurement error resulted from near field-of-view geometric optics considerations: because of the lidar's periscope arrangement, plumes within 200 meters of the lidar were not fully quantified by the lidar receiver. Both of these factors could result in underestimation of the maximum plume height when the plume was close to the lidar instrument.

## 4 EMISSION RATE CALCULATIONS

Emission rates were calculated for each test using a mass balance box model. This model requires that we define the plume characteristics sufficiently to calculate the mass transported across the downwind boundary of the field being tested. Because sampling equipment was modified and introduced several times over the course of the reporting period (Table 2.2), the data available for the calculation of emission factors depends on the phase of the experiment in which those data were collected. Data collected in 1994 were analyzed using the simple box model (see model types below) only. These tests include all of our fig and walnut harvest data and our first year of almond harvest data. Emission factors were calculated from vertical profiles of wind speed and PM concentrations measured in 1995 downwind of almond and cotton harvesting operations using the block and logarithmic integration methods (see section 4.2) as well as the simple box model. These data provide a comparison by which to judge the 1994 results (see sections 5.1 and 5.2). Emission factors were also calculated from the cotton harvesting data collected in 1995 using our most recently derived block, logarithmic, linear, and box modeling methods described below. These results can be compared to those of the two previously reported methods (see section 5.2). Emission factors reported for wheat harvesting, land preparation operations, and PM emissions from dairies and feedlots were calculated from data collected in 1995 - 1998 (Table 2.2) using slight modifications of this latest computational method (section 4.3). Ammonia emission factors were calculated from vertical profiles of wind speed and ammonia concentrations measured in 1996, 1997, and 1999 (section 4.4) and from estimates of dietary nitrogen and animal population parameters. The ammonia emission factors are reported in mass per head per year.

Our approach to measuring PM<sub>10</sub> fugitive dust emissions is to collect samples upwind and downwind of cotton production activities. The upwind samples are used to subtract a "background" concentration from the downwind samples, thereby isolating the fugitive dust source. The emission rates are calculated using a model that combines the wind speed and direction, area harvested, and the upwind and downwind concentrations as input parameters. Equation 4.1 shows how the flux is calculated.

$$E = \frac{u \cdot C \cdot t \cdot H \cdot \cos(\mathbf{q})}{w} \quad (4.1)$$

where

$u$  = horizontal wind speed,

$C$  = net concentration (downwind - upwind),

$t$  = time period of the test,

$H$  = height of the plume,

$\mathbf{q}$  = difference of the wind direction from ideal, and

$w$  = width of field "treated".

The horizontal flux across the vertical plane at the downwind edge of the field is related to the emission flux within the field. To quantify the horizontal flux, we need to know its lower and upper limits. The lower limit is obtained from the wind profile, while the upper limit is obtained

from the concentration profile, when they are available. The initial calculations presented in this report assume a fixed plume height with uniform dust concentration and wind velocity from the ground surface to the top of the plume.

Three different methods – the line, block and logarithmic profile models – were used to fit the PM<sub>10</sub> vertical concentration profiles. The height at which the best-fit function of the downwind concentration profile intersected the average upwind concentration was the calculated plume height, H. A fourth model, the box model was used to describe the PM<sub>10</sub> flux in cases of uniform downwind vertical concentration profiles.

**Line Profile Model.** In the line profile model, the three downwind PM<sub>10</sub> concentrations were fit to a line as a function of height. Linear vertical profiles have been used previously for PM profiles downwind of unpaved roads (Venkatram, Fitz et al. 1999).

**Block Profile Model.** The block model essentially ‘connects the dots’ of the three PM measurements in each vertical profile. The block fit assumed the 1 m concentration was constant down to z<sub>0</sub>, the PM<sub>10</sub> concentration was linear from 1 to 3 m, and linear from 3 to 9 m. Above the highest PM<sub>10</sub> measurement at 9 m, the vertical concentration profile was extrapolated linearly using the 3 to 9 m line until the block profile intersected the average upwind PM<sub>10</sub> concentration at H.

**Logarithmic Profile Model.** Downwind PM<sub>10</sub> vertical profiles were also fit with natural logarithmic decay curves as a function of height. The block and logarithmic profile methods were previously shown to give similar results for almond and cotton harvesting operations (see sections 5.1 and 5.2 ).

**Box Model.** The box model transforms the measured PM and wind speed profiles to a profile of uniform PM<sub>10</sub> concentration and wind speed by defining the height, H<sub>box</sub>, required to give the same total integrated PM<sub>10</sub> mass flux. The box model height was determined by different methods for use with data generated in different years, due to the increasing availability of PM<sub>10</sub> vertical profiles. In 1994 and 1995, the box model height was estimated to be 4 m. In subsequent data reduction, the height was determined by regressing the line-fit integrated mass fluxes for all of the profiles for which the most appropriate model was not the box versus the product: [net 1 m PM<sub>10</sub> concentration \* 1 m wind speed \* H<sub>box</sub>]. Height in this product was empirically adjusted until a unit slope was achieved; indicating the equivalent box height that would produce a PM<sub>10</sub> integrated mass flux equal to that measured using the functional models.

#### **4.1 PM from 1994 data**

In 1994, most measurements were made at three meters above ground. Visual observations of the plume were used to establish a plume height of four meters. We used this value for the box height for each test. Ideally, the wind direction would be perpendicular to the downwind boundary of the test field. True wind direction was compensated by using the angle of the wind with respect to the angle of the field boundary. The wind speed was used, along with the plume height and the concentration of PM<sub>10</sub> in the plume to calculate the mass flux across the downwind boundary of the field. Emission rates for the operation were calculated from net mass

flux by including the area of field operated on during the test. These data are presented in sections 5.1 and 5.2 for all valid tests. We continue to calculate an emission factor using the simple box model in addition to our application of vertical profiling models (see section 4.3).

#### **4.2 PM from 1995 data**

The vertical profiles of  $PM_{10}$  collected in 1995 provided the first opportunity to calculate a plume height for some tests and test the assumptions used to analyze the 1994 data. Results of these calculations showed that 4 m, when used with  $PM_{10}$  concentrations and wind speed measured at 3 m, was an underestimate of the true box height for the average plume sampled in 1995.

For the simple box model, the height  $H$  was set to 4 meters, and the concentration and wind speed at 2 meters were assumed to be uniform from the surface to  $H$ . For the block and logarithmic vertical profiling models, the upper and lower limits of the calculation were determined from the data, a flux was calculated at nine points equally spaced between the limits (eleven points including the limits), and the net flux was obtained by integration using Simpson's Rule. The angle  $\theta$  is the difference between the line drawn perpendicular to the direction of the agricultural operation being measured and the wind direction. We set a limit of  $\pm 45^\circ$  on this angle. The width  $w$  is found by measuring the width of implement used and counting the number of passes in front of the sampler for the test.

#### **4.3 PM from 1995 – 1998 data**

Emission factors of  $PM_{10}$  for harvest and land preparation of row crops and for dairies and feedlots were calculated by the simple box, log, and block methods described above and by a linear method. A summary of all four calculations, a method for estimating error for vertical profile heights and emission factors and an explanation of confidence rating assignments are presented below. These methods were also applied to  $PM_{10}$  concentrations measured upwind and downwind of harvest operations for cotton and wheat during 1995. However, emission factors for orchard crops could not be calculated using these methods because of the difficulties in measuring a representative wind speed profile. Exceptions to the method were made to accommodate differences in the sample collection capabilities of the project from year to year and these are summarized in **Table 4.1**.

**Table 4.1 Summary of exceptions to emission factor calculations for PM emissions from row crops and livestock**

Year	Emission type	Analysis affected	Description
1995-96	PM from row crop harvest	Emission factors	upwind PM profiles not always available, so averages of 2 points or a single height measurement was used
1996	PM from cattle	Emission factors	upwind PM profiles not always available, so averages of 2 points or a single height measurement was used
1995-98	PM from row crop harvest and cattle	Emission factor confidence rating	Edge effects not considered to be important in harvesting operations, not evaluated.

Criteria were established to determine: (1) that the profile data were adequate for calculating a reliable emission factor, and (2) that the measurements were made under conditions free of interference from other sources. First, only data sets ("tests") comprised of both upwind and downwind profiles with valid PM<sub>10</sub> concentration measurements at three heights and concurrent meteorological data were accepted, with exceptions as noted above. If either the upwind or downwind profile had any PM<sub>10</sub> RCMA concentrations (see section 3.3) below the MDL, or PM or meteorological data at one or more heights was missing, that test was considered invalid. Second, the upwind profiles were scrutinized to ascertain whether or not the upwind tower was influenced by another source. Since the upwind locations were generally ½ to 1 mile away from the downwind samplers, contamination of the upwind may not have influenced how well the measured downwind profile represented the source. However, isolation of the dust source was critical for characterizing the plume using the profiling method, so the upwind criterion was part of the test acceptance protocol. Most of the complete upwind profiles were as expected for an upwind free of interference: the PM<sub>10</sub> concentrations did not vary with height when taking measurement uncertainties into account. However, when upwind mass concentrations at 1 m exceeded two times the 9 m upwind mass concentration, indicating the presence of an additional source upwind of the source being characterized the tests associated with these upwind profiles were considered invalid. Because the majority of upwind profiles had essentially uniform PM<sub>10</sub> concentrations with height, the average upwind PM<sub>10</sub> RCMA mass concentration was used to calculate all emission factors reported here. Use of the average upwind value resulted in calculated emission factors that did not differ significantly from the emission factors calculated using a linear profile fit to the upwind data. The final criterion used to evaluate profile validity was meteorological conditions. Wind speed and direction both affect the ability of the stationary tower array to adequately capture the PM<sub>10</sub> plume from the moving point source (e.g., the tractor and implement). The wind speed was considered valid if the average speed at 2 m height over the test period was between 1.0 and 6.5 m/s. The upper limit on wind speed was intended to minimize the sampling and quantification of wind blown dust emissions and the

lower limit is two times the quantifiable range of the cup anemometers. Wind direction was a less clear-cut test validation variable because most of the land preparation operations were conducted at an angle to the field boundaries. The measured average wind direction and its standard deviation were used to qualify the level of confidence in the emission factors for each test.

#### 4.3.1 Integration of lidar data

Simultaneous collection of PM profiles, lidar scans and tractor location data on November 6, 1998 provided a comprehensive data set that allowed the development of methods for interpreting all the PM profiles, including those collected before lidar data were available. The observations from the comprehensive data collected on this day were used to develop assessment criteria for profile model fits and plume height reasonableness, and to provide insight into the factors affecting the quality of the PM<sub>10</sub> profile data.

Five categories of downwind profile shape are possible based on three measurement heights (see section 4.3.3). Four of these types were represented in the data (see section 5.0). Many of the measured downwind vertical profiles showed an overall decrease in PM<sub>10</sub> concentration with increasing height (Case 1, see section 4.3.3) and could be fit reasonably well with the linear model. Regions of non-linearity that occurred over limited height intervals in the test-averaged lidar vertical profiles (Figure 4.1) are consistent with the Case 3, 4, and 5 profile shapes for the point sampler tests. For example, the 98-047 lidar profile between 8 and 12 meters resembles a Case 4 ("greater than") profile and the 98-045 and -046 lidar profiles below 6 meters both resemble Case 5 ("less than") profiles. There are also height intervals in all of the measured lidar profiles that can be interpreted as Case 3 ("uniform") profiles, depending on the height-to-height measurement uncertainty. Thus, the complex profile shapes measured with the PM towers are likely the result of sampling over a limited height range with very few samplers. Lidar data also confirmed that the dust plumes measured over a short time interval often had higher concentrations above the ground than at the ground (data not shown). The time-averaged lidar data in Figure 4.1 suggest that the Case 4 and 5 vertical PM profiles captured actual small-scale deviations from a larger-scale overall linear decrease in concentration with increasing height. For the test conditions on 11/06/98, the lidar data suggest that towers of up to 50 m height would have been required to adequately sample the entire plume with point samplers (Figure 4.1).

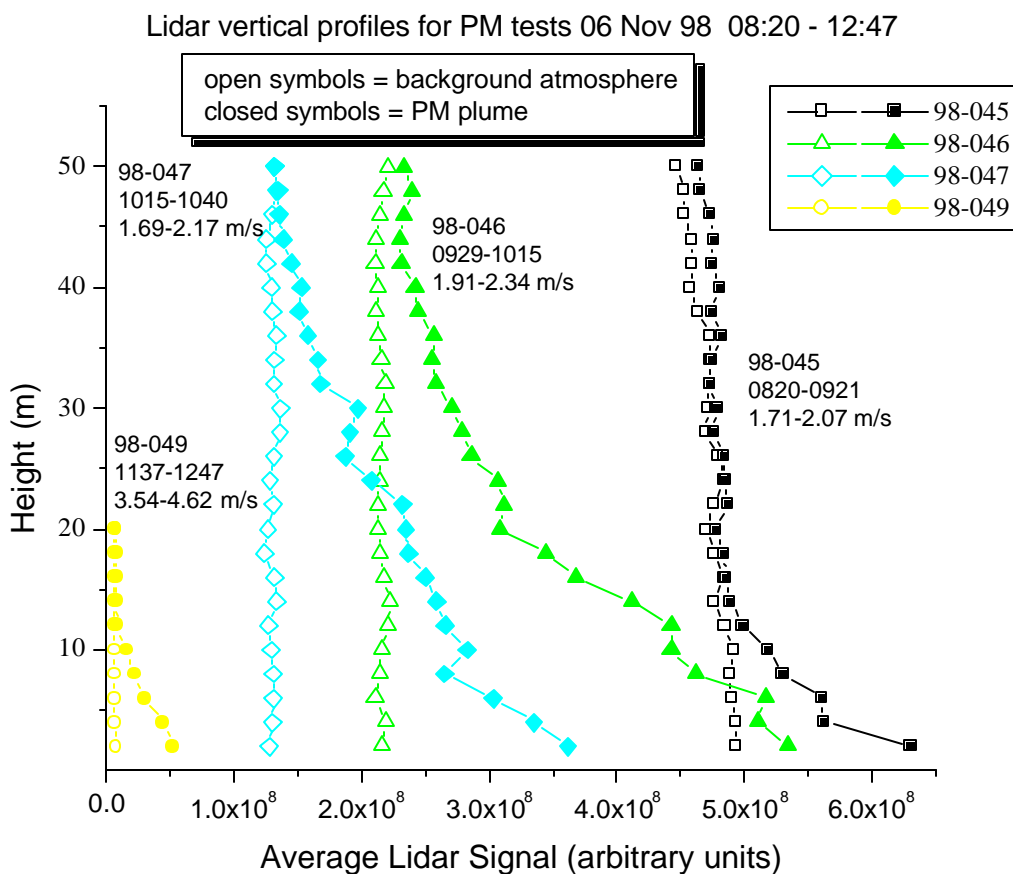


**Figure 4.1 Lidar vertical profiles for PM tests 06 Nov 1998.**

Maximum plume heights determined for individual lidar vertical scans (collected over a < 30 sec period) showed significant variability over the duration of a single PM test, but test-to-test variability in the averaged plume heights was smaller and comparable to the heights determined by fitting the point sampler vertical profiles to the line, block and log models (Figure 4.2). The test-averaged plume heights over only those range locations where the point sampler towers were located (Figure 4.1), agreed fairly well with the average heights from all ranges during a test period (Figure 4.2, compare open and closed bars). This indicates that, on average, the plume monitored at a specific location on the downwind edge of the field had the same height, within measurement uncertainty, as the plume over the entire crosswind length of the tractor pass.

For the lidar vertical profiles based on data only from the tower ranges (Figure 4.1), lidar field-of-view effects (see Section 3.7) could partly explain the significantly lower plume heights quantified for test 98-049 (Figure 4.1) because the tower was located only 180m from the lidar during this test whereas it was over 500 m from the lidar for the other three tests. However, the

agreement between the lidar height and the best-fit heights for all three point sampler models (Figure 4.2) suggest that field-of-view effects were not significant for this test and the smaller plume height measured by the lidar was real. A more likely explanation for the decrease in plume height during test 98-049 was the higher wind speed during this test (3.5 – 4.6 m/s) compared to the tests earlier in the day (1.7 – 2.3 m/s). The decrease in the lidar signal background in Figure 4.1 with time of day was likely due to relative humidity effects on the lidar response. The measured test period average (s.d.) relative humidity (%) values were 63.7 (3.2), 52.3 (1.7), 49.1 (0.8), 43.8 (0.8) for tests 98-045, 98-046, 98-047, 98-049, respectively. Thus, as relative humidity decreased, the lidar background signal decreased, as expected.

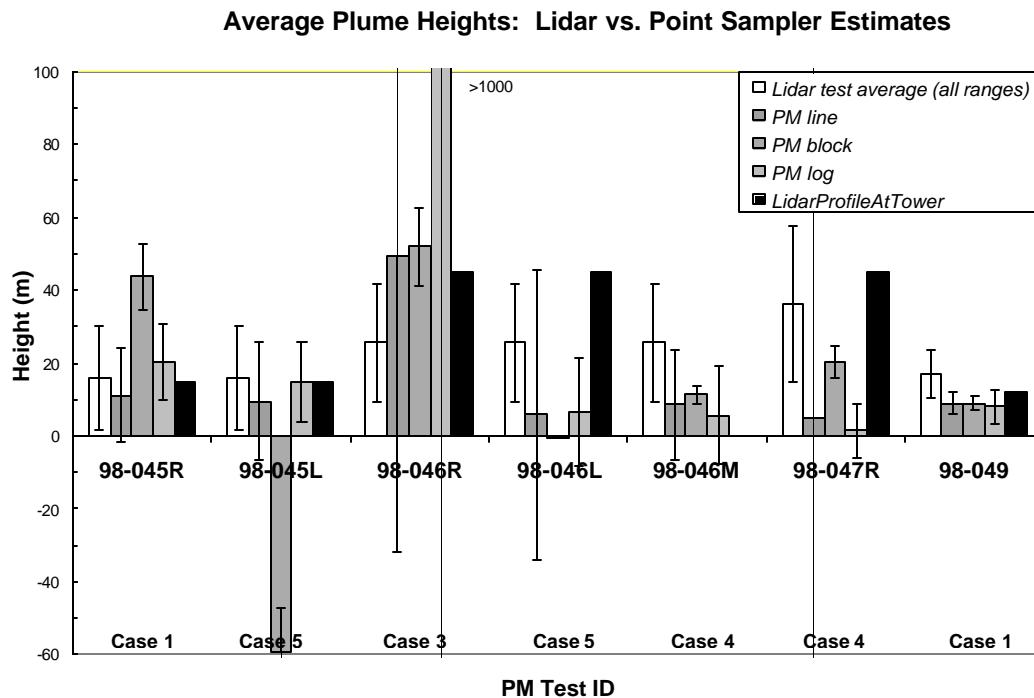


**Figure 4.2 Average plume heights: Lidar vs. point sampler estimates.**

#### 4.3.2 Plume Height and Uncertainty Calculations

Functional fits to the vertical profiles of PM<sub>10</sub> concentration were used to calculate the average heights of the plumes sampled from the harvest and land preparation operations for row crops and the dairies and feedlots and the most appropriate functional fits to each downwind profile type was determined. Three different methods – the line, block and logarithmic profile models – were used to fit the PM<sub>10</sub> vertical concentration profiles. The height at which the best-fit function of the downwind concentration profile intersected the average upwind concentration was the calculated plume height, H. A fourth model, the box model was used to describe the PM<sub>10</sub> flux in cases of uniform downwind vertical concentration profiles (see above).

Uncertainties in the modeled plume heights were estimated using error propagation techniques (Coleman and Steele 1989). Standard errors on the slope and intercept of the model fits to the downwind concentration profiles and the standard deviation in the upwind concentration measurements were used to propagate errors for the plume height estimate. The uncertainty calculations are described in Appendix H. The reported uncertainties do not take into account the uncertainty in individual upwind RCMA concentration measurements.

#### 4.3.3 Emission Factor Calculations

PM<sub>10</sub> emission factors for agricultural operations such as tilling and harvesting are logically quantified on the basis of the area of land worked because the source being quantified is the field where the operation takes place, not the moving tractor/implement. Emission factors for confined animal production facilities were also calculated on this basis. Vertical profiles of wind speed and PM<sub>10</sub> RCMA concentration were used to calculate emission factors for all of the agricultural operations. Because gravimetric mass was consistently well correlated with the “reconstructed mass” composite variable (RCMA) and the elemental analyses were sufficiently more sensitive than the gravimetric measurements (see section 3.3), all emission factors were calculated from PM<sub>10</sub> RCMA concentrations. When the RCMA mass concentration was below the MDL at any of the three sampling heights, emission factors were not calculated for that test.

Each downwind PM<sub>10</sub> profile was classified according to its shape into one of 5 types:

- Case 1 – decreasing PM<sub>10</sub> with height (“decline”);
- Case 2 – increasing PM<sub>10</sub> with height (“incline”);
- Case 3 – uniform PM<sub>10</sub> with height (“uniform”);
- Case 4 – 3 m concentration highest (“greater than”);
- Case 5 – 3 m concentration lowest (“less than”).

Three different methods – the line, block and logarithmic profile models – were used to fit the PM<sub>10</sub> RCMA vertical concentration profiles as described previously (see section 4.2). A fourth model, the box model, was used to describe the PM<sub>10</sub> flux in cases of uniform downwind vertical concentration profiles. The choice of the appropriate model for each downwind concentration profile type was based on analysis of simultaneous lidar data collected during some of the field tests ([Holmén, 2000 #39]– Appendix H).

For each model, a horizontal PM<sub>10</sub> flux was calculated as the product of the net (i.e., downwind – upwind) PM<sub>10</sub> concentration [mg m<sup>3</sup>],  $C(h)$ , and the average horizontal wind speed [m s<sup>-1</sup>],  $U(h)$ , at ten equally spaced height intervals [m],  $dh$ , between  $z_0$  and the top of the plume,  $H$ . The plume height was defined by the intersection of the downwind profiles with the average upwind concentration (as in section 4.2). The flux was integrated over the height of the plume using Simpson’s Rule, and normalized by the time of the test,  $t$ , the upwind width of soil worked during the test period,  $w$ , and the angle between the measured wind direction and the direction perpendicular to the field edge,  $\mathbf{q}$ , to compute the PM<sub>10</sub> emission factor [mg m<sup>-2</sup>]:

$$E = \int_{z_0}^H \frac{U(h)C(h)t \cos \mathbf{q}}{w} dh \quad (4.2)$$

Considering the field illustrated in figure 4.3, the integration in equation 3 can be simplified by moving all variables not dependent on  $h$  out of the integral and computing the flux first. Thus, the product of mass concentration, in mass per unit volume, and wind speed, in units of length in the **y direction** per time, is integrated over  $z$  (out of the plane of the page) to yield flux in mass per unit length in the **x direction** per time. This product can then be multiplied by the total time of the test period and the inverse of the length in the **y direction** covered during the test, normalized for wind direction deviation from perpendicular, to give the emission factor in mass per unit area where the lengths in the area are in the x and y directions. One should note that the  $\cos \theta$  is dimensionless.

Uncertainties in the calculated emission factors were estimated using error propagation techniques (Coleman and Steele 1989) for the line, block and logarithmic fit models. The  $PM_{10}$  RCMA measurement uncertainties and the test period wind speed standard deviation at each measurement height were used to estimate the uncertainty in the horizontal flux at each of the ten model heights. Details about the uncertainty calculations are in Appendix H.

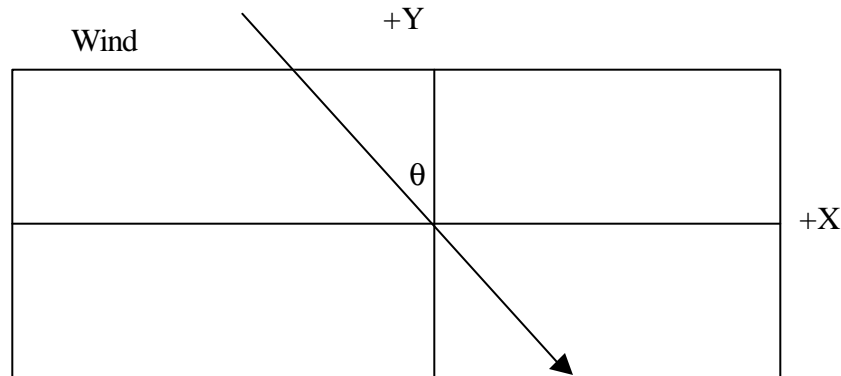


**Figure 4.3: Illustration of emission factor calculation parameters. The X-axis is the direction of tractor travel and the Y-axis represents the width of the field (W, in equation 3) treated during the test period. The wind direction vector is at approximately the limit of acceptance of 45 degrees from perpendicular to the X-axis.**

Emission factors for the  $PM_{10}$  from dairies and feedlots were reduced further to the units of  $\text{lbs } (PM_{10}) * \text{d}^{-1} * 1000\text{head}^{-1}$ . This was accomplished by dividing each emission factor ( $\text{mg } (PM_{10}) * \text{m}^{-2}$ ) by the duration of each test individually, multiplying by the area of the facility ( $\text{m}^2$ ) and dividing by the number of animals. Measurements of the feedlot for the purposes of applying the box model did not provide an accurate estimate of the area occupied by the animals, since it included feed-handling facilities, roads, and other areas. Since the number of animals on the feedlot during each sampling period is well known, a normative stocking density of  $150 \text{ft}^2 * \text{head}^{-1}$  was assumed in estimating the populated area of the feedlot for this calculation.

Conversely, the area of the dairy was much better defined by our measurements, while the number of animals was less well known. For these reasons, a compilation of the areas of all of the corrals was used in the calculation as the area of the facility and the approximate number of 2000 head was derived from the owner's statement that he was milking 1000 cows.

#### 4.3.4 Emission Factor Confidence Rating

Each calculated emission factor was assigned an overall test rating based on five qualifiers that attempt to assess the ability of the emission factor estimate to quantify the actual nonpoint source emissions. The overall test ratings ranged from A to E- and were designed to account for a decreased reliability in the computed emission factor when: the upwind concentrations were equal to or exceeded the downwind concentrations at any height ( $Q_{up}$ ); the wind direction deviated from ideal ( $Q_{wd}$ ); the test suffered from multiple passes due to edge effects ( $Q_{edge}$ ); the fit to Case 5 profiles was poor ( $Q_{fit}$ ); or emission factor relative uncertainty (EFU) was high. Each of these qualifiers is described in Table 4.2 and was based on observations made for all tests.

**Table 4.2 Emission factor confidence ratings summary**

Qualifier	Criteria/Rationale	Scale
1. Q <sub>up</sub> upwind conc	Number of upwind PM <sub>10</sub> RCMA concentrations that exceed the average downwind concentration at the same height  <u>special case</u> : if only the 9 m downwind < upwind, test rating = “A” under assumption that highest sample was above plume.	A = 0 exceed, or special case B = 1 exceeds C = 2 exceeds D = 3 exceeds
2. Q <sub>wd</sub> wind direction	<b>a.</b> test wind direction std. dev. > 25°  <b>b.</b> (test wind direction) - (best wind direction) > 45°  note: best wind direction = 90° to downwind edge of sampling array.	reduce letter rating (assigned on basis of Q <sub>up</sub> ) by:  1 scale (i.e., A B, B C) if <u>either</u> <b>a.</b> or <b>b.</b> true 2 scales (i.e., A C, B D) if <u>both</u> <b>a.</b> and <b>b.</b> true
3. Q <sub>edge</sub> edge effects	X <sub>loc</sub> ~ 0 any time during test  If test included passes at the field edge immediately upwind of the tower, test deserved lower quality rating (negative Q <sub>edge</sub> ).	- = edge effects present  + = no edge effects
4. Q <sub>fit</sub> Case 5 fit	assesses how well linear model described fit.  $[PM]_{9m} - [PM]_{3m} > \frac{1}{2} [PM]_{1m} - [PM]_{9m}$  $[PM]_{9m} - [PM]_{3m} < \frac{1}{2} [PM]_{1m} - [PM]_{9m}$	- = poor linear fit  + = better linear fit
5. EFU relative emission factor uncertainty	accounts for unidentified qualifying factors.  $\left[ \frac{\text{emission factor uncertainty}}{\text{emission factor}} \right] > 20\%$	reduce letter rating by one scale (i.e., A B, B C) if true

#### 4.4 Ammonia from Measurements

The ammonia mass flux, in mass of ammonia emitted per unit width of the facility per time, was calculated using the box model method as flux is calculated from PM concentrations. The mass flux model assumes that movement of the ammonia due to diffusion is negligible, as is deposition

or chemical transformation within the vicinity of the source. The general box model calculation solves the following equation (4.3), where the left-hand side is integrated over the measurement heights and the right-hand side incorporates the width of the facility for calculation of emission factors.

$$\sum_{i=1}^l C_i \times V_i \times \cos(\mathbf{q}) \times \Delta Z_i = E \times w \quad (4.3)$$

where  $C_i$  = Concentration (mass/volume) at height  $i$ ,

$V_i$  = wind speed (length/time) at height  $i$ ,

$q$  = wind direction angle from perpendicular to the facility

$\Delta Z_i$  = height (length) of layer  $i$ ,

$E$  = Emission flux (mass/area), and

$w$  = width of facility (length)

The emission factor is then computed as the mass of ammonia per animal per unit time, using equation (4.5):

$$F = E \times W \times \frac{1}{N} \quad (4.5)$$

where  $F$  = Emission factor (mass/head \* time), and

$N$  = number of animals

In our application of equation (4.4) we defined 10 height intervals between the surface roughness height and the top of the plume. We then computed ammonia concentrations and wind speeds for each height. The surface roughness height ( $i = 1$  in eq. (4.4)) was obtained by calculating the point above ground where the logarithmic wind speed profile projected to zero. A logarithmic fit was made to the wind speed to facilitate calculation of wind speed for each layer  $i$  in the data sets from all of the field trials. The methods used to compute the concentrations and heights at each layer in the summation from the measurements of ammonia air concentration and wind speed evolved as a response to the differences in the physical deployment of the samplers for each field trial.

The calculations of ammonia concentration for each layer  $i$  were made using the two methods described above (see section 4.2). For the data collected in 1996 a linear relationship between the two measured concentrations and the natural log of the height provided a slope and intercept used to compute the height at which the downwind concentration equaled the upwind concentration ( $i = 1$ , eq. (4)). For the data collected in 1997, a similar method was applied to more than two measured concentrations, fitting a series of linear curves to the concentration profile in a block form. This form assumes that from the roughness height to the first measured point, the concentration is constant at the first measured value. Between all the measured points, the concentration is interpolated from the measurements. The top of the plume is defined by extrapolating the valid measured concentration at the greatest height to the upwind concentration. Our 1999 field trial produced concentration measurements at 3 heights, allowing for the use of both methods. We used either a logarithmic or linear function to fit the measured concentrations with height depending on which provided the better fit. We found that logarithmic

fits were more appropriate for measurements of higher concentrations, and linear fits were better for lower concentrations.

We have used several methods to incorporate the variability in the rates of emission from different regions of the facilities into our estimate of the overall emission rate. Measurements made using the passive filter packs placed at 50 - 100 meter intervals along the downwind edge of the dairy in 1996 were averaged and divided by the concentration measured by active samplers at the same height on the vertical profile. The resulting ratio was used to normalize the ammonia air concentrations measured at both heights on the profile for incorporation into the mass flux model. Two vertical profiles were used at the feedlot in summer of 1996, such that independently computed emission rates were averaged for an estimate of the facility-wide emission rate. In analyzing the 1997 data we computed the ammonia mass flux at the point of the vertical measurements then scaled that value to the measurements made using the passive filter packs at approximately 90 meter intervals along the downwind edge of the dairy. The resulting scaled fluxes were integrated again over the downwind width of the dairy. The data from the 1999 field trials was reduced in much the same way as that used in 1997, except that up to three emission flux estimates based on vertical profiles were calculated. The larger number of directly calculated emission flux measurements were well correlated with the wind speed corrected concentrations measured at single heights. This relationship defined the effective height of the ammonia plume, assuming concentration constant with height, for application of the box model to calculate emission flux at each measurement location. These fluxes were then integrated over the width of the facility to compute an overall ammonia flux.

Because the box model method of computing mass flux relies on the wind to carry the ammonia to the locations for measurement, measurements made under conditions of unstable or inappropriate wind direction were not used to compute emission rates. A reliable measurement period was defined as one in which the average wind direction was within the arc described by radians drawn from the measurement location to the upwind corners of the facility. This criteria was applied to data collected in all of the field trials. Also, the capacity of the impregnated active filters (@ 400 mg/filter) was exceeded in many of the measurements at the feedlot during the first field trial. Emission factors were not calculated when the primary filter of the 7 meter measurement exceeded capacity.

#### **4.5 Ammonia from dietary nitrogen balance**

The methods we used to estimate emission rates from animal management parameters were based on estimates of nitrogen excretion and ammonia volatilization as a percent of nitrogen excreted. Experimental nitrogen excretion data for dairy calves and cows were used to estimate the ammonia emissions at the dairy in the 1996 field trial (Morse and DePeters 1996). In this application, we used a nitrogen excretion factor for yearling heifers equal to the average of the values for calves and cows. For the feedlot in the 1996 field trial, the nitrogen excretion rates were estimated from dietary and animal performance data, as described by Meyer et al. (Meyer, Ashbaugh et al. 1997) Two groups of cattle were fed different diets, according to body

weight. The weight of cattle entering each group and the rate of gain realized by the animals were used with the protein content of the diets to estimate nitrogen intake, accretion, and excretion from standard table values (National Research Council 1988).

The dairies on which our 1999 field trial was conducted were very cooperative in providing dietary, animal weight, and milk production data for each of the feeding groups on their facilities. We used a combination of standard table values (National Research Council 1988) and values provided by the producers to estimate dry matter intake based on the weight of the cattle. Diet formulations were used to calculate nitrogen intake from dry matter intake and animal weight data were used to estimate nitrogen retention for each feeding group. Milk production data, both for quantity and protein content, were used to estimate milk nitrogen removed from the farm. Nitrogen excretion was calculated as the difference between nitrogen intake and the sum of nitrogen retention and excretion in milk.

Emission factors were estimated based on both 50% and 70% manure nitrogen volatilized as ammonia for data collected in the first field trial. Subsequently, we determined the percent of manure nitrogen volatilized as ammonia through a series of feeding and laboratory experiments (James, Meyer et al. 1999). So for the data collected during the third field trial, we estimated ammonia emission rates separately for calves, heifers, and milking cows using these experimentally derived volatilization rates, then summed them for a facility-wide emission factor.

## 5 RESULTS FROM FIELD MEASUREMENTS

Results in this section are divided by source and presented chronologically. Tables 5.2 and 5.8 and the text at the end of section 5.2.2 are the result of our initial development of the vertical profiling method of calculating emission factors from data collected at multiple heights. Work done at that time only assessed 3 models, the box, the block, and the logarithmic. Starting with section 5.1.2, the methods developed for the Atmospheric Environment manuscripts (see Appendix H) and explained therein were used to re-calculate emission factors from all of the data collected from 1995 through 1998 under sampling conditions comparable to the recently established protocols. All data collected under other sampling conditions were not reported in these subsequent sections. Those calculation methods include 4 models, adding a linear method to the original 3 models. The much larger data set and new knowledge contributed by the lidar allowed a much more definitive assessment of which conditions favored which models and how to use the models together as complementary tools, rather than defining one model as best for all circumstances.

The results of a series of six comprehensive tests conducted during diskings when a full complement of ancillary data (lidar, laser rangefinder) were collected were used to develop a framework for analyzing all of the upwind-downwind point  $PM_{10}$  concentration profiles measured during this project and identify conditions under which the field sampling strategies affect the reproducibility of  $PM_{10}$  concentration measurements. Results of recently developed lidar data reduction techniques were used to verify that the shapes of the plumes measured as three-point  $PM_{10}$  vertical profiles were representative of the average plumes recorded during the sampling period. From this assessment, a best-fit function for quantifying plume height and emissions was identified for each category of vertical profiles observed in the  $PM_{10}$  data. These observations based on comparisons of lidar and point sampler data were used to develop an emission factor quality rating system.

The computation and rating of  $PM_{10}$  emission factors using this framework is restricted to those profiles for which three valid measurements of concentration were collected. Additionally, application of this method requires simultaneously collected wind speed measurements representative of the meteorological conditions at the tower where the  $PM_{10}$  concentrations were measured. Because of these requirements, all of the samples collected in 1994 and all of the measurements of  $PM_{2.5}$  are insufficient for emission factor calculation by these protocols, as they lack three measurement heights. Similarly, many tests conducted in early 1995 lacked multiple height wind speed data or, in the case of many almond tests, wind speed measurements were not made under the same conditions as  $PM_{10}$  concentrations. However, estimates of  $PM_{10}$  emission factors calculated from these data are still of interest. Emission factors computed using earlier methods (see sections 4.1 and 4.2) are compiled here along with other assessments of data that do not fit the model for emission factor analysis derived from the lidar and  $PM_{10}$  concentration profile comparisons. The recently calculated best fit emission factors follow the earlier work in each of the source category sections.

Comparison of the average plume heights and vertical profile shapes determined by lidar to the profiles measured with the point samplers on 11/06/98 led to assignment of particular best-fit models to the PM<sub>10</sub> profiles for each of the four observed profile shape categories (see section 4.3.3). Although there were some tests that were difficult to categorize, overall the model selected for each category tended to have the lowest calculated uncertainties for both plume height and emission factor. However, the large number of Case 4 and 5 profiles suggests that many plumes were not fully characterized by the three sampling heights. The spatial resolution and wide vertical scanning range of the lidar data on 11/06/98 confirmed that both local maxima and minima occurred in the overall plume profile, but the limited point sampler heights can bias the overall plume shape interpretation for plumes that are highly irregular or very tall (i.e., greater than highest point sampler height).

The calculated emission factors (and uncertainties) for all models are shown in Tables 5.3, 5.9, 5.11, 5.13, 5.15, 5.17, 5.19, and 5.21 for comparison; the bold type values represent the best-fit model plume height and emission factor values for each profile type. As the test results indicate, there was general agreement in the emission factors computed by the different functional fits to the profiles for an individual test when all four models could be calculated (Cases 1, 4 and 5). Thus, the magnitude of the computed emission factors was not biased by the selection of the best-fit model.

## 5.1 Orchard Crops

Sampling of PM was conducted upwind and downwind of operations in orchard crops in 1994, 1995, and 1998. Crops characterized in 1994 included almonds and a survey of figs and walnuts (Table 2.1). Almond harvesting operations were again monitored in 1995 and 1998. Emission rates were calculated from PM<sub>10</sub> and PM<sub>2.5</sub> measurements made in 1994 using the simple box model. This model does not require the characterization of the vertical wind speed profile, but uses the wind speed measured at 3 m to compute the PM flux (see section 4.1). Single height wind speed data was collected in 1994 (Table 2.2). Additionally, most of the PM and meteorological data collected in 1994 were measurements outside of the orchards (PM concentrations entering and leaving the orchards at the perimeters). Appendix A includes a summary of all 1994 field tests.

The emission factors for fig harvest operations are low compared to other operations tested. Combined with the small amount of acreage in the San Joaquin Valley, the net emissions from fig harvesting are minor. It should be noted that we have only tested fig harvest operations on one ranch and one soil type; other harvesting practices and soil types may lead to different emission factors than those measured. We have no valid walnut data. The 3 good tests collected in 1994 (see Appendix A) were of 2 simultaneous operations which could not be quantified separately using these data.

### 5.1.1 1994 Field Tests

An effective method for assessing the PM<sub>10</sub> emission potential of operations within an orchard canopy without calculating emission factors compares the horizontal distribution of PM<sub>10</sub> concentrations. Figure 5.1, Figure 5.2, and Figure 5.3 show typical horizontal distributions of PM<sub>10</sub> aerosols at 3 meters height downwind of orchards with clay and silt soil textures. Figures 5.1 through 5.4 illustrate the possibility of a relationship between PM<sub>10</sub> transport distance and soil texture. Other variables such as wind speed, temperature, and relative humidity may have also played a role in producing the observed differences in the ground level extent of the dust plume. Although meteorological data were collected for these tests, the database to incorporate them with the PM data was not developed yet in 1994. A more complete hypothesis of the impact of soil texture on dust emissions is a fundamental aspect of the research quantifying PM10 potential (section 7).

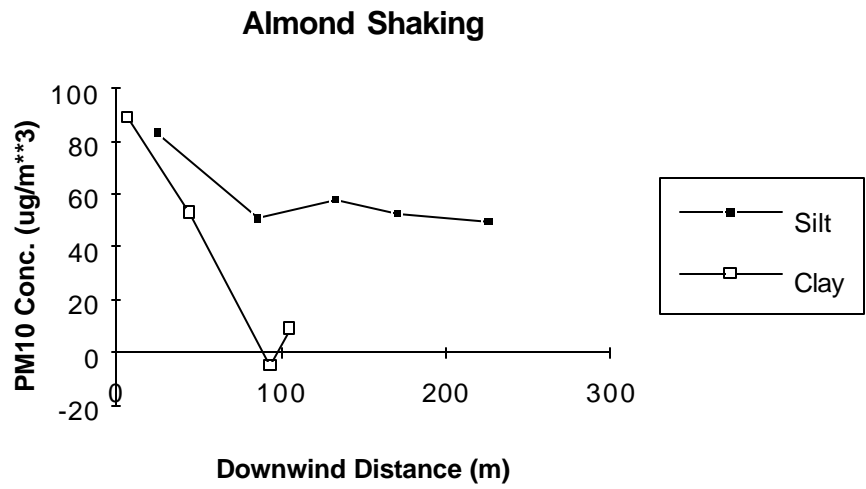


**Figure 5.1 Example of the PM<sub>10</sub> horizontal distribution downwind of an almond harvest tree shaking operation for silt and clay soil textures.**

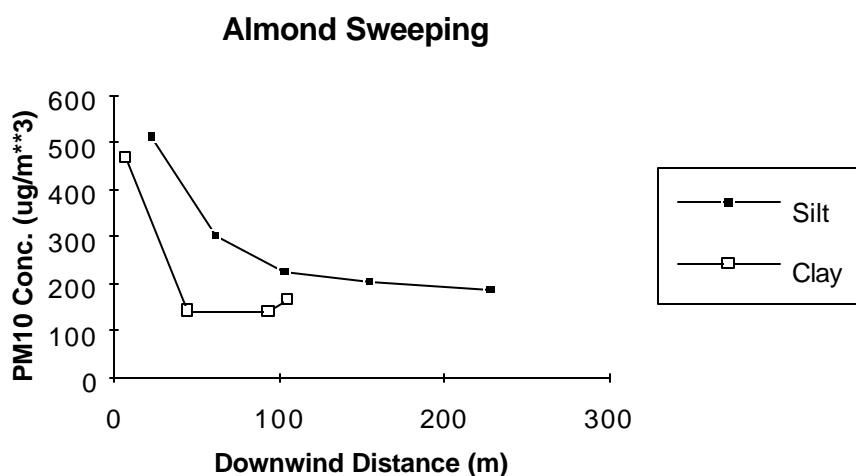


**Figure 5.2** Example of the PM<sub>10</sub> horizontal distribution downwind of an almond harvest sweeping (windrowing) operation for silt and clay soil textures.

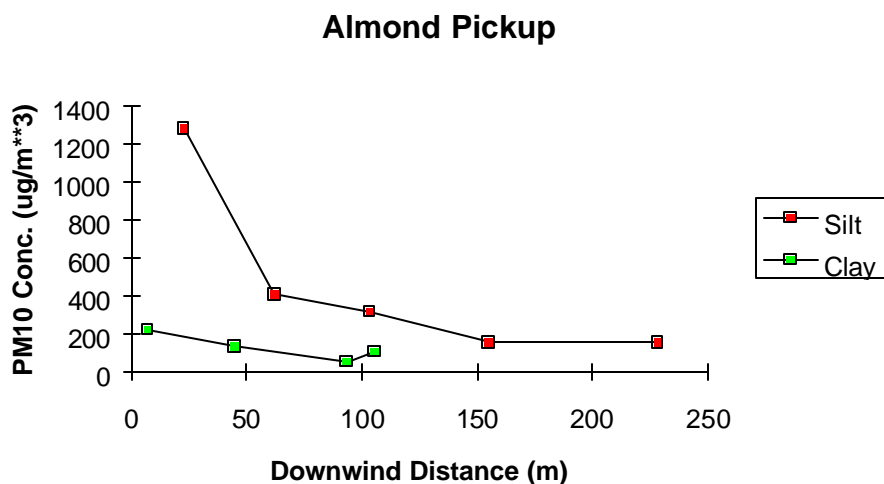


**Figure 5.3** Example of the PM<sub>10</sub> horizontal distribution downwind of an almond harvest, nut pickup operation for silt and clay soil textures.

Some of the vertical profiles of aerosols collected during 1994 field tests were above detectable limits for total suspended particulate matter. An example of the vertical distribution of aerosols is illustrated in Figure 5.4. In this example, the fine aerosols are relatively uniform by height while the coarse aerosols show a pronounced vertical gradient. An absence of profiles of PM<sub>10</sub> led us to calculate emission factors from 1994 data using the simple box model.

### Test 95, Fig Harvest-Pickup

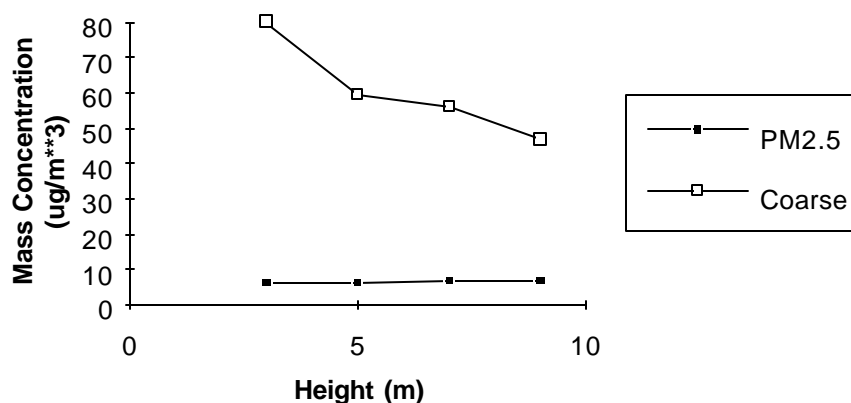


**Figure 5.4 Vertical distribution of aerosols from vertical profile tower.**

Calculation of emission factors using the simple box model yielded the following results. The average  $PM_{10}$  emission factors for the fig harvest operations were  $13 \pm 8$   $kg/km^2$  for the sweeping operation and  $39 \pm 4$   $kg/km^2$  for the pickup. This is significantly lower than the emission factors obtained for almond harvesting. Table 5.1 compares the emission factors measured from fig harvesting to those measured from almond harvesting. Part of the reason for the lower emission factors from fig harvesting is the lack of blower use in sweeping figs. It is not clear why the pickup operation for figs is low compared to that for almonds, although there was some rain before the fig pickup operation and the soil moisture was slightly higher than for almonds. Figure 5.5 and Figure 5.6 show the  $PM_{10}$  and  $PM_{2.5}$  emission factors for fig harvest in comparison to other agricultural operations tested. Note that the vertical scale is logarithmic, which exaggerates the smaller emission factors relative to the larger ones.

**Table 5.1 Comparison of fig harvest to almond harvest emission factors ( $kg/km^4$ )**

Operation	Fig Harvest		Almond Harvest	
	$PM_{10}$	$PM_{2.5}$	$PM_{10}$	$PM_{2.5}$
Shaking	N/A	N/A	15	--
Sweeping	$13 \pm 8$	$2 \pm 2$	$197 \pm 155$	$24 \pm 14$
1 <sup>st</sup> Pickup	$39 \pm 4$	$5 \pm 2$	$1438 \pm 395$	$170 \pm 78$
2 <sup>nd</sup> Pickup	N/A	N/A	$1840 \pm 1810$	$179 \pm 175$

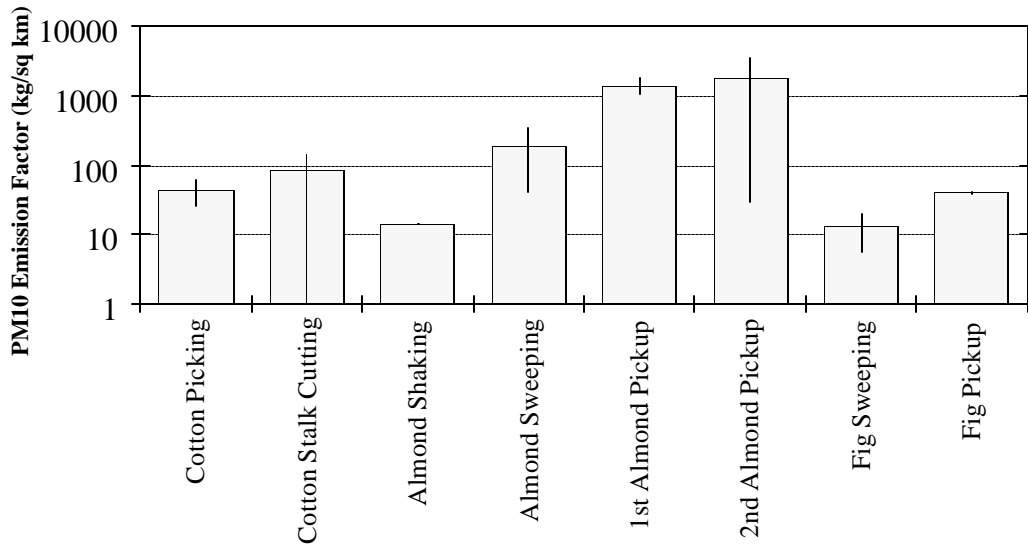


**Figure 5.5 PM<sub>10</sub> emission factors for eight agricultural operations**

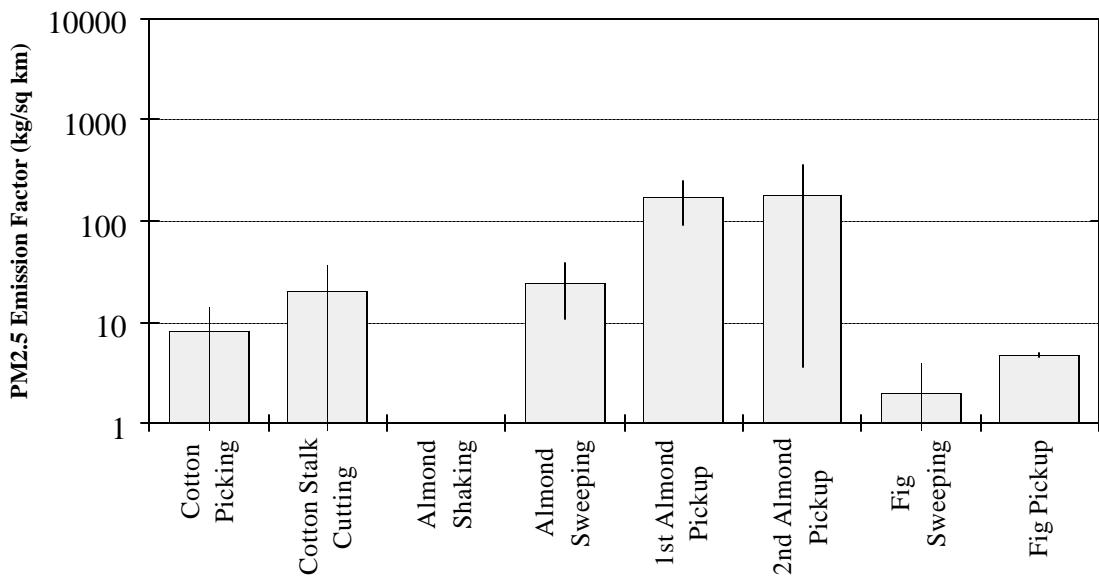


**Figure 5.6 PM<sub>2.5</sub> emission factors for eight agricultural operations**

### 5.1.2 1995 Field Tests

Almond harvesting was, chronologically, the first operation tested in 1995 and our profiling methods were developed during that field sampling campaign. Consequently, many of those tests were conducted with vertical profiles of either wind speed or PM concentrations, but not both. Or, wind speed and PM concentrations were not both measured under the same

conditions with regard to being either within or outside of the tree canopy. It is vitally important that the wind speed measurements describe the exact wind field that carries the PM being sampled. Otherwise, it is meaningless to describe the PM flux as the product of a wind profile that is spatially unrelated to the PM profile. This fact did not become apparent until the detailed investigation conducted in 1998 to compare almond pick-up implements (see section 5.1.3).

Emission factors were initially calculated from the 1995 almond harvesting tests using all of the valid data, regardless of the position of the instruments with respect to the canopy. These preliminary data (Table 5.2) illustrate the relative importance of the almond harvest operations as PM<sub>10</sub> sources both among the three almond operations and by comparison with cotton harvesting.

**Table 5.2 PM<sub>10</sub> emission factors (kg/km<sup>4</sup>) by three calculation methods**

	Log Integration	Block Integration	Simple Box Model
Almond Shaking	1670±1303 (4)	1647±1074 (4)	823±558 (4)
Almond Sweeping	1466±1042 (2)	1935±1403 (2)	1087±631 (2)
Almond Nut Pickup	4467±5830 (7)	3233±1956 (7)	1201±647 (8)

Measurements of PM<sub>10</sub> concentration and wind speed profiles made in 1995 were reviewed to select only those tests in which both the PM<sub>10</sub> and the wind speed were measured in the same wind field. These results provide emission factors that are most directly interpretable to quantification of the PM<sub>10</sub> leaving the perimeter of an almond orchard (Table 5.3). Emission factor uncertainties have not been calculated for measurements made in 1995.

**Table 5.3 PM<sub>10</sub> emission factors for almond pick-up tests during which both PM<sub>10</sub> and wind speed were measured outside of the canopy.**

TestID	date	time of test	Xloc (m)	Upwind	RCMA (ug m-3)				Plume height (m)			Emission Factor (mg m-2)					Qup	Qwd
					9m	3m	1m	Linear	Block	Log	Linear	Block	Log	Box	case			
Almonds																		
95-044 I1	9/9/95	1155 to 1236	22	87.33 (38.78)	169.7 (10.8)	1197.2 (65.5)	877.1 (46.3)	10.57	<b>9.54</b>	5.32E+03	2841.39	<b>1663.30</b>	-6.18E+07	1995.09	4	A	B	
95-044 D1	9/9/95	1155 to 1236	32	87.33 (38.78)	203.5 (12.80)	525.3 (31.1)	1009.2 (55.6)	<b>9.92</b>	11.34	1.54E+06	<b>1995.09</b>	924.96	-3.21E+10	2841.39	1	A	B	
95-046 D1	9/9/95	1347 to 1447	44	87.33 (38.78)	746.9 (42.7)	1165.4 (66.9)	367.9 (22.2)	-29.20	<b>18.59</b>	3.05E+00	1647.52	<b>2365.12</b>	3.96E+01	539.37	4	A	B	
95-054 D1	9/13/95	0745 to 0825	102	175.80 (80.33)	711.5 (39.6)	1317.2 (76.0)	1118.8 (65.1)	19.49	<b>15.03</b>	1.85E+15	18806.94	<b>5259.02</b>	-4.35E+20	1812.52	4	A	A	
95-055 D1	9/13/95	0825 to 855	144	102.45 (23.41)	6.70 (1.10)	613.0 (36.4)	549.8 (33.8)	8.14	<b>8.05</b>	5.09E+03	978.55	<b>431.37</b>	-2.51E+07	457.45	4	A	B	
95-060 D1	9/16/95	0700 to 0740	38	218.87 (168.74)	130.4 (8.6)	1565.3 (85.7)	1761.7 (98.0)	<b>8.74</b>	8.63	6.13E+04	<b>9248.42</b>	2870.09	-1.18E+09	1763.53	1	A	A	

Values in parentheses are uncertainties; NC = not calculated (unreasonable value).

Q<sub>UP</sub> = upwind qualifier; Q<sub>WD</sub> = wind direction qualifier;

Plume heights and emission factors in **bold** type are the best-fit figures based on profile shape (see section 4.3.3).

**Table 5.4 Environmental conditions during almond pick-up tests.**

TestID	Date	Op	Wind DIR*	RH %	SolarRac Watt/m2	Bulk Ri	Wind Speed (m/s)				Temperature (deg C)				%Soil moist	%Silt Content
							1m	2m	4m	7.5m	1m	2m	4m	7.5m		
95-044	09/09/95	Pick-up	265.9	26.27	858.333	-0.068	0.000	1.390	0.000	2.103	30.199	29.68	28.394	27.636	4.80	8.75
95-046	09/09/95	Pick-up	243.6	22.57	812.625	-0.036	0.000	1.907	0.000	3.082	31.750	31.60	30.298	29.604	4.80	8.75
95-054	09/13/95	Pick-up	261.4	80.63	227.929	-0.019	0.000	1.110	0.000	1.598	18.176	18.45	18.076	18.114	2.50	11.34
95-055	09/13/95	Pick-up	225.7	69.47	357.483	-0.043	0.000	1.258	0.000	1.670	21.762	21.41	20.605	20.560	2.50	11.34
95-060	09/16/95	2nd Pick-up	245.4	68.37	44.538	-0.045	0.447	0.916	1.188	1.997	17.904	18.40	17.735	17.829	3.00	14.90

\*best wind = 270°

### 5.1.3 1998 Field Tests

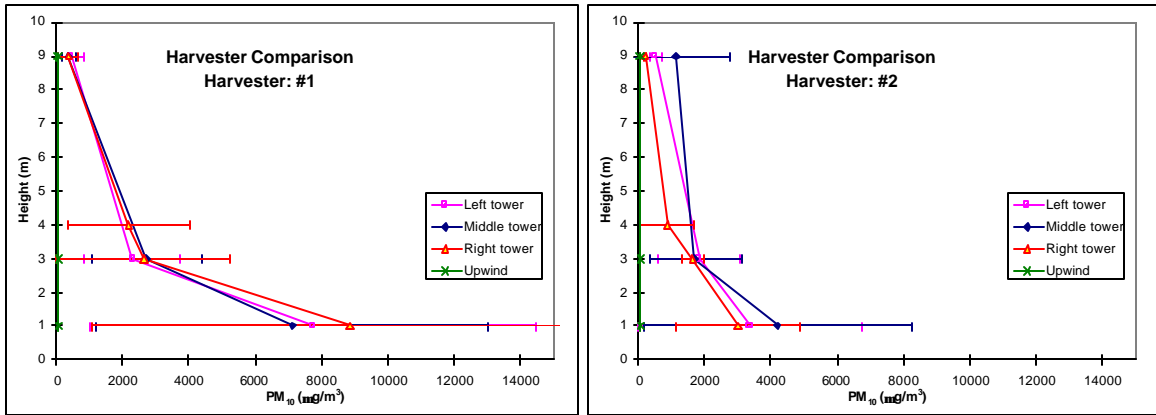
A test was conducted in July 1998 to measure PM<sub>10</sub> dust emissions under controlled conditions from older and newer models of the two major manufacturers of almond harvesting equipment. The tests identify the extent of reduced emissions that can be expected from replacing older harvesters with newer ones. The tests also identify differences in emissions that could result from management practices of the grower. The full text of the report is included in appendix B. Multiple simultaneous tests were conducted on older and newer model harvesters from Flory Industries and Weiss-McNair, Inc. and an older model Ramacher harvester to determine whether there is a difference between the older and newer designs. The harvesters will be referred to here only by code, not by manufacturer. Three sampling towers were used to collect replicate test data simultaneously (see section 3.1.2). The tests were conducted on two different orchards; one with solid-set and one with micro-spray irrigation. Each harvester was tested in a configuration that had the fan blower pointing toward the particle samplers during operation so that the dust plume was carried over the samplers as the harvester passed them. Two meteorological towers were used to collect wind speed and direction data. One was located outside the orchard; the other was located inside. The meteorological data were examined to confirm valid test conditions.

The tree canopy creates a much different environment inside the orchard than exists outside, so the outside meteorology is not representative of the conditions experienced at the samplers. It is useful to examine the outside meteorology for overall sampling conditions, but it can not be used to calculate emission fluxes. The almond harvesters create their own winds, too, so the meteorology within the canopy is strongly affected by the harvest activities. Each time a harvester passes the sampler, it creates strong winds that are not necessarily aligned with the natural air movement in the canopy. Furthermore, the natural wind profile in the canopy is not logarithmic with height as is normally the case in the outside environment. Instead, the tree structure modifies the winds; the highest wind speeds are found close to the ground where there are few leaves and branches to slow it. The slowest winds are found at canopy height, about 3-5 meters above ground. Above the tree canopy, the wind speeds typically increase logarithmically with height. These factors combine to make it impossible to calculate emission fluxes for the harvester tests. Instead, this report will focus on the PM<sub>10</sub> mass concentrations for each harvester and field tested.

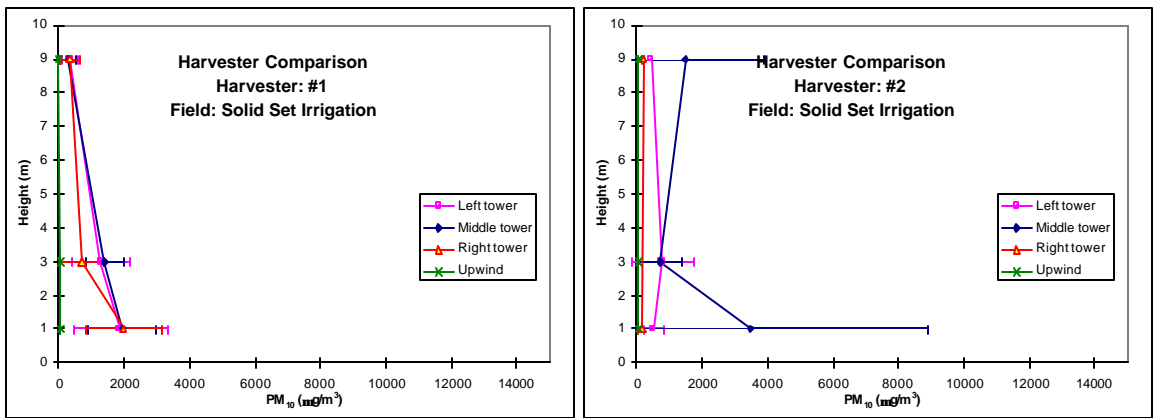
The  $PM_{10}$  mass was measured at three heights on three towers for each test. A complete set of tests included one with the harvester two tree rows from the towers picking up nuts on the outside of the harvested trees, one with the harvester three rows from the towers picking up from between the two rows of harvested trees, and one with the harvester four rows from the towers picking up nuts on the outside again. In Figure 5.7 the uncertainty bar represents the standard deviation of all measurements that were averaged for that figure.

Figure 5.7 shows a set of plots for harvesters 1 and 2 on both fields, and on each field separately. In Figure 5.7a it appears harvester 1 created higher  $PM_{10}$  concentrations than the older harvester 2. Upon closer inspection, though, this seems to be the case only on the micro-spray irrigated field, and only at 1m above the soil surface. This may be due to the way in which dust and trash is ejected from the machine and to the field management practiced on the micro-spray irrigated field. In any case, dust ejected closer to the ground should deposit sooner than dust ejected higher up. On the solid-set irrigated field the  $PM_{10}$  concentrations created by the newer harvester 1 were lower than those from the older harvester 2.

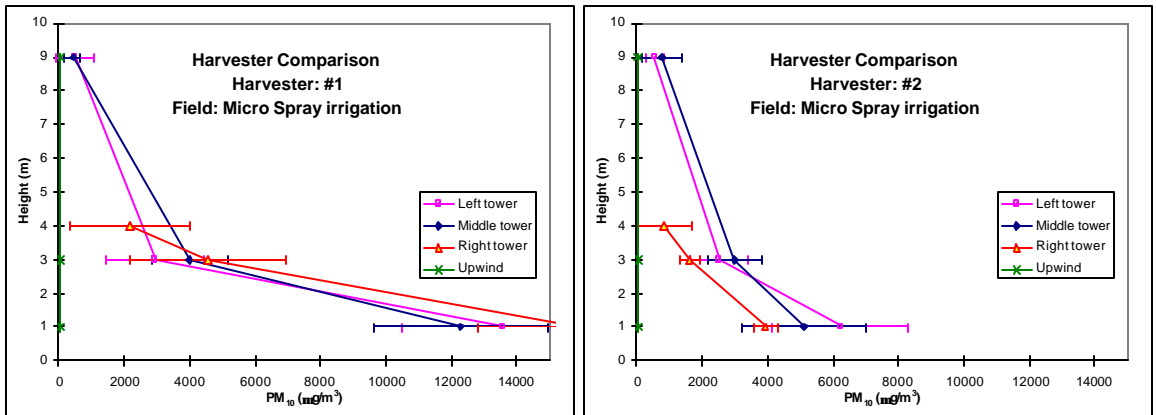
On both fields, the newer harvester 3 also shows lower  $PM_{10}$  concentrations than the older model. For this harvester, too, the  $PM_{10}$  concentrations from the micro-spray irrigated field were higher than for the solid-set irrigated field. The  $PM_{10}$  concentration profile for the newer harvester 3 is similar to that for harvesters 1 and 2. Harvester 5 produced much higher  $PM_{10}$  concentrations than the other two harvesters.



(a)



(b)



(c)

Figure 5.7 PM<sub>10</sub> concentrations downwind of harvester #1 and #2, (a) all tests, (b) solid-set irrigation, (c) micro-spray irrigation.

The PM<sub>10</sub> mass measurements from each tower were averaged to obtain mean PM<sub>10</sub> concentrations by height for each harvester test. Each average vertical PM<sub>10</sub> profile was then integrated from 1m to 9m using Simpson’s Rule to obtain an average PM<sub>10</sub> concentration for the dust plume. The most appropriate way to compare the performance of the harvesters is to examine the PM<sub>10</sub> concentrations normalized to the amount of windrow trash that passed through a 2mm screen. The results of this calculation are shown in Table 5.5. For the solid–set irrigated field, the newer harvester #2 showed overall lower concentrations than the older harvester #1 relative to the amount of windrow trash, but it showed higher concentrations for the micro–spray irrigated field. The newer harvester #4 showed decreases over the older harvester #3 in both fields, though the decrease was larger for the solid–set irrigated field than for the micro–spray irrigated field. The overall change in PM<sub>10</sub> concentrations for both fields combined, normalized to the amount of windrow trash, ranged from +32% to -35%.

**Table 5.5 PM<sub>10</sub> concentrations normalized to amount of windrow trash <2mm prior to harvest (µg/m<sup>4</sup>/g)**

	Harvester			Harvester			5
	1	2	% Difference	3	4	% Difference	
Solid–Set	4.1	2.4	-42%	12.1	4.7	-61%	9.8
Near	2.5	2.3	-9%	30.8	2.8	-91%	7.6
Middle	0.5	2.5	368%	8.6	3.9	-55%	24.1
Far	25.6	1.5	-94%	10.0	5.9	-40%	8.1
Micro–Spray	3.8	6.7	76%	5.5	3.5	-37%	12.1
Near	4.6	5.2	13%	6.3	1.7	-73%	16.2
Middle	2.6	6.1	130%	4.6	3.7	-20%	13.4
Far	4.2	8.4	101%	5.7	4.9	-14%	7.2
Both fields	4.1	5.4	32%	7.4	4.8	-35%	11.4
Near	3.4	3.8	13%	8.8	1.8	-79%	12.4
Middle	2.0	4.1	103%	6.1	5.1	-17%	16.1
Far	7.6	8.8	16%	7.9	6.6	-16%	7.6

Overall, for both fields combined, both new harvesters (#2 and #4) showed very similar PM<sub>10</sub> concentrations relative to the amount of windrow trash. The newer harvester #2 showed better results on the solid–set irrigated field, while the newer harvester #4 showed better results on the micro–spray irrigated field. It is not possible to recommend one brand of harvester over the other. Harvester #5, on the other hand, showed 2-4 times the PM<sub>10</sub> concentrations, relative to the amount of windrow trash, as the other two brands.

## 5.2 Cotton Harvest

### 5.2.1 1994 Field Tests

Table 5.6 lists emission rate results for the valid cotton harvest tests conducted in 1994. These data are also shown in Figure 5.8. Emission rates calculated from data collected in 1994 were calculated using the simple box model (see section 4.1).

**Table 5.6 PM<sub>10</sub> emission rates from cotton operations, 1994**

Test No.	Implement used	Soil Type	Operation	PM <sub>10</sub> Emission Rate (kg/km <sup>2</sup> )
94-049	Deere 9950 4-row pickers	Clay, silt	1st Picking	79 ± 31
94-050	Deere 9950 4-row pickers	Clay, silt	1st Picking	29 ± 9
94-068	2-row and 4-row pickers	Clay	1st Picking	65 ± 20
94-069	2-row and 4-row pickers	Clay	1st Picking	49 ± 15
94-070	2-row and 4-row pickers	Clay	1st Picking	34 ± 10
94-079	Deere 9950 4-row pickers	Clay	1st Picking	32 ± 12
94-087	Deere 5-row pickers	Clay	1st Picking	42 ± 12
94-088	Deere 5-row pickers	Clay	1st Picking	22 ± 7
94-089	Deere 5-row pickers	Clay	1st Picking	42 ± 18
94-083	Alloway Ram 9-row flail shredder	Clay	Stalk Cutting	34 ± 12
94-084	Alloway Ram 9-row flail shredder	Clay	Stalk Cutting	16 ± 7
94-091	Rhino RC20 shredder	Clay	Stalk Cutting	106 ± 44
94-092	Rhino RC20 shredder	Clay	Stalk Cutting	118 ± 49
94-093	Rhino RC20 shredder	Clay	Stalk Cutting	165 ± 49

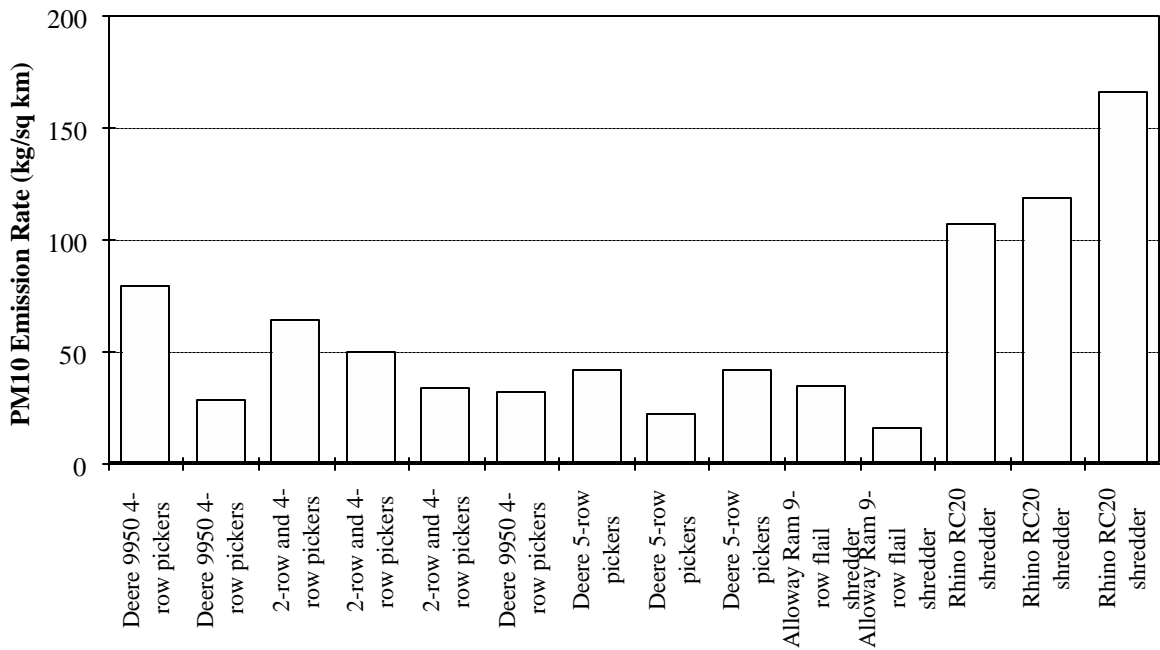


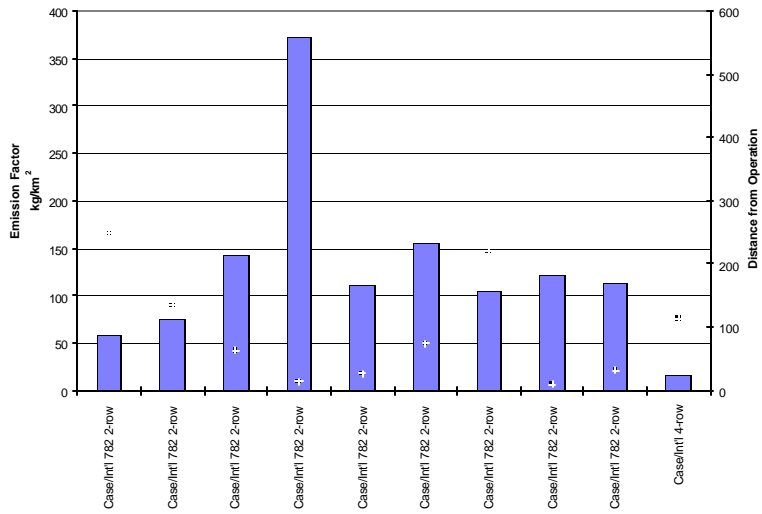
**Figure 5.8 PM<sub>10</sub> emission rates from cotton operations, 1994**

The data in Figure 5.8 and Table 5.6 indicate that the PM<sub>10</sub> emissions from cotton picking operations were fairly consistent from test to test. The emissions from stalk cutting operations were much more variable, and averaged about twice the emissions from picking. The Rhino RC20 shredder operating on clayey soils showed higher emission rates than the Alloway Ram shredder on clayey soils. These differences between equipment manufacturers may be real, or they may result from test conditions. Note that the two Alloway Ram Flail Shredder tests were conducted at over 100 meters downwind of the operation. The Rhino shredder tests were conducted less than 20 meters downwind of the operation. This may be the cause of the difference between the shredder tests. There were, however, too few valid tests of stalk shredding in this data set to draw any conclusions about equipment.

### 5.2.2 Assessment of simple box model emission factor calculations using 1995 Field Tests

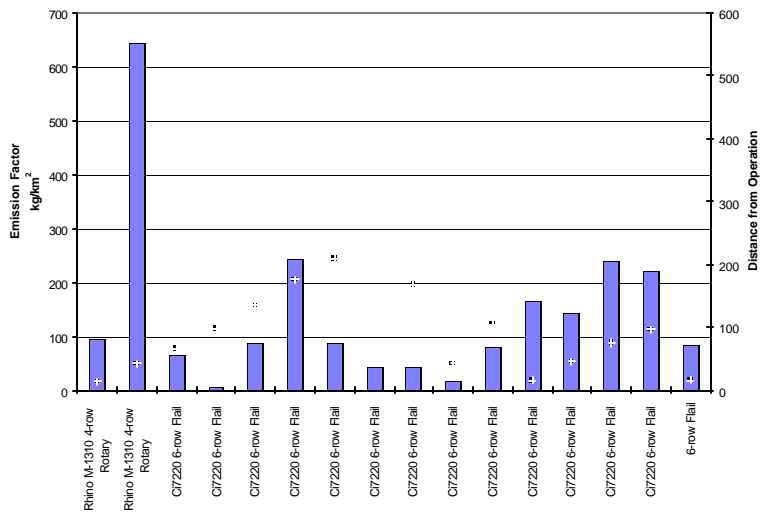
Emission rates, presented in Figure 5.9, Figure 5.10, and Figure 5.11 for cotton picking, stalk cutting, and stalk incorporation, respectively, were calculated using the simple box model from concentrations and wind speeds measured at a single height as described above (see section 4.1). Figure 5.9 shows the emission rates from picking tests conducted in 1995. The symbol shows the mean distance between the picking operation and the first downwind sampler. There seems to be a relationship between the distance and the emission rate; this relationship could be caused by application of the simple box model calculation method to PM<sub>10</sub> concentrations measured at a single height. Single height measurements result in sampling different portions of the plumes that vary in size and concentration with distance from the implement. Further, the

emission rates are higher than those found in 1994; when measurements were made further from the operation. They averaged  $114 \pm 100$  kg/km<sup>2</sup> in 1995, but only  $44 \pm 18$  kg/km<sup>2</sup> in 1994.



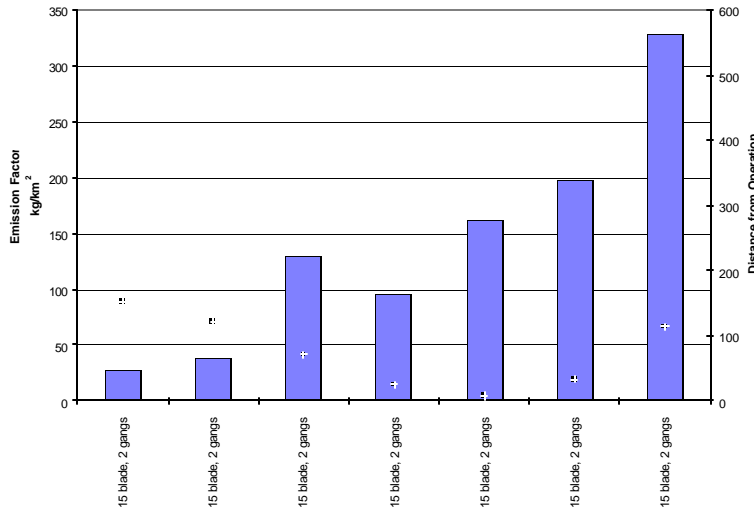
**Figure 5.9 PM<sub>10</sub> emission factor for 1995 cotton picking tests**

Figure 5.10 shows the emission rates from stalk shredding tests conducted in 1995. The relationship between emission rate and downwind distance of the measurement is not as apparent as for the picking tests, but there is a wide variation between individual tests. The rates for this operation were also higher than for 1994 tests; they averaged  $141 \pm 152$  kg/km<sup>2</sup> in 1995, but  $90 \pm 64$  kg/km<sup>2</sup> in 1994.



**Figure 5.10 PM<sub>10</sub> emission factor for 1995 cotton stalk shredding tests**

Figure 5.11 shows the emission rates from stalk incorporation tests conducted in 1995. Once again, the relationship between emission rate and downwind distance of the measurement is not obvious, but there is a wide variation between individual tests. We did not measure emission rates for this operation in 1994, but for 1995 they averaged  $140 \pm 104 \text{ kg/km}^2$ .



**Figure 5.11 PM<sub>10</sub> emission factor for 1995 cotton stalk incorporation tests**

These data indicate the presence of a bias in emission factors calculated using the simple box model which weights the tests conducted closer to the source over those conducted at a distance. An investigation of these effects was conducted using the vertical profiles of PM<sub>10</sub> mass concentrations and wind speeds to recalculate emission factors for cotton harvesting operations (see section 4.2).

Table 5.7 shows the correlation statistics for emission factors calculated for 1995 cotton harvesting operations using the two vertical profile models and the box model with height set at 4 m. For these data, we tested a procedure to calculate PM<sub>2.5</sub> emission factors using vertical profile fits to concentration measurements at two heights. We discontinued this procedure for post-1995 data pending the addition of PM<sub>2.5</sub> measurements at more heights. The PM<sub>2.5</sub> emission factors calculated for 1995 using vertical profile methods should be considered preliminary.

The block integration and log integration of the vertical profiles result in similar PM<sub>10</sub> emission fluxes, but the simple box model results in a lower estimate by a factor of 1.9-2.3 (Table 5.8). For PM<sub>2.5</sub>, the box model is lower than the block or log integration by a factor of 1.7-1.8. This is probably due to the fact that the plume height is not correctly accounted for in the simple box model. The agreement between the log and block integration suggests that either one adequately accounts for the plume height and vertical variation of the plume, and that the number and spacing of the vertical measurements collected are adequate to define the plume. Inspection of individual test results, though, suggests that the block integration provides a better

fit to the plume height. The logarithmic integration sometimes give unrealistic plume heights due to a poor fit to the measured values. This is not surprising, as there is no *a priori* reason to believe that the particle concentrations should have a logarithmic vertical profile. Note that we developed procedures [Holmén, 2000 #38; Holmén, 2000 #39] to identify which model should be used for the vertical integration based on lidar profiles.

Table 5.8 shows the emission flux results for each calculation method for the cotton harvest tests conducted in 1995. The average and standard deviation of the individual test results are shown. The number of tests is given in parentheses. The variation in the test results may be due to differences in underlying soil type, but they may also be due to differences in soil moisture or some other variable. There is not a significant difference between the log and block integrations, but the box model is significantly lower than either the log or block integration in most cases.

**Table 5.7 Correlation statistics for models**

	PM <sub>10</sub>			PM <sub>2.5</sub>		
	Slope	Intercept	r <sup>2</sup>	Slope	Intercept	r <sup>2</sup>
Block (y) vs. Log (x)	0.99	+57.3	.928	0.90	-1.3	.982
Block (y) vs. Box (x)	2.33	-18.8	.896	1.80	+10.6	.868
Log (y) vs. Box (x)	1.90	+35.3	.883	1.74	+23.0	.899

**Table 5.8 PM<sub>10</sub> Emission flux (kg/km<sup>4</sup>) by three calculation methods**

	Log Integration	Block Integration	Simple Box Model
Cotton Picking	340±223 (11)	265±172 (13)	115±79 (16)
Cotton Stalk Cutting	258±157 (15)	278±209 (21)	119±99 (22)
Cotton Stalk Incorporation	319±165 (9)	237±207 (10)	103±90 (11)

The calculation of emission flux from area sources using measured concentrations requires a careful characterization of the horizontal flux at the downwind edge of the source. The results presented here indicate that the vertical profile of wind speed and concentration must be properly accounted for to obtain an accurate result. Either the log integration or the block integration seems to be adequate to characterize the vertical profile of particle concentrations, but the block integration gives more realistic results for plume height. The log integration gives unrealistically high plume heights when the fit is poor, and also gives unrealistically high concentrations near the surface.

Measurement of area source emission fluxes must account for the vertical profile of both wind and particle concentrations. The block integration method using measurement heights of 1m, 3m, and 9m gives satisfactory results. The logarithmic integration gives similar results, on average, but fails in some cases. The simple box model underestimates the emission flux when used with a plume height of 4 meters. The box model results could be improved by selecting a plume height of 7-9 meters.

### 5.2.3 1996-1998 Field Tests

Cotton harvest operations were also monitored in 1996 and 1998 (Table 2.1). Data collected from these tests has been combined with the data collected in 1995 (presented above) and emission factors were calculated using the log, linear, block, and box methods (see section 4.3). The number of tests reported using these calculations varies slightly from the number reported previously due to the stringent application of data validity screening (see section 4.3). We believe that consistent application of these protocols for data validation greatly improves the consistency of resulting emission factors between practices and over time. The support of the lidar data in assessing plume height and other assumptions made in the calculations give these emission factors higher confidence than was possible using the previous computations. The inclusion of error calculations to estimate uncertainty and quality ratings also greatly improves the usefulness of these emission factors. Table 5.9 and Table 5.11 present these latest calculations of emission factors for cotton harvest operations; picking, stalk incorporation, and stalk cutting. The plume heights and emission factors in bold type are the result of the best fit to the concentration data, as defined in section 4.3. Average and standard deviations of the  $PM_{10}$  emission factors calculated by this method from data collected in 1995 were:  $190 \pm 167$  mg/m<sup>2</sup> (17), and  $188 \pm 219$  mg/m<sup>2</sup> (29) for cotton harvest, and stalk cutting, respectively with the number of tests averaged in parenthesis. These averages compare well with the initial calculations using the vertical profiles of  $PM_{10}$  mass concentration (see above).

**Table 5.9 Emission factors for cotton picking compiled from field data collected in 1995-1998.**

TestID	date	time	Xloc (m)	RCMA (ug m-3)				Plume height (m)			Emission Factor (mg m-2)				case	Qup	Qwd	EFU
				Upwind	9m	3m	1m	Linear	Block	Log	Linear	Block	Log	Box				
cotton																		
95-093 D1	10/18/95	1330 to 1530	253.50	69.57 (6.05)	104.40 (6.32)	184.88 (10.50)	209.18 (11.60)	<b>11.66</b>	11.60	19.05	<b>88.63</b>	88.72	97.35	65.65	1	A	A	7%
95-094 D1	10/18/95	1530 to 1700	139.50	69.57 (6.05)	142.10 (9.19)	157.65 (9.15)	197.09 (11.80)	<b>16.53</b>	36.98	110.99	<b>233.90</b>	496.92	927.34	105.55	1	A	A	9%
95-095 D1	10/18/95	1700 to 1750	69.00	90.12 (13.02)	218.20 (13.05)	456.29 (26.16)	433.40 (25.16)	12.71	<b>12.23</b>	20.32	265.95	<b>278.56</b>	287.80	134.01	4	A	A	6%
95-096 D1	10/18/95	1750 to 1838	20.50	90.12 (13.02)	174.98 (10.85)	669.83 (38.46)	742.52 (43.49)	<b>10.21</b>	10.03	12.60	<b>503.58</b>	520.06	442.48	274.95	1	A	A	6%
95-123 D1	10/29/95	1700 to 1904	217.00	156.99 (69.17)	159.63 (9.23)	315.45 (17.55)	290.28 (16.64)	8.84	<b>9.10</b>	8.21	99.73	<b>117.47</b>	72.55	59.93	4	A	A	11%
95-124 D1	10/29/95	2105 to 2205	23.00	156.99 (69.17)	135.21 (8.32)	257.71 (15.91)	323.14 (20.69)	<b>7.88</b>	7.93	7.58	<b>22.11</b>	20.92	16.41	21.18	1	A	B	13%
95-136 D1	11/6/95	1417 to 1509	5.00	57.25 (17.02)	54.22 (3.70)	105.20 (6.98)	184.96 (12.60)	<b>8.37</b>	10.06	9.48	<b>183.54</b>	163.84	148.58	260.12	1	A	A	9%
95-136 IA	11/6/95	1417 to 1509	5.00	57.25 (17.02)	61.72 (4.15)	185.61 (10.76)	291.61 (16.89)	<b>9.06</b>	9.80	10.81	<b>367.43</b>	345.38	312.10	458.63	1	A	A	8%
95-137 D1	11/6/95	1509 to 1602	10.00	57.25 (17.02)	85.57 (5.59)	160.78 (9.84)	134.95 (8.71)	11.76	<b>12.22</b>	13.73	204.87	<b>240.23</b>	173.07	127.66	4	A	A	7%
95-137 IA	11/6/95	1509 to 1602	10.00	57.25 (17.02)	84.24 (6.48)	114.05 (7.12)	180.77 (12.22)	<b>10.34</b>	16.85	17.46	<b>184.55</b>	231.75	206.24	192.83	1	A	A	8%
95-138 D1	11/6/95	1743 to 1917	94.00	81.36 (0)	140.25 (8.23)	201.87 (11.42)	251.79 (14.42)	<b>12.81</b>	14.73	29.58	<b>101.41</b>	108.26	151.52	50.48	1	A	B	8%
95-138 IA	11/6/95	1743 to 1917	94.00	81.36 (0)	121.65 (6.94)	245.83 (14.00)	277.55 (16.58)	<b>11.08</b>	10.95	16.19	<b>102.91</b>	103.57	103.57	58.12	1	A	B	9%
95-146 I1	11/14/95	919 to 959	25.00	112.25 (32.76)	145.11 (8.6)	77.49 (5.2)	125.22 (8.5)	<b>-0.66</b>	-0.66	2.98	<b>0.08</b>	NC	-4.26	-1.40	1	C	A	NC
95-147 I2	11/14/95	1202 to 1302	28.00	81.52 (16.13)	119.50 (7.0)	97.87 (5.2)	162.67 (8.5)	<b>20.68</b>	20.68	3.4E+20	<b>619.65</b>	203.07	-1.8E+24	2.76	1	A	B	NC
96-095 I1	11/10/96	1548 to 1727	74.00	101.16 (26.24)	151.73 (8.43)	229.94 (10.03)	407.85 (17.14)	<b>9.70</b>	14.53	12.33	<b>83.50</b>	88.83	71.67	54.57	1	A	A	15%
96-101 I1	11/15/96	1302 to 1427	46.00	26.72 (4.17)	99.02 (4.56)	136.7 (6.03)	155.95 (6.77)	21.48	<b>23.43</b>	183.40	203.20	<b>214.33</b>	750.80	92.62	4	A	B	13%
96-108 D1	11/20/96	1022 to 1206	119.00	14.09 (1.35)	25.55 (1.46)	71.21 (4.06)	27.32 (1.68)	5.69	<b>10.51</b>	3.12	34.77	<b>41.56</b>	162.48	8.82	4	A	A	262%

Values in parentheses are uncertainties; NC = not calculated (unreasonable value).

Q<sub>UP</sub> = upwind qualifier; Q<sub>WD</sub> = wind direction qualifier; EFU = relative emission factor uncertainty = (calculated uncertainty/emission factor)100.

Plume heights and emission factors in **bold** type are the best-fit figures based on profile shape case.

**Table 5.10 Environmental conditions during cotton picking tests.**

TestID	Date	OP	Wind DIR	RH %	Solar Rad Watt/m2	Bulk Ri	Temperature (deg C)				Wind Speed (m/s)				% Soil Moist	% Silt Content
							1 m	2 m	4 m	7.5 m	1 m	2 m	4 m	7.5 m		
95-093	10/18/95	1st Picking	342.1	36.89	584.87	-0.03	28.762	28.47	27.324	26.962	1.77	2.13	2.58	2.87	4.20	16.10
95-094	10/18/95	1st Picking	346.5	35.59	329.74	-0.01	28.881	28.87	27.918	27.648	1.92	2.47	3.09	3.54	4.20	16.10
95-095	10/18/95	1st Picking	350.8	37.18	129.24	-0.01	27.567	27.88	27.188	27.152	1.50	1.96	2.58	3.06	4.20	16.10
95-096	10/18/95	1st Picking	346.3	42.57	16.19	0.07	24.276	25.47	25.385	25.787	0.73	1.18	1.66	2.10	4.20	16.10
95-123	10/29/95	Cotton Picking	333.3	49.14	1.17	0.13	18.932	20.37	20.711	21.938	0.92	1.22	1.64	2.52	4.40	10.08
95-124	10/29/95	Cotton Picking	285.8	61.77	0.00	0.10	14.55	15.66	16.028	17.753	1.13	1.49	2.04	2.84	4.00	10.08
95-136	11/06/95	Cotton Picking	342	41.41	352.89	-0.01	21.971	22.19	21.322	21.08	2.08	2.26	2.62	2.84	5.50	16.59
95-136	11/06/95	Cotton Picking	342	41.41	352.89	-0.01	21.971	22.19	21.322	21.08	2.08	2.26	2.62	2.84	5.50	16.59
95-137	11/06/95	Cotton Picking	349.8	41.15	210.16	-0.01	21.624	21.99	21.235	21.054	1.83	1.98	2.33	2.50		
95-138	11/06/95	Cotton Picking	313	53.17	0.06	0.11	13.942	15.48	16.136	17.361	1.00	1.47	2.07	2.55		
95-146	11/14/95	Cotton Picking	148.9	58.90	420.60	-0.03	18.6	18.5	17.9	17.8	0.45	1.33	1.42	1.51	9.50	4.07
95-147	11/14/95	Cotton Picking	140.9	39.70	524.60	-0.03	24.9	25.3	24.1	24	0.45	1.34	1.41	1.45	9.50	4.07
96-095	11/10/96	Picking	152.9 **	54.36	54.56	-1.31	18.19	18.53	19.66	20.07	0.52	0.59	1.42	1.67	12.40	15.00
96-101	11/15/96	Picking	343.65	43.67	481.67	0.66	17.28	16.47	16.53	16.29	1.80	1.91	2.21	2.36	17.40	20.70
96-108	11/20/96	2nd Picking	2.89	87.72	294.31	0.19	16.99	17.47	16.62	16.34	2.22	2.22	2.95	3.09		17.70

\*best wind = 315 °; \*\* = best wind = 90 °; otherwise, best wind = 360 °



**Table 5.11 Emission factors and uncertainties for cotton stalk cutting**

TestID	date	time	Xloc (m)	Upwind	RCMA (ug m-3)			Plume height (m)			Emission Factor (mg m-2)				case	Qup	Qwd	EFU
					9m	3m	1m	Linear	Block	Log	Linear	Block	Log	Box				
Stalk Cutting																		
95-097 D1	10/19/95	1400 to 1450	20.00	115.26 (56.66)	111.14 (6.70)	180.66 (11.90)	240.74 (14.77)	<b>8.22</b>	8.65	8.60	<b>89.15</b>	80.63	69.10	128.65	1 A	A	15%	
95-098 D1	10/19/95	1523 to 1533	48.00	115.26 (56.66)	254.83 (20.23)	374.88 (27.16)	379.25 (25.06)	<b>17.08</b>	15.98	62.14	<b>915.08</b>	890.71	2027.02	447.03	1 A	A	3%	
95-098 I1	10/19/95	1523 to 1533	6.00	115.26 (56.66)	103.32 (10.79)	498.97 (32.15)	696.37 (48.61)	<b>8.69</b>	8.82	9.33	<b>762.76</b>	736.24	600.86	984.02	1 A	A	5%	
95-099 D1	10/20/95	1421 to 1523	71.50	88.76 (0)	93.07 (5.78)	109.80 (6.53)	112.41 (6.68)	<b>10.77</b>	10.55	14.50	<b>27.97</b>	28.62	26.33	25.25	1 A	A	18%	
95-099 I1	10/20/95	1421 to 1523	29.50	88.76 (0)	49.66 (3.17)	146.34 (8.84)	213.97 (12.57)	<b>6.71</b>	6.57	5.65	<b>69.55</b>	59.96	46.82	133.67	1 A	A	12%	
95-100 D1	10/20/95	1536 to 1605	104.00	88.76 (0)	70.47 (4.42)	73.03 (4.41)	127.98 (8.00)	<b>4.49</b>	-33.85	3.16	<b>9.21</b> NC	5.42	27.96		1 B	B	24%	
95-100 I2	10/20/95	1536 to 1605	20.00	88.76 (0)	64.38 (4.93)	118.12 (7.83)	168.07 (12.39)	<b>6.51</b>	6.28	5.44	<b>27.95</b>	22.18	18.89	56.54	1 A	A	16%	
95-101 D1	10/20/95	1605 to 1703	140.00	88.76 (0)	70.47 (4.42)	73.03 (4.41)	127.98 (8.00)	<b>4.49</b>	-33.85	3.16	<b>11.94</b> NC	6.78	36.25		1 B	B	28%	
95-101 I2	10/20/95	1605 to 1703	56.00	88.76 (0)	99.43 (5.99)	182.00 (11.33)	181.76 (11.52)	9.90	<b>9.78</b>	11.12	94.80	<b>102.49</b>	77.74	85.96	4 A	A	11%	
95-106 I3	10/22/95	1113 to 1152	49.00	119.94 (15.09)	116.01 (7.3)	184.00 (10.9)	137.03 (9.6)	9.89	<b>9.89</b>	1.6E+05	13.44	<b>63.83</b> NC	NC		4 A	A	NC	
95-110 I3	10/24/95	958 to 1016	15.00	113.04 (16.12)	228.62 (14.9)	317.97 (19.5)	612.14 (38.6)	<b>11.11</b>	11.11	6.6E+09	<b>216.55</b>	108.08	NC	NC	1 A	A	NC	
95-125 D1	10/31/95	1455 to 1631	33.00	35.55 (6.73)	87.28 (5.49)	137.19 (8.06)	110.92 (6.83)	13.22	<b>15.22</b>	14.69	74.44	<b>90.80</b>	62.27	40.71	4 A	C	13%	
95-126 D1	10/31/95	1631 to 1723	101.50	35.55 (6.73)	182.62 (11.08)	211.14 (12.25)	275.46 (15.63)	<b>18.74</b>	39.93	205.84	<b>260.88</b>	502.50	1372.69	114.33	1 A	A	6%	
95-127 D1	10/31/95	1723 to 1824	111.00	35.55 (6.73)	182.62 (11.08)	211.14 (12.25)	275.46 (15.63)	<b>18.74</b>	39.93	205.84	<b>262.52</b>	522.92	1488.41	99.74	1 A	B	40%	
95-127 I1	10/31/95	1723 to 1824	18.00	35.55 (6.73)	132.11 (9.12)	306.34 (21.68)	899.24 (52.82)	<b>7.87</b>	12.33	8.74	<b>317.45</b>	292.28	254.58	359.06	1 A	B	40%	
95-139 D1	11/7/95	1433 to 1507	17.00	95.01 (48.64)	110.25 (7.63)	501.31 (29.04)	1008.39 (58.05)	<b>8.19</b>	9.23	8.86	<b>361.66</b>	316.64	285.91	546.64	1 A	A	9%	
95-140 D1	11/7/95	1507 to 1554	47.00	95.01 (48.64)	116.50 (7.17)	251.30 (15.74)	444.39 (26.18)	<b>8.45</b>	9.96	9.62	<b>205.19</b>	184.22	167.73	302.65	1 A	A	359%	
95-140 I1	11/7/95	1507 to 1554	16.00	95.01 (48.64)	78.38 (5.32)	461.64 (26.70)	725.84 (43.36)	<b>8.45</b>	8.74	8.99	<b>381.78</b>	356.40	300.50	546.45	1 A	A	359%	
95-141 D1	11/7/95	1554 to 1620	77.00	95.01 (48.64)	185.11 (12.19)	246.25 (16.25)	381.05 (23.23)	<b>10.76</b>	17.84	19.71	<b>112.63</b>	145.76	133.78	120.19	1 A	A	4%	
95-142 D1	11/7/95	1620 to 1635	98.00	95.01 (48.64)	135.20 (10.21)	428.44 (26.28)	855.86 (51.22)	<b>8.35</b>	9.82	9.38	<b>247.04</b>	219.80	202.18	324.26	1 A	A	8%	
95-142 I3	11/7/95	1620 to 1635	25.00	95.01 (48.64)	141.90 (12.17)	653.89 (39.48)	1177.56 (74.31)	<b>8.67</b>	9.55	9.90	<b>371.80</b>	341.59	309.11	461.36	1 A	A	8%	
95-148 D1	11/15/95	1424 to 1500	18.00	91.30 (3.54)	92.35 (5.82)	246.74 (14.88)	330.83 (20.31)	<b>8.85</b>	9.04	9.78	<b>75.42</b>	72.24	60.14	35.69	1 A	A	31%	
95-149 D1	11/15/95	1501 to 1605	59.15	91.30 (3.54)	143.15 (8.97)	192.04 (11.64)	247.17 (14.98)	<b>12.15</b>	15.36	26.25	<b>18.55</b>	20.92	26.33	6.22	1 A	B	22%	
96-096 D1	11/11/96	1435 to 1735	67.00	214.89 (31.90)	160.87 (6.75)	189.71 (7.88)	297.56 (11.1)	<b>4.39</b>	-2.24	3.05	<b>12.15</b> NC	8.00	31.14		1 C	C	38%	
96-097 D1	11/12/96	1405 to 1535	467.00	214.89 (31.90)	72.97 (3.27)	150.15 (6.19)	164.61 (6.7)	<b>-2.87</b>	-2.03	0.51	NC	NC	0.66	-30.49	1 D	D	NC	
96-097 I2	11/12/96	1405 to 1535	35.00	214.89 (31.90)	166.18 (7.65)	183.84 (8.24)	258.6 (10.46)	<b>3.75</b>	-9.31	2.39	<b>8.31</b> NC	6.99	26.51		1 C	C	176%	
96-098 D1	11/12/96	1620 to 1650	12.00	220.15 (41.46)	193.28 (9.67)	312.39 (15.32)	551.69 (22.86)	<b>7.02</b>	7.65	6.56	<b>80.34</b>	58.20	56.90	99.80	1 A	A	174%	
96-102 I2	11/15/96	1713 to 1828	71.50	25.94 (10.65)	56.49 (2.65)	261.24 (12.17)	392.52 (15.69)	<b>10.45</b>	11.04	12.94	<b>276.79</b>	265.45	238.14	240.72	1 A	B	7%	
98-043 I1	11/5/98	0945 to 1032	21.00	60.30 (20.66)	45.89 (2.86)	55.01 (3.93)	125.16 (5.27)	<b>5.89</b>	-1.06	4.46	<b>68.35</b> NC	50.88	127.83		1 A	A	12%	
98-044 I2	11/5/98	1050 to 1150	22.00	60.30 (20.66)	40.19 (2.25)	46.96 (2.61)	71.88 (3.07)	<b>3.00</b>	-10.80	1.94	<b>8.91</b> NC	11.05	34.72		1 D	A	51%	

Values in parentheses are uncertainties; NC = not calculated (unreasonable value).

$Q_{UP}$  = upwind qualifier;  $Q_{WD}$  = wind direction qualifier; EFU = relative emission factor uncertainty = (calculated uncertainty/emission factor)100.

Plume heights and emission factors in **bold** type are the best-fit figures based on case.

**Table 5.12 Environmental conditions during cotton stalk cutting tests.**

TestID	Date	OP	Wind	RH	Solar Rad	Bulk	Temperature (deg.C)				Wind Speed (m/s)				%Soil	%Silt
			DIR	%	Watt/m2	Ri	1 m	2 m	4 m	7.5 m	1 m	2 m	4 m	7.5 m	moist	content
95-097	10/19/95	Stalk Cutting/Shred	342.6	30.72	601.32	-0.03	30.46	30.33	29.34	29.06	1.68	1.86	2.03	2.20	4.70	16.10
95-098	10/19/95	Stalk Cutting/Shred	331.8	30.37	460.50	-0.01	30.64	30.67	29.71	29.57	2.09	2.41	2.54	2.63		
95-099	10/20/95	Stalk Cutting/Shred	334.1	26.60	536.10	-0.02	31.46	31.21	30.13	29.90	2.19	2.47	2.63	2.76		
95-100	10/20/95	Stalk Cutting/Shred	338.8	24.60	392.72	-0.02	31.62	31.36	30.46	30.23	1.77	1.99	2.15	2.23		
95-101	10/20/95	Stalk Cutting/Shred	334.2	25.75	263.91	-0.01	31.01	31.18	30.24	30.12	2.35	2.77	2.93	3.12		
95-106	10/22/95	Stalk Cutting	347.3	24.60	620.50	-0.003	18.60	18.50	17.60	17.30	0.00	4.71	0.00	6.63		
95-110	10/24/95	Stalk Cutting	143.7	31.40	440.60	-0.032	17.00	16.90	16.50	16.40	0.00	1.46	0.00	1.56		
95-125	10/31/95	Stalk Cutting	316.4	47.72	169.95	-0.01	21.05	21.42	20.71	20.66	1.55	1.70	1.83	1.99	4.70	10.08
95-126	10/31/95	Stalk Cutting	348.2	52.67	23.63	0.04	18.94	19.94	19.58	19.86	1.11	1.25	1.53	1.93		
95-127	10/31/95	Stalk Cutting	53.2	53.13	0.04	0.06	16.95	18.64	18.49	18.89	1.13	1.46	1.81	2.28		
95-139	11/7/95	Stalk Cutting	350.4	34.24	325.81	-0.02	23.49	23.79	23.02	22.86	1.48	1.58	1.75	1.81		
95-140	11/7/95	Stalk Cutting	4.4	34.14	211.98	-0.01	23.14	23.59	22.93	22.85	1.55	1.64	1.79	1.84		
95-141	11/7/95	Stalk Cutting	356.3	35.15	120.26	0.00	22.51	23.20	22.64	22.65	1.36	1.39	1.61	1.55		
95-142	11/7/95	Stalk Cutting	355.5	36.26	56.53	0.03	21.79	22.71	22.23	22.31	0.95	1.03	1.32	1.39		
95-148	11/15/95	Stalk Cutting	34.6	40.43	336.16	-0.03	25.61	26.00	24.78	24.66	0.45	1.46	1.64	1.72	9.50	4.07
95-149	11/15/95	Stalk Cutting	78.8	41.42	176.57	-0.01	24.86	25.08	24.54	24.50	0.45	1.42	1.50	1.55	9.50	4.07
96-096	11/11/96	Stalk Cutting	334	44.54	135.54	-0.48	22.13	21.85	22.79	23.09	0.78	0.94	1.29	1.56	12.10	15.40
96-097	11/12/96	Stalk Cutting	8.3	51.57	262.94	0.51	21.94	21.10	21.42	21.25	1.14	1.24	1.63	1.69	13.10	16.80
96-098	11/12/96	Stalk Cutting	7.05	63.35	18.78	-2.01	18.11	18.25	19.74	20.01	0.67	0.97	1.40	1.42		
96-102	11/15/96	Stalk Cutting	308.29	56.52	-0.03	-0.40	11.81	11.62	12.26	12.69	1.88	2.19	2.73	3.38	16.70	16.30
98-043	11/5/98	Stalk Cutting	329.04	63.86	507.02	0.09	16.36	15.83	15.55	15.19	4.91	5.16	5.77	5.76	8.60	4.20
98-044	11/5/98	Stalk Cutting	320.34	52.84	397.20	0.06	17.89	17.30	16.94	16.42	6.49	7.00	7.90	8.09	8.60	4.20

\*best wind = 315 °; \*\* = best wind = 90 °; otherwise, best wind = 360 °

### 5.3 Wheat Harvest

Testing of PM emissions from wheat harvests began in 1995 and were continued through 1999 (Table 2.1). Unfortunately, tests conducted in 1995 did not include vertical profiles of wind speed, so calculation of emission factors by the vertical integration methods was not feasible. Data collected in 1996-1998 were analyzed using our most current methods (see section 4.3) and results are presented in Table 5.13.

**Table 5.13 Emission factors and uncertainties for wheat harvest**

TestID	date	time	Xloc (m)	RCMA (ug m-3)				Plume height (m)			Emission Factor (mg m-2)				case	Qup	Qwd	EFU
				Upwind 9m	3m	1m	Linear	Block	Log	Linear	Block	Log	Box					
Wheat																		
96-051 I3	6/22/96	1230 to 1324	27.00	42.25 (9.53)	298.14 (13.29)	1302.64 (56.39)	590.58 (24.66)	8.21	<b>11.78</b>	4.99	1341.08	<b>1719.21</b>	1288.88	693.53	4 A	A	362%	
96-052 I4	6/22/96	1343 to 1452	36.00	42.25 (9.53)	126.83 (6.06)	795.09 (34.54)	741.98 (31.32)	10.92	<b>10.89</b>	11.85	1090.68	<b>1169.38</b>	903.56	940.29	4 A	A	7%	
96-053 I5	6/22/96	1516 to 1637	40.00	42.25 (9.53)	66.74 (3.28)	704.23 (30.04)	714.33 (30.77)	<b>10.32</b>	10.27	10.79	<b>1222.46</b>	1291.87	1001.58	1160.02	1 A	A	131%	
96-054 I6	6/24/96	0945 to 1105	47.00	64.04 (21.92)	59.78 (2.89)	539.47 (23.17)	382.26 (15.74)	9.03	<b>9.94</b>	7.21	412.20	<b>485.64</b>	331.63	324.49	4 A	A	112%	
96-058 I1	6/27/96	1738 to 1950	46.00	18.54 (9.80)	36.18 (1.69)	216.8 (8.7)	418.2 (16.4)	<b>9.45</b>	10.68	10.68	<b>584.49</b>	530.19	480.30	664.23	1 A	A	6%	
96-061 I3	6/28/96	1250 to 1451	46.00	32.42 (1.47)	50.07 (2.28)	439.44 (17.82)	1243.32 (37.82)	<b>8.37</b>	10.32	8.50	<b>779.98</b>	633.03	617.01	1116.57	1 A	B	135%	
96-063 I5	6/28/96	1724 to 1836	23.00	32.42 (1.47)	15.41 (1.35)	176.59 (7.23)	854 (34.54)	<b>7.34</b>	9.26	6.67	<b>1036.90</b>	671.01	757.19	1557.58	1 A	A	8%	
96-068 I1	7/3/96	1355 to 1522	63.00	78.86 (0)	135.63 (5.63)	231.69 (9.47)	255.89 (10.67)	<b>14.24</b>	14.14	28.76	<b>225.88</b>	225.94	264.85	151.00	1 A	A	3%	
96-068 D4	7/3/96	1355 to 1522	258.50	78.86 (0)	46.22 (2.12)	80.26 (3.2)	89.02 (3.69)	<b>3.04</b>	3.25	2.17	<b>3.27</b>	2.98	4.98	8.67	1 A	A	47%	
96-069 D4	7/5/96	0845 to 0940	463.35	84.77 (0)	79.08 (3.78)	92.93 (4.25)	57.04 (3.92)	5.04	<b>6.54</b>	4.10	-15.50	<b>-2.36</b>	-9.55	-17.14	4 A	A	67%	
96-069 I3	7/5/96	0845 to 0940	113.00	84.77 (0)	152.85 (6.52)	281.88 (11.89)	233.11 (9.73)	12.94	<b>13.69</b>	14.65	163.59	<b>189.12</b>	135.79	91.67	4 A	A	5%	
96-070 D4	7/5/96	1048 to 1210	545.15	84.77 (0)	50.79 (2.72)	48.5 (2.31)	43.02 (2.79)	38.24	98.03	65791.49	-244.54	-621.58	-126826.1	<b>-57.23</b>	3 C	C	148%	
96-070 I4	7/5/96	1048 to 1210	91.00	84.77 (0)	180.67 (7.66)	327.63 (13.39)	323.76 (13.37)	15.23	<b>14.57</b>	30.92	569.60	<b>579.05</b>	671.26	327.60	4 A	A	3%	
97-032 I1	6/17/97	1638 to 1813	336.00	43.56 (2.80)	134.36 (5.38)	447.55 (17.82)	586.65 (23.33)	<b>11.69</b>	12.03	16.81	<b>1287.46</b>	1273.03	1298.73	919.85	1 A	A	3%	
97-033 I2	6/18/97	0940 to 1116	586.00	32.41 (7.50)	163.45 (6.58)	254.41 (10.33)	344.56 (14.24)	<b>15.69</b>	20.08	52.09	<b>365.05</b>	409.02	601.52	246.50	1 A	B	10%	
97-034 D1	6/18/97	1600 to 1706	126.50	46.57 (9.57)	184.47 (7.2)	163.2 (6.85)	517.62 (21.05)	<b>7.16</b>	-25.79	8.69	<b>287.51</b>	NC	246.17	396.14	5 A	A	26%	
97-034 I3	6/18/97	1600 to 1706	126.50	46.57 (9.57)	339.28 (13.6)	564.37 (22.43)	1104.37 (44.91)	<b>11.07</b>	19.10	18.11	<b>907.38</b>	1063.44	911.79	889.58	1 A	A	25%	
97-035 D1	6/18/97	1706 to 1756	21.00	46.57 (9.57)	130.46 (5.77)	607.39 (24.86)	804.18 (32.6)	<b>9.13</b>	9.17	11.54	<b>954.33</b>	949.72	874.72	1031.81	1 A	A	34%	
97-036 D1	6/18/97	1756 to 1923	42.00	46.57 (9.57)	97.26 (3.81)	703.69 (28.52)	496.55 (19.62)	7.92	<b>8.69</b>	6.69	979.29	<b>1164.15</b>	787.54	786.55	4 A	A	2388%	
97-041 I1	6/21/97	1306 to 1413	141.80	67.01 (59.36)	78.36 (3.22)	68.42 (3.35)	182.25 (7.88)	<b>6.62</b>	2.00	5.84	<b>42.90</b>	18.00	31.38	64.97	5 C	E	114%	

Values in parentheses are uncertainties; NC = not calculated (unreasonable value).

$Q_{UP}$  = upwind qualifier;  $Q_{WD}$  = wind direction qualifier; EFU = relative emission factor uncertainty = (calculated uncertainty/emission factor)100.

Plume heights and emission factors in **bold** type are the best-fit figures based on case.

**Table 5.14 Environmental conditions during wheat harvest tests.**

TestID	Date	Wind DIR	RH %	Solar Rad Watt/m <sup>2</sup>	Bulk Ri	Temperature (deg C)				Wind Speed (m/s)				Soil Moist (%)	Silt Content
						1 m	2 m	4 m	7.5 m	1 m	2 m	4 m	7.5 m		
96-051	6/22/96	6.2	41.32	1029.5	0.27	25.85	25.05	24.94	24.8	2.356	2.425	2.522	2.599	4.10	20.60
96-052	6/22/96	356.42	36.8	989.38	0.19	27.93	27.04	26.88	26.66	2.927	3.032	3.189	3.28	4.10	20.60
96-053	6/22/96	6.98	27.45	799.67	0.13	29.81	28.86	28.68	28.42	3.578	3.738	3.905	4.014	4.10	20.60
96-054	6/24/96	14.47	40.34	800.31	0.23	23.65	22.73	22.83	22.64	2.566	2.681	2.798	2.855	5.10	22.60
96-058	6/27/96	348.92	38.29	271.88	0.09	23.89	23.11	23.41	23.31	2.566	2.889	3.233	3.514	3.90	19.70
96-061	6/28/96	39.92	42.59	842.5	0.62	22.6	22.63	21.63	21.29	1.984	2.047	2.147	2.292	3.90	19.70
96-063	6/28/96	349.38	37.86	393.91	0.13	24.27	24.73	23.82	23.51	2.679	2.81	3.279	3.772	3.90	19.70
96-068	7/3/96	314.59 *	27.35	929.82	0.15	35.94	35.29	34.2	33.59	3.327	3.762	4.23	4.437	2.40	15.70
96-069	7/5/96	306.75 *	31.47	659.87	0.22	24.58	23.34	23.4	23.13	2.674	3.018	3.356	3.528	2.40	15.70
96-070	7/5/96	291.91 *	30.12	984.56	0.23	30.13	29	28.5	28.04	2.821	3.208	3.572	3.797	2.40	15.70
97-032	6/17/97	341.2	25.06	429.97	0.08	37.96	37.23	36.67	36.32	2.831	0.447	4.842	5.41		
97-033	6/18/97	319.61	34.34	806.58	0.78	30.03	28.14	28.43	28.02	1.62	1.782	1.961	2.02	2.30	9.70
97-034	6/18/97	35.94	24.61	665.62	0.22	36.53	38.53	35.19	34.7	2.623	2.788	3.126	3.473	2.30	9.70
97-035	6/18/97	29.17	23.76	478.74	0.16	36.29	37.65	35.25	34.78	2.61	2.81	3.273	3.674	2.30	9.70
97-036	6/18/97	0.59	23.37	236.33	0.07	35.19	37.14	34.81	34.48	2.679	2.79	3.497	3.942	2.30	9.70
97-041	6/21/97	55.71	16.59	688.73	0.58	30.18	31.56	29.24	29.01	1.638	1.67	1.726	1.78	2.20	7.00

\*best wind = 315 °; \*\* = best wind = 90 °; otherwise, best wind = 360 °

### 5.4 Land Preparation

Land preparation operations have been monitored following cotton and wheat harvests. These operations include root cutting, stubble discing, chiseling or ripping, finish discing, and listing. Root cutting is unique to cotton, but is included here for comparison with stubble discing.

The five highest best-fit emission factors (538 – 776 mg m<sup>-2</sup>) were seen for profiles collected on hot dry summer days for ripping and after dark in winter for stubble discing (Tables 5.15, 5.16). Similar field conditions, however, also resulted in a much lower ripping emission factor of 112 mg m<sup>-2</sup> (test 97-050), thus complicating interpretation between different tests. There were no stubble discing tests conducted under conditions similar to 95-150 and 95-151 that had lower emission factors, but the single test of stubble discing following wheat, in midday in summer (97-045), had a comparable emission factor (430 mg m<sup>-2</sup>). When the downwind concentrations were uniform with height (Case 3) emissions were generally low but downwind PM<sub>10</sub> values were significantly higher than upwind concentrations. The low emission factors were not due to the use of the box model, however, because the box model emission factors showed fairly good agreement (within a factor of 2) with the emission factors calculated by the other models for the other profile types (Table 5.15). Interestingly, the lowest 5 emission factors were measured in winter when temperatures were cooler and soil moisture was relatively high (Table 5.15 and 5.16), suggesting that environmental conditions greatly influence emission rates. The calculated emission factors for land preparation activities (Table 5.15) showed no correlation with wind speed, increased with decreasing relative humidity, were generally lower when soil moisture was higher and generally increased with increasing vertical temperature differential.

Differences in PM<sub>10</sub> emission factors from two operations, for which a representative number of repeated measurements were made, disking and ripping, were used to examine the importance of implement type. The average emission factor for ripping operations, 512 ± 288 mg m<sup>-2</sup>, was significantly larger than that for disking, 134 ± 154 mg m<sup>-2</sup>. However, direct comparison of

implement-average emissions is not reliable because differences in environmental conditions (e.g., relative humidity and wind direction variability) between individual tests appear to have a larger impact on measured emissions than does implement type. Variability in measured emissions due to environmental factors is highlighted by three Case 1 ripping tests collected on 6/26/97 (see Table 5.16). The emission factors for two tests (97-046,  $765 \pm 36 \text{ mg m}^{-2}$  and 97-051,  $776 \pm 27 \text{ mg m}^{-2}$ ) were similar and significantly higher than disking tests conducted under similar relative humidity conditions (98-050,  $74.2 \pm 6.3 \text{ mg m}^{-2}$ ) but the emissions from the third ripping test, 97-050,  $112 \pm 5.3 \text{ mg m}^{-2}$ , was much lower and similar to emissions measured for disking. The much higher deviation of wind direction from the ideal direction during this third ripping test likely explains these results and highlights the complexity of comparing emission tests with different implements unless all other environmental factors are held constant.

Cultivation operations such as weeding have been generally regarded as a form of tillage. Several measurements of  $\text{PM}_{10}$  emission factors for mechanical cotton cultivation conducted in spring of 1998 show that emissions from this practice can be of similar magnitude as disking (Table 5.17). These tests also indicate a correlation between  $\text{PM}_{10}$  emissions from cultivation and soil moisture (Table 5.18).

**Table 5.15 Emission factors and uncertainties for land preparation.**

TestID	date	time	Xloc (m)	RCMA (ug m-3)				Plume height (m)			Emission Factor (mg m-2)				case	Qup	Qwd	EFU
				Upwind	9m	3m	1m	Linear	Block	Log	Linear	Block	Log	Box				
Stubble disc																		
95-118 I7	10/27/95	1255 to 1400	128.00	142.71 (32.24)	138.43 (8.3)	185.36 (10.8)	255.66 (15.1)	<b>9.61</b>	4.74	2.3E+46	<b>257.68</b>	39.96	-1.4E+50	6.77	1	A	B	NC
95-128 D1	11/3/95	1001 to 1139	155.00	66.74 (66.74)	81.34 (5.14)	131.87 (7.64)	141.40 (8.27)	<b>10.94</b>	10.73	15.30	<b>49.31</b>	50.20	49.84	17.08	1	B	B	9%
95-129 D1	11/3/95	1139 to 1200	124.00	66.74 (66.74)	81.34 (5.14)	131.87 (7.64)	141.40 (8.27)	<b>10.94</b>	10.73	15.30	<b>27.47</b>	27.97	27.77	9.56	1	B	B	470%
95-130 D1	11/3/95	1238 to 1300	74.00	66.74 (66.74)	178.31 (12.67)	334.42 (21.30)	411.68 (26.01)	<b>12.75</b>	13.29	26.79	<b>231.04</b>	235.80	371.34	35.58	1	A	A	4%
95-130 I2	11/3/95	1238 to 1300	15.00	66.74 (66.74)	109.27 (8.79)	247.61 (15.32)	563.74 (35.59)	<b>8.09</b>	10.84	9.05	<b>136.73</b>	125.27	102.45	26.35	1	A	A	7%
95-131 D1	11/3/95	1300 to 1333	27.50	66.74 (66.74)	156.97 (11.06)	206.65 (12.99)	464.86 (26.95)	<b>8.52</b>	19.90	10.97	<b>140.80</b>	249.66	126.36	24.82	1	A	A	6%
95-132 D1	11/3/95	1333 to 1342	10.50	66.74 (66.74)	158.22 (14.31)	464.61 (29.88)	841.23 (54.70)	<b>9.17</b>	10.79	11.58	<b>286.12</b>	278.54	254.11	52.62	1	A	A	5%
95-150 D1	11/15/95	1838 to 1910	11.00	143.67 (19.13)	192.89 (12.08)	732.80 (42.53)	1272.34 (74.77)	<b>8.70</b>	9.55	9.95	<b>537.91</b>	491.69	438.93	319.33	1	A	B	9%
95-151 D1	11/15/95	1910 to 1947	32.50	143.67 (19.13)	195.25 (12.96)	966.70 (56.03)	2090.62 (117.39)	<b>8.14</b>	9.40	8.82	<b>542.20</b>	471.01	430.39	472.14	1	A	A	125%
97-045 D1	6/24/97	0956 to 1137	87.00	55.91 (20.94)	92.5 (3.7)	485.1 (18.5)	325.9 (12.4)	9.40	<b>10.70</b>	7.50	352.00	<b>430.00</b>	271.00	270.00	4	A	B	17%
98-045 R1	11/6/98	0820 to 0921	23.00	23.56 (4.88)	57.5 (2.8)	64.5 (3.0)	113.3 (4.7)	<b>11.10</b>	43.90	20.50	<b>50.00</b>	117.00	55.00	58.00	1	A	A	146%
98-045 L1	11/6/98	0820 to 0921	26.00	23.56 (4.88)	46.0 (4.1)	43.7 (2.9)	79.2 (3.3)	<b>9.60</b>	-59.50	14.80	<b>28.40</b>	NC	27.00	36.00	5	A	A	145%
98-046 R1	11/6/98	0929 to 1015	30.00	23.56 (20.94)	62.7 (4.5)	69.3 (3.7)	65.9 (3.9)	49.20	51.90	5931.00	164.00	180.00	5924.00	<b>35.00</b>	3	A	A	NC
98-046 M1	11/6/98	0929 to 1015	63.00	23.56 (20.94)	29.1 (2.0)	58.2 (2.7)	40.0 (1.8)	8.50	<b>11.30</b>	5.60	21.50	<b>28.00</b>	18.00	14.00	4	A	A	10%
98-046 L1	11/6/98	0929 to 1015	30.00	23.56 (20.94)	94.2 (5.8)	47.4 (3.3)	131.8 (6.3)	<b>5.80</b>	-0.60	6.70	<b>117.00</b>	NC	61.00	89.00	5	A	A	18%
98-047 D1	11/6/98	1015 to 1040	98.00	23.56 (20.94)	56.5 (5.1)	78.5 (3.8)	47.6 (3.1)	5.00	<b>20.50</b>	1.60	70.00	<b>32.40</b>	-2.80	7.60	4	A	A	9%
98-048 D1	11/6/98	1050 to 1115	123.00	23.56 (20.94)	56.8 (3.4)	164.5 (7.7)	243.3 (10.3)	<b>11.10</b>	12.20	15.60	<b>58.90</b>	57.00	54.00	64.00	1	A	B	8%
98-049 D1	11/6/98	1137 to 1347	56.00	23.56 (20.94)	12.5 (0.9)	95.0 (4.1)	96.9 (4.0)	<b>9.00</b>	9.10	8.00	<b>93.50</b>	100.40	73.00	107.00	1	A	B	9%
98-050 D1	11/6/98	1404 to 1450	34.00	17.37 (4.04)	44.9 (2.9)	74.5 (3.7)	114.8 (5.5)	<b>12.20</b>	16.50	22.40	<b>74.20</b>	80.00	81.00	74.00	1	A	B	8%
finish disc																		
96-111 I5	11/26/96	1240 to 1320	100.00	14.14 (20.0)	42.12 (2.68)	82.27 (4.17)	111.37 (6.09)	<b>13.22</b>	14.88	26.15	<b>124.29</b>	127.82	152.70	80.17	1	A	A	3%
96-112 I6	11/26/96	1330 to 1404	114.00	14.14 (20.0)	49.18 (3.73)	115.89 (5.71)	276.84 (13.04)	<b>9.26</b>	13.68	11.02	<b>142.35</b>	136.07	117.41	150.42	1	A	A	4%
96-113 I7	11/26/96	1518 to 1615	188.00	14.14 (20.0)	48.15 (3.65)	142.46 (6.36)	208.66 (9.39)	<b>11.48</b>	12.52	16.90	<b>97.53</b>	96.13	94.93	74.65	1	A	A	5%
96-117 D1	12/2/96	1655 to 1815	25.00	11.46 (2.13)	26.2 (2.0)	52.1 (2.7)	83.0 (3.6)	<b>11.20</b>	14.00	17.10	<b>91.00</b>	94.00	92.00	65.00	1	A	A	9%
96-118 D1	12/4/96	1041 to 1151	60.00	33.72 (2.18)	59.1 (3.0)	53.6 (2.9)	51.5 (2.6)	-17.80	-8.40	0.01	NC	NC	0.00	<b>9.20</b>	3	A	B	NC
96-119 D1	12/4/96	1237 to 1411	185.00	33.72 (2.18)	39.9 (2.2)	37.3 (2.1)	35.4 (1.9)	-2.50	-5.10	0.50	NC	NC	-0.03	<b>0.60</b>	3	D	B	NC
96-119 M1	12/4/96	1237 to 1411	77.00	33.72 (2.18)	40.4 (2.0)	46.6 (2.2)	43.9 (2.2)	16.50	17.50	26.20	6.60	7.50	6.50	<b>3.50</b>	3	A	B	NC
96-120 D1	12/5/96	1046 to 1200	70.00	30.64 (4.32)	29.2 (1.7)	32.4 (2.1)	25.5 (1.6)	4.90	<b>6.30</b>	3.90	-5.40	<b>-0.50</b>	-2.90	-5.60	4	D	A	NC
ripping																		
97-046	6/24/97	1342 to 1635	75.00	55.91 (20.94)	56.4 (2.3)	250.6 (10.3)	299.9 (12.0)	<b>10.00</b>	10.00	11.00	<b>765.00</b>	770.00	623.00	853.00	1	A	A	5%
97-050	6/26/97	0820 to 0950	233.00	48.07 (9.85)	60.8 (2.5)	161.1 (6.8)	205.9 (8.2)	<b>10.70</b>	10.90	13.10	<b>112.00</b>	110.00	97.00	130.00	1	A	A	5%
97-051	6/26/97	1000 to 1040	234.00	48.07 (9.85)	255.1 (11.0)	434.8 (18.0)	598.5 (24.1)	<b>14.70</b>	18.10	40.10	<b>776.00</b>	840.00	1109.00	651.00	1	A	A	3%
97-048	6/25/97	1231 to 1410	128.00	67.0 (15.01)	101.1 (4.2)	241.8 (10.2)	221.6 (8.8)	9.60	<b>9.50</b>	10.80	306.00	<b>331.00</b>	268.00	299.00	4	A	A	5%
97-049	6/25/97	1411 to 1551	68.00	67.0 (15.01)	239 (10.3)	167.7 (6.9)	396.3 (14.9)	<b>7.50</b>	-5.50	10.60	<b>577.00</b>	NC	502.00	696.00	5	A	A	6%
root cutting																		
96-103 D1	11/16/96	1008 to 1100	176.00	25.3 (4.67)	28.8 (2.5)	55.2 (3.2)	165.1 (5.1)	<b>8.70</b>	10.90	9.30	<b>30.00</b>	25.00	23.00	40.00	1	A	A	12%
96-104 D1	11/16/96	1249 to 1300	72.00	25.3 (4.67)	30.8 (2.0)	63.6 (2.9)	81.3 (3.7)	<b>10.70</b>	11.20	13.60	<b>36.00</b>	34.00	31.00	33.00	1	A	A	8%

Values in parentheses are uncertainties; NC = not calculated (unreasonable value).

Q<sub>UP</sub> = upwind qualifier; Q<sub>WD</sub> = wind direction qualifier; EFU = relative emission factor uncertainty = (calculated uncertainty/emission factor)100.

Plume heights and emission factors in **bold** type are the best-fit figures based on case.

**Table 5.16 Environmental conditions during land preparation tests.**

TestID	Date	Crop	Op	Wind DIR*	RH %	SolarRac Watt/m2	Bulk Ri	Temperature (deg C)				Wind Speed (m/s)				%Soil moist	%Silt Conten
								1m	2m	4m	7.5m	1m	2m	4m	7.5m		
95-118	10/27/95	Cotton	Disk	11.80	29.60	498.7	-0.028	25.2	25.5	24.5	24.3	1.81	1.85	2.03	2.14		
95-128	11/03/95	Cotton	Disk	346.50	61.62	358.9	-0.01	17.94	22.43	17.29	17.1	NA	2.68	NA	3.07	6.10	12.89
95-129	11/03/95	Cotton	Disk	2.70	53.61	348.93	-0.01	19.1	23.72	18.47	18.2	NA	3.22	NA	3.64		
95-130	11/03/95	Cotton	Disk	351.70	51.71	506.63	-0.01	20.13	25.35	19.2	19	NA	3.55	NA	4.12	5.70	12.89
95-131	11/03/95	Cotton	Disk	346.50	50.18	568.99	-0.01	20.51	26.76	19.66	19.4	NA	3.06	NA	3.51		
95-132	11/03/95	Cotton	Disk	346.30	47.7	510.65	-0.01	20.48	28.01	19.94	19.8	NA	3.24	NA	3.64	5.90	12.89
95-150	11/15/95	Cotton	Disk	353.2	57.83	0	0.34	16.19	18	19.41	20.6	0.45	0.93	1.40	1.65		
95-151	11/15/95	Cotton	Disk	2.1	58.25	0.04	0.55	15.69	18.38	19.41	20.3	0.45	0.75	1.00	1.16		
97-045	06/24/97	Wheat	Disk	324.31	30.72	874.89	0.52	27.86	26.19	26.29	26	2.684	2.947	3.335	3.5	2.32	17.90
98-045R	11/06/98	Cotton	Disk	11.43	63.68	352.44	1.16	11.62	11.29	11.19	11.1	1.707	1.91	1.676	2.07	12.95	7.00
98-045L	11/06/98	Cotton	Disk	11.43	63.68	352.44	1.16	11.62	11.29	11.19	11.1	1.707	1.91	1.676	2.07	12.95	7.00
98-046R	11/06/98	Cotton	Disk	338.75	52.26	480.94	1.22	14.33	13.13	13.02	12.8	1.906	2.107	2.19	2.34	12.95	7.00
98-046M	11/06/98	Cotton	Disk	338.75	52.26	480.94	1.22	14.33	13.13	13.02	12.8	1.906	2.107	2.19	2.34	12.95	7.00
98-046L	11/06/98	Cotton	Disk	338.75	52.26	480.94	1.22	14.33	13.02	13.02	12.8	1.906	2.107	2.19	2.34	12.95	7.00
98-047	11/06/98	Cotton	Disk	317.6	49.13	483.6	2.5	15.68	14.18	13.96	13.7	1.691	1.925	2.038	2.17	12.95	7.00
98-048	11/06/98	Cotton	Disk	312.12	46.45	381.61	0.45	16.04	14.85	14.63	14.4	2.709	3.083	3.451	3.59	12.95	7.00
98-049	11/06/98	Cotton	Disk	312.12	43.67	382.21	0.2	17.21	16.38	16.11	15.8	3.538	3.958	4.442	4.62	11.50	2.30
98-050	11/06/98	Cotton	Disk	309.50	41.17	246.51	0.16	18.3	17.65	17.43	17.1	3.688	4.198	4.706	4.93	11.50	2.30
Finish Disc																	
96-111	11/26/96	Cotton	Disk	1.70	59.8	593.2	0.1	15.5	14.7	14.7	14.3	3.42	3.82	5.7	5.6	20.80	
96-112	11/26/96	Cotton	Disk	352	58.8	516.9	0.1	15.8	15	15	14.7	3.1	3.4	4.75	5.14	20.80	
96-113	11/26/96	Cotton	Disk	359.4	66.7	142.8	0.1	15	14.5	14.8	14.7	2.02	2.28	3.34	3.41	20.80	
96-117	12/02/96	Cotton	Disk	347.01	79.82	0.18	-2.39	7.26	7.35	8.31	8.9	0.896	1.266	1.998	2.16	18.15	
96-118	12/04/96	Cotton	Disk	134.18*	72.44	566.62	0.51	11.16	10.14	10.04	9.9	2.522	2.792	3.141	3.24	18.00	
96-119	12/04/96	Cotton	Disk	119.6*	59.78	454.29	0.39	13.35	12.43	12.43	12.3	2.484	2.702	3.002	3.13	16.25	20.00
96-119M	12/04/96	Cotton	Disk	119.6*	59.78	454.29	0.39	13.35	12.43	12.43	12.3	2.484	2.702	3.002	3.13	16.25	20.00
96-120	12/05/96	Cotton	Disk	140.27*	80.04	72.52	-0.02	11.3	10.97	11.44	11.5	4.098	4.649	5.498	5.92	16.65	14.50
97-046	06/24/97	Wheat	Rip	358.26	22.49	893.47	0.19	33.11	31.08	31.28	30.9	3.036	3.444	3.884	4.11	2.32	
97-050	06/26/97	Wheat	Rip	317.45	40.45	586.59	0.36	25.21	23.71	24.17	23.9	1.994	2.113	2.404	2.45	2.21	
97-051	06/26/97	Wheat	Rip	331.62	36.92	806.5	0.41	27.72	25.62	26.32	26.1	2.008	2.174	2.475	2.49	2.21	
97-048	06/25/97	Wheat	Rip	347.78	23.34	799.46	0.26	34.39	32.37	32.44	32.1	2.601	2.928	3.303	3.43	2.21	
97-049	06/25/97	Wheat	Rip	358.83	21.62	915.05	0.17	35.49	33.7	33.66	33.4	3.016	3.435	3.91	4.13	2.21	
96-103	11/16/96	Cotton	Root c	139.21*	53.93	585.39	0.6	14.96	14.11	13.84	13.5	1.79	2.118	2.629	2.83	12.20	27.00
96-104	11/16/96	Cotton	Root c	141.97*	46.58	371.9	0.26	16.95	16.12	16.08	15.8	2.076	2.54	3.359	3.67	12.20	27.00
96-114	11/27/96	Cotton	Root c	58.24	91.77	479.03	1.37	10.6	9.93	10.08	10	1.229	1.259	1.366	1.43	19.80	

\*best wind = 315 °; \*\* = best wind = 90 °; otherwise, best wind = 360 °

**Table 5.17 Emission factors and uncertainties for cultivation**

TestID	date	time	Xloc (m)	Upwind	RCMA (ug m-3)			Plume height (m)			Emission Factor (mg m-2)				case	Qup	Qwd	EFU			
					9m	3m	1m	Linear	Block	Log	Linear	Block	Log	Box							
weeding																					
98-001 D1	6/4/98	0905 to 1026	26.00	20.90	34.99	25.36	(6.04)	(2.09)	(1.21)	32.31 (1.4)	<b>-0.86</b>	-1.10	1.47	NC	NC	-5.71	<b>18.33</b>	3	A	A	NC
98-001 I1	6/4/98	0905 to 1026	26.00	20.90	38.8	27.12	(6.04)	(2.07)	(1.36)	(1.55)	-2.77	-0.73	0.83	NC	NC	-1.43	<b>18.55</b>	3	A	A	NC
98-002 D1	6/4/98	1026 to 1205	71.00	20.90	21.96	35.12	(6.04)	(1.05)	(1.66)	(1.55)	<b>10.21</b>	9.90	13.47	<b>27.85</b>	28.92	26.01	21.73	1	A	B	17%
98-002 I2	6/4/98	1026 to 1205	26.00	20.90	30.59	33.03	(6.04)	(1.86)	(1.43)	(1.4)	42.20	37.81	10105.50	74.25	68.71	4642.90	<b>18.30</b>	3	A	B	NC
98-003 D1	6/4/98	1231 to 1429	122.00	20.16	34.46	26.51	(5.16)	(1.5)	(1.21)	(1.27)	-4.25	-1.93	0.39	NC	NC	-0.31	<b>9.40</b>	3	A	B	NC
98-003 I3	6/4/98	1231 to 1429	29.00	20.16	31.17	24.27	(5.16)	(1.52)	(1.09)	(1.09)	-3.54	-1.17	0.59	NC	NC	-0.38	<b>7.29</b>	3	A	B	NC
98-004 D1	6/4/98	1231 to 1429	161.00	20.16	38.42	74.52	(5.16)	(1.73)	(3.38)	(5.82)	<b>8.72</b>	11.07	11.83	<b>248.03</b>	243.54	230.98	325.31	1	A	B	23%
98-004 I4	6/4/98	1231 to 1429	14.00	20.16	43.66	38.59	(5.16)	(3.2)	(1.74)	(3.18)	<b>9.05</b>	-22.44	13.28	<b>147.57</b>	NC	131.25	162.63	5	A	B	22%
98-005 D1	6/5/98	0834 to 0929	294.00	15.28	38.08	61.31	15.28	40.86	44.29	70.4	<b>16.13</b>	15.41	53.76	<b>329.03</b>	324.74	555.04	191.00	5	A	A	5%
98-005 I5	6/5/98	0834 to 0929	20.00	15.28	40.86	44.29	(2.86)	(3.87)	(2.28)	(3.03)	<b>12.66</b>	62.21	32.74	<b>256.54</b>	784.56	347.09	212.59	1	A	A	5%
98-007 I7	6/5/98	1133 to 1301	79.00	15.28	29.58	46.82	(2.86)	(1.31)	(1.99)	(2.78)	<b>12.91</b>	15.81	25.57	<b>107.77</b>	112.03	121.05	93.84	1	A	A	8%
98-008 I8	6/5/98	1308 to 1442	80.00	24.55	33.57	56.74	(4.75)	(1.53)	(2.33)	(2.94)	<b>12.19</b>	12.72	19.20	<b>68.38</b>	67.78	66.92	61.68	1	A	B	16%
98-009 I9	6/5/98	1450 to 1625	95.00	24.55	49.5	44.81	(4.75)	(1.95)	(1.99)	(3.33)	<b>9.64</b>	-27.23	16.30	<b>76.10</b>	NC	73.91	77.06	5	A	B	15%
98-010 IA	6/6/98	0755 to 0922	36.00	21.96	26.98	27.33	(6.71)	(1.28)	(1.48)	(1.68)	<b>8.61</b>	110.47	10.39	<b>31.54</b>	129.46	25.92	38.22	1	B	A	9%
98-011 IB	6/6/98	0932 to 1136	91.00	21.96	24.29	30.01	(6.71)	(1.21)	(1.33)	(1.89)	<b>8.85</b>	12.86	9.89	<b>37.36</b>	33.11	30.36	48.29	1	A	A	12%

Values in parentheses are uncertainties; NC = not calculated (unreasonable value).

Q<sub>UP</sub> = upwind qualifier; Q<sub>WD</sub> = wind direction qualifier; EFU = relative emission factor uncertainty = (calculated uncertainty/emission factor)100.

Plume heights and emission factors in **bold** type are the best-fit figures based on case.

**Table 5.18 Environmental conditions during cultivation tests**

TestID	Date	Crop	Op	Wind DIR*	RH %	SolarRac Watt/m2	Bulk Ri	Temperature (deg C)				Wind Speed (m/s)				%Soil moist	%Silt Conten
								1m	2m	4m	7.5m	1m	2m	4m	7.5m		
Weeding																	
98-001	06/04/98	Cotton	Weedi	343.1	59.5	676.1	0.4	18.4	18.2	17.6	17.3	2.42	2.56	2.75	2.82	8.85	3.01
98-002	06/04/98	Cotton	Weedi	352.4	51.2	834.1	0.8	20.5	20.2	19.6	19.3	2.07	2.14	2.31	2.33	9.80	3.01
98-003	06/04/98	Cotton	Weedi	320.4	40	762.3	0.6	23.5	23.6	22.5	22.2	2.15	2.26	2.37	2.43	17.90	4.10
98-004	06/04/98	Cotton	Weedi	320.4	40	762.3	0.6	23.5	23.6	22.5	22.2	2.15	2.26	2.37	2.43	2.60	3.01
98-005	06/05/98	Cotton	Weedi	335.3	65.3	507.2	0.1	18.3	17.9	17.4	17.1	3.85	4.15	4.58	4.85	7.30	3.52
98-007	06/05/98	Cotton	Weedi	334	45.2	762.8	0.2	24.3	23.8	23.2	22.8	3.24	3.47	3.73	3.85	4.80	3.50
98-008	06/05/98	Cotton	Weedi	328.8	38.4	673.1	0.5	26	26.6	25.1	24.7	2.34	2.5	2.69	2.71	6.45	3.50
98-009	06/05/98	Cotton	Weedi	343.3	37.3	537.8	0.3	26.8	26.9	25.9	25.7	2.68	2.89	3.06	3.16	3.60	3.50
98-010 IA	06/06/98	Cotton	Weedi	330	69.2	496.9	0.2	18.2	17.6	17.4	17.2	3.5	3.79	4.06	4.26	5.05	4.00
98-011 IB	06/06/98	Cotton	Weedi	337.2	53.1	662.9	0.2	22.2	22.3	21.2	20.8	3.07	3.26	3.58	3.7		

\*best wind = 315 °; \*\* = best wind = 90 °; otherwise, best wind = 360 °

## **5.5 PM from confined cattle facilities**

Emission factors of PM<sub>10</sub> from open lot dairies were calculated from measurements made downwind of a single facility in October and April (Table 5.19). The PM<sub>10</sub> emission factor was highly influenced by relative humidity, with the highest measured emission factor coincident with the lowest relative humidity. The facility where these measurements were made did not have free stalls for any of the cows. With the exception of young heifers (<500 lbs), all animals were housed in open lots with paved, flushed feed lanes and free-standing shade structures. Highest production cows were misted with water at the feed lanes during high temperature episodes. No dust control measures were in use at the dairy during either sampling period and an unpaved road used by dairy personnel ran between the cow enclosures and the downwind sampling array.

Emission factors of PM<sub>10</sub> from large feedlots were calculated from measurements made downwind of a feedlot in both winter and summer seasons (Table 5.21). PM from the feedlot was also highly influenced by relative humidity, but the lowest measured relative humidity was not coincident with the highest emission factor, probably because that measurement was made in March, when the ground surface was relatively wet. During the July sampling period water trucks were used for dust control in all of the animal enclosures and on the unpaved portions of roads surrounding the feedlot.

**Table 5.19 Best fit PM<sub>10</sub> emission factors from open lot dairies**

TestID	date	time	Xloc (m)	RCMA (ug m-3)				Plume height (m)			Emission Factor (mg m-2)				case	Qup	Qwd	EFU	E. Factor lbs per 1000hd*d
				Upwind	9m	3m	1m	Linear	Block	Log	Linear	Block	Log	Box					
Dairy																			
95-075	10/03/95	1500 to 1701	220.00	101.6 (20.8)	113.4 (6.8)	191.0 (11.2)	81.3 (5.1)	4.30	<b>9.90</b>	2.60	-684.50	<b>31.37</b>	-10.57	7.88	4	B	A	15%	48.29
95-076	10/03/95	1746 to 2003	130.00	80.1 (11.3)	224.0 (12.9)	791.8 (44.8)	1169.5 (69.6)	<b>9.90</b>	10.52	13.30	<b>223.14</b>	217.81	207.54	30.82	1	A	A	19%	255.01
95-077	10/03/95	2021 to 2301	130.00	138.3 (45.9)	97.8 (5.7)	109.4 (6.5)	419.0 (25.5)	<b>5.50</b>	-11.90	4.40	<b>20.01</b>	NC	12.29	-2.07	1	C	C	109%	26.62
95-077	10/03/95	2021 to 2301	220.00	138.3 (45.9)	133.9 (7.6)	391.1 (22.3)	195.1 (10.8)	<b>5.90</b>	8.90	3.60	<b>25.66</b>	36.85	25.82	7.43	5	A	C	108%	34.14
95-078	10/04/95	1358 to 1700	220.00	290.2 (59.9)	330.9 (18.6)	430.1 (24.3)	503.1 (30.0)	<b>8.90</b>	9.40	10.20	<b>35.60</b>	33.58	29.69	5.16	1	A	C	33%	27.86
95-086	10/06/95	1600 to 1700	220.00	105.9 (18.8)	233.0 (14.6)	346.2 (21.4)	142.0 (9.3)	3.40	<b>15.70</b>	1.60	-15.00	<b>87.65</b>	-2.33	10.16	4	A	A	5%	272.12
95-089	10/07/95	1245 to 1452	140.00	108.9 (24.7)	154.1 (9.4)	225.0 (13.2)	209.6 (12.3)	13.10	<b>12.80</b>	20.40	-10.93	<b>64.88</b>	63.22	10.29	4	A	A	14%	95.16
95-090	10/07/95	1600 to 1800	220.00	163.6 (20.0)	284.2 (16.6)	406.1 (23.2)	512.0 (29.3)	<b>12.70</b>	14.90	29.40	<b>150.05</b>	161.59	221.24	17.72	1	A	A	8%	232.93
96-024	4/19/96	1330 to 1635	128.00	13.24 (0.00)	30.48 (1.5)	64.53 (3.66)	78.4 (3.81)	<b>13.19</b>	13.54	23.77	<b>62.61</b>	62.48	66.54	51.86	1	A	A	8%	63.04
96-025	4/19/96	1647 to 2000	128.00	43.51 (0.00)	43.2 (1.89)	66.29 (3.37)	99.34 (4.2)	<b>8.67</b>	9.91	8.94	<b>36.80</b>	31.15	29.12	48.28	1	A	A	13%	30.20
96-026	4/20/96	0322 to 0538	128.00	17.5 (0.00)	13.8 (0.92)	27.18 (2.01)	64.88 (3.04)	<b>7.32</b>	8.06	6.51	<b>6.12</b>	3.89	4.20	8.14	1	A	A	100%	8.38
96-027	4/20/96	0830 to 1213	128.00	12.37 (0.00)	17.21 (0.93)	53.73 (2.66)	106.37 (4.5)	<b>9.18</b>	10.93	10.22	<b>55.75</b>	49.51	45.57	73.99	1	A	B	18%	52.72
96-028	4/20/96	1213 to 1455	128.00	12.37 (0.00)	22.49 (1.2)	33.02 (1.48)	81.64 (3.89)	<b>8.59</b>	16.73	9.61	<b>29.45</b>	27.45	23.77	39.31	1	A	B	13%	33.86
96-029	4/20/96	1600 to 1900	128.00	37.34 (0.00)	29.56 (1.38)	63.07 (2.63)	113.04 (4.95)	<b>7.87</b>	8.37	7.25	<b>489.35</b>	387.45	377.49	730.22	1	A	A	9%	506.41
96-030	4/20/96	1935 to 0000	128.00	15.67 (0.00)	15.84 (0.93)	28.3 (1.33)	45.25 (2.06)	<b>8.84</b>	10.10	9.29	<b>22.53</b>	19.29	17.71	27.44	1	A	A	22%	15.26
96-031	4/21/96	0000 to 0200	128.00	15.67 (0.00)	13.86 (1.13)	22.91 (1.53)	44.2 (2.08)	<b>7.61</b>	8.60	6.98	<b>3.63</b>	2.48	2.49	4.79	1	A	A	17%	5.63
96-033	4/21/96	1455 to 1915	128.00	57.35 (0.00)	46.08 (2.03)	77.57 (3.42)	250.15 (11.51)	<b>6.90</b>	7.49	5.94	<b>133.26</b>	77.26	99.38	217.46	1	A	A	13%	88.65
96-034	4/21/96	1915 to 2133	128.00	43.47 (0.00)	56.6 (2.53)	147.23 (5.95)	314.08 (12.75)	<b>8.81</b>	11.01	9.50	<b>38.92</b>	33.08	29.34	45.33	1	A	A	26%	52.53
96-037	4/22/96	1630 to 2000	128.00	35.73 (0.00)	70.4 (2.89)	124.27 (5.01)	174.85 (6.94)	<b>12.24</b>	14.51	21.36	<b>98.98</b>	100.50	103.79	89.24	1	A	A	11%	87.80
96-038	4/22/96	2000 to 2247	128.00	110.89 (0.00)	38.23 (1.69)	186.88 (7.54)	316.55 (12.53)	<b>6.94</b>	6.58	5.53	<b>14.10</b>	10.05	7.73	24.61	1	A	A	14%	15.73
96-039	4/23/96	0007 to 0202	128.00	47.62 (0.00)	47.6 (2.19)	70.06 (3.2)	99.98 (4.37)	<b>8.81</b>	9.99	9.21	<b>-7.00</b>	-5.94	-5.38	-7.97	1	A	C	42%	-20.06
96-040	4/23/96	0202 to 0405	128.00	47.62 (0.00)	43.47 (2.04)	48.11 (2.22)	88.06 (3.9)	<b>6.41</b>	3.74	5.21	<b>-2.37</b>	-1.01	-1.50	-3.62	1	A	C	32%	-3.59
96-043	4/23/96	1915 to 2330	128.00	54.81 (0.00)	46.49 (1.97)	115.61 (5.02)	225.79 (8.97)	<b>8.19</b>	9.16	7.93	<b>56.98</b>	44.02	40.57	71.21	1	A	A	28%	41.63
96-042	4/23/96	1605 to 1915	128.00	57.41 (0)	60.8 (2.6)	144.73 (5.89)	255.47 (10.66)	<b>8.98</b>	10.28	9.61	<b>139.11</b>	121.52	112.20	180.40	1	A	A	7%	136.39
96-046	4/24/96	1250 to 1630	128.00	89.27 (0.00)	56.49 (2.42)	62.99 (2.63)	5.36 (0.49)	8.89	<b>-25.30</b>	12.36	-75.27	NC	-65.47	-85.29	4	C	C	NC	
96-047	4/24/96	1715 to 2000	128.00	44.33 (0.00)	62.7 (2.89)	121.92 (5.05)	24.72 (1.48)	4.45	<b>12.17</b>	2.50	-200.10	<b>86.24</b>	-40.15	-21.11	4	A	A	7%	119.00
96-048	4/24/96	2000 to 2350	128.00	26.6 (0.00)	26.27 (1.33)	58.47 (2.51)	6.84 (0.54)	4.62	<b>9.93</b>	2.93	-1042.23	<b>188.11</b>	-192.32	-156.04	4	B	B	9%	152.35

Values in parentheses are uncertainties; NC = not calculated (unreasonable value).

Q<sub>UP</sub> = upwind qualifier; Q<sub>WD</sub> = wind direction qualifier; EFU = relative emission factor uncertainty = (calculated uncertainty/emission factor)100.

Plume heights and emission factors in **bold** type are the best-fit figures based on case.

**Table 5.20 Environmental conditions during dairy tests.**

TestID	Date	Wind DIR	RH %	Solar Rad Watt/m2	Bulk Ri	Temperature (deg C)				Wind Speed (m/s)			
						1 m	2 m	4 m	7.5 m	1 m	2 m	4 m	7.5 m
95-075	10/3/95	319.1	21.60	468.776	-0.023	32.422	32.70	31.594	31.372	1.909	2.090	2.337	2.540
95-076	10/3/95	347.5	43.21	23.544	0.353	23.326	25.95	25.798	27.218	0.844	0.985	1.202	1.707
95-077	10/3/95	58.2	65.27	0.006	0.354	16.603	18.79	19.524	21.965	0.610	0.891	1.193	1.578
95-078	10/4/95	221.1	29.74	523.650	-0.047	26.228	26.11	25.155	24.914	1.180	1.372	1.550	1.634
95-086	10/6/95	345.4	16.34	362.667	-0.013		30.66	29.642	29.463	2.142	2.348	2.542	2.780
95-089	10/7/95	262.4	30.91	685.608	-0.035		26.70	25.471	25.150	1.581	1.892	2.257	2.516
95-090	10/7/95	329.6	27.72	240.292	-0.017		28.30	27.368	27.258	1.926	2.118	2.390	2.741
96-024	4/19/96	340.22	34.99	NA	0.20	18.65	18.94	17.89	17.67	2.98	3.09	3.32	3.52
96-025	4/19/96	340.63	37.07	NA	0.00	17.72	18.25	17.56	17.52	3.08	3.31	3.65	3.96
96-026	4/20/96	5.77	92.61	NA	-7.89	4.97	6.23	6.65	7.64	0.82	1.12	1.46	1.29
96-027	4/20/96	350.65	63.09	NA	1.63	13.63	13.95	12.9	12.7	2.32	2.41	2.34	2.71
96-028	4/20/96	322.24	39.53	NA	0.33	17.45	17.67	16.49	16.2	2.88	2.97	3.19	3.37
96-029	4/20/96	340.46	32.31	NA	0.12	18.15	18.48	17.48	17.28	3.79	4.00	4.35	4.63
96-030	4/20/96	334.46	62.69	NA	-2.86	11.78	12.62	12.34	12.55	2.52	2.87	3.06	3.76
96-031	4/21/96	323.25	83.09	NA	-5.65	7.98	8.96	8.98	9.39	1.14	1.40	1.57	2.24
96-033	4/21/96	350.64	34.85	NA	0.17	19.99	20.35	19.33	19.12	2.86	3.00	3.25	3.44
96-034	4/21/96	351.38	52.55	NA	-21.15	14.73	16.22	15.98	16.58	0.80	0.93	0.94	1.55
96-037	4/22/96	346.25	34.69	NA	-1.90	23.62	24.37	23.49	23.43	2.04	2.20	2.29	2.60
96-038	4/22/96	342.47	66.53	NA	-36.30	15.7	17.22	17.39	18.89	0.49	0.66	0.45	0.98
96-039	4/23/96	183.99	83.96	NA	-11.33	11.92	13.05	13.05	13.95	0.86	1.13	1.08	1.47
96-040	4/23/96	158.46	89.57	NA	-21.18	9.74	10.98	11.3	12.24	0.51	0.65	0.71	0.98
96-042	4/23/96	355.83	28.6	NA	0.08	28.59	29.15	28.03	27.82	3.121	3.298	3.5	3.836
96-043	4/23/96	347.35	52.91	NA	-15.57	20.13	21.68	22.04	22.81	1.09	1.36	1.36	2.08
96-046	4/24/96	352.65	37.72	NA	0.23	26.7	26.9	25.72	25.4	3.09	3.21	3.34	3.68
96-047	4/24/96	348.35	40.11	NA	0.02	26.59	27.21	26.28	26.16	4.42	4.74	5.17	5.64
96-048	4/24/96	345.4	61.1	NA	-0.03	20.66	21.39	20.88	20.98	3.85	4.19	4.65	5.15

\*best wind = 315 °; \*\* = best wind = 90 °; otherwise, best wind = 360 °

**Table 5.21 Best fit PM<sub>10</sub> emission factors from feedlots**

TestID	date	time	Xloc (m)	RCMA (ug m-3)				Plume height (m)			Emission Factor (mg m-2)				case	Qup	Qwd	EFU	E. Factor lbs per 1000hd*d
				Upwind	9m	3m	1m	Linear	Block	Log	Linear	Block	Log	Box					
96-003 D1	3/27/96	1800 to 1920	440.00	65.76 (0.00)	244.28 (11.01)	896.76 (39.67)	558.58 (25.18)	9.93	<b>11.92</b>	7.58	-2.89	<b>-3.77</b>	-2.09	-1.57	4	A	B	39%	-2.08
96-006 D1	3/29/96	1307 to 1700	440.00	20.82 (0.00)	42.22 (1.88)	99.22 (4.43)	94.89 (4.13)	12.96	<b>12.63</b>	18.35	20.96	<b>21.98</b>	19.63	13.79	4	A	B	13%	5.19
96-007 D1	3/29/96	1700 to 1919	440.00	20.82 (0.00)	48.23 (2.29)	128.6 (5.71)	91.93 (4.02)	10.91	<b>12.39</b>	9.45	2.02	<b>2.52</b>	1.48	1.09	4	A	B	60%	0.80
96-013 D1	3/30/96	1144 to 1554	440.00	21.38 (0.00)	56.36 (2.33)	102.82 (4.4)	93.77 (3.91)	15.80	<b>15.27</b>	30.52	29.66	<b>31.10</b>	33.83	15.38	4	A	A	8%	5.49
96-020 D1	3/31/96	1350 to 1633	440.00	7.9 (0.00)	60.65 (2.56)	159.62 (6.79)	178.19 (7.63)	<b>13.99</b>	13.73	26.39	<b>22.76</b>	22.83	25.25	16.00	1	A	B	17%	7.33
96-021 D2	3/31/96	1948 to 2347	376.50	6.02 (0.00)	47.75 (2.03)	194.34 (7.7)	165.03 (6.66)	11.93	<b>11.99</b>	13.76	24.04	<b>26.60</b>	20.08	14.99	4	A	C	125%	6.49
96-022 D2	3/31/96	2347 to 0205	376.50	6.02 (0.00)	45.52 (2.09)	316.83 (12.07)	367.29 (14.84)	<b>11.13</b>	11.02	13.68	<b>41.81</b>	42.54	35.93	32.04	1	A	A	25%	13.19
96-023 D2	4/1/96	0205 to 0357	376.50	6.02 (0.00)	71.88 (3.07)	220.82 (8.77)	165.44 (7.06)	12.32	<b>13.10</b>	13.12	28.30	<b>33.60</b>	22.39	14.45	4	A	A	15%	13.25
96-073 D1	7/27/96	2203 to 0017	400.00	171.98 (0.00)	257.13 (10.15)	436.28 (17.93)	432.83 (16.83)	11.21	<b>10.75</b>	17.12	28.32	<b>29.36</b>	29.99	16.54	4	A	A	10%	9.60
96-073 I1	7/27/96	2203 to 0017	400.00	171.98 (0.00)	155.62 (6.56)	302.61 (12.84)	496.12 (20.00)	<b>8.41</b>	9.22	8.28	<b>19.36</b>	15.53	13.83	20.55	1	A	A	12%	6.33
96-074 D1	7/28/96	0154 to 0340	400.00	47.8 (0.00)	244.85 (10.81)	424.76 (17.91)	454.98 (17.64)	<b>14.76</b>	14.00	47.06	<b>32.43</b>	31.65	65.59	13.85	1	A	A	19%	19.35
96-074 I1	7/28/96	0154 to 0340	400.00	47.8 (0.00)	130.8 (5.87)	250.43 (10.37)	435.94 (17.72)	<b>10.93</b>	14.86	16.40	<b>18.45</b>	19.69	18.37	13.20	1	A	A	22%	11.00
96-078 D1	7/29/96	0109 to 0505	400.00	32.32 (0.00)	333.25 (12.99)	341.55 (13.23)	597.44 (21.68)	<b>11.23</b>	198.60	33.83	<b>39.64</b>	770.22	75.34	26.80	1	A	A	28%	9.51
96-076 I1	7/28/96	1245 to 1810	455.50	40.19 (0.00)	193.41 (8.3)	273.14 (11.12)	182.78 (7.13)	8.06	<b>23.45</b>	2.22	114.86	<b>239.64</b>	-55.25	55.51	4	A	A	6%	31.58
96-075 D1	7/28/96	0505 to 0703	400.00	47.8 (0.00)	320.83 (13.03)	365.06 (15.99)	414.96 (16.77)	<b>28.41</b>	40.66	3720.49	<b>102.02</b>	146.73	6359.11	25.96	1	A	A	23%	72.64
96-075 I1	7/28/96	0505 to 0703	400.00	47.8 (0.00)	235.1 (9.63)	339.31 (13.33)	418.54 (16.8)	<b>18.82</b>	22.58	107.11	<b>60.91</b>	69.36	191.55	26.22	1	A	A	23%	43.37
96-079 D1	7/29/96	0310 to 0505	400.00	32.32 (0)	333.25 (12.99)	341.55 (13.23)	597.44 (21.68)	<b>12.08</b>	226.54	37.30	<b>31.35</b>	654.29	60.22	21.97	1	A	A	15%	21.29
96-080 D1	7/29/96	1709 to 1946	455.50	24.51 (0.00)	10.81 (0.73)	891.39 (32.16)	549.14 (20.53)	7.13	<b>8.17</b>	5.53	92.70	<b>109.73</b>	79.52	73.89	4	A	A	10%	30.85
96-082 D1	7/29/96	2322 to 0123	400.00	32.54 (0.00)	289.09 (11.49)	646.1 (25.96)	662.37 (24.69)	<b>12.72</b>	12.02	25.89	<b>37.50</b>	37.51	51.16	18.12	1	A	C	77%	13.79
96-084 I1	7/30/96	1510 to 1746	455.50	34.12 (0.00)	217.15 (9.24)	476.89 (18.03)	312.8 (13.32)	11.51	<b>14.93</b>	8.68	64.66	<b>85.86</b>	48.51	35.55	4	A	B	4%	24.30
96-087 I1	7/30/96	2235 to 0009	455.50	64.54 (0)	353.66 (14.38)	809.14 (30.68)	501.88 (20.0)	10.58	<b>14.44</b>	7.17	44.94	<b>70.28</b>	26.75	16.23	4	A	A	41%	36.08
96-088 D1	7/31/96	1134 to 1352	455.50	54.77 (0.00)	559.37 (21.68)	613.49 (24.11)	335.87 (13.1)	-2.44	<b>57.20</b>	0.24	NC	<b>518.24</b>	-0.53	40.83	4	A	A	5%	165.79
96-088 I1	7/31/96	1134 to 1352	455.50	54.77 (0.00)	275.71 (11.5)	384.3 (15.44)	338.21 (14.02)	23.86	<b>24.24</b>	102.27	115.85	<b>126.41</b>	233.00	41.16	4	A	A	5%	40.44
96-089 D1	7/31/96	1450 to 1640	455.50	54.77 (0.00)	300.73 (12.44)	197.03 (9.53)	679.86 (25.85)	<b>6.85</b>	-4.20	8.48	<b>59.22</b>	NC	49.86	77.01	5	A	B	7%	37.35
96-089 I1	7/31/96	1450 to 1640	455.50	54.77 (0.00)	280.09 (11.2)	202.08 (8.27)	239 (9.76)	<b>-12.44</b>	-10.22	0.15	NC	NC	-0.09	22.70	5	A	B	NC	NC
96-090 D1	7/31/96	1643 to 1845	455.50	52.96 (0.00)	318.75 (12.7)	600.77 (24.12)	495.84 (19.72)	12.86	<b>13.20</b>	18.87	96.93	<b>107.39</b>	95.70	58.30	4	A	A	5%	38.86
96-090 I1	7/31/96	1643 to 1845	455.50	52.96 (0.00)	404.07 (16.00)	498.48 (20.11)	487.06 (19.16)	40.33	<b>36.03</b>	5759.29	266.14	<b>245.74</b>	12587.09	57.15	4	A	A	4%	88.92

Values in parentheses are uncertainties; NC = not calculated (unreasonable value).

Q<sub>UP</sub> = upwind qualifier; Q<sub>WD</sub> = wind direction qualifier; EFU = relative emission factor uncertainty = (calculated uncertainty/emission factor)100.

Plume heights and emission factors in **bold** type are the best-fit figures based on case.

**Table 5.22 Environmental conditions during feedlot tests.**

TestID	Date	Wind DIR	RH %	Solar Rad Watt/m2	Bulk Ri	Temperature (deg C)				Wind Speed (m/s)			
						1 m	2 m	4 m	7.5 m	1 m	2 m	4 m	7.5 m
96-003	3/27/96	48.42 *	43.99	NA	-0.44	16.67	17.48	17.00	17.65	1.64	1.80	2.20	2.52
96-006	3/29/96	340.48 *	33.6	NA	0.43	17.45	17.90	16.75	16.54	2.17	2.44	2.68	2.97
96-007	3/29/96	37.12 *	47.45	NA	-0.18	14.15	14.78	14.08	14.26	1.97	2.26	2.63	3.09
96-013	3/30/96	336.48 *	29.55	NA	0.33	20.89	21.25	19.91	19.66	2.23	2.50	2.82	3.04
96-020	3/31/96	348.69 *	16.87	NA	0.51	25.54	26.24	24.85	24.65	1.69	1.83	2.02	2.16
96-021	3/31/96	21.68 **	46.47	NA	-0.67	15.78	16.44	15.99	16.25	2.29	2.58	2.97	3.53
96-022	3/31/96	61.06 **	56.89	NA	-3.14	10.83	11.55	11.41	12.49	1.57	1.85	1.93	2.80
96-023	4/1/96	54.87 **	58.74	NA	-0.89	10.54	11.20	11.17	12.54	2.12	2.44	2.91	3.61
96-073	7/27/96	72.47 **	45.83	-0.05	-0.81	26.67	26.56	27.54	28.17	1.03	1.27	1.80	2.25
96-074	7/28/96	63.43 **	52.91	-0.05	-3.63	23.69	23.98	25.20	25.96	0.74	0.91	1.33	1.71
96-075	7/28/96	104.49 **	50.43	16.11	-0.69	24.50	24.34	25.13	25.45	1.28	1.29	1.71	2.27
96-076	7/28/96	320.96	22.48	723.06	0.09	37.68	39.21	36.57	36.16	3.64	3.95	4.40	4.87
96-078	7/29/96	68.53 **	42.58	-0.05	-2.35	25.50	25.60	26.71	27.33	0.87	1.02	1.43	1.89
96-079	7/29/96	114.44 **	45.87	-0.03	-3.28	24.94	25.12	26.17	26.72	0.77	0.77	1.01	1.48
96-080	7/29/96	323.25	24.32	252.11	0.06	37.79	39.92	37.31	37.08	2.64	2.87	3.18	3.60
96-082	7/29/96	36.74 **	42.91	-0.05	-1.59	27.70	27.61	29.04	29.84	0.82	1.03	1.52	1.98
96-084	7/30/96	300.47	24.85	598.9	0.08	39.07	40.88	37.94	37.55	3.80	4.04	4.35	4.55
96-088	7/31/96	317.92	21.52	893.56	0.13	37.58	39.48	36.35	35.86	3.34	3.59	3.91	4.23
96-089	7/31/96	310.03	21.78	736.12	0.08	39.49	40.89	38.29	37.81	4.114	4.433	4.807	5.142
96-090	7/31/96	321.61	24.82	387.41	0.07	39.43	41.20	38.69	38.38	3.25	3.53	3.93	4.32

\*best wind = 315 °; \*\* = best wind = 90 °; otherwise, best wind = 360 °

## 5.6 Ammonia from confined cattle facilities

Ambient PM<sub>10</sub> measurements in California's San Joaquin Valley frequently exceed state and federal PM<sub>10</sub> air quality standards. During the winter months, a large fraction of the PM<sub>10</sub> is attributed to secondary particles, including ammonium nitrate and ammonium sulfate. These particles are formed in the atmosphere by chemical reactions between ammonia gas and SO<sub>2</sub> and NO<sub>x</sub> gases. They are also primarily in the PM<sub>2.5</sub> size range, and may lead to violations of the recently promulgated fine particle standard.

Although it is believed that up to 60% of the total ammonia emissions result from livestock facilities, including large dairies and feedlots, there is little experimental data to verify it. We have conducted several field studies on dairies and feedlots in the San Joaquin Valley to measure the concentrations of ammonia upwind and downwind. The results of these field studies have been used to estimate the emissions of ammonia from a large dairy during the winter. We have found that the emissions are highly variable from different parts of the dairy, and that it is necessary to spatially characterize the emissions.

Ammonia emission factors were calculated from air sample measurements and animal dietary information (see section 4.4) collected at 1 feedlot and 3 dairies. The results are most logically divided by the year in which the data were collected, since methods for sample collection and/or emission factor calculation changed over time.

### 5.6.1 1996 Field Tests

Average ammonia emission factors measured were 74 lb./head yr. with an uncertainty of 130 lb./head yr. for dairy cattle and 130 +/- 144 lb./head yr. for beef cattle. These figures are in the same range as ammonia emission factors currently used to assess emissions from livestock wastes in California (Figure 5.12). The significant variation in the emission factors can be partially explained as a diurnal fluctuation. Ammonia emissions at the feedlot estimated from dietary formulations and daily body weight gains data to estimate nitrogen intake and excretion and at the dairy using empirical nitrogen excretion data from calf and cow feeding trials were in the same range as the ammonia emission factors based on field measurements.

The precision of the mass flux model for area sources was evaluated using simultaneous measurements of the ammonia concentration at two heights, in two locations. Figure 5.13 shows the correlation between emissions measured at two points on the downwind edge of the feedlot. Restrictions in the acceptable wind direction for application of the model, and cases where the capacity of the filters was exceeded, limited the data set to four points. The linear fit of these data indicates that there is a systematic difference between the emission rates calculated from concentrations measured at two points on the fence line. This difference illustrates the need to adequately characterize concentrations along the fence line, as we did for the data collected at the dairy, using the passive filter packs. Additionally, the spatial variation seen here indicates a significant difference in emission rates for different parts of the facility.

The correlation in Figure 5.13 also serves to validate the apparent variation seen in the ammonia emission factors determined in this work. Figure 5.13 illustrates that a wide range of emissions

was measured repeatably by this method. This variation in the data collected at the feedlot can be largely attributed to a diurnal fluctuation. However, there were not enough data available to verify this trend. Figure 5.14 compares ammonia emission factors averaged for day-time with those for night-time at the feedlot and the dairy. Of the data collected at the dairy, there was a single time period when we measured very high emissions. Although this time period was the same time of day, approximately 13:00, as the highest emissions recorded at the feedlot, the data collected at the dairy do not show a diurnal trend. Samples collected within one hour of the same time on different days do not provide similar results. In fact, exclusion of this point from the average day-time emission factor brings that average to about the value of the night-time average emissions for the dairy. This difference in the diurnal trend seen at the two facilities may be explained if the single spike in emissions seen at the dairy was due to temperature, or another meteorological condition that is not wind speed or direction. Diurnal fluctuations in temperature, humidity and atmospheric stability were more constant from day to day in the summer conditions at the feedlot than in the winter conditions at the dairy. The pertinent conditions may have been very similar for all collection periods at the dairy, whether they were day-time or night-time samples, except the one. The meteorological data collected during this study is yet to be examined for this variable. Alternately, the apparently smoother diurnal variation seen at the feedlot may be due to a bias in data collection. A large number of samples from the feedlot were not included in the calculation of averages due to exceedences of filter capacity. These samples were all collected at night, so that estimations of night-time emission rates at the feedlot may be biased low. This sample methodology bias does not necessarily exist, however, as ammonia concentrations are expected to be higher at night, due to a lower mixing height. Ammonia fluxes will not directly follow concentrations because of the dependence of flux on wind speed.

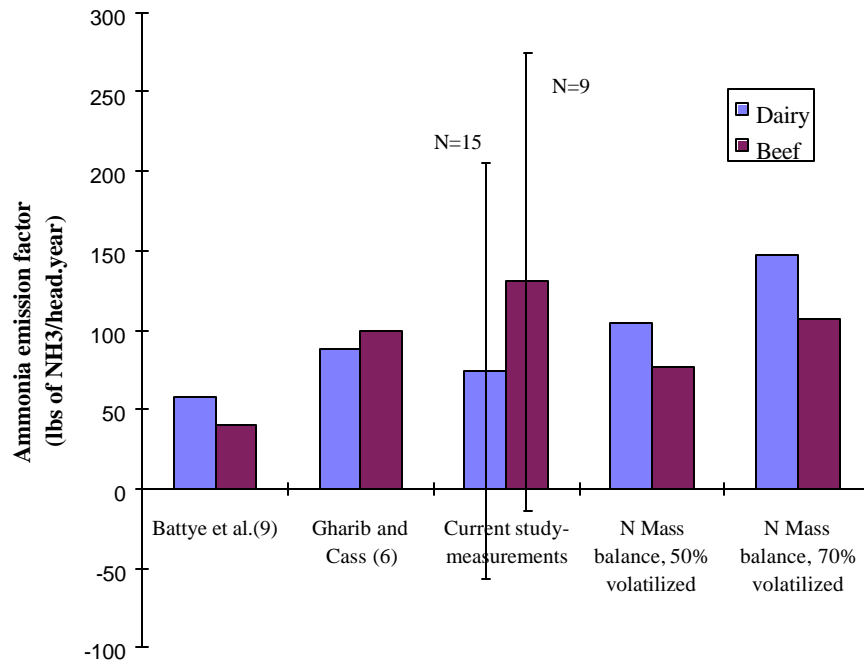


**Figure 5.12 Ammonia emission factors for dairy and beef cattle derived from mass flux model.**

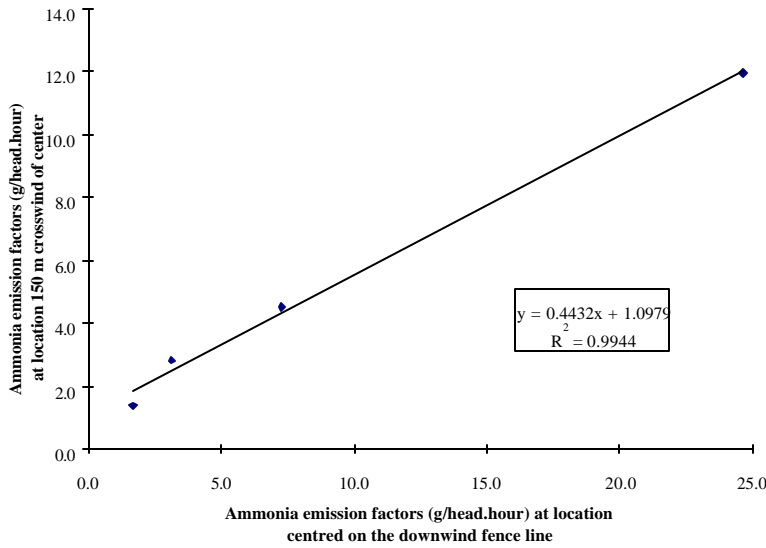


**Figure 5.13 Comparison of ammonia emission rates derived from mass flux model of measurements made at two locations on the downwind fence line.**

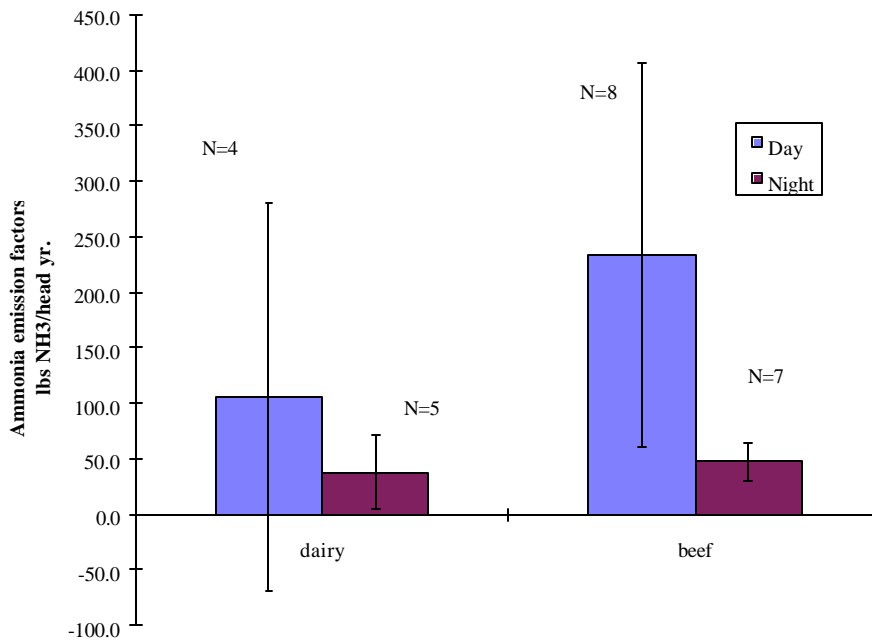


**Figure 5.14 Ammonia emission factors for day-time and night-time for dairy and beef cattle derived from mass flux model.**

### 5.6.2 1997 Field Tests

The emission factors calculated for this study are shown in Table 5.23. They range from a high of 227 lb/head-yr in the late morning to a low of 24 lb/head-yr during the night. Table 5.23 also

shows the surface roughness height as determined from the wind profile and the maximum plume height as determined from the measured ammonia concentrations. Figure 5.15 shows the emission factors according to the time of day they were measured.

The measurements reported here are within the range estimated by Meyer, et al. (Meyer, Ashbaugh et al. 1997) and Battye, et al. (Battye, Battye et al. 1994), but are significantly larger than those of Schmidt and Winegar (Schmidt and Winegar 1996) and Gharib and Cass (Gharib and Cass 1984). The diurnal variation of the emission factor will be of interest to modelers, although additional measurements are needed to define the diurnal variation more completely.

**Table 5.23 Results of ammonia emission factor calculation.**

	Test 2	Test 3	Test 4	Test 5	Test 6
$z_0$ (m)	0.0047	0.0045	0.0070	0.0684	0.1101
Max Height (m)	9.0	14.1	17.2	11.3	13.6
Emission factor (lb/head-yr)	227	95	102	54	24

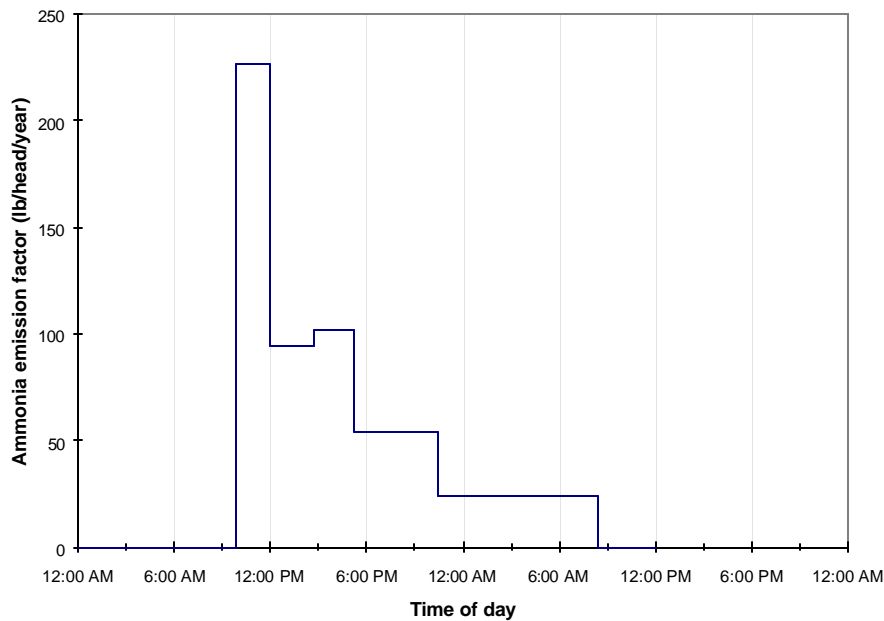


**Figure 5.15 Diurnal trend in ammonia emission factors from 1997 data.**

### 5.6.3 1999 Field Tests

The average horizontal ammonia fluxes measured during north wind episodes at each sampling location on dairies 1 and 2, with standard deviations, are presented in figures 5.16A and 5.16B, respectively. Fluxes measured on dairy 1 were averaged from 8 periods at all 9 locations and 1 period at 8 locations. Although only 3 locations were monitored for the 7 periods during which

wind was from the south, data describe the same trend as shown (data not shown). The fluxes presented for dairy 2 were calculated from results of 4 periods of valid data collected at 7 locations and 3 sampling periods at 6 locations. Negative and zero fluxes were included in the averages and standard deviations of  $\text{NH}_3$  flux. In 3 cases, the vertical integration resulted in negative computed fluxes when the ammonia concentration was greater at either 4 m or 10 m than at 2 m and the net concentration at 2 m was less than  $25 \text{ mg/m}^3$ . In many cases the  $\text{NH}_3$  concentrations measured using the passive samplers was less than the limit of detection, resulting in a zero flux. Negative fluxes were calculated when upwind concentrations were detectable (by the reference method) and downwind concentrations were not, and flux was also zero when both upwind and downwind concentrations were below the limits of detection. To disregard these data because of the sensitivity limitations of the methods would bias the averages to the periods of highest  $\text{NH}_3$  emission. Including them may be underestimating the average flux, but the standard deviations of the averages provide an estimate of the overall uncertainty in the calculations.

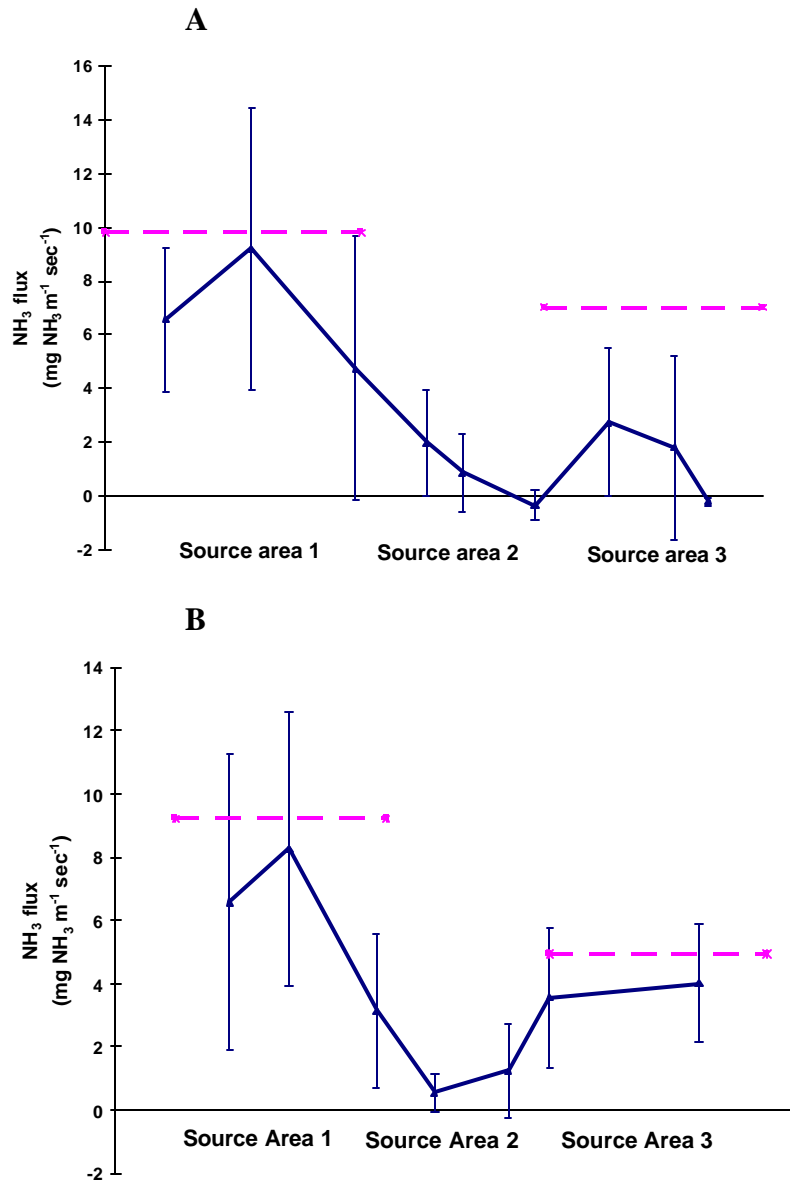


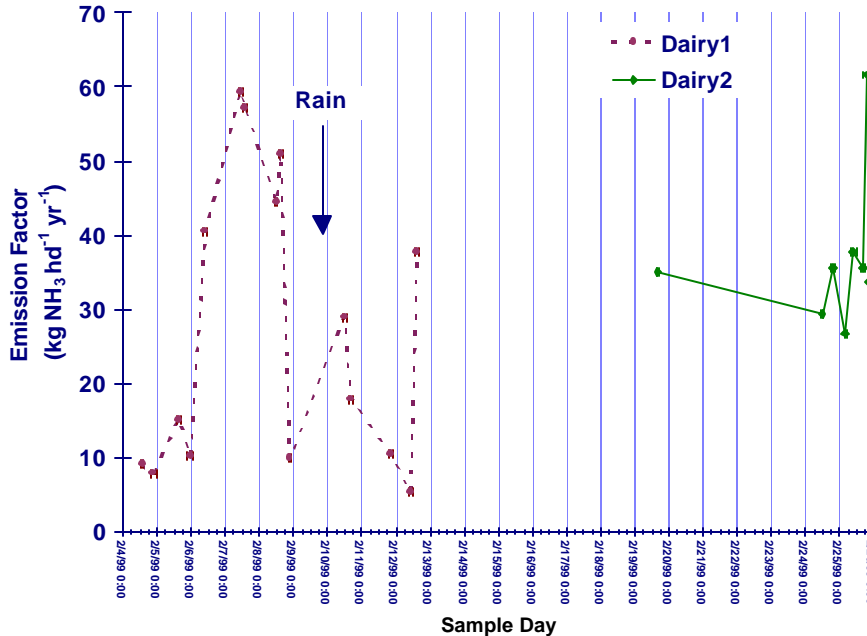
**Figure 5.16 Average  $\text{NH}_3$  fluxes calculated from measurements.**

**Table 5.24 Ammonia concentration profiles and mass fluxes at downwind locations instrumented with active (bubbler) samplers.**

TestID	Date	Time	Tower #	NH3 concentration ( $\mu\text{g m}^{-3}$ )				Plume heights (m)		Ammonia Flux ( $\mu\text{g m}^{-1} \text{s}^{-1}$ )			Emission Factor	
				upwind	2 m	4 m	10 m	Block	Log	Block	Log	Box	fit	( $\text{kg hd}^{-1} \text{yr}^{-1}$ )
99-002	2/4/99	1230-1448	D1	44.204 (5.105)	329.366 (12.083)	327.317 (15.904)	218.209 (10.610)	19.6	75.1	5783.3	13100.6	2982.2	block	9.149
			D2	111.016 (7.237)	80.399 (6.817)	43.834 (8.383)		9.9	9.8	-211.6	456.2	698.7	log	
			D3	127.155 (7.461)	111.375 (7.321)	79.508 (8.768)		16.6	33.2	1206.4	1665.9	867.5	log	
99-003	2/4/99	2046-2210	D1	46.665 (13.752)	670.216 (23.468)	617.257 (21.941)	177.670 (14.044)	12.4	17.0	6836.7	7006.2	5049.2	log	7.966
				40.079 (3.797)	467.902 (15.679)	735.151 (23.798)	299.796 (15.095)	13.6	9.3	10211.8	8070.8	5856.1	log	
99-004	2/5/99	1116-1358	D1	116.892 (6.316)	81.764 (5.509)	52.946 (7.066)		12.7	12.9	819.7	799.3	1051.4	log	10.224
			D2	51.821 (5.176)	123.599 (6.575)	89.170 (7.469)		18.6	2.6	1510.7	-273.4	160.7	log	
			D3	40.079 (3.797)	123.606 (6.142)	63.718 (4.909)	37.473 (6.533)	9.4	7.9	90.0	776.6	1421.3	log	
99-005	2/5/99	1358-1700	D2	732.346 (23.741)	625.025 (28.422)	247.871 (13.030)		13.9	22.5	19030.7	21448.7	17590.3	log	40.548
99-006	2/6/99	0836-1122	D1	14.54 (5.290)	662.734 (21.636)	565.187 (25.831)	289.122 (14.644)	16.0	32.1	23036.2	29121.3	19863.1	log	59.289
99-007	2/7/99	0931-1207	D1	949.18 (16.3)	567.824 (42.694)	236.698 (25.773)		14.3	16.0	24917.0	24662.0	28913.5	log	57.042
99-008	2/7/99	1207-1517	D1	715.009 (23.199)	569.029 (18.724)	275.572 (11.148)		15.6	27.8	24050.7	28630.0	21780.3	log	50.939
99-010	2/8/09	1325-1605	D1	695.062 (22.694)	519.208 (17.357)	126.474 (8.505)		11.9	14.7	6493.7	6477.6	5877.0	log	9.877
99-011	2/8/99	2010-2237	D1	16.104 (5.878)	509.663 (23.111)	369.461 (16.972)	135.405 (7.698)	13.1	17.0	16569.6	16987.8	18979.1	log	28.962
99-012	2/10/99	0942-1326	D1	60.034 (4.613)	60.632 (4.501)	54.456 (5.694)		47.3	24251.7	5976.6	796630.6	1689.3	block	17.919
			D2	95.144 (4.345)	73.609 (3.876)	35.833 (4.134)		13.1	17.4	2688.6	2771.4	3039.4	log	
			D3	464.301 (16.171)	312.532 (12.012)	145.939 (10.969)		15.3	20.4	8989.3	9483.7	8920.1	log	
99-013	2/10/99	1513-1714	D1	33.381 (7.428)	36.326 (7.138)	36.488 (9.743)		-1341.4	0.0	1563.5	0.1	641.3	block	11.800
			D2	101.199 (7.037)	88.154 (6.888)	50.104 (8.262)		17.9	46.6	2690.5	4177.9	1944.2	log	
			D3	17.859 (6.016)	414.166 (18.906)	296.846 (13.887)	163.371 (6.996)	16.5	25.0	2487.7	2242.6	7797.0	log	
99-014	2/11/99	1144-1528	D1	88.234 (4.784)	87.336 (4.853)	75.713 (5.804)		39.9	5097.4	4356.2	182115.2	1384.6	block	10.533
			D2	98.748 (4.977)	90.102 (4.745)	57.749 (5.200)		17.4	44.4	2084.8	3083.4	1591.4	log	
			D3	73.736 (12.460)	778.355 (26.096)	617.751 (21.207)	239.556 (12.719)	12.6	16.8	7193.9	7571.2	5957.8	log	
99-015	2/11/99	1914-2057	D1	181.186 (11.151)	191.085 (10.831)	121.166 (12.530)		14.1	21.9	1647.4	1813.8	908.5	log	5.384
			D2	333.145 (14.158)	365.835 (14.387)	128.038 (11.904)		11.4	12.5	3160.3	2606.8	2193.4	log	
			D3	95.981 (12.721)	531.782 (20.659)	423.335 (17.342)	253.201 (16.016)	15.5	25.1	4688.8	5656.8	3704.2	log	
99-016	2/12/99	0931-1046	D1	82.738 (10.007)	82.452 (9.348)	51.303 (12.032)		1.4	1.6	-983.9	10.7	-112.6	log	37.671
			D2	66.364 (12.523)	99.673 (11.881)	74.407 (15.017)		4.9	4.8	-534.1	-427.9	-251.7	log	
			D3	438.001 (15.196)	437.88 (15.266)	210.442 (9.752)		15.6	32.2	14575.8	18230.5	11650.5	log	
99-017	2/12/99	1334-1559	D1	72.862 (6.112)	58.083 (5.730)	21.41 (7.129)		13.5	19.9	1862.9	1989.3	1938.1	log	26.804
			D2	194.449 (8.480)	180.138 (7.902)	125.249 (8.113)		23.7	153.2	8872.7	25519.2	5172.2	block	
			D3	2.369 (6.637)	392.19 (18.56)	296.57 (14.8)	141.96 (9.89)	15.42	24.9	5208.0	5931.0	611.0	log	
99-018	3/16/99	1505-1711	D3	21.637 (4.123)	193.387 (9.653)	180.968 (9.807)	138.096 (10.114)	26.3	245.8	5044.3	27138.1	1826.0	block	35.674
99-020	3/21/99	1722-2100	D2	21.637 (4.123)	72.602 (3.046)	68.339 (2.997)	55.243 (3.047)	25.4	197.0	1700.3	7291.8	707.4	block	29.307
99-021	3/21/99	2100-0155	D2	77.105 (3.969)	79.742 (4.034)	60.185 (4.274)		28.5	445.4	3281.1	25564.4	1101.5	block	26.804

Time indicates period of sampling. Values in parentheses are uncertainties. Fit indicates which computed flux was assigned as the best-fit for purposes of calculating emission factors.

Emission factors are reported for the 23 periods for which the wind direction was appropriate for all sampling locations, including those during south wind events on dairy 1 (Table 5.24 and Figure 5.17). The dates of measurements made on dairy 2 are shifted by -37 days in order to show both data sets on the same plot. Although emission factors were generally lower during night periods than at midday, the larger temporal trend overwhelmed any diurnal trend in the data. A storm on the fifth day of sampling at dairy 1 saturated the corral surfaces, lowering emission as expected (Asman 1992). The very low emission factor for the period directly preceding the storm is likely due to a combination of high relative humidity and highly unstable atmospheric conditions (RH = 85%, bulk Richardson's number < -6). The only other period of unstable conditions was between 18:00 and 0:00 on the last day at dairy 1, for which the emission factor is consistent with the immediately previous measurement in time. The final period at dairy 1 was characterized by high wind speed (> 3.5 m/s at 4m) and the lowest RH of all sampling periods (42%), which accelerated drying and increased emissions. The higher emission factors measured on dairy 2 at midmorning and late afternoon may be evidence of a diurnal trend with animal activity, as they are the feeding times, but with data from only two days it is impossible to determine conclusively. Taken as three data sets, dairy 1 before the rain event, after the rain, and dairy 2, the emission factors show the expected decreasing trend with increasing relative humidity ( $r^2 = .2$ , data not shown) and increased with increasing temperature ( $r^2 = .3$ , data not shown). We also saw a trend of increasing emission with higher wind speed, which was expected, but this finding may be biased by the fact that wind speed is incorporated in the calculation of emission factor.



The average  $\text{NH}_3$  emission factor for the two dairies was  $29.5 \text{ kg hd}^{-1} \text{ yr}^{-1}$  when calculated from the measurements and  $30.3 \text{ kg hd}^{-1} \text{ yr}^{-1}$  when calculated by N balance. The agreement between the two methods indicates the robustness of the measurement method. Climatic conditions during the sampling periods were cooler and wetter than the conditions of the laboratory experiments from which the  $\text{NH}_3$  volatilization estimates were derived ( $27^\circ \text{C}$ , dried air). This should result in an overestimation, since hot, dry conditions increase  $\text{NH}_3$  volatilization (Asman 1992). Urea was demonstrated to be the only significant source of  $\text{NH}_3\text{-N}$  in the laboratory experiments. These were run until the manure was well dried with no additional input of moisture. Conversely, the areas occupied by the cattle in the field trial were saturated throughout the measurement periods, which could cause field measured  $\text{NH}_3$  to include some contribution from organic forms of N. In this study, the climactic factors inhibiting  $\text{NH}_3$  volatilization during the field trials appear to balance the N sources that are not included in the laboratory derivation, resulting in a good agreement between the methods. This may not be the case in other circumstances.

A comparison of average  $\text{NH}_3$  fluxes calculated from measurements made downwind of the various sources within the two dairies with fluxes calculated by N balance for two general populations on each dairy show some consistent trends (Figure 5.16). Nitrogen balance estimates predict similar  $\text{NH}_3$  fluxes from source areas 1 and 3, while measurements indicate higher emission from source area 1 on both dairies. The primary reason for this difference was the manure management practices: source areas 3 included free stalls which were flushed, while source areas 1 were dry lot corrals from which manure was only flushed from about 20% of the area in dairy 1 and not removed in dairy 2. The lower measured fluxes, relative to N balance calculations, from source area 3 on dairy 1 compared to dairy 2 are most likely due to the fact that dairy 1 was removing manure from all of the milking cows while dairy 2 was flushing the manure from the 60% of the milking cows.

## 6 CONCLUSIONS FROM FIELD MEASUREMENTS

In order to better meet the regulatory needs of both California and national agencies for empirically derived PM<sub>10</sub> emission factors for specific agricultural operations, the data presented in section 5.0 has been summarized in these conclusions. The five years (1994 - 1998) of field testing results from this study that have been used to compute PM<sub>10</sub> emission rates were filtered to identify only those data for which the emission factor confidence rating was very high. The emission factor confidence rating applied in selecting data for the summaries was comprised of the elements identified in the systematic examination of the emission rates calculated for land preparation activities and the attendant lidar data as presented in section 4.3 and Appendix H. Due to the changes made in the equipment and the methods involved in collecting the data over the reporting period, some of the qualifiers in the rating system were more stringently applied to some sub-sets of the data than to others. This was necessary to attain the optimal compromise between data quality and recovery. The application of each qualifier in the rating system to each specific source category is explained as the data is presented below.

The PM<sub>10</sub> emission factors calculated for land preparation activities showed some trends by operation (i.e. discing vs. ripping, see section 5.4), though there were individual tests that could be interpreted as exceptions to these trends. For the following summary, the selected PM<sub>10</sub> emission factors have been grouped by commodity and operation with the exception of the confined animal facilities, which were grouped only by commodity (i.e. dairy or beef). The strongest trends in PM<sub>10</sub> emission factors with environmental conditions were the relationships observed with relative humidity and soil moisture. As is illustrated in the categorical summaries below, there appears to be a critical relative humidity of 40% below which it is more likely that large emission factors will be measured. Data collected for discing operations and almond pickup indicate a more definite relationship of PM<sub>10</sub> emission factors with soil moisture, with 10% soil moisture appearing to be a critical level observed to reduce emissions under the discing study conditions and 4% soil moisture defining the difference for almond pickup. Similar observations have been made by other researchers and a correlation of relative humidity with soil moisture indicates the relationship between these two important variables and PM<sub>10</sub> emission factors (Holmén, James et al. 2001). Where data is available, average emission factors have been calculated for each source from those tests conducted in conditions below and above 40% relative humidity, with the exception of discing tests which are averaged for soil moisture conditions below and above 10%. Almond harvesting tests were averaged for soil moisture conditions below and above 4% and cotton weeding tests were averaged for soil moisture conditions below and above 8%.

**Table 6.1 Summary of average PM<sub>10</sub> emission factors.**

SOURCE	all valid - all conditions standard			most confident - selected standard			notes	
	average	deviation	number	average	deviation	number		
<b>almond</b>								
shaking <sup>II</sup>	1670	1303	4				log model only	
sweeping <sup>II</sup>	1466	1042	2				log model only	
pickup <sup>III</sup>	4106.19	3210.43	5	> 4 %	2007.83	351.08	3	high and low soil moisture
				< 4 %	7253.72	2820.93	2	
<b>fig</b>								
sweeping <sup>I</sup>	13	8	N/A					box model, high soil moisture
pickup <sup>I</sup>	39	4	N/A					no blowers
<b>cotton harvest <sup>IV</sup></b>				<b>cotton harvest <sup>VI</sup></b>				high and low relative humidity
picking	189.80	166.61	17	<40%	200.36	99.31	3	
				>40%	217.65	148.23	7	
stalk cutting	188.17	218.68	29	<40%	348.94	301.03	9	
				>40%	134.88	109.17	3	
<b>wheat harvest <sup>IV</sup></b>				<b>wheat harvest <sup>VI</sup></b>				high and low relative humidity
combining	649.86	513.96	20	<40%	889.64	346.02	7	
				>40%	none			
<b>land preparation <sup>IV</sup></b>				<b>land preparation <sup>VI</sup></b>				high relative humidity only
root cutting	33.00	4.24	2	>40%	33.00	4.24	2	
discing	134.24	153.97	27	<10%	244.94	121.13	5	high and low soil moisture
				>10%	72.66	46.22	12	
chiseling	512.20	287.53	5	<40%	612.25	208.56	4	high and low relative humidity
				>40%	112.00	0.00	1	
weeding	89.21	107.98	15	> 8 %	5.98	10.73	6	high and low soil moisture
				< 8 %	144.70	108.05	9	
<b>confined animal facilities <sup>V</sup></b>				<b>confined animal facilities <sup>V</sup></b>				high and low relative humidity
dairy	80.42	102.64	26	<40%	113.26	126.22	12	
				>40%	54.70	64.08	10	
<i>lbs/d*1000hd</i>	90.51	116.74	26	<40%	112.95	142.25	12	
				>40%	53.39	80.89	10	
beef	79.21	107.32	27	<40%	158.11	159.26	9	high and low relative humidity
				>40%	42.31	24.21	12	
<i>lbs/d*1000hd</i>	28.87	35.28	26	<40%	43.28	46.88	11	
				>40%	23.24	20.10	11	

<sup>I</sup> Valid Upwind (UP) and Downwind (DN) PM<sub>10</sub> and wind speed (WS) at one height.

<sup>II</sup> 2 or more valid UP and DN and WS.

<sup>III</sup> 2 or more valid UP and WS, 3 valid DN; PM and WS outside canopy; PM measured 100 m or less from operation.

<sup>IV</sup> 2 or more uncontaminated UP and WS, 3 valid DN; sampler placement as in Holmén et al., 2001.

<sup>V</sup> 1 valid UP, 3 valid DN, WD within 45 ° of optimal, EFU < 100%.

<sup>VI</sup> 2 or more uncontaminated UP and WS, 3 valid DN; sampler placement as in Holmén et al., 2001; Q<sub>UP</sub> = A, Q<sub>WD</sub> = A, EFU <100%.

Figures in *italics* indicate averaged results presented in English units.

Summarization of the PM<sub>10</sub> emission factors measured in this study by 1) reducing the data set to those tests which are assigned the highest confidence ratings and 2) grouping the data by commodity, operation, and relative humidity produced average emission factors which represent the most directly applicable interpretation of the results of the first five years of this study currently possible.

## 6.1 Orchard Crops

Measurement of emission factors was attempted for walnuts, figs, and almonds. The three valid walnut tests (see Appendix A) were conducted during two simultaneous operations which could not be quantified separately using these data, so no PM<sub>10</sub> emission factors are reported for walnuts. Fig harvesting operations of sweeping and pickup were monitored in 1994 only, so vertical profiles of the PM<sub>10</sub> concentrations and wind speeds were not collected. Also, the climatic conditions during the fig sampling were unusually wet and it became necessary for the operator to sweep the figs without the blowers (which would be too rough on the high-moisture-content fruit) and to conduct the pickup on unusually wet ground. Therefore, the PM<sub>10</sub> emission factors summarized in Table 6.1 are computed from single height measurements and are likely a lower-bound estimate of emissions, due to the unusual circumstances.

Two independent calculations of PM<sub>10</sub> emission factors were performed on PM<sub>10</sub> and wind speed profiles collected at almond harvesting operations (shaking, sweeping, and pickup) in 1995. The initial computations used the logarithmic model (see section 4.2) applied to all tests with valid PM<sub>10</sub> concentration measurements at least two heights, a valid upwind measurement, and appropriate wind direction. Subsequent calculations used the methods described by Holmén et al. (2001) and confined the evaluation to those tests conducted under conditions shown to be appropriate to the application of those methods. In this evaluation, only six almond pickup tests were conducted under the appropriate conditions of having both PM<sub>10</sub> and wind speed measurements in the same wind field. One of these tests was conducted significantly more than 100 m from the operation (95-055, Table 5.3) and the calculated emission factor for that test is much lower than all of the other tests conducted under similar conditions, so that data point is considered invalid for the purposes of this summary. There were no tests of almond shaking or sweeping that met all of the requirements of the published method.

A trend can be observed between PM<sub>10</sub> emission factors and soil moisture in the five almond pickup tests of highest confidence. Interestingly, the trend with relative humidity and almond PM<sub>10</sub> emission factors is opposite that expected, with the highest emission factors recorded under the highest relative humidity (see Table 5.4). This fact indicates clearly that the soil moisture is a more meaningful predictor of PM<sub>10</sub> emissions from almond pickup than relative humidity. For this reason, the average emission factors summarized in Table 6.1 are provided for conditions of low (< 4%) and high (> 4%) soil moisture.

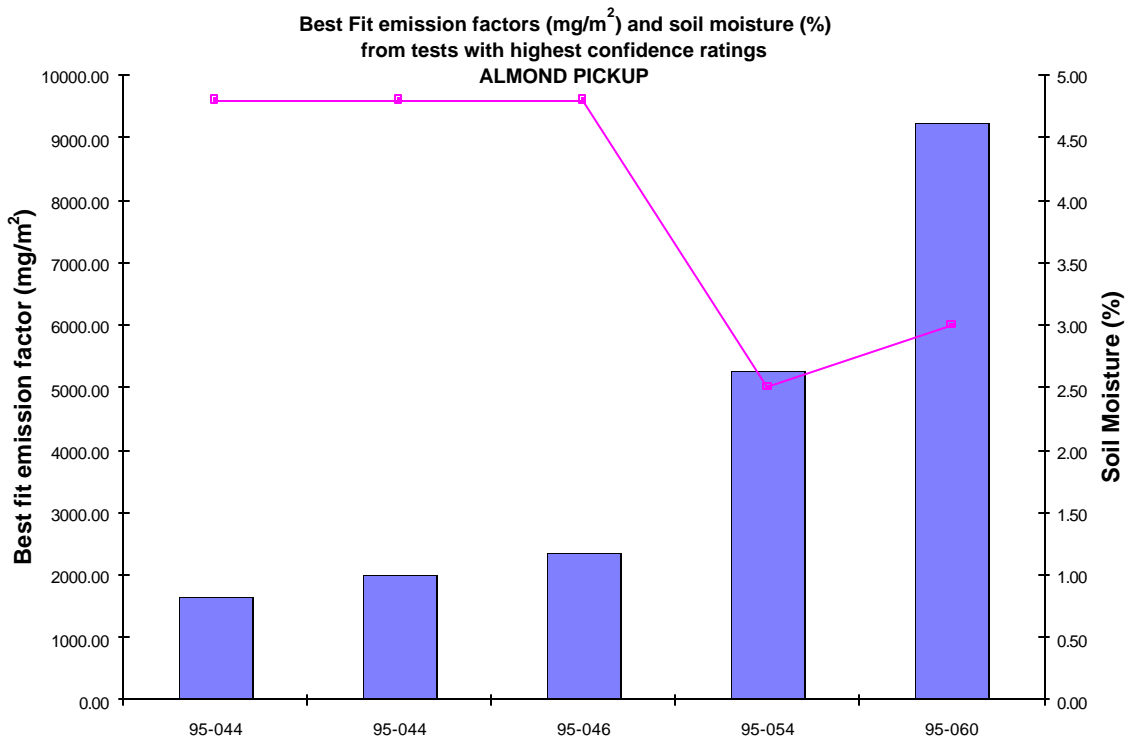


**Figure 6.1  $\text{PM}_{10}$  emission factors ( $\text{mg}/\text{m}^2$ ) and soil moisture (%) from 1995 tests of highest confidence for Almond pickup operations.**

## 6.2 Cotton Harvest

Tests of PM<sub>10</sub> emission factors from cotton harvest were grouped by operation into picking, stalk cutting, and stalk incorporation. Only tests with upwind PM<sub>10</sub> concentrations measured at 2 or more heights were included in this final summary to insure that instances of upwind contamination would be reliably identified (see section 4.3.4). Additionally, individual tests for which more than one concentration measured upwind was greater than the downwind concentration measured at the same height were excluded from this summary as were tests during which the average or standard deviation of the wind direction exceeded limits set by the confidence rating  $Q_{wd}$  (see Table 4.2). Tests for which the emission factor relative uncertainty exceeded 100% were also excluded.

### 6.2.1 Cotton Picking

Ten tests of cotton picking met all of the emission factor confidence criteria. All of these were conducted on a single ranch on 4 fields with very similar loam or clay loam soil types using the same Case-Harvester 2-row pickers. Seven tests were conducted in 1995 and the eighth in 1996. Soils analysis results are available for all of these tests except 95-137 and both moisture and dry sieve fraction less than 75  $\mu\text{m}$  were essentially the same in 5 tests (soil moisture = 4 % and silt content = 16 %), but silt content was lower (10 %) in test 95-123 and moisture was higher (12.4 %) in test 96-095. These two tests resulted in relatively low PM<sub>10</sub> emission factors, which may have been due to soil conditions or increased relative humidity.

The two tests conducted in conditions with the highest relative humidity (tests 95-123 and 96-095) have two of the three lowest calculated PM<sub>10</sub> emission factors. Also, tests conducted under identical (using side-by-side towers) or nearly identical conditions (95-136 and 95-137) have similar PM<sub>10</sub> emission factors. However, tests 95-094 through 95-096, conducted sequentially as relative humidity increased have increasing PM<sub>10</sub> emission factors. This phenomenon may be related to the change in atmospheric stability as the sun set, or it may be due to the fact that the distance between the pickers and the samplers decreased steadily in this series of tests. It is apparent that changes in relative humidity alone fail to describe the differences in PM<sub>10</sub> emission factors. Because the cotton picking data for which confidence ratings are highest do not show a solid trend in PM<sub>10</sub> emission factors with relative humidity, the average values for this operation under conditions of high and low relative humidity are essentially the same. This fact may be due, in part, to the fact that cotton picking can only be performed when the cotton is dry such that cotton is generally picked at times of low relative humidity.

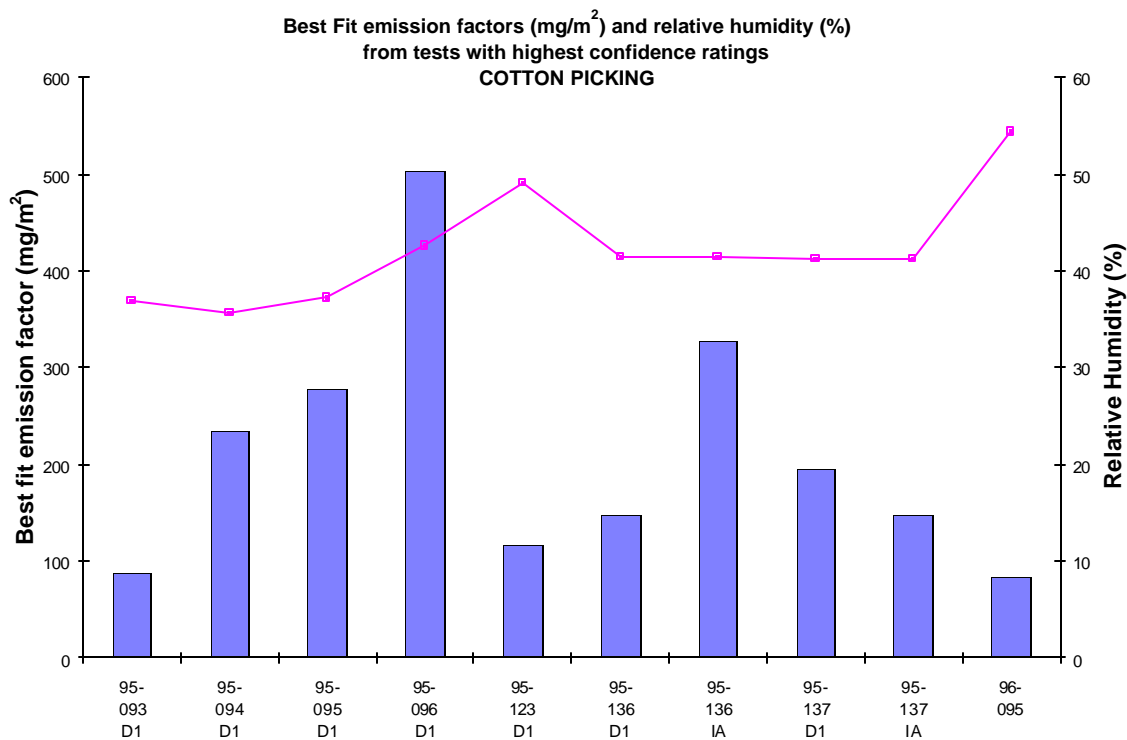


**Figure 6.2  $\text{PM}_{10}$  emission factors ( $\text{mg}/\text{m}^2$ ) and relative humidity (%) for cotton picking tests with highest confidence ratings.**

### 6.2.2 Cotton Stalk Cutting

Twelve tests of cotton stalk cutting met all of the emission factor confidence criteria. Eleven of the tests were conducted in 1995 and one in 1998. The first six tests were conducted on one farm, on three separate fields, the seventh test was on a second farm and the eighth on a third. Soil types ranged from loam (tests 95-097, 95-098, 95-110, 95-139, 95-141, and 95-142) through clay loam (95-106, 95-126) to clay (95-148 and 98-043). Soils analysis data are not available for tests 95-139 through 95-142, though the soil moisture and silt content can be inferred from samples collected for cotton picking tests conducted on the same fields immediately prior to the stalk cutting. Making this assumption, the moisture and silt content of fields used in tests 95-097 through 95-142 were similar to one another and differed from the fields used in tests 95-148 and 98-043. Soil moisture was about double and soil silt content was lower for the last two tests, with silt contents between 10 and 20 % for the earlier tests and below 5 % for the later tests. The last two tests resulted in the two lowest  $\text{PM}_{10}$  emission factors measured in this set. These data present an apparent relationship between these soil parameters and  $\text{PM}_{10}$  emission factors for cotton stalk cutting in which higher soil moisture and lower soil silt content correlate with lower measured emission factors.

Two types of stalk cutting implements were represented in the valid tests; a 4-row rotary type was used for tests 95-097 and 95-098 and a 6-row flail type was used for the subsequent tests. While the side-by-side measurements made during test 95-098 agree very well and appear to indicate a larger PM<sub>10</sub> emission factor for the rotary type stalk cutter, the equally valid test 95-097 does not support this hypothesis. Test 95-097 was taken earlier in the afternoon when the solar radiation was stronger, wind speeds were slightly lower, and the difference between temperature at the ground and aloft was greater than during test 95-098. The plume would be expected to loft higher under these conditions and dispersion upward could result in inaccurate measurements and underestimation of PM<sub>10</sub> emission. Unfortunately, lidar data are not available for these tests and, considering the fact that the sampling towers were within 50 meters of the tractors for both tests, there is no data available to indicate that either test is a better measurement of the true PM<sub>10</sub> emission factor for rotary type stalk cutters than the other.

The range in relative humidity was greater for cotton stalk cutting tests than for cotton picking tests, as picking is only practiced under conditions of favorable cotton moisture content and trends are apparent between PM<sub>10</sub> emission factors for stalk cutting and relative humidity. The test performed under conditions of lowest relative humidity (95-098) measured the highest PM<sub>10</sub> emission factor and the test with the highest relative humidity (98-043) had the lowest PM<sub>10</sub> emission factor. For the cotton stalk cutting tests, this clearer delimitation of PM<sub>10</sub> emission factor with relative humidity results in a lower average emission factor under conditions of higher relative humidity (> 40%) than when relative humidity is lower. Tests 95-139 to 95-142, collected sequentially under identical or nearly identical conditions, illustrate the variability in emission factor that cannot be accounted for in the measured variables.

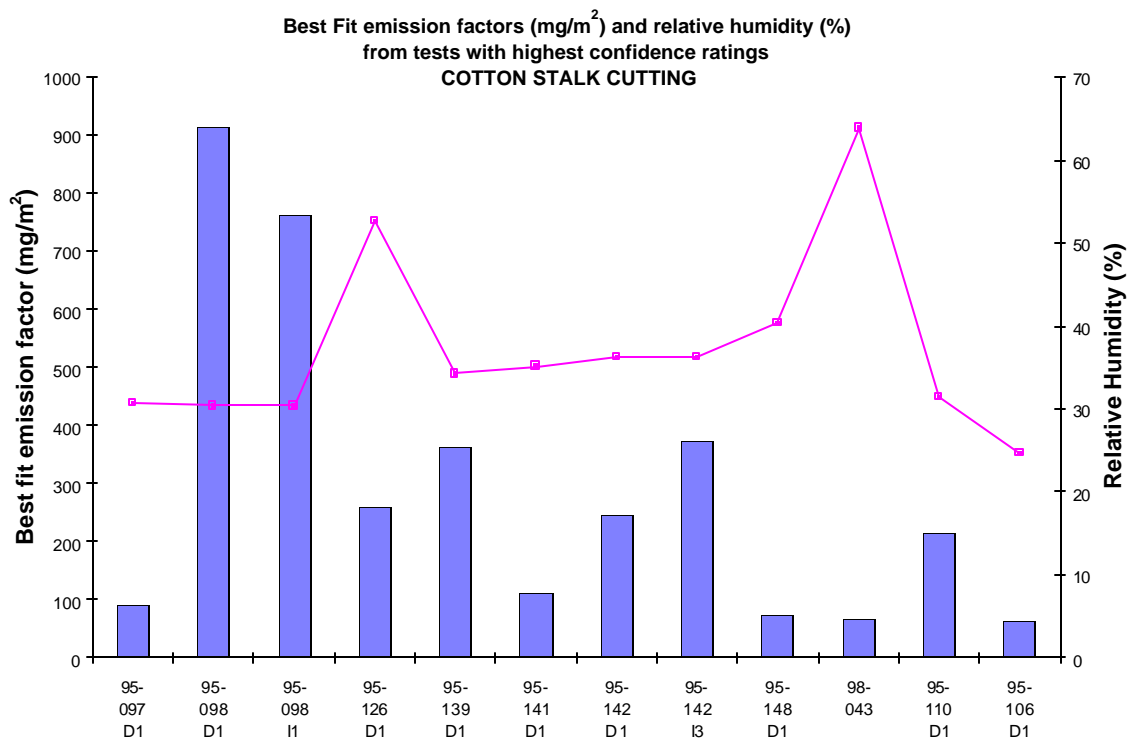


**Figure 6.3  $\text{PM}_{10}$  emission factors ( $\text{mg}/\text{m}^2$ ) and relative humidity (%) for cotton stalk cutting tests with highest confidence ratings.**

### 6.2.3 Cotton Root Cutting

Two tests of root cutting following cotton harvest met the emission factor confidence criteria. This practice has not been widely adopted, but its ability to break down the furrows and loosen the cotton plant residue from the soil makes it an attractive alternate practice to stubble discing for cotton. The tests were conducted sequentially on the same field under nearly identical conditions. This limited data set indicates that there may be a relationship between relative humidity and  $\text{PM}_{10}$  emission factors for cotton root cutting. It also indicates that, under these conditions, the average emission from root cutting is less than that for stubble discing. However, soil moisture data is not available for the tests of root cutting, and this information is essential for a meaningful comparison of the two practices (see section 6.4.1).

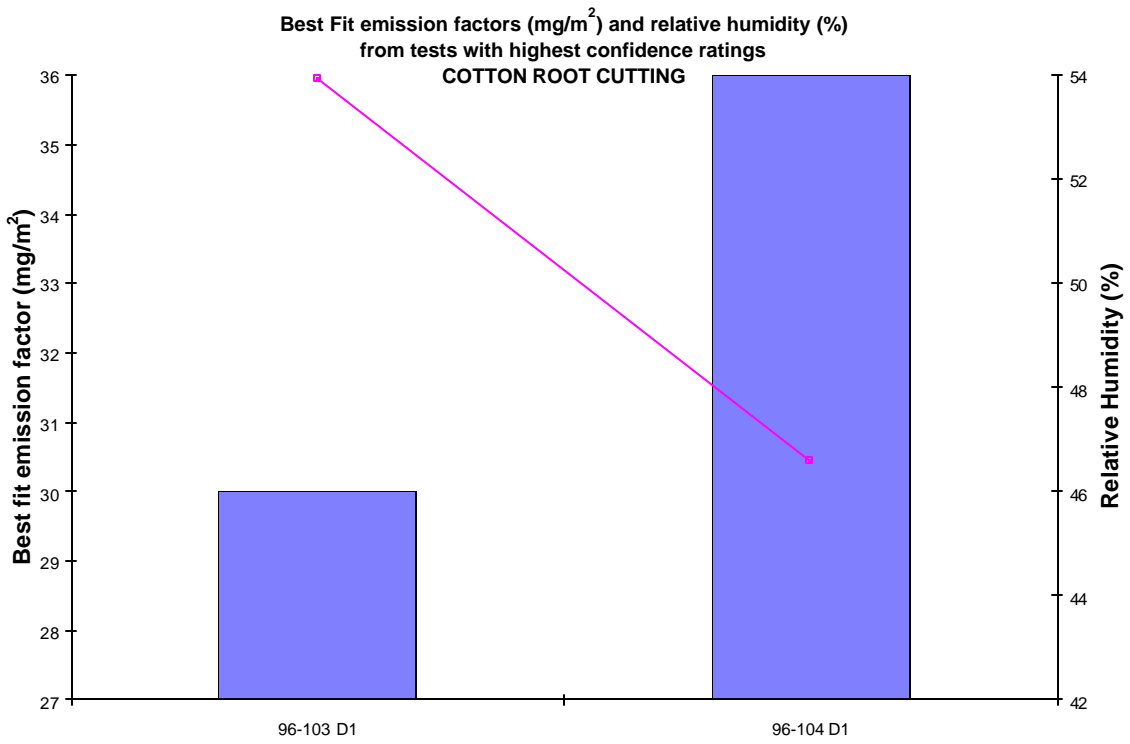


**Figure 6.4  $\text{PM}_{10}$  emission factors ( $\text{mg}/\text{m}^2$ ) and relative humidity (%) for cotton root cutting tests with highest confidence ratings.**

### 6.3 Wheat Harvest

As with tests of cotton harvest operations, only tests with upwind  $PM_{10}$  concentrations measured at 2 or more heights were included in this final summary and individual tests for which more than one concentration measured upwind was greater than the downwind concentration measured at the same height were excluded, as were tests during which the average or standard deviation of the wind direction exceeded limits set by the confidence rating  $Q_{wd}$  (see Table 4.2). Tests for which the emission factor relative uncertainty exceeded 100% were also excluded.

The single operation identified with wheat harvest, combining, is represented in this summary by six tests for which measurement data met all reliability criteria. The first three were conducted in 1996 and the rest in 1997 on a single farm on three different fields with loam and clay loam soil types. Soil moisture and 75  $\mu m$  dry sieved fraction data are available for all tests except 97-032 and soil moistures were very low, from 2.3 to 4.2%. Silt contents were about 20% for tests conducted in 1996 and 10% for the 1997 tests. All tests were conducted using the same combines.

There appears to be no readily discernible trend in  $PM_{10}$  emission factors from wheat harvesting with soil type or relative humidity, within the limited range of these variables during measurements. Tests 97-032 and 97-034 were conducted sequentially, with two towers side-by-side the same distance from the combine used in test 97-034, and the variance in  $PM_{10}$  emission factors from these tests indicate the variability that cannot be accounted for within the measured parameters. One possible source of error is the relatively large distance between the sampling tower and the combine during test 97-032, but the lack of lidar data for this test makes it impossible to identify any uncertainty in the estimate of plume height directly and the resulting data have been included in the summary average.

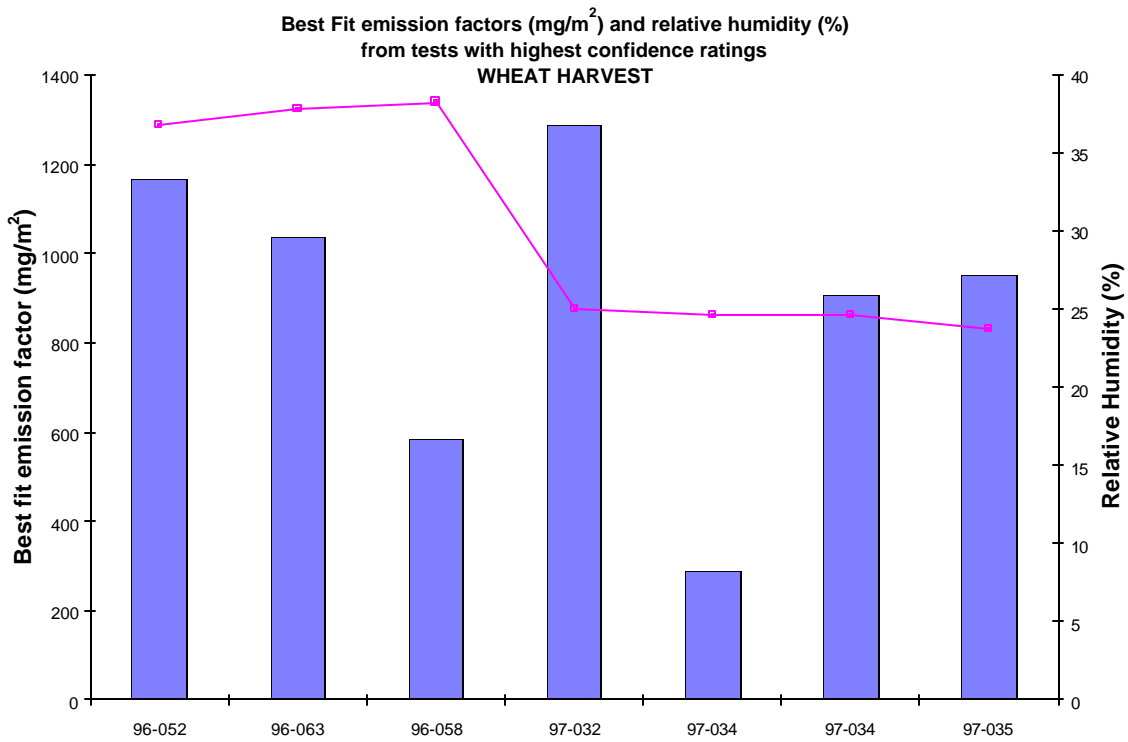


**Figure 6.5  $\text{PM}_{10}$  emission factors ( $\text{mg}/\text{m}^2$ ) and relative humidity (%) for wheat harvesting tests with highest confidence ratings.**

## 6.4 Land Preparation

The most recent focus of this project has been on land preparation activities. Stubble discing following cotton was the first land preparation operation monitored in 1995 followed by chiseling, finish discing, and listing following cotton in 1996 and stubble discing, chiseling, and finish discing following wheat in 1997. Finally, the stubble discing tests following cotton in 1998 provided the basis for the lidar-assisted evaluation of emission factor confidence ratings. Unfortunately, none of the listing tests fulfill the emission factor confidence criteria, which is similar to that for the harvest of wheat and cotton (see sections 6.2 and 6.3), and only results for discing and chiseling are summarized below. Criteria for land preparation tests require valid  $PM_{10}$  concentration measurements at three heights upwind, due to the increased likelihood of upwind interferences with these later-season operations when simultaneous activities on neighboring fields is more common. Also, wind direction requirements were relaxed for tests of land preparation activities relative to those for harvest because these operations are conducted at an angle to the edge of the field making the distinction of wind direction within 45 degrees of perpendicular to the edge of the field less relevant to data interpretation. Thus, tests of land preparation are included in the following summary regardless of wind direction.

### 6.4.1 Discing

Sixteen of the seventeen discing tests that met all of the emission factor confidence criteria were following cotton and only test 97-045 was following wheat. Twelve of the tests were conducted during stubble discing, immediately following stalk cutting or harvesting (in the case of 97-045) and five were conducted during second discing following chiseling (tests 96-111 through 96-119). Two farms and three different fields are represented in these data. The implements used in all of the tests were similar with respect to the variables measured in this study; the discs all had 2 gangs or rows of blades and were pulled by a track-drive diesel tractor. The finish disc (used in tests 96-111 through 96-119) was wider and the individual blades were smaller in circumference than those of the stubble discs and no rollers were used following the finishing disc.

Emission factors for  $PM_{10}$  from discing show a distinct relationship with soil moisture and soil silt content, with lower emission factors measured in conditions of higher soil moisture and lower soil silt contents. Soil moisture was lower during stubble discing than for finish discing because soil brought up to the surface (where it is collected for the analysis) by the chisel was wetter than soil sampled following the harvest. The farm where tests in 1998 were conducted had soil of much lower silt content (dry sieve fraction less than 75  $\mu m$ ) than the farm where all of the other tests in this summary were conducted. It is difficult to distinguish between the effects of soil moisture and silt content using only these data, but the stubble discing tests conducted on fields of similar soil silt content but much different soil moisture can be compared by comparison of stubble discing (tests 95-128 to 95-132) to finish discing (tests 96-111 to 96-119), making the assumption that the difference in soil moisture is the most significant difference between these operations. Since this comparison indicates that increased soil moisture decreased  $PM_{10}$  emission factors, average emission factors are presented for soil moisture above and below 10%.

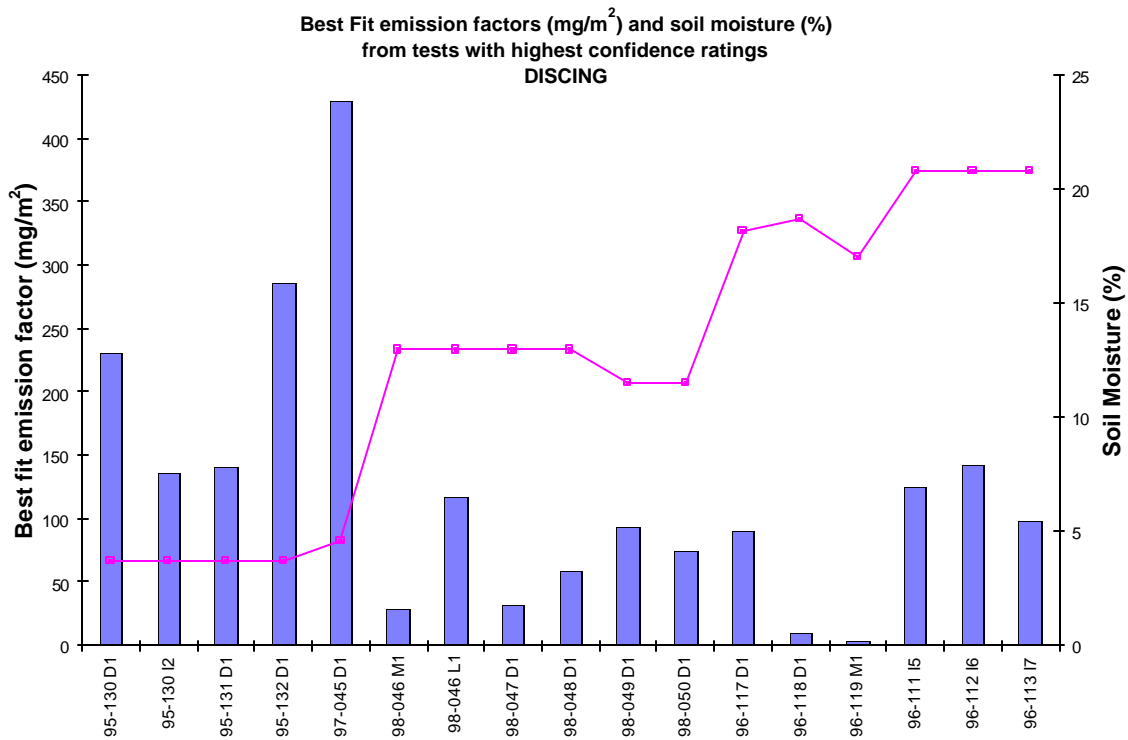


**Figure 6.6 PM<sub>10</sub> emission factors (mg/m<sup>2</sup>) and soil moisture (%) for discing tests with highest confidence ratings.**

Data are presented for tests 95-130 and 98-046 conducted under identical conditions using two towers for each test, and the variance in PM<sub>10</sub> emission factors calculated for these tests indicate the variation that cannot be accounted for by the variables measured in this study.

#### 6.4.2 Chiseling

Five chiseling tests met all of the emission factor validity criteria. All of these tests were following wheat harvest and stubble discing on the same farm and field using the same implement. Soil moisture was about 2% for all of the tests. There appears to be a relationship between PM<sub>10</sub> emission factors from chiseling and relative humidity. Test 97-050 was the only test conducted under conditions of relative humidity above 40% and has the lowest PM<sub>10</sub> emission factor. While differences in relative humidity cannot account for all of the variation seen in the PM<sub>10</sub> emission factors calculated for chiseling, the trend was also seen in other agricultural operations and these chiseling data are summarized for conditions above and below 40% relative humidity.

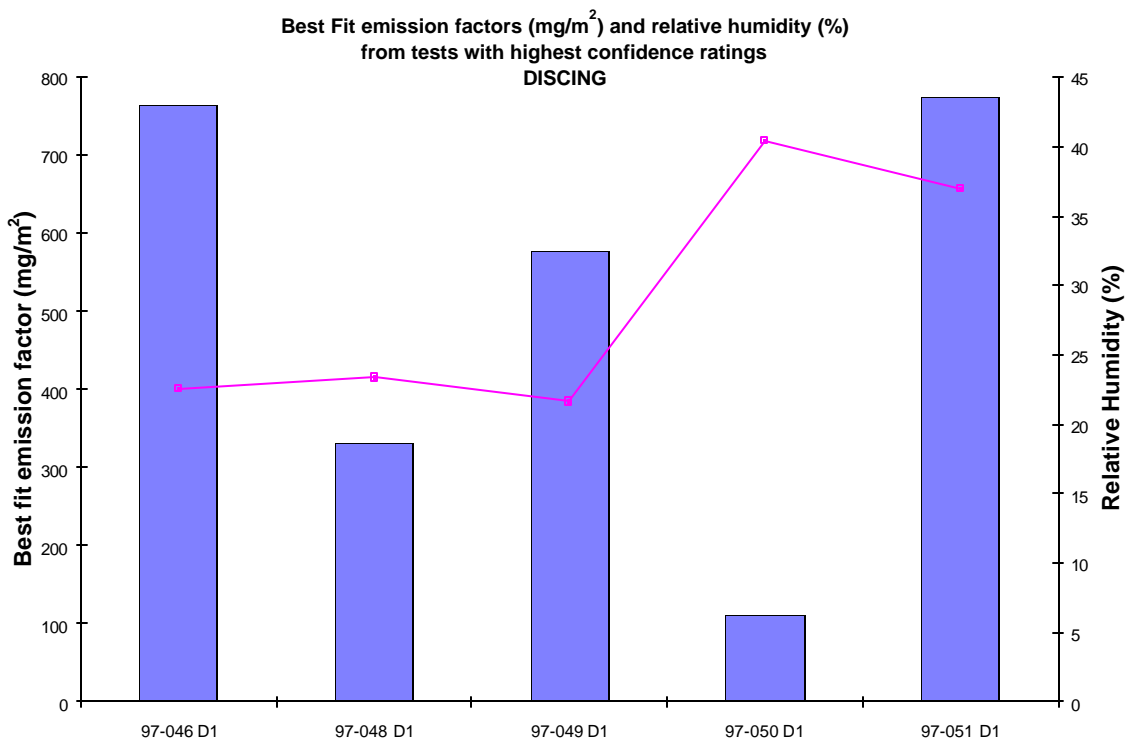


**Figure 6.7  $\text{PM}_{10}$  emission factors ( $\text{mg}/\text{m}^2$ ) and relative humidity (%) for chiseling tests with highest confidence ratings.**

#### 6.4.3 Weeding

Fifteen cotton cultivation tests met all of the emission factor confidence criteria. Weeding, for these tests, was conducted using a Lilliston 6 blade cultivator 6.6 m wide pulled by a wheeled tractor at approximately 2.2 m/s. Several tests (98-001 through 98-005) were conducted with two simultaneous profiles, thus each pair of emission factors provides a good estimate of the repeatability of the measurements. Emissions of  $\text{PM}_{10}$  from these weeding operations, conducted on a clay loam soil, appear to be strongly affected by soil moisture. The data presented in Figure 6.8 illustrates a marked increase in  $\text{PM}_{10}$  emissions when soil moisture drops below 8 %.

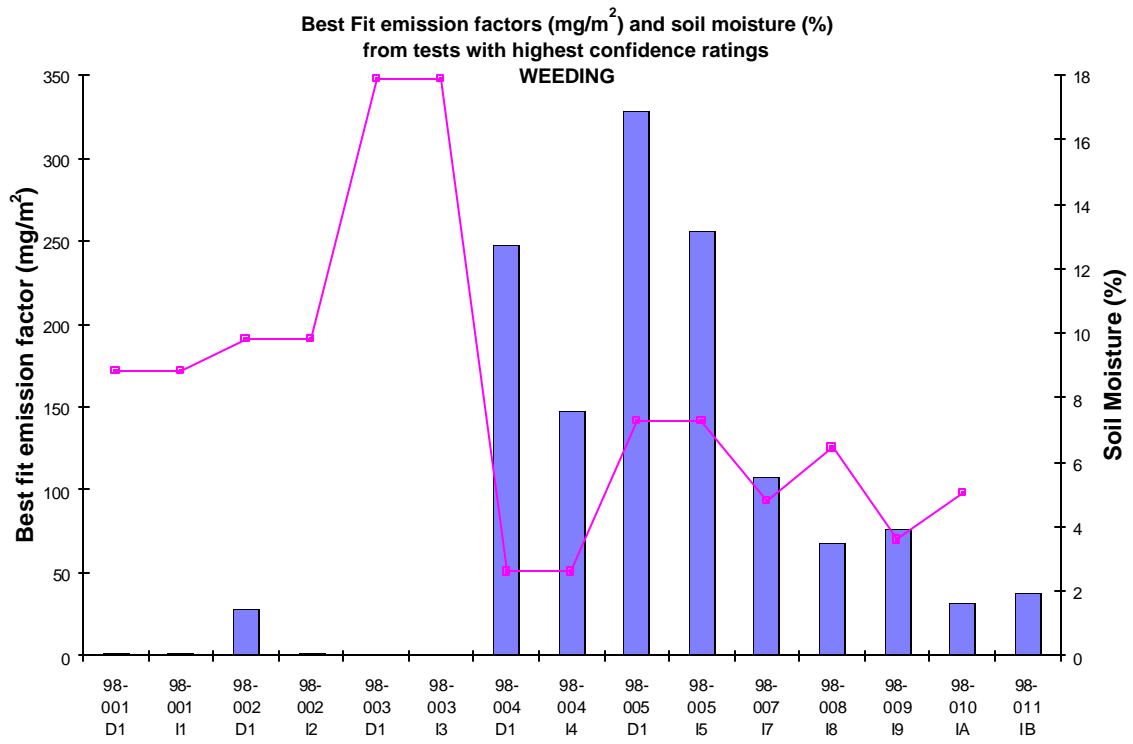


**Figure 6.8  $\text{PM}_{10}$  emission factors ( $\text{mg}/\text{m}^2$ ) and soil moisture (%) for weeding tests with highest confidence ratings.**

## 6.5 Confined Animal Facilities

Vertical profiles of PM<sub>10</sub> were collected downwind of confined animal facilities in 1995 and 1996. Emission factor confidence criteria used to select data for inclusion in this summary is similar to that used for the row crops but does not require upwind PM<sub>10</sub> concentrations be measured at multiple heights due to the relative unlikelihood of upwind contamination from the hay fields and vineyards upwind of the facilities. However, tests for which the upwind PM<sub>10</sub> concentration exceeded the downwind concentration at the height of measurement (3 m) were excluded from this summary. Average wind direction was restricted to within 45 degrees of perpendicular to the edge of the facility to ensure that the source was being measured quantitatively and tests with emission factor uncertainties of more than 100% were excluded from this summary.

The relationship between PM<sub>10</sub> emission factors for confined animal facilities and relative humidity is most apparent in the correlation where it can be seen that high PM<sub>10</sub> emissions are most likely in conditions of relative humidity under 40%. Thus, emission factors for dairy and beef are presented for conditions of less than and greater than 40% relative humidity.

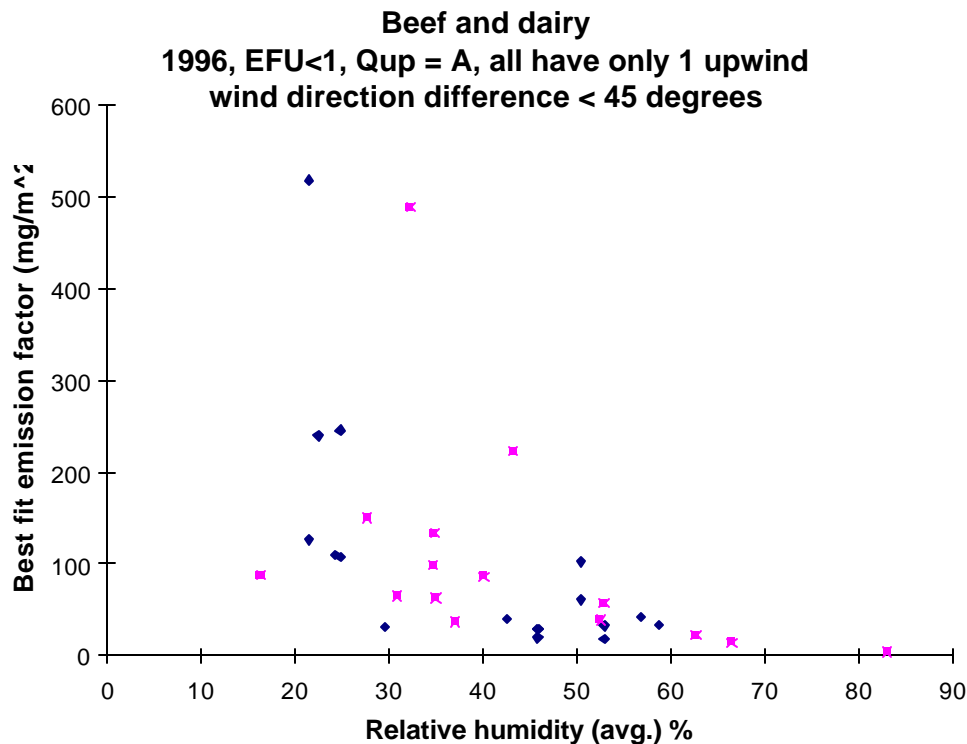


**Figure 6.9 Correlation of PM<sub>10</sub> emission factors (mg/m<sup>2</sup>) and relative humidity (%) for confined cattle tests with highest confidence ratings.**

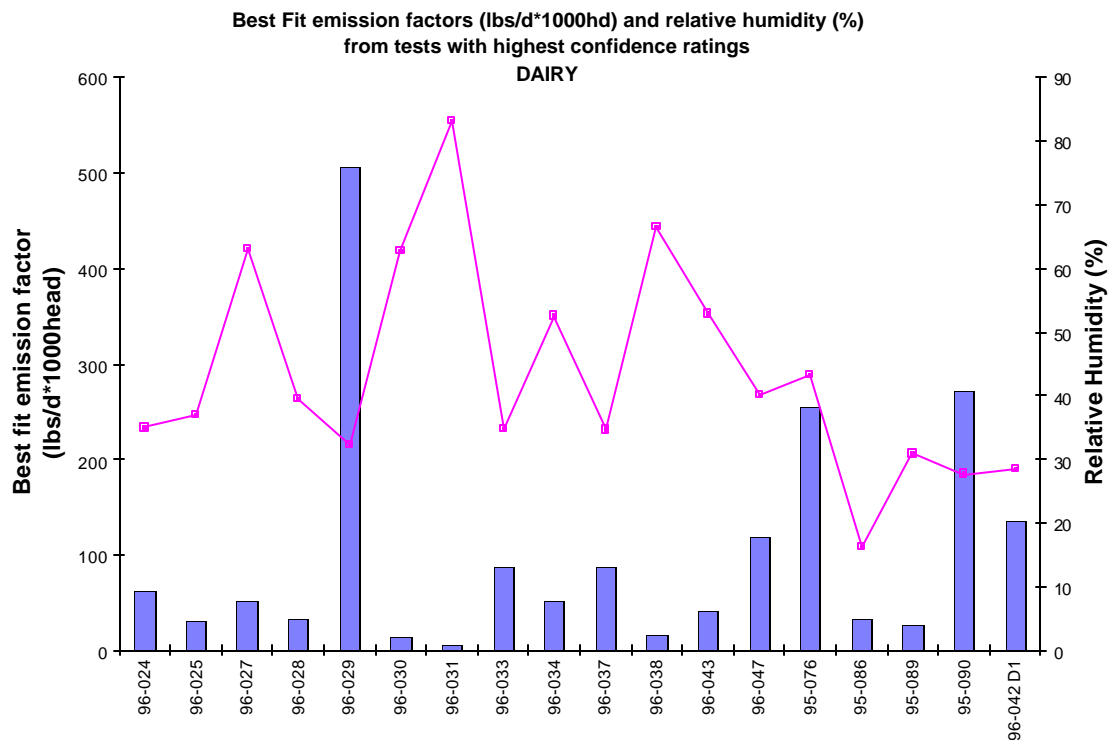


**Figure 6.10 PM<sub>10</sub> emission factors (lbs/d\*1000hd) and relative humidity (%) for dairy tests with highest confidence ratings.**

### 6.5.1 Dairy

Eighteen measurements of PM<sub>10</sub> emission factors from the dairy met the confidence rating criteria (Figure 6.10). Data collected in 1996 represent winter conditions (April) and those from 1995 represent summer conditions (October). The 1996 data show a strong relationship to relative humidity with the largest emission factor measured in the lowest relative humidity (test 96-029) and the lowest emission factor measured in the highest relative humidity (test 96-031). There is also a trend in the 1995 data collected during daytime (tests 95-086, 089, and 090; see table 5.19) linking relative humidity to PM<sub>10</sub> emission factors. The single nighttime test conducted in the summer indicates that PM<sub>10</sub> emissions in the early night hours (see Table 5.19 for exact times) can be elevated in the summertime, regardless of humidity. This phenomena can reasonably be attributed to the observed increased animal activity at dusk in the summer. Soil moisture and solar radiation data are not available for these tests but emission factors were lowest during night and morning hours and highest in the late afternoon and early evening. There was no precipitation during the time period over which samples were collected at this dairy and no dust control measures were applied.

## 6.5.2 Beef Feedlot

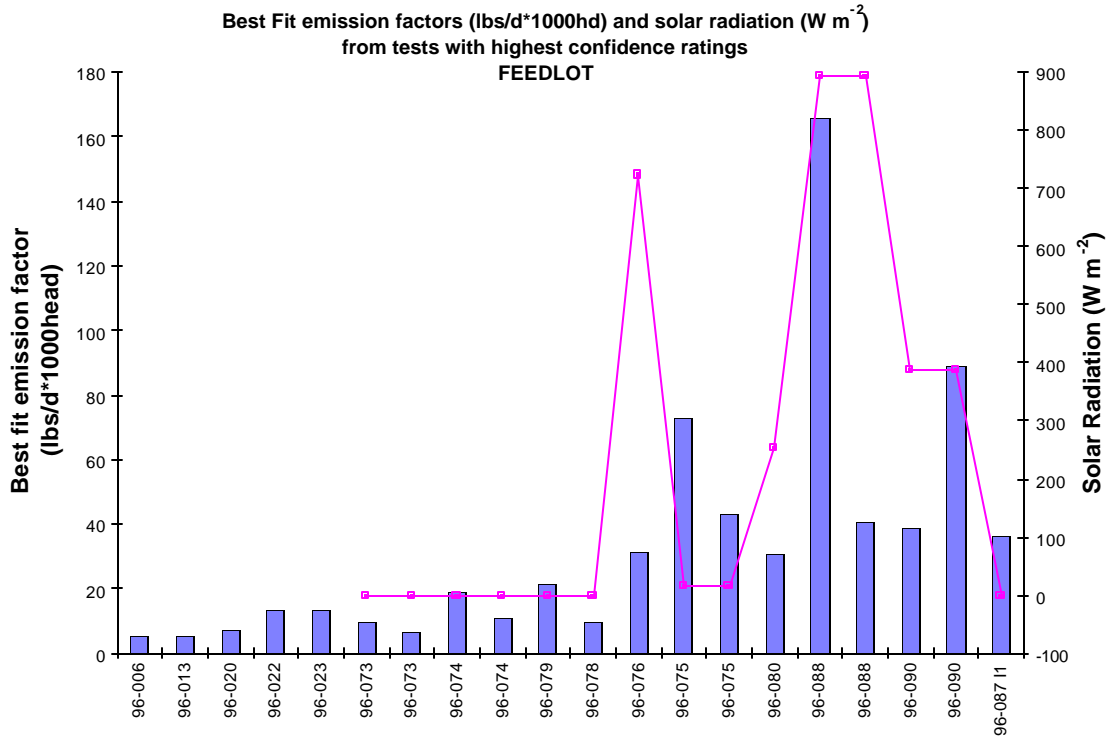


**Figure 6.11**  $PM_{10}$  emission factors (lbs/d\*1000hd) and solar radiation ( $W/m^2$ ) for feedlot tests with highest confidence ratings.

Measurements of  $PM_{10}$  were made at the feedlot in both March and July of 1996 (Figure 5.11). Solar radiation data is available for measurements made in July and a trend can be observed between  $PM_{10}$  emission and solar radiation. There is also a definite increase in  $PM_{10}$  emission in the summer season over that measured in the winter. Of the winter tests in this summary, the first three (96-006, 96-013, and 96-020) were conducted during daylight hours. Since emissions measured in those tests are not higher than emissions measured in the nighttime tests in the winter (tests 96-022 and 96-023), it is unlikely that variation in  $PM_{10}$  emission factor can be directly attributed to changes in solar radiation. However, it may be indicative of some underlying phenomena. The observed seasonal differences may be due to soil moisture but unfortunately, soil moisture data are not available for these tests. It is also likely that the peaks in  $PM_{10}$  emission factors observed at nighttime may be due to increased nighttime animal activity in the hot summer months.

## 6.6 Ammonia emission factors

Ammonia emission factors were quantified for a feedlot and three dairies using both direct measurements of ammonia concentrations and dietary nitrogen balance. In all cases, the average ammonia emission factors calculated by the two methods were comparable. Generally, ammonia emission factors calculated from dietary nitrogen will provide the most broadly applicable means for estimating average ammonia emission rates for any particular dry lot facility. However, in order to provide an estimate of the diurnal and seasonal variations of ammonia emissions from confined animal facilities, a summary of the measured ammonia emissions is also valuable. Calculated uncertainties for ammonia emission factors have not been developed as yet. Therefore, all of the data compiled from valid measurements over the term of the project (1996 to 1999) are summarized in this section with discussion to clarify the relative value of each data set.

**Table 6.2 Ammonia emission factors for open lot feedlots and dairies.**

SOURCE	SEASON	PERIOD	Ammonia emission factors (kg hd <sup>-1</sup> yr <sup>-1</sup> )		
			AVERAGE	STDEV	NUMBER
1996 field sampling campaign					
*Feedlot	Winter	Day	13.36	10.64	8
		Night	28.48	11.30	8
Feedlot	Summer	Day	105.92	78.09	4
		Night	21.65	7.86	5
1999 field sampling campaign					
Dairy	Winter	Day	48.11	79.39	8
		Night	17.05	15.20	7
Dairy	Winter	Day	32.35	17.40	15
		Night	26.95	17.94	8

\*Winter feedlot factors are computed from single height measurements only, and are of lower certainty than other factors in the table.

Day = test start times from 5:00 am to 5:00 pm. Night = from 5:00 pm to 5:00 am.

### 6.6.1 Beef Feedlot

Field measurements of ammonia emissions underwent a similar evolution of methods to that of the PM<sub>10</sub> emission factors. Measurements made at the feedlot in the winter did not include vertical profiles of ammonia concentration and measurements at the feedlot in the summer were seldom successful due to exceeding the capacity of the sampling apparatus. The feedlot ammonia emission factors presented in Table 6.2 are compiled from data collected during time periods when the wind direction was within 45 degrees of ideal and the use of secondary filters demonstrated that ammonia concentrations were measured accurately. Each emission factor is computed as an average of ammonia fluxes measured at two or more locations downwind of the facility to account for spatial variability in the source. The culling of lower confidence data results in relatively few data points, which may not be adequately representative of the source. Additionally, fewer measurement locations were used to characterize the heterogeneity of the

feedlot compared to the subsequent measurements made at the dairy in 1999, so confidence in the ammonia emission factors for feedlots is lower than that for dairies. Most importantly, emission factors for the feedlot in winter were calculated from ammonia concentrations measured at one height using the box model without the benefit of simultaneously collected profiles from which to judge the appropriate height of the plume. Therefore, the winter feedlot data should be used only for range finding and be considered highly uncertain.

Because the contribution of secondary particulate matter to  $PM_{10}$  is most significant in the winter, only one set of measurements was made in the summer, at the feedlot in 1996. A comparison of both the magnitude and the diurnal variation of ammonia emissions between winter and summer indicate the expected trends. While night time ammonia emission factors are similar in the two seasons, day time emissions in the summer were over 5 times those measured in the winter. Additional research is needed to verify this trend, however, using the concentration measured at a single height in the box model (as was done for the winter data) produces similar night time emission factors for the summer feedlot as were computed using the profiles, but underestimates the summer day time emission factors by an order of magnitude (10 times) (data not shown). Therefore, the ammonia emission factors for the feedlot in the summer most likely describe a real diurnal trend, because they are based on vertical profiles of ammonia concentration. The absence of a diurnal trend in the ammonia emission factors for the feedlot in the winter may be an artifact of the single height measurement technique, or it may be real (see discussion of diurnal trends in ammonia emission factors for dairies in the winter, section 6.6.2), but would need to be verified by measurements of the vertical profile of ammonia concentrations in the winter.

#### 6.6.2 Dairies

The ammonia emission factors for dairies averaged for Table 6.2 include only those tests for which the wind direction was within the arc described by lines drawn from the downwind measurement site to the two upwind corners of the facility. All of the included ammonia emission factors for dairies are computed from measurements of the vertical profile of ammonia concentration. Measurements were made at two heights in 1996 and at three heights in 1999, which indicates that emission factors computed from measurements made in 1999 are of lower uncertainty than the 1996 data. However, the climatic conditions were different in the two years and it is useful to consider both data sets in an interpretation of the diurnal trends in ammonia emissions from dairies.

Ammonia emission factors were computed from measurements made at three different dairies, one in 1996, and two in 1999. While all of the measurements were made in the winter season, the period of the 1996 measurements was characterized by spring-like conditions without rain or the temporal variability of frontal systems but both field trips in 1999 were interrupted by significant rain events. This fact may account for the observed variation in the evidence of diurnal patterns in ammonia emission factors of dairies between the two years. The more stable conditions of the 1996 field sampling period produced a larger difference between the day and night time averaged emission factors than the highly variable climate conditions experienced

during the 1999 field campaign. It is important to note that the larger number of tests used to compute the 1999 averages, and the relatively low standard deviations of those averages, indicate that the 1999 data merit higher confidence than the 1996 dairy ammonia emission factors.

## 6.7 Ongoing Research Directions

**Table 6.3 Completed measurements of PM<sub>10</sub> requiring further analysis and data reduction for the calculation of emission factors.**

<b>PM Tests Summary (1999-2000)</b>				Seasons: (Nov-Apr) Winter; (May-Oct) Summer	
<b>County</b>	<b>Crop</b>	<b>Practice</b>	<b>Operation</b>	<b># of Tests</b>	<b>Season/Yr.</b>
<b>1999</b>					
Kings	Wheat	Land Preparation	Discing	3	Summer 99
Kings	Wheat	Land Preparation	Floating	4	Summer 99
Kings	Wheat	Land Preparation	Ripping	4	Summer 99
Kings	Tomatoes	Land Preparation	Discing	11	Summer 99
Kings	Tomatoes	Land Preparation	Floating	3	Summer 99
Kings	Tomatoes	Land Preparation	Land Planing	4	Summer 99
Kings	Garbonzo	Land Preparation	Discing	3	Summer 99
Kings	Garbonzo	Land Preparation	Land Planing	8	Summer 99
Kings	Melon	Land Preparation	Discing	6	Summer 99
Kings	Melon	Land Preparation	Floating	1	Summer 99
Kings	Tomatoes	Harvest	Picking	4	Summer 99
Tulare	Milk	Dairy	Sleeping	3	Winter 99
Tulare	Milk	Dairy	Feeding	1	Winter 99
Tulare	Milk	Dairy	Activity	1	Winter 99
Tulare	Milk	Dairy	Loafing	14	Winter 99
Kings	Cotton	Harvest	Gin	7	Winter 99
<b>2000</b>					
Fresno	Wheat	Land Prep	Floating	23	Summer 00
Fresno	Tomatoes	Land Prep	Discing	6	Summer 00
Fresno	Cotton	Land Prep	Ripping	11	Winter 00
Fresno	Cotton	Land Prep	Discing	4	Winter 00

Recent field sampling activities associated with this study (Table 5.3) have addressed the need for better understanding of PM<sub>10</sub> emission factors for land preparation operations. There has been an emphasis on testing similar operations on similar fields following different crops and on fields of different soil texture properties following the same crop. These tests have been conducted with the intent to distinguish between the effects of soil moisture, soil silt content, and crop on PM<sub>10</sub> emission factors for tillage operations. The PM samples collected at the dairy in 1999 were specifically used to understand the contribution of nitrate particulates to the measurements of ammonia and are not useful for the calculation of PM emission factors.

The importance of soil properties such as moisture and silt content demonstrate how crucial it is to integrate the soils data that has been generated for this study with the PM<sub>10</sub> emission factors data. This database development will be an important task for this project in 2001 as will the

implementation of an improved sampling protocol and an assessment of analytical uncertainty in the measurement of soil parameters. These steps should result in better data recovery and greatly enhance the interpretability of the PM<sub>10</sub> emission factors calculated from the concentrations measurements.

The PM<sub>10</sub> concentrations and wind speeds used to calculate the emission factors presented in this report are currently archived in a collection of databases at Crocker Nuclear Laboratory (see Appendix G for structure information). Efforts are currently underway to automate data retrieval and emission factor calculation. These activities will be pursued concurrently with the development of the soil properties databases and the reduction of data from measurements made in 1999 and 2000. As these higher level data integration and quality assurance protocols and mechanisms are developed, a vehicle will be derived for the distribution of both raw data and computed emission factors to the research community. The air quality group will draw on experience gained in making data from the IMPROVE program available through a dial-in service to accomplish this task.

## 7 ASSOCIATED RESEARCH: PM<sub>10</sub> POTENTIAL

### Introduction

Airborne particles are a regulated (criteria) air pollutant. Current regulations control the concentration of PM<sub>10</sub>, i.e. particulate matter less than 10 µm aerodynamic diameter. Particles of this size are hazardous to human health, as they can penetrate pulmonary defenses and lodge deep in the lung. In general, particles larger than 1-2 µm are created mostly from natural processes and are dominated by soil dust. Smaller particles are generally created from combustion sources and from chemical reactions between airborne gases. Considerable evidence exists that the smaller particles are more hazardous to health than are the larger particles (Pope, Thun et al. 1995); (Schwartz, Dockery et al. 1996); (Klemm, Mason et al. 2000), but the larger particles have not been exonerated and are still subject to regulation.

The concept of dustiness index has been explored by other researchers, including the British Occupational Hygiene Society Technology Committee Working Party on Dustiness Estimation (BOHS 1988), (Chung and Burdett 1994), (Heitbrink 1990), and (Hjemsted and Schneider 1996). Three different principles of dust generation were used by these researchers; a single drop of material into an enclosed chamber, a rotating drum to allow multiple drops of material, and fluidization by forcing air upward through the material. All methods produce a dustiness index that relates the mass of dust produced to the mass of soil that produced it. The BOHS working party evaluated the operating principles of the single drop method in detail (BOHS 1988) by varying the mass of material dropped, the drop height, and the method of dropping it (single drop or stream). They concluded that the dust yield is strongly influenced by the size of sample and the height of drop, and that reproducibility is greater when the sample is released as a stream. They also found differences in dustiness depending on the sample grain size distribution.

We have designed a dust resuspension chamber to examine the PM<sub>10</sub> characteristics of soil samples collected in California's San Joaquin Valley (SJV). The chamber allows us to determine the potential for PM<sub>10</sub> production from soils collected in the San Joaquin Valley and the relative energy required to generate PM<sub>10</sub> from the soil. In this section we describe the operating parameters of the resuspension chamber system and apply some observed relationships between soil texture and PM<sub>10</sub> production to predict the PM<sub>10</sub> potential of SJV soils. Experiments performed in the UC Davis CNL dust resuspension – collection chamber have shown that the ability of soil to release PM<sub>10</sub> under controlled laboratory conditions depends on the soil texture, as defined by the percent sand, silt, and clay measured by wet sieving. Soils with the same dry silt content obtained by dry sieving, do not necessarily have equivalent potential to emit PM<sub>10</sub>. An index of PM<sub>10</sub> emissions may improve our ability to estimate PM<sub>10</sub> emissions from more easily measured parameters.

### Description:

The Crocker Nuclear Laboratory resuspension system consists of three major components:

- Dust Resuspension Chamber
- Dust Collection Chamber
- PM<sub>10</sub> inlet and IMPROVE Sampler

### Dust Resuspension Chamber:

The dust resuspension chamber is designed as a fluidized bed to agitate and suspend the ~ PM<sub>50</sub> from the soil sample facilitating collection of PM<sub>10</sub> from the produced air stream (Figure 7.1). The chamber consists of a stainless steel tube with a conical taper at both ends, and has a volume of 247.2 cm<sup>3</sup>. An aluminum tube of 1.0 cm diameter extends from the top of the dust resuspension chamber to the inside of the dust collection chamber.

The soil sample is placed in the bottom, on a 2.5 cm diameter fritted glass filter. The soil sample is agitated at 3.5 lpm for 15 seconds to put the PM<sub>50</sub> particles in suspension. Higher flow rates through the soil sample do not change the particle size collection characteristics, as they are determined by the sampler inlet, but would remove larger particles from the soil sample. The dust resuspension chamber has a separate flow meter and pump to control the flow of air into the soil sample.

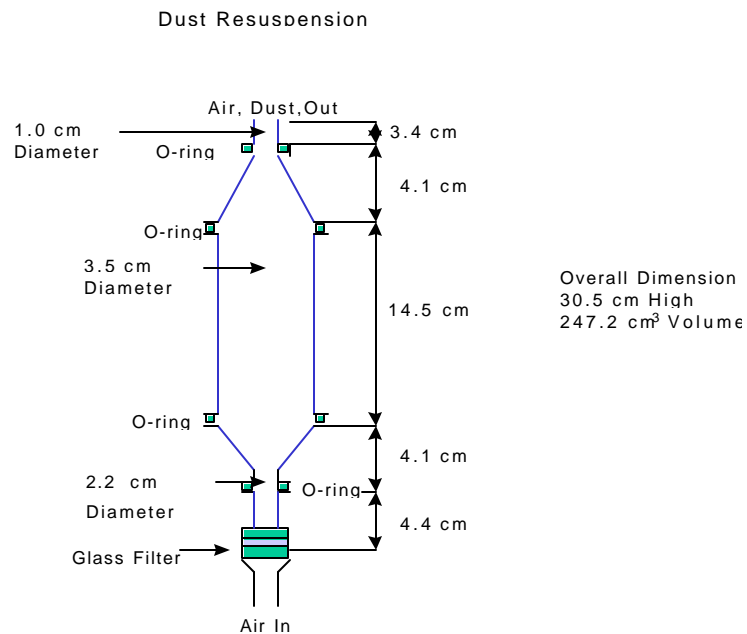


**Figure 7.1 Diagram of dust resuspension chamber**

## 7.1 Dust Collection Chamber:

The dust collection chamber (Figure 7.2) is a painted wood box with interior dimensions 50 cm high by 37 cm wide by 50 cm deep. It has a 19.8 cm by 30.5 cm Plexiglas window in the front and a hole in the bottom for the  $PM_{10}$  inlet. The inlet hole is sealed to the inlet tube. Filtered air enters the collection chamber through a hole in the top to allow clean make-up flow to enter as dust-laden air is removed by the sampler. The total working volume of the test chamber is 92.5 liters.

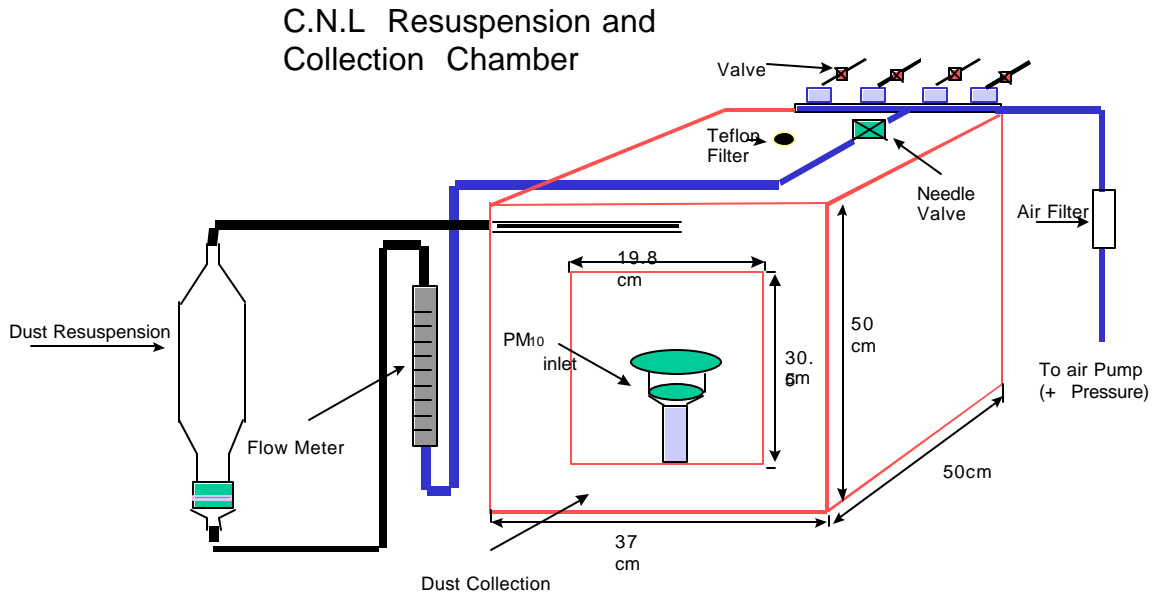


**Figure 7.2 Diagram of CNL resuspension and collection chamber**

## 7.2 $PM_{10}$ Inlet and the IMPROVE Sampler

A Sierra Andersen  $PM_{10}$  inlet is used to collect the resuspended dust at a flow rate of 16.7 lpm. This inlet is widely used in sampling networks to obtain a  $10\ \mu\text{m}$  size cut. Particles greater than  $10\ \mu\text{m}$  aerodynamic diameter are removed from the air stream by inertial separation.

The  $PM_{10}$  inlet is attached to an IMPROVE (Interagency Monitoring of PROtected Visual Environments) sampler consisting of four independent filter cassettes, a common flow controller, a vacuum pump, and a flow rate measurement system. The active sample filter can be changed instantly by activating and deactivating the controlling solenoids. In this manner, up to four sequential filter samples can be collected without opening the chamber or taking time for filter changes.

**Experimental:**

Most dust resuspension systems that measure the “dustiness” potential of material are concerned with size modes coarser than PM<sub>10</sub>. (Singh, Gregory et al. 1994). Since the main concerns of this project is with soil particles that remain suspended in the ambient air, the soil samples are dried and sieved to obtain the fraction less than or equal to 75µm in physical diameter prior to introduction to the resuspension chamber. Tests have also been run on other soil size fractions to determine how much PM<sub>10</sub> can be obtained from different fractions of the soil. To measure the maximum PM<sub>10</sub> potential of the soil, only oven-dried soil is used. The moisture content of resuspended soil, as well as the humidity of the atmosphere, may have an effect upon PM<sub>10</sub> potential of soils. The ambient relative humidity and temperature are kept relatively constant between experiments to ensure intercomparability.

Approximately 1g of sieved soil material (particles less than 75 µm physical diameter) is placed in the dust resuspension chamber, which is then sealed with a clamp. A measured volume of air (3.5 lpm for 15 seconds) is forced through the soil sample at the base of the fluidizing bed. The 3.5 lpm flow rate corresponds to a velocity of 15.4 cm/s at the bottom of the resuspension chamber, and is sufficient to suspend dust particles of ~50 µm aerodynamic diameter. The suspended particles are then carried into the middle section of the resuspension chamber, where the velocity drops to 10.6 cm/s due to the expansion of the chamber cross-section. Particles with an aerodynamic diameter greater than ~40 µm cannot be carried past the middle section of the resuspension chamber. Smaller particles are carried out of the resuspension chamber and into the collection chamber.

After the dust is separated from the soil sample in the resuspension chamber, it is introduced to the collection chamber at the top via the 1 cm diameter aluminum tube. The dust is mixed throughout the chamber and is collected through a Sierra Anderson PM<sub>10</sub> inlet connected to an IMPROVE sampler containing four filter cartridges. The dust is collected on 47 mm Teflon filters that are changed regularly to obtain a time record of dust concentration. The design flow rate for the inlet is 16.7 lpm. Because the flow rate from the dust generation chamber lasts only 15 seconds and is only a fraction of the sampler flow rate, the remaining sample volume is replaced by fresh air introduced through a filtered hole in the top of the chamber.

Several methods of PM<sub>10</sub> sample collection have been tried in developing the PM<sub>10</sub> index measurement protocol. Initially, the first sample was collected for one minute, followed by two minutes for the second, four minutes for the third, and eight minutes for the fourth filter. Thus, the total sampling time was 15 minutes. In this time, the amount of PM<sub>10</sub> collected on the fourth filter dropped to a nearly negligible amount, indicating that fifteen minutes was sufficient to collect all the dust that was introduced into the chamber. This time period corresponds to nearly three volume changes of the dust collection chamber.

Collection time was then increased such that all the PM<sub>10</sub> produced by a 15-second “puff” was collected on a single filter in 15 minutes, then the PM<sub>10</sub> produced by two cycles of a 15-second “puff” was collected during two 15-minute collections, then three cycles on a third filter, and

finally four cycles on a fourth filter. The total time for PM<sub>10</sub> production and collection in this method is 150 minutes, but results in more complete removal of PM<sub>10</sub> from the soil sample. The total suspension time, though, is only 150 seconds, to minimize disaggregation of particles that may be bound tightly together. The masses of PM<sub>10</sub> collected on the four sequential filters in this manner are used to compute the PM<sub>10</sub> potential of the soil through application of the following theory.

## Theory

The differential equation for the mass of dust in the collection chamber can be written as:

$$\frac{dM(t)}{dt} = E - D - R, \quad (7.1)$$

where  $M(t)$  is the mass of dust suspended in the collection chamber at time  $t$ ,  $E$  is the emission rate into the chamber,  $D$  is the deposition rate to the walls and floor of the chamber, and  $R$  is the sampling removal rate. These last three terms can be written as

$$E = k_1 M_s(t), \quad (7.2)$$

$$D = \frac{M(t) \times V_d}{H} = \frac{A \times M(t) \times V_d}{V}, \text{ and} \quad (7.3)$$

$$R = \frac{M(t) \times F}{V} \quad (7.4)$$

where  $k_1 M_s(t)$  is the mass emission from the soil sample,  $H$  is the height at which the sample is introduced into the collection chamber,  $A$  is the floor area of the collection chamber,  $V_d$  is the deposition velocity of the dust,  $V$  is the collection chamber volume, and  $F$  is the sample collection flow rate. The dust concentration in the chamber can now be written as

$$\frac{dM(t)}{dt} = k_1 M_s(t) - \left[ \frac{A \times V_d + F}{V} \right] \times M(t). \quad (7.5)$$

In a normal laboratory atmosphere, the initial dust concentration in the chamber can be neglected relative to the concentration generated from resuspending a soil sample. We do not yet know the form of the input mass emission rate as a function of time ( $R_1 M_s(t)$ ), but if it is constant during the experiment the equation becomes a first order differential equation of the form

$$\frac{dM(t)}{dt} = k_3 - k_2 \times M(t) \quad (7.6)$$

with a solution given by

$$M(t) = \frac{k_3}{k_2} [1 - e^{-k_2 t}]. \quad (7.7)$$

Note that if the input mass emission rate is initially very high, then drops quickly (e.g., a puff entering the collection chamber), the form of the equation simplifies to

$$M(t) = M_0 \times e^{-k_2 t} \quad (7.8)$$

after the initial puff is over. This functional form (cumulative mass =  $a \cdot (1 - e^{-bt})$ ) has the desired properties of an asymptotic limit ( $a$ ) and a time constant ( $b$ ) that depends on the chamber operating parameters. The asymptotic limit represents the potential of the soil to emit PM<sub>10</sub>, as tested using our operating conditions. This parameter represents the cumulative mass that would be measured if we extended the suspension sampling time indefinitely (and if soil particles did not break down due to the extended agitation). The time constant is related to the volume of the test chamber and the removal rate (sample flow rate) of air within the chamber.

The PM<sub>10</sub> Index is calculated by fitting the cumulative mass  $M$  collected on the four sequential filters as a function of time  $t$  to the equation  $M = a(1 - e^{-bt})$ . The parameter  $a$  is the asymptote of the exponential curve and represents the PM<sub>10</sub> Index; i.e. it is the maximum amount of PM<sub>10</sub> that would be released by repeated “puffs” if disaggregation did not occur. The parameter  $b$  represents how rapidly the PM<sub>10</sub> is released. An example of the curve fit for any of the resuspension data is shown in Figure 7.3.

## Results:

A series of 44 soil samples representing a wide range of agricultural and urban uses and the entire spectrum of soil textures were resuspended to obtain PM<sub>10</sub> indices. These soils were chosen as representative of a variety of textures, crops, and other sources of fugitive dust and were not necessarily collected at the same sites as where aerosols (PM emission) were measured. Average PM<sub>10</sub> masses collected on each of the four filters used in the resuspension are presented in Table 7.1, grouped by the texture of the soils. The data for the average clay soil is presented graphically in Figure 7.3, indicating the PM<sub>10</sub> potential = 18.203 mg/g.

**Table 7.1 Averages of cumulative mass (mg/g) as a function of time for tested soils.**

Filter	Time (min)	Clay		Loam		Clay Loam		Silty Clay Loam		Sandy Loam		Silty Clay	
		Average	St.Dev	Average	St.Dev	Average	St.Dev	Average	St.Dev	Average	St.Dev	Average	St.Dev
1	15	4.599	0.37	3.819	0.07	3.240	0.14	3.510	0.04	2.933	0.81	5.002	0.02
2	45	13.384	0.31	9.364	0.03	8.854	0.32	9.395	0.08	7.012	1.12	11.096	0.02
3	90	16.993	0.04	11.890	0.12	12.228	0.61	13.125	0.03	9.107	0.88	14.354	0.08
4	150	19.503	0.50	12.724	0.21	13.946	0.89	14.700	0.02	10.097	0.87	15.888	0.08

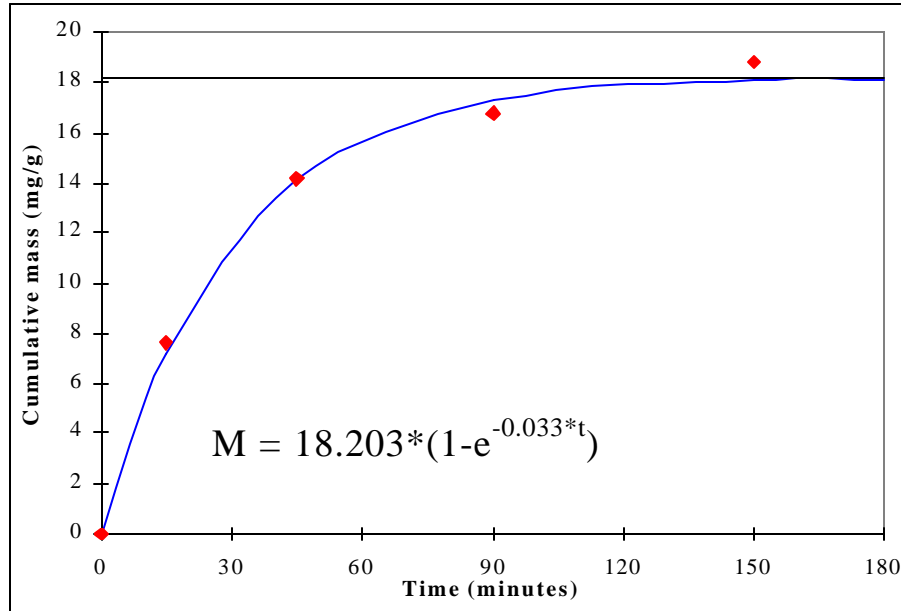


**Figure 7.3 PM<sub>10</sub> Index curve for the clay soils data in table 7.2.**

The potential of soil to emit PM<sub>10</sub> quantified for these 44 soils is reproducible and displays a strong relationship between the PM<sub>10</sub> Index and the properties of the soil texture (Sand %, and Clay %). Two linear equations were derived from this data set describing the dependence of PM<sub>10</sub> potential on sand and clay percentages of the soil. These relationships were then tested by analyzing 11 soils samples, spanning different textures and collected simultaneously with the measurements of PM<sub>10</sub> emission factors described in this report, for PM<sub>10</sub> Index soil samples. The textures, collection dates, and associated PM<sub>10</sub> emission factor test numbers are presented in Table 7.2 and the cumulative mass curves are shown in Figure 7.4.

**Table 7.2 Partial list of the USDA soil tested from San Joaquin Valley**

County	Test #	Array	Date	Soil Texture
Kings	95-114-115	N1	10/25/95	Clay
Merced	95-001-003	F1	7/6/95	Loam
Kings	95-040-042	P2	9/8/95	Clay Loam
Kings	96-051-053	S2	6/22/96	Silty Clay Loam
Kings	96-099	S6	11/14/96	Loam
Kings	96-096	S5	11/14/96	Sandy Loam
Kings	97-045	S1	6/24/97	Sandy Loam
Kings	97-041	S3	6/21/97	Silty Clay Loam
Fresno	98-001	J1	6/4/98	Clay Loam
Kings	98-012	P1	6/11/98	Clay Loam
Kings	98-012-014	P2	9/13/98	Sandy Loam

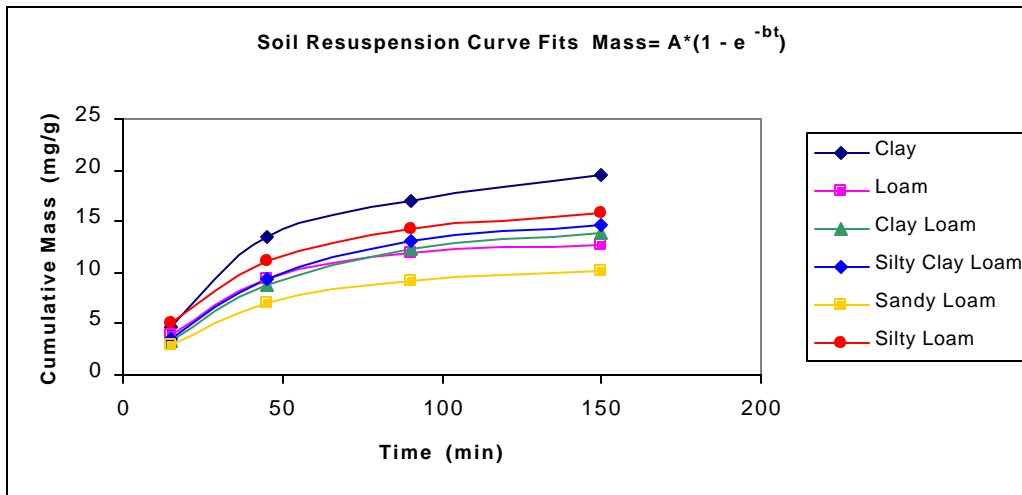


**Figure 7.4 Cumulative mass for resuspension of select soils collected simultaneously with  $PM_{10}$  emission factor measurements.**

The results of these resuspension tests tend to group according to soil textures (Figure 7.4). The clay and silty clay samples have the highest cumulative mass ( $PM_{10}$  potential), the clay loam and loam samples are next, the sandy loam follows next, and sand samples have the lowest  $PM_{10}$  potential. The analysis of additional soil samples with high sand content should help clarify this grouping. The other soils tend to have cumulative mass ( $PM_{10}$  potentials) that are similar for similar textures (fractions of sand, silt, and clay).

These findings are in agreement with the relationships initially observed between soil textural properties and  $PM_{10}$  potential. Thus, the linear equations formulated from the original data set ( $y = mx + b$  ;  $y = PM_{10}$  Index and  $x = \% \text{ Sand or } \% \text{ Clay}$ ) were used to calculate the  $PM_{10}$  Index for all soils collected in association with this study. Table 7.3 and Figure 7.5 show the relationship between the measured  $PM_{10}$  potential and the  $PM_{10}$  Index calculated as the average of computations made using % sand and % clay for the selected soils for which measurements were made.

**Table 7.3 USDA soils tested for PM<sub>10</sub> index .**

County	Test #	Array	Date	Soil Texture	Experimental PM <sub>10</sub>	Calculated PM <sub>10</sub>
Kings	95-114-115	N1	10/25/95	Clay	20.545	20.073
Merced	95-001-003	F1	7/6/95	Loam	13.445	13.369
Kings	95-040-042	P2	9/8/95	Clay Loam	16.385	15.754
Kings	96-051-053	S2	6/22/96	Silty Clay Loam	15.794	15.546
Kings	96-099	S6	11/14/96	Loam	13.266	11.679
Kings	96-096	S5	11/14/96	Sandy Loam	9.924	9.798
Kings	97-045	S1	6/24/97	Sandy Loam	11.089	11.219
Kings	97-041	S3	6/21/97	Silty Clay Loam	16.212	16.395
Fresno	98-001	J1	6/4/98	Clay Loam	14.667	14.717
Kings	98-012	P1	6/11/98	Clay Loam	14.006	13.973
Kings	98-012-014	P2	9/13/98	Sandy Loam	9.924	10.551

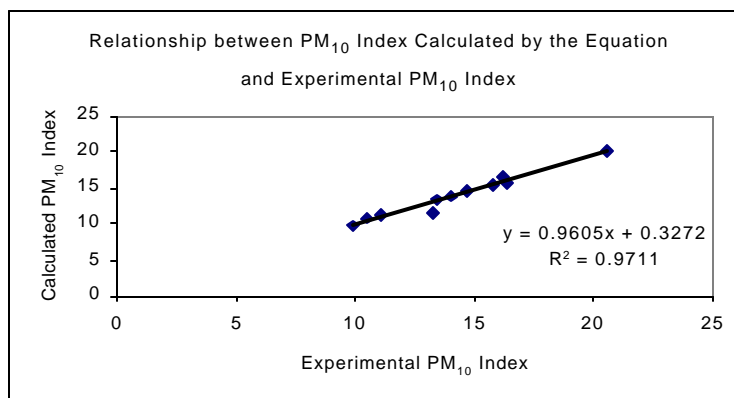


**Figure 7.5 Relationship between PM<sub>10</sub> Index calculated by the straight line and experimental PM<sub>10</sub> Index.**

Figure 7.6 shows the distribution of soil texture for all the soils analyzed in the development of the PM<sub>10</sub> Index. These soil textures span the same range of soils collected for the study of PM<sub>10</sub> emissions from agricultural operations. The sand ranges from ~5% to over 90%, silt ranges from

less than 5% to over 40%, and the clay ranges from less than 5% to about 55%. Since the application of this empirically derived relationship of PM<sub>10</sub> Index with soil texture appears to be robust across much of this range, we have used measured sand % and clay % to compute PM<sub>10</sub> indices for all of the soils collected simultaneously with PM<sub>10</sub> emission factor measurements.

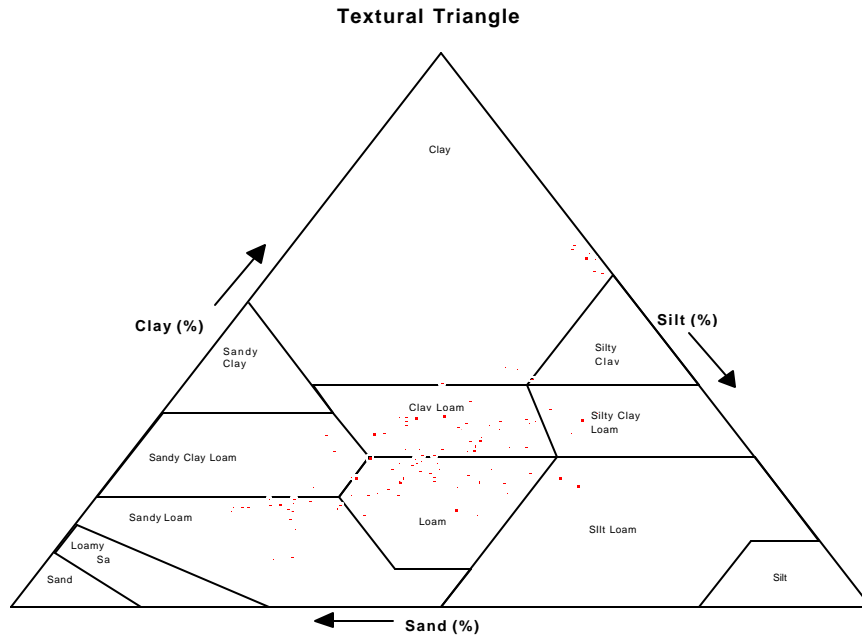


**Figure 7.6 Distribution of soil texture for soils analyzed, based on wet sieving.**

PM<sub>10</sub> Indices in Tables 7.4 to 7.7 were derived from the relationship between the PM<sub>10</sub> Index and the standard soil texture parameters sand, silt, and clay. The PM<sub>10</sub> Index is presented for 0-75 μm fraction of dry-sieved soil. The sand, silt, and clay were measured by wet sieving and represent the soil particle size distribution for completely disaggregated soil. There is an excellent correlation between the PM<sub>10</sub> Index and all three soil size fractions, but the best relationship is with the percent clay and sand, and the relationship with the percent silt has the lowest correlation.

There is a poor relationship between the PM<sub>10</sub> Index and the soil dry silt content (i.e., the <75 μm fraction obtained by dry sieving), this fraction includes aggregates of smaller particles. The relationship shows much more scatter than for any of the soil texture parameters obtained by wet sieving.

**Summary and Conclusions:**

The utility of any parameter used to estimate dust emissions depends on it being more easily measured than a measurement of the actual emissions. At this time, the U.S. EPA recommends using the dry silt content of a soil to estimate the emissions through the use of published

empirical equations. However, the dry silt content of a soil is not readily available for large tracts of land and must therefore be measured for each soil. For use in agricultural emissions the soil texture is much more readily available in soil surveys published by the USDA. Our results show that the PM<sub>10</sub> Index is better correlated to the readily available soil texture than to the dry silt content. For this reason, we expect it to be a better parameter to use in emission calculations. We plan to pursue the relationship between the PM<sub>10</sub> Index and our measurements of dust emissions from various agricultural operations, including different soil types and with varying moisture content. If there is a good relationship between the dust emissions and the operation and soil conditions, we will be better able to predict dust emissions from readily available parameters.

We have developed a laboratory procedure to describe the potential of soil to release PM<sub>10</sub> dust into the atmosphere. When applied to soil samples collected in California's San Joaquin Valley the PM<sub>10</sub> Index is highly correlated with the soil texture determined by wet sieving. For example, clay and silty clay soil have a higher potential to emit PM<sub>10</sub> dust, and sandy and loamy sand soil have lower potential to emit PM<sub>10</sub> dust.

Although there is a good relationship between the soil texture parameters (sand, silt, and clay) and the PM<sub>10</sub> Index, there is a poor relationship between the dry silt content (fraction of soil <75 µm by dry sieving) and the PM<sub>10</sub> Index. The dry silt content is currently used to estimate dust emissions for a variety of activities, including agricultural operations, that produce fugitive dust. We expect the PM<sub>10</sub> Index to be more consistently related to measured dust emissions after accounting for differences between agricultural operations and soil moisture.

Additional research is planned to further define the potential of soils to emit PM<sub>10</sub>. This research will include additional soil textures that extend the range of soil testing beyond the 11 soil types (soil texture) analyzed so far. Examination of the PM<sub>10</sub> potential of soil fractions other than the "silt" fraction (<75µm) is also planned.

Field	Array	Test #	Date	Soil type	Sand	Silt	Clay	Silt Cont	PM <sub>10</sub> Index
					(%)	(%)	(%)	(%)	
4	F1	95-001-003	7/6/95	Loam	29.6	49.3	21.1	15.7	13.369
19	F2	95-004-007	7/7/95	Silt Loam	21.5	55.3	23.3	19.4	14.221
20	F3	95-008-010	7/10/95	Silt Loam	23.8	53.8	22.4	20.7	13.949
2	F4	95-015-017	7/12/95	Loam	30.6	46.4	24.7	15.5	13.501
341	P1	95-051-059	9/12/95	SaCl Loam	57	23.8	19.2	11.7	11.1
350	P2	95-040-042	9/8/95	Clay Loam	24.4	37.6	38	8.04	15.754
342	P3	95-043-046	9/10/95	Clay Loam	33.7	37.8	28.5	8.75	13.929
328	P4	95-047-05	9/11/95	Loam	48.2	32	20.4	11.49	11.819
328A	P5	95-057-059	9/18/95	Loam	41.3	34.6	24	11.14	12.841
328B	P6	95-060-062	9/18/95	Loam	45.1	32.4	22.6	14.9	12.384
350B	P7	95-063-065	9/18/95	Clay Loam	39	33.3	27.8	14.11	13.452
Sec. 1.6	N1	95-114-115	10/25/95	Clay	1.5	38.2	60.3	10.47	20.074
Sec. 1.7	N2	95-143-149	11/14/95	Clay	1.5	34.8	63.7	4.07	20.485
Vineyard	R1	95-092	10/10/95	Sandy Loam	64	27.2	8.8	21.83	9.361
Sec. 10	S1	95-093-096	10/18/95	Loam	32.3	39.9	27.8	16.1	13.957
Sec. 2	S2	95-095-113	10/20/95	Loam	49.2	32.4	18.4	19.69	12.653
Sec. 13E	S3	95-125-127	10/30/95	Clay Loam	40.6	33.5	26	10.08	13.127
Sec. 13	S5	95-128-132	11/3/95	Clay Loam	39.5	37	23.5	12.89	13.796
Sec. 1S	S6	95-136-138	11/6/95	Loam	24.8	42.8	32.4	16.59	15.047
Sec. 1N	S7	95-135	11/5/95	Loam	25.6	41.2	33.2	13.19	15.082

**Table 7.4 Results from soil samples collected in 1995**

**Table 7.5 Results from soil samples collected in 1996**

Field	Array	Test #	Date	Soil Texture	Sand	Silt	Clay	Silt Cont	PM <sub>10</sub> Index
Sec.10 NE	S1	N/A	6/21/96	Clay Loam	23.2	43.7	33.1	20.7	15.249
Sec.10 NE	S1	N/A	6/21/96	Clay Loam	29.9	39.4	30.7	16.7	14.450
Sec.10 NE	S1	N/A	6/21/96	Clay Loam	27.2	40.9	31.9	18.4	14.798
Sec.10 SE	S2	96-049-050	6/21/96	Loam	40.5	33.9	25.6	17.2	13.063
Sec.10 SE	S2	96-049-050	6/21/96	Loam	41.8	32.2	26	19.9	13.008
Sec.10 SE	S2	96051-053	6/22/96	Silty Clay Loam	19.2	49.6	31.2	22	15.313
Sec.10 SE	S2	96-051-053	6/22/96	Silty Clay Loam	16.8	49.7	33.6	19.2	15.779
Sec.10 SE	S2	96-054-056	6/24/96	Silty Clay Loam	14.4	50.8	34.8	22.6	16.000
Sec.18 SW	S3	96-057-063	6/27/96	Clay Loam	39.9	31.7	28.4	20.7	13.433
Sec.18 SW	S3	96-057-063	6/27/96	Clay Loam	35.7	36	28.3	18.6	13.734
Sec.5 E	S5	96-095	11/10/96	Sandy Loam	67.5	19.8	12.7	15.3	9.520
Sec.5 E	S5	96-095	11/10/96	Sandy Loam	67.8	19	13.1	14.3	9.547
Sec.5 E	S5	96-095	11/10/96	Sandy Loam	65.5	21.2	13.3	15.4	9.744
Sec.5 E	S5	96-096	11/11/96	Sandy Loam	65.1	21.3	13.6	15.4	9.798
Sec.5 E	S5	96-097	11/12/96	Loam	40.6	41	18.4	18.8	12.207
Sec.5 E	S5	96-103-104	11/16/96	Sandy Loam	58.4	26.9	14.7	27	10.436
Sec.10 W	S6	96-099	11/14/96	Sandy Loam	54.8	28.5	16.7	14.5	10.940
Sec.10W	S6	96-099	11/14/96	Loam	44.2	41	14.8	13.7	11.515
Sec.10 W	S6	96-099	11/14/96	Loam	34.9	47.2	18	15.9	12.583
Sec.11 E	S8	96-101	11/15/96	Loam	44.7	31.8	23.6	20.7	12.511
Sec.11 E	S8	96-108	11/20/96	Clay Loam	41.8	28.9	29.4	15.9	13.411
Sec.11 E	S8	96108	11/20/96	Clay Loam	45.3	28.2	26.5	18.2	12.805
Sec.11 E	S8	96108	11/20/96	Clay Loam	42.6	29.1	28.3	19.1	13.228
Sec.1 W	S9	96105	11/18/96	Clay Loam	40.2	32.9	27	17.3	13.244
Sec.1 W	S9	96-105	11/18/96	Clay Loam	37.6	32	30.3	16.5	13.836
Sec.1 W	S9	96-105	11/18/96	Clay Loam	33.5	38	28.5	17.5	13.933
Sec.11 E	SA	96-115	12/2/96	Clay Loam	27.9	42	30.1	18.1	14.531
Sec.11 E	SA	96-116	12/2/96	Clay Loam	21.3	43.2	35.5	15.1	15.662
Sec.11 E	SA	96-117	12/2/96	Clay Loam	39	31.8	29.2	12.9	13.600
Sec.11 E	SC	96-118	12/4/96	Clay Loam	39.3	33	27.7	19	13.395
Sec.11 E	SC	96-119	12/4/96	Clay Loam	31	38.1	30.9	20	14.399
Sec.11 E	SC	96-120	12/5/96	Loam	41.1	33.6	25.4	14.5	12.993
Block 6	F1	96-064-066	7/2/96	Loam	39.5	43.1	17.4	14.4	12.164
Block 9	F2	96-067-071	7/3/96	Loam	37.4	46	16.6	15.3	12.234
Block 9	F2	96-067-071	7/3/96	Loam	32.1	47.5	20.4	16.1	13.084

**Table 7.6 Results from soil samples collected in 1997**

Field	Array	Test #	Date	Soil Texture	Sand	Silt	Clay	Silt Cont	PM <sub>10</sub> Index
Sec. 2	S1	97-033-036	6/18/97	Loam	50.4	29.6	20	9.7	11.686
Sec.2	S1	97-039-040	6/20/97	Sandy Loam	59.5	24.6	8	11.8	10.53
Sec.2	S1	97-047	6/24/97	Sandy Loam	53.1	29.1	17.8	17.9	11.219
Sec. 14	S3	97-041	6/21/97	Silty Clay Loam	18.7	41.3	39.9	7	16.395

**Table 7.7 Results from soil samples collected in 1998**

Field	Array	Test #	Date	Soil Texture	Sand	Silt	Clay	Silt Cont	PM <sub>10</sub> Index
Sec. 10 W	J1	98-001-004	6/4/98	Clay Loam	32.1	33.9	34.1	3	14.717
Sec. 10 W	J1	98-005-009	6/5/98	Clay Loam	37.2	29.9	32.9	3.5	14.188
Sec. 10 W	J1	98-010-011	6/6/98	Clay Loam	37.1	28.6	33.8	4.1	14.299
PF7	P1	98-012-014	6/11/98	Clay Loam	38.5	27.7	34.4	5.6	14.207
PF7	P1	98-012-014	6/11/98	Clay Loam	41.1	26.7	32.2	3.3	13.818
PF7	P1	98-015-017	6/11/98	Clay Loam	44.9	23.5	31.7	2.8	13.473
PF7	P1	98-015-017	9/11/98	Clay Loam	42.5	25.6	32.1	4.3	13.702
PF7	P1	98-018-020	6/11/98	Clay Loam	41.2	27.1	31.8	4	13.758
PF7	P1	98-018-020	6/11/98	Clay Loam	41.6	26.8	31.7	3.4	13.716
PF7	P1	98-021-023	6/12/98	Clay	26.2	31.4	42.3	4.3	16.121
PF7	P1	98-021-023	6/12/98	Clay Loam	29.9	33.9	36.3	7.3	15.124
PF7	P1	98-024-027	6/12/98	Clay	29.8	30	40.9	2.5	15.683
PF7	P1	98-024-027	6/12/98	Clay Loam	28	34.2	37.3	2.6	15.386
PF4	P2	98-028-030	9/13/98	Sandy Loam	62.9	18.9	18.2	5.6	10.546
PF4	P2	98-028-030	9/13/98	Sandy Loam	59.7	21.4	18.8	4.8	10.853
PF4	P2	98-031-033	9/13/98	Sandy Loam	58.7	24.2	17.1	7.9	10.726
PF4	P2	98-031-033	9/13/98	Sandy Loam	59.6	22.4	18	7.4	10.771
PF4	P2	98-034-036	9/13/98	Sandy Loam	65	17.5	17.6	6.7	10.316
PF4	P2	98-034-036	9/13/98	Sandy Loam	63	18.9	18.2	6.8	10.535
PF4	P2	98-037-039	9/14/98	Sandy Loam	56.6	23.7	19.6	4.4	11.179
PF4	P2	98-037-039	9/14/98	Sandy Loam	59.34	22.1	18.51	5.4	10.846
PF4	P2	98-040-042	9/14/98	Sandy Loam	60	20.6	19.4	4.7	11.041
PF4	P2	98-040-042	9/14/98	Sandy Loam	63.8	18.2	18.1	3.7	10.474
Sec. 10 W	J2	98-043-044	11/5/98	Clay Loam	37.7	28.2	34.2	3.4	14.306
Sec. 10 W	J2	98-043-044	11/5/98	Clay Loam	37.5	29.7	32.8	5	14.156
Sec. 10 W	J2	98-045-048	11/5/98	Clay Loam	31.7	36.1	32.2	11.8	14.515
Sec. 10 W	J2	98-045-048	11/5/98	Clay Loam	31.9	37.8	32.8	2.3	14.571
Sec. 10 W	J2	98-049-050	11/5/98	Clay Loam	36.9	29	34.1	2.3	14.354
Sec. 10 W	J2	98-049-050	11/5/98	Clay Loam	35.8	30.3	33.9	2.2	14.412

## REFERENCES CITED

- Asman, W. (1992). Ammonia emission in Europe: Updated emission and emission variations. Bilthoven, The Netherlands, National institute of public health and environmental protection.
- Battye, R., W. Battye, et al. (1994). Development and selection of ammonia emission factors. Durham, N.C., EC/R incorporated.
- BOHS (1988). "Progress in dustiness estimation." American Industrial Hygiene Association Journal **32**(4): 535-544.
- Bond, T. C., T. L. Anderson, et al. (1999). "Calibration and Intercomparison of Filter-based Measurements of Visible Light Absorption by Aerosols." Aerosol Sci. Technol. **30**: 582-600.
- Cahill, T. A. (1995). Compositional analysis of atmospheric aerosols. Particle-Induced X-Ray Emission Spectrometry. S. A. E. Johansson, J. L. Campbell and K. G. Malmqvist. New York, John Wiley & Sons, Inc.
- Cahill, T. A., L. L. Ashbaugh, et al. (1981). Comparisons between size-segregated resuspended soil samples and ambient aerosols in the western United States. Atmospheric Aerosol: Source/Air Quality Relationships. Washington, D.C., American Chemical Society: 269-285.
- Cahill, T. A., R. A. Eldred, et al. (1977). "Statistical techniques for handling PIXE data." Nuclear Instruments and Methods **142**: 259-261.
- Cahill, T. A., R. A. Eldred, et al. (1989). "Indirect measurement of hydrocarbon aerosols across the US by nonsulfate hydrogen-remaining gravimetric mass correlations." Aerosol Sci. Technol. **10**: 421-429.
- Campbell, D., S. Copeland, et al. (1995). "Measurement of Aerosol Absorption Coefficient from Teflon Filters Using Integrating Plate and Integrating Sphere Techniques." Aerosol Sci. Technol. **22**: 287-292.
- Chow, J. C., J. G. Watson, et al. (1992). "PM<sub>10</sub> source apportionment in California's San Joaquin Valley." Atmos. Environ. **26A**: 3335-3354.
- Chung, K. Y. K. and G. J. Burdett (1994). "Dustiness testing and moving toward a biologically relevant dustiness index." Annals of Occupational Hygiene **38**(6): 945-949.

- Coe, D., L. Chinkin, et al. (1998). Evaluation and improvement of methods for determining ammonia emissions in the San Joaquin Valley. Sacramento, California Air Resources Board.
- Coleman, H. W. and W. G. Steele, Jr. (1989). Experimentation and Uncertainty Analysis for Engineers. New York, John Wiley & Sons.
- Cowherd, C., Jr., K. Axetall, Jr., et al. (1974). Development of Emission Factors for Fugitive Dust Sources. Kansas City, MO, Midwest Research Institute: EPA 450/3-74-037.
- Cowherd, C., Jr. and J. S. Kinsey (1986). Identification, assessment and control of fugitive particulate emissions. Research Triangle Park, NC, US EPA.
- Cuscino, T. A., Jr., J. S. Kinsey, et al. (1984). The role of agricultural practices in fugitive dust emissions. Kansas City, MO, Midwest Research Institute: Report for California Air Resources Board.
- Eldred, R. A., T. A. Cahill, et al. (1997). "Composition of PM<sub>2.5</sub> and PM<sub>10</sub> aerosols in the IMPROVE network." J. Air & Waste Manage. Assoc. **47**: 194-201.
- Eldred, R. A., T. A. Cahill, et al. (1988). IMPROVE- A new remote area particulate monitoring system for visibility studies. Air Pollution Control Association 81st Annual Meeting, Dallas, TX.
- Eldred, R. A., T. A. Cahill, et al. (1990). Measurement of fine particles and their chemical components in the IMPROVE/NPS network. Visibility and Fine Particles. C. V. Mathai, Air & Waste Management Association: 187-196.
- Eldred, R. A., T. A. Cahill, et al. (1989). Particulate characterization at remote sites across the U.S.: First year results of the NPS/IMPROVE network. Air & Waste Management Association 82nd Annual Meeting, Anaheim, CA, Air & Waste Management Association.
- Fitz, D. (1997).
- Flocchini, R. G., T. A. Cahill, et al. (1994). Study of fugitive PM-10 emissions for selected agricultural practices on selected agricultural soils. Davis, CA, University of California: 60pp.
- Gharib, S. and G. R. Cass (1984). Ammonia emission in the South Coast Air Basin 1982. Pasadena, CA, Environmental Quality Laboratory, California Institute of Technology.

- Heitbrink, W. A. (1990). "Factor affecting the Heubach and MRI dustiness tests." American Industrial Hygiene Association Journal **51**(4): 210-216.
- Hjemsted, K. and T. Schneider (1996). "Documentation of a dustiness drum test." Annals of Occupational Hygiene **40**(6): 627-643.
- Holmén, B. A., W. E. Eichinger, et al. (1998). "Application of elastic lidar to PM<sub>10</sub> emissions from agricultural nonpoint sources." Environ. Sci. Technol. **32**: 3068-3076.
- Holmén, B. A., T. A. James, et al. (2001). "Lidar-assisted measurement of PM<sub>10</sub> emissions from agricultural tilling in California's San Joaquin Valley II: Emission Factors." Atmospheric Environment **35**(19): 3265-3277.
- Jackson, M. L. (1956). Soil Chemical analysis-Advanced course. Madison, Wisconsin, University of Wisconsin.
- James, T. A., T. W.-M. Fan, et al. (2000). Size and elemental characterization of dust from agricultural sources. Second international conference on air pollution from agricultural operations specialty conference, St. Joseph, MI.
- James, T. A., R. T. Matsumura, et al. (1996). Strategies for Measuring Fugitive Dust Emissions. International Conference on Air Pollution from Agricultural Operations, February 7-8, Kansas City, MO, Midwest Plan Service.
- James, T. A., D. Meyer, et al. (1999). "Effects of dietary nitrogen manipulation on ammonia volatilization from manure from Holstein heifers." Journal of Dairy Science **82**: 2430-2439.
- John, W. and G. Reischl (1980). "A cyclone for size-selective sampling of ambient air." APCA Journal **30**: 872-876.
- Johnston, W. E. and H. O. Carter (2000). "Structural adjustment, resources, global economy to challenge California agriculture." California Agriculture **54**(4): 16-22.
- Klemm, R. J., R. M. J. Mason, et al. (2000). "Is daily mortality associated specifically with fine particles? Data reconstruction and replication of analyses." Journal of the Air and Waste Management Association **50**(7): 1251-1222.
- Malm, W. C., J. F. Sisler, et al. (1994). "Spatial and seasonal trends in particle concentration and optical extinction in the US." Journal of geophysical research **99**(D1): 1347-1370.

- Meyer, D., L. L. Ashbaugh, et al. (1997). Estimated ammonia emission from manure decomposition. International Symposium for Ammonia and Odour Control from Animal Production Facilities, Vinkeloord, The Netherlands.
- Morse, D. and E. DePeters (1996). Digestibility of nutrients and their presence in manure. Continuing Education conference, Coalinga, CA.
- National Research Council (1988). Nutrient Requirements of Dairy Cattle. Washington, D.C., National Academy of Science.
- Pope, C. A., M. J. Thun, et al. (1995). "Particulate air pollution as a predictor of mortality in a prospective study of U.S. adults." American Journal of Respiratory and Critical Care Medicine **151**(3, part1): 669-674.
- Rabaud, N. E., T. A. James, et al. (2001). "A passive sampler for the determination of airborne ammonia concentrations near large-scale animal facilities." Environmental Science & Technology **35**: 1190-1196.
- Schmidt, C. E. and E. Winegar (1996). Results of the measurement of PM10 precursor compounds from dairy industry livestock waste. Diamond Bar, CA, South Coast Air Quality Management District.
- Schwartz, J., D. W. Dockery, et al. (1996). "Is daily mortality associated specifically with fine particles?" Journal of the Air and Waste Management Association **46**(10): 927-939.
- Singh, U. B., J. M. Gregory, et al. (1994). Dust production from a controlled energy environment. 1994 International summer meeting of the American Society of Agricultural Engineers, Crown Center, Kansas City, ASAE.
- Tomlinson, A. P., W. J. Powers, et al. (1996). "Dietary protein effects on nitrogen excretion and manure characteristic of lactating cows." Transactions of the American Society of Agricultural Engineers **39**: 1441-1448.
- U.S.E.P.A. (1995). Compilation of Air Pollution Emission Factors. Research Triangle Park, NC, United States Environmental Protection Agency.
- Venkatram, A., D. Fitz, et al. (1999). "Using a dispersion model to estimate emission rates of particulate matter from paved roads." Atmos. Environ. **33**: 1903-1102.
- Willems, J. J. H. and H. Harssema (1995). Measuring ammonia emissions from stables with natural ventilation based on passive sampling. Atmospheric Ammonia: Emission, Deposition and Environmental Impacts, Culham, Oxford England, Institute of Terrestrial Ecology, Midlothian.



## 8 APPENDIX A – INVENTORY OF 1994 FIELD TESTS

### Inventory of 1994 field tests using upwind-downwind sampling array

Test No.	Commodity	Operation	County	Site Name	Soil Texture	Date	Start Time	End Time	Valid Test?	Comments
94A-001	Almond	Sweeping-1st	Kern	Paramount Farms Field #306	Silty & Clayey	08/23/94	0800	0900	Yes	OK
94A-002	Almond	Sweeping-1st	Kern	Paramount Farms Field #306	Silty & Clayey	08/23/94	0900	1018	No	Wind angle > 45°
94A-003	Almond	Ambient-Night	Kern	Paramount Farms Field #306	Silty & Clayey	08/24/94	0000	0400	Yes	OK
94A-004	Almond	Field Blank	Kern	Paramount Farms Field #306	Silty & Clayey	08/23/94			No	Field Blank
94A-005	Almond	Pickup-1st	Kern	Paramount Farms Field #306	Silty & Clayey	08/24/94	0650	0739	Yes	OK
94A-006	Almond	Pickup-1st	Kern	Paramount Farms Field #306	Silty & Clayey	08/24/94	0739	0833	Yes	OK
94A-007	Almond	Pickup-1st	Kern	Paramount Farms Field #306	Silty & Clayey	08/24/94	0833	0933	No	Wind direction too variable
94A-008	Almond	Ambient-Night	Kern	Paramount Farms Field #306	Silty & Clayey	08/25/94	0000	0600	No	Ambient test, no harvesting
94A-009	Almond	Pickup-1st	Kern	Paramount Farms Field #306	Silty & Clayey	08/25/94	0712	0752	Yes	OK
94A-010	Almond	Pickup-1st	Kern	Paramount Farms Field #306	Silty & Clayey	08/25/94	0752	0813	Yes	OK
94A-011	Almond	Pickup-1st	Kern	Paramount Farms Field #306	Silty & Clayey	08/25/94	0813	0910	No	Wind angle > 45°
94A-012	Almond	Field Blank	Kern	Paramount Farms Field #306	Silty & Clayey	08/25/94			No	Field Blank
94A-013	Almond	Ambient-Night	Kern	Paramount Farms Field #302	Sandy	09/06/94	0000	0600	No	Ambient test, no harvesting
94A-014	Almond	Shaking-2nd	Kern	Paramount Farms Field #302	Sandy	09/06/94	1248	1336	Yes	OK
94A-015	Almond	Shaking-2nd	Kern	Paramount Farms Field #302	Sandy	09/06/94	1336	1501	Yes	OK
94A-016	Almond	Field Blank	Kern	Paramount Farms Field #302	Sandy	09/05/94			No	Field Blank
94A-017	Almond	Sweeping-2nd	Kern	Paramount Farms Field #302	Sandy	09/07/94	1136	1224	Yes	OK
94A-018	Almond	Pickup-2nd	Kern	Paramount Farms Field #302	Sandy	09/09/94	1109	1230	Yes	OK
94A-019	Almond	Pickup-2nd	Kern	Paramount Farms Field #302	Sandy	09/09/94	1230	1423	Yes	OK
94A-020	Almond	Field Blank	Kern	Paramount Farms Field #302	Sandy	09/07/94			No	Field Blank
94A-021	Almond	Sweeping-2nd	Kern	Paramount Farms Field #326N	Sandy	09/10/94	1108	1323	No	Wind angle > 45°
94A-022	Almond	Pickup-2nd	Kern	Paramount Farms Field #326N	Sandy	09/12/94	1300	1403	No	Wind angle > 45°
94A-023	Almond	Pickup-2nd	Kern	Paramount Farms Field #326N	Sandy	09/12/94	1403	1600	Yes	OK
94A-024	Almond	Pickup-2nd	Kern	Paramount Farms Field #326N	Sandy	09/12/94	1600	1726	No	Wind angle > 45°
94A-025	Almond	Shaking-2nd	Kern	Paramount Farms Field #306	Silty & Clayey	09/14/94	0805	0940	No	Number of passes missing
94A-026	Almond	Sweeping-2nd	Kern	Paramount Farms Field #306	Silty & Clayey	09/20/94	0720	0820	Yes	OK

Test No.	Commodity	Operation	County	Site Name	Soil Texture	Date	Start Time	End Time	Valid Test?	Comments
94A-027	Almond	Sweeping-2nd	Kern	Paramount Farms Field #306	Silty & Clayey	09/20/94	0820	0955	Yes	OK
94A-028	Almond	Ambient-Day	Kern	Paramount Farms Field #306	Silty & Clayey	09/20/94	0955	1220	No	Ambient test, no harvesting
94A-029	Almond	Pickup-2nd	Kern	Paramount Farms Field #306	Silty & Clayey	09/21/94	0719	0745	Yes	OK
94A-030	Almond	Pickup-2nd	Kern	Paramount Farms Field #306	Silty & Clayey	09/21/94	0745	0825	Yes	OK
94A-031	Almond	Pickup-2nd	Kern	Paramount Farms Field #306	Silty & Clayey	09/21/94	0830	0933	Yes	OK
94A-032	Almond	Field Blank	Kern	Paramount Farms Field #306	Silty & Clayey	09/21/94			No	Field Blank
94A-033	Fig	Sweeping-2nd	Merced	Debenedetto-Bliss Ranch	Sandy	09/26/94	0850	0948	Yes	OK
94A-034	Fig	Sweeping-2nd	Merced	Debenedetto-Bliss Ranch	Sandy	09/26/94	0948	1039	Yes	OK
94A-035	Fig	Field Blank	Merced	Debenedetto-Bliss Ranch	Sandy	09/26/94			No	Field Blank
94A-036	Fig	Field Blank	Merced	Debenedetto-Bliss Ranch	Sandy	09/26/94			No	Field Blank
94A-037	Fig	Sweeping-2nd	Merced	Debenedetto-Bliss Ranch	Sandy	09/26/94	1342	1453	Yes	OK
94A-038	Fig	Sweeping-2nd	Merced	Debenedetto-Bliss Ranch	Sandy	09/26/94	1535	1700	Yes	OK
94A-039	Fig	Sweeping-2nd	Merced	Debenedetto-Bliss Ranch	Sandy	09/26/94			No	Field Blank
94A-040	Fig	Sweeping-2nd	Merced	Debenedetto-Bliss Ranch	Sandy	09/26/94			No	Field Blank
94B-041	Cotton	Picking-1st	Kern	Kern Lake Ranch, Section 6-1	Sandy	10/03/94			No	Wind direction too variable
94A-042	Cotton	Stalk Cutting	Kern	Kern Lake Ranch, Section 6-1	Sandy	10/07/94	1237	1308	Yes	OK
94A-043	Cotton	Stalk Cutting	Kern	Kern Lake Ranch, Section 6-1	Sandy	10/07/94	1308	1507	Yes	OK
94A-044	Cotton	Stalk Cutting	Kern	Kern Lake Ranch, Section 6-1	Sandy	10/07/94	1507	1646	No	Wind angle > 45°
94A-045	Cotton	Field Blank	Kern	Kern Lake Ranch, Section 6-1	Sandy	10/07/94			No	Field Blank
94B-046	Cotton	Picking-1st	Kern	Kern Lake Ranch, Section 18-3	Clayey	10/08/94			No	Number of passes missing
94B-047	Cotton	Picking-1st	Kern	Kern Lake Ranch, Section 18-3	Clayey	10/08/94			No	Number of passes missing
94A-048	Cotton	Picking-1st	Kern	Buena Vista Ranch, Section 34-1,2	Clayey, Silty	10/10/94	1137	1521	Yes	OK
94A-049	Cotton	Picking-1st	Kern	Buena Vista Ranch, Section 34-1,2	Clayey, Silty	10/10/94	1521	1700	Yes	OK
94A-050	Cotton	Picking-1st	Kern	Buena Vista Ranch, Section 34-1,2	Clayey, Silty	10/10/94	1701	1821	Yes	OK
94A-051	Cotton	Field Blank	Kern	Buena Vista Ranch, Section 34-1,2	Clayey, Silty	10/10/94			No	Field Blank
94B-052	Fig	Pickup-2nd	Merced	Debenedetto-Bliss Ranch	Sandy	10/12/84	1101	1249	Yes	OK
94B-053	Fig	Pickup-2nd	Merced	Debenedetto-Bliss Ranch	Sandy	10/12/84	1249	1551	No	Wind angle > 45°
94A-054	Fig	Pickup-2nd	Merced	Debenedetto-Bliss Ranch	Sandy	10/12/84	1837	2039	No	Wind angle > 45°

Test No.	Commodity	Operation	County	Site Name	Soil Texture	Date	Start Time	End Time	Valid Test?	Comments
94A-055	Fig	Ambient-Night	Merced	Debenedetto-Bliss Ranch	Sandy	10/12/84	2200	0400	No	Ambient test, no harvesting
94A-056	Fig	Field Blank	Merced	Debenedetto-Bliss Ranch	Sandy	10/12/84			No	Field Blank
94A-057	Fig	Field Blank	Merced	Debenedetto-Bliss Ranch	Sandy	10/12/84			No	Field Blank
94A-058	Cotton	Picking-1st	Kern	Kern Lake Ranch, Section 10, SE 2/3	Clayey, Loam	10/14/94	0903	1139	No	Number of passes missing
94A-059	Cotton	Picking-1st	Kern	Kern Lake Ranch, Section 10, SE 2/3	Clayey, Loam	10/14/94	1139	1243	Yes	OK
94A-060	Cotton	Ambient-Day	Kern	Kern Lake Ranch, Section 10, SE 2/3	Clayey, Loam	10/14/94	1400	1700	No	Ambient test, no harvesting
94A-061	Cotton	Field Blank	Kern	Kern Lake Ranch, Section 10, SE 2/3	Clayey, Loam	10/14/94			No	Field Blank
94B-062	Almond	Pickup-Comparison	Kern	Paramount Farms Field # 306	Silty & Clayey	09/20/94	1308	1337	No	Wind angle > 45°
94B-063	Almond	Pickup-Comparison	Kern	Paramount Farms Field # 306	Silty & Clayey	09/27/94	1640	1750	No	Wind angle > 45°
94B-064	Almond	Pickup-Comparison	Kern	Paramount Farms Field # 310	Clayey	10/17/94	1051	1154	No	Wind angle > 45°
94B-065	Almond	Pickup-Comparison	Kern	Paramount Farms Field # 310	Clayey	10/17/94	1306	1432	No	Wind angle > 45°
94B-066	Almond	Pickup-Comparison	Kern	Paramount Farms Field # 308	Clayey	10/18/94	0734	0820	No	Wind angle > 45°
94B-067	Almond	Pickup-Comparison	Kern	Paramount Farms Field # 308	Clayey	10/18/94	1009	1101	No	Wind angle > 45°
94A-068	Cotton	Picking-1st	Fresno	Boston Ranch, Section 8, West Half	Clayey	10/21/94	0923	1105	Yes	OK
94A-069	Cotton	Picking-1st	Fresno	Boston Ranch, Section 8, West Half	Clayey	10/21/94	1105	1301	Yes	OK
94A-070	Cotton	Picking-1st	Fresno	Boston Ranch, Section 8, West Half	Clayey	10/21/94	1301	1612	Yes	OK
94A-071	Cotton	Field Blank	Fresno	Boston Ranch, Section 8, West Half	Clayey	10/21/94			No	Field Blank
94A-072	Walnut	Shaking	Kings	Fukano/Deremer	Sandy	10/22/94	1116	1350	No	Wind angle > 45°
94A-073	Walnut	Sweeping, Shaking	Kings	Fukano/Deremer	Sandy	10/22/94	1350	1526	Yes	OK
94A-074	Walnut	Sweeping, Pickup	Kings	Fukano/Deremer	Sandy	10/22/94	1526	1718	Yes	OK
94A-075	Walnut	Sweeping, Pickup	Kings	Fukano/Deremer	Sandy	10/22/94	1718	1759	Yes	OK
94A-076	Walnut	Pickup	Kings	Deremer	Sandy	10/23/94	1217	1307	No	Wind angle > 45°
94A-077	Walnut	Pickup	Kings	Deremer	Sandy	10/23/94	1307	1504	No	Wind angle > 45°

Test No.	Commodity	Operation	County	Site Name	Soil Texture	Date	Start Time	End Time	Valid Test?	Comments
94B-078	Walnut	Sweeping	Kings	Deremer	Sandy	10/23/94	1409	1649	No	Number of passes missing
94A-079	Cotton	Picking-1st	Kern	Buena Vista, Section 31, West Half	Clayey	10/27/94	1617	1828	Yes	OK
94A-080	Cotton	Picking-1st	Kern	Buena Vista, Section 31, West Half	Clayey	10/27/94	1828	1943	No	Number of passes missing
94A-081	Cotton	Ambient	Kern	Buena Vista, Section 31, West Half	Clayey	10/27/94	1943	2042	No	Ambient test, no harvesting
94A-082	Cotton	Picking-1st	Kern	Buena Vista, Section 31, West Half	Clayey	10/28/94	0912	1036	Yes	OK
94A-083	Cotton	Stalk Cutting	Kern	Buena Vista, Section 31, West Half	Clayey	10/28/94	0000	0001	Yes	OK
94A-084	Cotton	Stalk Cutting	Kern	Buena Vista, Section 31, West Half	Clayey	10/28/94	0001	0001	Yes	OK
94A-085	Cotton	Field Blank	Kern	Buena Vista, Section 31, West Half	Clayey	10/28/94			No	Field Blank
94A-086	Cotton	Field Blank	Kern	Buena Vista, Section 31, West Half	Clayey	10/28/94			No	Field Blank
94A-087	Cotton	Picking-1st	Kings	Corcoran Ranch, Sect. 27, East Half	Clayey	10/30/94	0000	0001	Yes	OK
94A-088	Cotton	Picking-1st	Kings	Corcoran Ranch, Sect. 27, East Half	Clayey	10/30/94	0001	0001	Yes	OK
94A-089	Cotton	Picking-1st	Kings	Corcoran Ranch, Sect. 27, East Half	Clayey	10/30/94	1518	1702	Yes	OK
94A-090	Cotton	Field Blank	Kings	Corcoran Ranch, Sect. 27, East Half	Clayey	10/30/94			No	Field Blank
94A-091	Cotton	Stalk Cutting	Kings	Corcoran Ranch, Sect. 27, East Half	Clayey	11/01/94	0723	1007	Yes	OK
94A-092	Cotton	Stalk Cutting	Kings	Corcoran Ranch, Sect. 27, East Half	Clayey	11/01/94	1330	1518	Yes	OK
94A-093	Cotton	Stalk Cutting	Kings	Corcoran Ranch, Sect. 27, East Half	Clayey	11/01/94	1518	1610	Yes	OK
94A-094	Cotton	Field Blank	Kings	Corcoran Ranch, Sect. 27, East Half	Clayey	11/01/94			No	Field Blank
94A-095	Cotton	Picking-1st	Fresno	Terranova Ranch, Field # 63	Sandy	11/03/94	1645	1742	Yes	OK
94A-096	Cotton	Picking-1st	Fresno	Terranova Ranch, Field # 63	Sandy	11/03/94	1742	1839	Yes	OK
94A-097	Cotton	Field Blank	Fresno	Terranova Ranch, Field # 63	Sandy	11/03/94			No	Field Blank
94A-098	Cotton	Field Blank	Fresno	Terranova Ranch, Field # 63	Sandy	11/03/94			No	Field Blank
94A-099	Cotton	Stalk Cutting	Fresno	Terranova Ranch, Field # 63	Sandy	11/05/94	1457	1628	Yes	OK
94A-100	Cotton	Stalk Cutting	Fresno	Terranova Ranch, Field # 62	Sandy	11/06/94	1146	1219	No	Wind direction too variable
94B-101	Cotton	Stalk Cutting	Fresno	Terranova Ranch, Field # 62	Sandy	11/06/94	1256	1503	No	Number of passes missing
94B-102	Cotton	Stalk Cutting	Fresno	Terranova Ranch, Field # 62	Sandy	11/06/94	1500	1547	No	Number of passes missing
94B-103	Cotton	Picking-1st	Kings	Newton Brothers, Section 17	Clayey	11/07/94	0922	1240	No	Number of passes missing

Test No.	Commodity	Operation	County	Site Name	Soil Texture	Date	Start Time	End Time	Valid Test?	Comments
94B-104	Cotton	Picking-1st	Kings	Newton Brothers, Section 17	Clayey	11/07/94	1246	1418	No	Number of passes missing
94B-105	Cotton	Picking -1st	Fresno	Boston Ranch, section 18	Clayey	10/20/94	1002	1337	No	Wind direction too variable
94B-106	Cotton	Picking -1st	Fresno	Boston Ranch, section 18	Clayey	10/20/94	1532	1810	No	Wind direction too variable

## 9 APPENDIX B – INVENTORY OF 1995 FIELD TESTS

### Inventory of 1995 field tests using upwind-downwind sampling array

TESTID	COMMODITY	OPERATION	COUNTY	SOIL TEXTURE	SITEDESC	TESTDATE	TESTSTART	TESTEND	Valid Test?
95-001	Wheat	Harvest	Merced	Loam	Fancher Ranch, Field 4	7/6/95	1100	1130	No
95-002	Wheat	Harvest	Merced	Loam	Fancher Ranch, Field 4	7/6/95	1130	1200	No
95-003	Wheat	Harvest	Merced	Loam	Fancher Ranch, Field 4	7/6/95	1210	1220	No
95-004	Wheat	Harvest	Merced	Silt Loam	Fancher Ranch, Field 19	7/7/95	0943	1000	No
95-005	Wheat	Harvest	Merced	Silt Loam	Fancher Ranch, Field 19	7/7/95	1000	1100	No
95-006	Wheat	Harvest	Merced	Silt Loam	Fancher Ranch, Field 19	7/7/95	1100	1200	No
95-007	Wheat	Harvest	Merced	Silt Loam	Fancher Ranch, Field 19	7/7/95	1200	1300	No
95-008	Wheat	Harvest	Merced	Silt Loam	Fancher Ranch, Field 20	7/10/95	1025	1100	No
95-009	Wheat	Harvest	Merced	Silt Loam	Fancher Ranch, Field 20	7/10/95	1100	1200	No
95-010	Wheat	Harvest	Merced	Silt Loam	Fancher Ranch, Field 20	7/10/95	1200	1330	No
95-011	Wheat	Harvest	Merced	Loam	Fancher Ranch, Field 2	7/11/95	1100	1300	No
95-012	Wheat	Harvest	Merced	Loam	Fancher Ranch, Field 2	7/11/95	1300	1500	No
95-013	Wheat	Harvest	Merced	Loam	Fancher Ranch, Field 2	7/11/95	1607	1802	No
95-014	Wheat	Harvest	Merced	Loam	Fancher Ranch, Field 2	7/11/95	1812	1920	No
95-015	Wheat	Harvest	Merced	Loam	Fancher Ranch, Field 2	7/12/95	1035	1138	No
95-016	Wheat	Harvest	Merced	Loam	Fancher Ranch, Field 2	7/12/95	1138	1215	No
95-017	Wheat	Harvest	Merced	Loam	Fancher Ranch, Field 2	7/12/95	1215	1240	No
95-018->023	Research	Land Planning	Yolo	Silt Loam	Campbell Tract, Davis	8/15/95	1220	1240	No
95-024->037	Transportation	Paved Roads - Emissions	Sacramento	NA	Florin/Stockton Intersection	8/23/95	1200	1600	No
95-038	Almonds	Second Shaking	Kern	Sandy Clay Loam	Paramount Farms, Field 341	9/7/95	0948	1006	No
95-039	Almonds	Second Shaking	Kern	Sandy Clay Loam	Paramount Farms, Field 341	9/7/95	1007	1030	No
95-040	Almonds	First Shaking	Kern	Clay Loam	Paramount Farms, Field 350	9/8/95	0952	1041	No
95-041	Almonds	First Shaking	Kern	Clay Loam	Paramount Farms, Field 350	9/8/95	1243	1259	No
95-042	Almonds	First Shaking	Kern	Clay Loam	Paramount Farms, Field 350	9/8/95	1331	1426	No
95-043	Almonds	Second Pickup	Kern	Clay Loam	Paramount Farms, Field 342	9/9/95	1101	1155	No
95-044	Almonds	Second Pickup	Kern	Clay Loam	Paramount Farms, Field 342	9/9/95	1155	1236	Yes
95-045	Almonds	Second Pickup	Kern	Clay Loam	Paramount Farms, Field 342	9/9/95	1305	1347	No
95-046	Almonds	Second Pickup	Kern	Clay Loam	Paramount Farms, Field 342	9/9/95	1347	1447	Yes
95-047	Almonds	Ambient	Kern	Loam	Paramount Farms, Field 328B,4-2	9/11/95	0857	1050	No
95-048	Almonds	Second Shaking	Kern	Loam	Paramount Farms, Field 328B,4-2	9/11/95	1050	1122	No
95-049	Almonds	Second Shaking	Kern	Loam	Paramount Farms, Field 328B,4-2	9/11/95	1130	1202	No
95-050	Almonds	Second Shaking	Kern	Loam	Paramount Farms, Field 328B,4-2	9/11/95	1237	1300	No
95-051	Almonds	Second Sweeping	Kern	Sandy Clay Loam	Paramount Farms, Field 341	9/12/95	0915	1045	No
95-052	Almonds	Second Sweeping	Kern	Sandy Clay Loam	Paramount Farms, Field 341	9/12/95	1045	1153	No
95-053	Almonds	Second Pickup	Kern	Sandy Clay Loam	Paramount Farms, Field 341	9/13/95	0720	0745	No
95-054	Almonds	Second Pickup	Kern	Sandy Clay Loam	Paramount Farms, Field 341	9/13/95	0745	0825	Yes
95-055	Almonds	Second Pickup	Kern	Sandy Clay Loam	Paramount Farms, Field 341	9/13/95	0825	0855	Yes
95-056	Almonds	Second Pickup	Kern	Sandy Clay Loam	Paramount Farms, Field 341	9/13/95	0857	0926	No
95-057	Almonds	Second Sweeping	Kern	Loam	Paramount Farms, Field 328A,5-1	9/15/95	0728	0824	No
95-058	Almonds	Second Sweeping	Kern	Loam	Paramount Farms, Field 328A,5-1	9/15/95	0842	0901	No
95-059	Almonds	Second Sweeping	Kern	Loam	Paramount Farms, Field 328A,5-1	9/15/95	0927	0952	No
95-060	Almonds	Second Pickup	Kern	Loam	Paramount Farms, Field 328B,4-2	9/16/95	0700	0740	Yes
95-061	Almonds	Second Pickup	Kern	Loam	Paramount Farms, Field 328B,4-2	9/16/95	0810	0812	No
95-062	Almonds	Second Pickup	Kern	Loam	Paramount Farms, Field 328B,4-2	9/16/95	0837	0842	No
95-063	Almonds	First Pickup	Kern	Clay Loam	Paramount Farms, Field 350	9/18/95	0805	0818	No
95-064	Almonds	First Pickup	Kern	Clay Loam	Paramount Farms, Field 350	9/18/95	0818	0834	No
95-065	Almonds	First Pickup	Kern	Clay Loam	Paramount Farms, Field 350	9/18/95	0834	0846	No
95-066	Almonds	Second Shaking	Kern	Clay Loam	Paramount Farms, Field 350	9/19/95	1310	1323	No
95-067	Almonds	Second Shaking	Kern	Clay Loam	Paramount Farms, Field 350	9/19/95	1439	1450	No
95-068	Almonds	Second Shaking	Kern	Clay Loam	Paramount Farms, Field 350	9/20/95	0803	0808	No
95-069	Almonds	Second Shaking	Kern	Clay Loam	Paramount Farms, Field 350	9/20/95	0810	0816	No
95-070	Almonds	Second Shaking	Kern	Clay Loam	Paramount Farms, Field 350	9/20/95	0821	0827	No
95-071	Almonds	Second Shaking	Kern	Clay Loam	Paramount Farms, Field 350	9/20/95	0843	0850	No
95-072	Almonds	Second Shaking	Kern	Clay Loam	Paramount Farms, Field 350	9/20/95	0952	1002	No
95-073	Almonds	Second Shaking	Kern	Clay Loam	Paramount Farms, Field 350	9/20/95	1043	1049	No
95-074	Almonds	Second Shaking	Kern	Clay Loam	Paramount Farms, Field 350	9/20/95	1104	1112	No
95-075	Milk	Dairy PM Feeding	Tulare	Loam	Griffioen Dairy	10/3/95	1500	1701	Yes
95-076	Milk	Dairy Dusk Activity	Tulare	Loam	Griffioen Dairy	10/3/95	1746	2003	Yes
95-077	Milk	Dairy Night Sleeping	Tulare	Loam	Griffioen Dairy	10/3/95	2021	2301	Yes
95-078	Milk	Dairy PM Feeding	Tulare	Loam	Griffioen Dairy	10/4/95	1358	1700	Yes
95-079	Milk	Dairy Dusk Activity	Tulare	Loam	Griffioen Dairy	10/4/95	1700	2000	No
95-080	Milk	Dairy Night Sleeping	Tulare	Loam	Griffioen Dairy	10/4/95	2000	2200	No
95-081	Milk	Dairy AM Feeding	Tulare	Loam	Griffioen Dairy	10/5/95	0600	1009	No
95-082	Milk	Dairy Midday Loafing	Tulare	Loam	Griffioen Dairy	10/5/95	0948	1355	No
95-083	Milk	Dairy PM Feeding	Tulare	Loam	Griffioen Dairy	10/5/95	1504	1700	No
95-084	Milk	Dairy Dusk Activity	Tulare	Loam	Griffioen Dairy	10/5/95	1700	2000	No
95-085	Milk	Dairy Night Sleeping	Tulare	Loam	Griffioen Dairy	10/5/95	2000	2222	No
95-086	Milk	Dairy PM Feeding	Tulare	Loam	Griffioen Dairy	10/6/95	1600	1700	Yes
95-087	Milk	Dairy Dusk Activity	Tulare	Loam	Griffioen Dairy	10/6/95	1700	2000	No

TESTID	COMMODITY	OPERATION	COUNTY	SOIL TEXTURE	SITEDESC	TESTDATE	TESTSTART	TESTEND	Valid Test?
95-088	Milk	Dairy Midday Loafing	Tulare	Loam	Griffioen Dairy	10/7/95	1000	1200	No
95-089	Milk	Dairy Midday Loafing	Tulare	Loam	Griffioen Dairy	10/7/95	1245	1452	Yes
95-090	Milk	Dairy PM Feeding	Tulare	Loam	Griffioen Dairy	10/7/95	1600	1800	Yes
95-091	Milk	Dairy Dusk Activity	Tulare	Loam	Griffioen Dairy	10/7/95	1800	2000	No
95-092	Raisins	Tray Burning	Fresno	Sandy Loam	Melkonian Vineyard	10/11/95	1000	1104	Yes
95-093	Cotton	Picking	Kings	Clay Loam	Stone Land Co., Section 10SE	10/18/95	1330	1530	Yes
95-094	Cotton	Picking	Kings	Clay Loam	Stone Land Co., Section 10SE	10/18/95	1530	1700	Yes
95-095	Cotton	Picking	Kings	Clay Loam	Stone Land Co., Section 10SE	10/18/95	1700	1750	Yes
95-096	Cotton	Picking	Kings	Clay Loam	Stone Land Co., Section 10SE	10/18/95	1750	1838	Yes
95-097	Cotton	Stalk Cutting	Kings	Clay Loam	Stone Land Co., Section 10SE	10/19/95	1400	1450	Yes
95-098	Cotton	Stalk Cutting	Kings	Clay Loam	Stone Land Co., Section 10SE	10/19/95	1523	1533	Yes
95-099	Cotton	Stalk Cutting	Kings	Clay Loam	Stone Land Co., Section 10SE	10/20/95	1421	1523	Yes
95-100	Cotton	Stalk Cutting	Kings	Clay Loam	Stone Land Co., Section 10SE	10/20/95	1536	1605	Yes
95-101	Cotton	Stalk Cutting	Kings	Clay Loam	Stone Land Co., Section 10SE	10/20/95	1605	1703	Yes
95-102	Cotton	Picking	KINGS	Loam	STONE LAND CO., SEC 2W	10/20/95	1903	1930	No
95-103	Cotton	Picking	KINGS	Loam	STONE LAND CO., SEC 2W	10/20/95	1930	2000	No
95-104	Cotton	Picking	KINGS	Loam	STONE LAND CO., SEC 2W	10/20/95	2000	2100	No
95-105	Cotton	Stalk Cutting	Kings	Clay Loam	Stone Land Co., Section 10SE	10/22/95	1051	1113	No
95-106	Cotton	Stalk Cutting	Kings	Clay Loam	Stone Land Co., Section 10SE	10/22/95	1113	1152	Yes
95-107	Cotton	Stalk Cutting	KINGS	Loam	STONE LAND CO., SEC 2W	10/22/95	1553	1605	No
95-108	Cotton	Ambient	KINGS	Loam	STONE LAND CO., SEC 2W	10/23/95	0850	1050	No
95-109	Cotton	Stalk Cutting	KINGS	Loam	STONE LAND CO., SEC 2W	10/24/95	0850	0916	No
95-110	Cotton	Stalk Cutting	KINGS	Loam	STONE LAND CO., SEC 2W	10/24/95	0958	1016	Yes
95-111	Cotton	Stalk Cutting	KINGS	Loam	STONE LAND CO., SEC 2W	10/24/95	1034	1100	No
95-112	Cotton	Stalk Cutting	KINGS	Loam	STONE LAND CO., SEC 2W	10/24/95	1116	1140	No
95-113	Cotton	Stalk Cutting	KINGS	Loam	STONE LAND CO., SEC 2W	10/24/95	1326	1402	No
95-114	Cotton	Picking	Kings	Clay	Newton Bros, Section 1, 6	10/25/95	1236	1445	No
95-115	Cotton	Picking	Kings	Clay	Newton Bros, Section 1, 6	10/25/95	1977	2051	No
95-116	Cotton	Picking	Kings	Clay	Newton Bros, Section 1, 6	10/26/95	0900	1120	No
95-117	Cotton	Picking	Kings	Clay	Newton Bros, Section 1, 6	10/26/95	1230	1430	No
95-118	Cotton	Stalk Incorporation	KINGS	Loam	STONE LAND CO., SEC 2W	10/27/95	1255	1400	Yes
95-119	Cotton	Stalk Incorporation	KINGS	Loam	STONE LAND CO., SEC 2W	10/27/95	1400	1456	Yes
95-120	Cotton	Ambient	KINGS	Loam	STONE LAND CO., SEC 2W	10/27/95	1646	1746	No
95-121	Cotton	Stalk Incorporation	Kings	Clay Loam	Stone Land Co., Section 18	10/29/95	1423	1434	No
95-122	Cotton	Stalk Incorporation	Kings	Clay Loam	Stone Land Co., Section 18	10/29/95	1445	1530	No
95-123	Cotton	Picking	Kings	Loam	Stone Land Co., Section 13E	10/29/95	1700	1904	No
95-124	Cotton	Picking	Kings	Loam	Stone Land Co., Section 13E	10/29/95	2105	2205	No
95-125	Cotton	Stalk Cutting	Kings	Loam	Stone Land Co., Section 13E	10/31/95	1455	1631	Yes
95-126	Cotton	Stalk Cutting	Kings	Loam	Stone Land Co., Section 13E	10/31/95	1631	1723	Yes
95-127	Cotton	Stalk Cutting	Kings	Loam	Stone Land Co., Section 13E	10/31/95	1723	1824	Yes
95-128	Cotton	Stalk Incorporation	Kings	Loam	Stone Land Co., Section 13W	11/3/95	1001	1139	Yes
95-129	Cotton	Stalk Incorporation	Kings	Loam	Stone Land Co., Section 13W	11/3/95	1139	1200	Yes
95-130	Cotton	Stalk Incorporation	Kings	Loam	Stone Land Co., Section 13W	11/3/95	1238	1300	Yes
95-131	Cotton	Stalk Incorporation	Kings	Loam	Stone Land Co., Section 13W	11/3/95	1300	1333	Yes
95-132	Cotton	Stalk Incorporation	Kings	Loam	Stone Land Co., Section 13W	11/3/95	1333	1342	Yes
95-133	Cotton	Stalk Incorporation	Kings	Loam	Stone Land Co., Section 13E	11/3/95	1452	1708	No
95-134	Cotton	Stalk Incorporation	Kings	Loam	Stone Land Co., Section 13E	11/3/95	1710	1800	No
95-135	Cotton	Picking	Kings	Clay Loam	Stone Land Co., Section 1N	11/5/95	1550	1633	Yes
95-136	Cotton	Picking	Kings	Clay Loam	Stone Land Co., Section 1S	11/6/95	1417	1509	Yes
95-137	Cotton	Picking	Kings	Clay Loam	Stone Land Co., Section 1S	11/6/95	1509	1602	Yes
95-138	Cotton	Picking	Kings	Clay Loam	Stone Land Co., Section 1S	11/6/95	1743	1917	Yes
95-139	Cotton	Stalk Cutting	Kings	Clay Loam	Stone Land Co., Section 1S	11/7/95	1433	1507	Yes
95-140	Cotton	Stalk Cutting	Kings	Clay Loam	Stone Land Co., Section 1S	11/7/95	1507	1554	Yes
95-141	Cotton	Stalk Cutting	Kings	Clay Loam	Stone Land Co., Section 1S	11/7/95	1554	1620	Yes
95-142	Cotton	Stalk Cutting	Kings	Clay Loam	Stone Land Co., Section 1S	11/7/95	1620	1635	Yes
95-143	Cotton	Picking	Kings	Clay	Newton Bros, Section 17	11/13/95	1338	1423	No
95-144	Cotton	Picking	Kings	Clay	Newton Bros, Section 17	11/13/95	1426	1605	No
95-145	Cotton	Picking	Kings	Clay	Newton Bros, Section 17	11/13/95	1605	1718	No
95-146	Cotton	Picking	Kings	Clay	Newton Bros, Section 17	11/14/95	0919	0959	Yes
95-147	Cotton	Picking	Kings	Clay	Newton Bros, Section 17	11/14/95	1202	1302	Yes
95-148	Cotton	Stalk Cutting	Kings	Clay	Newton Bros, Section 17	11/15/95	1424	1500	Yes
95-149	Cotton	Stalk Cutting	Kings	Clay	Newton Bros, Section 17	11/15/95	1501	1605	Yes
95-150	Cotton	Stalk Incorporation	Kings	Clay	Newton Bros, Section 17	11/15/95	1838	1910	Yes
95-151	Cotton	Stalk Incorporation	Kings	Clay	Newton Bros, Section 17	11/15/95	1910	1947	Yes

## APPENDIX C – INVENTORY OF 1996 FIELD TESTS

### Inventory of 1996 field tests using upwind-downwind sampling array

TESTID	COMMODITY	OPERATION	COUNTY	SITEDESC	TESTDATE	TESTSTART	TESTEND	SOIL TEXTURE(WET SIEVE)	VALID?
96-001->002	Beef	LOAFING - DAY	Kern	Three Brands Feedlot	3/27/96	0834	1033		No
96-003	Beef	DUSK ACTIVITY	Kern	Three Brands Feedlot	3/27/96	1800	1920		Yes
96-004->005	Beef	LOAFING - DAY	Kern	Three Brands Feedlot	3/28/96	1004	1330		No
96-006	Beef	LOAFING - DAY	Kern	Three Brands Feedlot	3/29/96	1307	1700		Yes
96-007	Beef	ACTIVITY - DUSK	Kern	Three Brands Feedlot	3/29/96	1700	1919		Yes
96-008->011	Beef	SLEEPING - NIGHT	Kern	Three Brands Feedlot	3/29/96	2135	0043		No
96-012	Beef	LOAFING - DAY	Kern	Three Brands Feedlot	3/30/96	0720	0930		No
96-013	Beef	LOAFING - DAY	Kern	Three Brands Feedlot	3/30/96	1144	1554		Yes
96-014->019	Beef	SLEEPING - NIGHT	Kern	Three Brands Feedlot	3/30/96	2017	2332		No
96-020	Beef	ACTIVITY - DUSK	Kern	Three Brands Feedlot	3/31/96	1350	1633		Yes
96-021	Beef	SLEEPING - NIGHT	Kern	Three Brands Feedlot	3/31/96	1948	2347		Yes
96-022	Beef	SLEEPING - NIGHT	Kern	Three Brands Feedlot	3/31/96	2347	0205		Yes
96-023	Beef	SLEEPING - NIGHT	Kern	Three Brands Feedlot	4/1/96	0205	0357		Yes
96-024	Milk	LOAFING - DAY	Tulare	Griffioen Dairy	4/19/96	1330	1635		Yes
96-025	Milk	ACTIVITY - NIGHT	Tulare	Griffioen Dairy	4/19/96	1647	2000		Yes
96-026	Milk	SLEEPING - NIGHT	Tulare	Griffioen Dairy	4/20/96	0322	0538		Yes
96-027	Milk	LOAFING - DAY	Tulare	Griffioen Dairy	4/20/96	0830	1213		Yes
96-028	Milk	LOAFING - DAY	Tulare	Griffioen Dairy	4/20/96	1213	1455		Yes
96-029	Milk	ACTIVITY - DUSK	Tulare	Griffioen Dairy	4/20/96	1600	1900		Yes
96-030	Milk	LOAFING - NIGHT	Tulare	Griffioen Dairy	4/20/96	1935	0000		Yes
96-031	Milk	SLEEPING - NIGHT	Tulare	Griffioen Dairy	4/21/96	0000	0200		Yes
96-032	Milk	LOAFING - DAY	Tulare	Griffioen Dairy	4/21/96	1021	1430		No
96-033	Milk	ACTIVITY - DUSK	Tulare	Griffioen Dairy	4/21/96	1455	1915		Yes
96-034	Milk	LOAFING - NIGHT	Tulare	Griffioen Dairy	4/21/96	1915	2133		Yes
96-035	Milk	SLEEPING - NIGHT	Tulare	Griffioen Dairy	4/22/96	0408	0608		No
96-036	Milk	LOAFING - DAY	Tulare	Griffioen Dairy	4/22/96	0608	0810		No
96-037	Milk	ACTIVITY - DUSK	Tulare	Griffioen Dairy	4/22/96	1630	2000		Yes
96-038	Milk	ACTIVITY - DUSK	Tulare	Griffioen Dairy	4/22/96	2000	2247		Yes
96-039	Milk	SLEEPING - NIGHT	Tulare	Griffioen Dairy	4/23/96	0007	0202		Yes
96-040	Milk	SLEEPING - NIGHT	Tulare	Griffioen Dairy	4/23/96	0202	0405		Yes
96-041	Milk	LOAFING - DAY	Tulare	Griffioen Dairy	4/23/96	0735	0950		No
96-042	Milk	LOAFING - DAY	Tulare	Griffioen Dairy	4/23/96	1605	1915		Yes
96-043	Milk	LOAFING - NIGHT	Tulare	Griffioen Dairy	4/23/96	1915	2330		Yes
96-044	Milk	SLEEPING - NIGHT	Tulare	Griffioen Dairy	4/23/96	2330	0200		No
96-045	Milk	SLEEPING - NIGHT	Tulare	Griffioen Dairy	4/24/96	0200	0400		No
96-046	Milk	LOAFING - DAY	Tulare	Griffioen Dairy	4/24/96	1250	1630		Yes
96-047	Milk	ACTIVITY - DUSK	Tulare	Griffioen Dairy	4/24/96	1715	2000		Yes
96-048	Milk	LOAFING - NIGHT	Tulare	Griffioen Dairy	4/24/96	2000	2350		Yes
96-049	Wheat	Harvest	Kings	Stone Land Co., Section 10SE	6/21/96	1428	1543	Clay Loam	No
96-050	Wheat	Harvest	Kings	Stone Land Co., Section 10SE	6/21/96	1546	1718	Clay Loam	No
96-051	Wheat	Harvest	Kings	Stone Land Co., Section 10SE	6/22/96	1230	1324	Silty Clay Loam	Yes
96-052	Wheat	Harvest	Kings	Stone Land Co., Section 10SE	6/22/96	1343	1452	Silty Clay Loam	Yes
96-053	Wheat	Harvest	Kings	Stone Land Co., Section 10SE	6/22/96	1516	1637	Silty Clay Loam	Yes
96-054	Wheat	Harvest	Kings	Stone Land Co., Section 10SE	6/24/96	0945	1105	Silty Clay Loam	Yes
96-055	Wheat	Harvest	Kings	Stone Land Co., Section 10SE	6/24/96	1118	1210	Silty Clay Loam	No
96-056	Wheat	Harvest	Kings	Stone Land Co., Section 10SE	6/24/96	1224	1428	Silty Clay Loam	No
96-057	Wheat	Harvest	Kings	Stone Land Co., Section 18NE	6/27/96	0955	1138	Clay Loam	No
96-058	Wheat	Harvest	Kings	Stone Land Co., Section 18SE	6/27/96	1738	1950	Clay Loam	Yes
96-059	Wheat	Harvest	Kings	Stone Land Co., Section 18SE	6/27/96	0804	1054	Clay Loam	No
96-060	Wheat	Harvest	Kings	Stone Land Co., Section 18SE	6/28/96	1110	1222	Clay Loam	No
96-061	Wheat	Harvest	Kings	Stone Land Co., Section 18SE	6/28/96	1250	1451	Clay Loam	Yes
96-062	Wheat	Harvest	Kings	Stone Land Co., Section 18SE	6/28/96	1516	1643	Clay Loam	No
96-063	Wheat	Harvest	Kings	Stone Land Co., Section 18SE	6/28/96	1724	1836	Loam	Yes
96-064	Wheat	Harvest	Merced	Fancher Ranch, Field 6	7/2/96	1642	1745	Loam	No
96-065	Wheat	Harvest	Merced	Fancher Ranch, Field 6	7/2/96	1746	1813	Loam	No
96-066	Wheat	Harvest	Merced	Fancher Ranch, Field 6	7/3/96	0828	0946	Loam	No
96-067	Wheat	Harvest	Merced	Fancher Ranch, Field 9	7/3/96	0920	1018	Loam	No
96-068	Wheat	Harvest	Merced	Fancher Ranch, Field 9	7/3/96	1355	1522	Loam	Yes
96-069	Wheat	Harvest	Merced	Fancher Ranch, Field 9	7/5/96	0845	0940	Loam	Yes
96-070	Wheat	Harvest	Merced	Fancher Ranch, Field 9	7/5/96	1048	1210	Loam	Yes
96-071	Wheat	Harvest	Merced	Fancher Ranch, Field 9	7/5/96	1423	1550	Loam	No

TESTID	COMMODITY	OPERATION	COUNTY	SITEDESC	TESTDATE	TESTSTART	TESTEND	SOIL TEXTURE(WET SIEVE)	VALID?
96-072	Beef	PM Loafing	Kern	Three Brands Feedlot	7/27/96	1202	1505		No
96-073	Beef	Night Sleeping	Kern	Three Brands Feedlot	7/27/96	2203	0017		Yes
96-074	Beef	Night Sleeping	Kern	Three Brands Feedlot	7/28/96	0154	0340		Yes
96-075	Beef	AM Feeding	Kern	Three Brands Feedlot	7/28/96	0505	0703		Yes
96-076	Beef	PM Loafing	Kern	Three Brands Feedlot	7/28/96	1245	1810		Yes
96-077	Beef	Dusk Activity	Kern	Three Brands Feedlot	7/28/96	2019	2220		No
96-078	Beef	Night Sleeping	Kern	Three Brands Feedlot	7/29/96	0109	0310		Yes
96-079	Beef	Night Sleeping	Kern	Three Brands Feedlot	7/29/96	0310	0505		Yes
96-080	Beef	Dusk Activity	Kern	Three Brands Feedlot	7/29/96	1709	1946		Yes
96-081	Beef	End of Activity	Kern	Three Brands Feedlot	7/29/96	1947	2200		No
96-082	Beef	Night Sleeping	Kern	Three Brands Feedlot	7/29/96	2322	0123		Yes
96-083	Beef	Night Sleeping	Kern	Three Brands Feedlot	7/30/96	0123	0402		No
96-084	Beef	PM Napping	Kern	Three Brands Feedlot	7/30/96	1510	1746		Yes
96-085->086	Beef	Dusk Activity	Kern	Three Brands Feedlot	7/30/96	1850	2007		No
96-087	Beef	PM Napping	Kern	Three Brands Feedlot	7/30/96	2235	0009		Yes
96-088	Beef	Daily Loafing	Kern	Three Brands Feedlot	7/31/96	1134	1352		Yes
96-089	Beef	Daily Loafing	Kern	Three Brands Feedlot	7/31/96	1450	1640		Yes
96-090	Beef	PM Loafing	Kern	Three Brands Feedlot	7/31/96	1643	1845		Yes
96-091->092	Beef	PM Loafing	Kern	Three Brands Feedlot	7/31/96	1845	1955		No
96-093->094	Beef	PM Sleeping	Kern	Three Brands Feedlot	7/31/96	2149	2335		No
96-095	Cotton	Picking	Kings	Stone Land Co., Section 2E	11/10/96	1548	1727	Sandy Loam	Yes
96-096	Cotton	Stalk Cutting	Kings	Stone Land Co., Section 2E	11/11/96	1435	1735	Sandy Loam	Yes
96-097	Cotton	Stalk Cutting	Kings	Stone Land Co., Section 2E	11/12/96	1405	1535	Loam	Yes
96-098	Cotton	Stalk Cutting	Kings	Stone Land Co., Section 2E	11/12/96	1620	1650	Loam	Yes
96-099	Cotton	Listing	Kings	Stone Land Co., Section 10W	11/14/96	0926	1056	Sandy Loam	No
96-100	Cotton	Picking	Kings	Stone Land Co., Section 12W	11/15/96	1016	1136	Loam	No
96-101	Cotton	Picking	Kings	Stone Land Co., Section 11E	11/15/96	1302	1427	Loam	Yes
96-102	Cotton	Stalk Cutting	Kings	Stone Land Co., Section 12W	11/15/96	1713	1828	Loam	Yes
96-103	Cotton	Root Cutting	Kings	Stone Land Co., Section 2E	11/16/96	1008	1050	Sandy Loam	Yes
96-104	Cotton	Root Cutting	Kings	Stone Land Co., Section 2E	11/16/96	1249	1358	Sandy Loam	Yes
96-105	Cotton	Listing	Kings	Stone Land Co., Section 1W	11/18/96	1010	1144	Clay Loam	No
96-106	Cotton	Listing	Kings	Stone Land Co., Section 1W	11/18/96	1226	1454	Clay Loam	No
96-107	Cotton	Picking	Kings	Stone Land Co., Section 11E	11/18/96	1548	1615	Clay Loam	No
96-108	Cotton	2nd Picking	Kings	Stone Land Co., Section 11E	11/20/96	1022	1206	Clay Loam	Yes
96-109	Cotton	Root Cutting	Kings	Stone Land Co., Section 12W	11/20/96	1548	1717	Clay Loam	No
96-110	Cotton	1st discing	Kings	Stone Land Co., Section 12W	11/26/96	0920	1056	Loam*	No
96-111	Cotton	1st Discing	Kings	Stone Land Co., Section 12W	11/26/96	1240	1320	Loam*	Yes
96-112	Cotton	1st Discing	Kings	Stone Land Co., Section 12W	11/26/96	1330	1404	Loam*	Yes
96-113	Cotton	1st Discing	Kings	Stone Land Co., Section 12W	11/26/96	1518	1615	Loam*	Yes
96-114	Cotton	Root Cutting	Kings	Stone Land Co., Section 12W	11/27/96	0855	1100	Loam*	Yes
96-115	Cotton	Chiseling	Kings	Stone Land Co., Section 11E	12/2/96	1035	1235	Clay Loam	No
96-116	Cotton	Chiseling	Kings	Stone Land Co., Section 11E	12/2/96	1235	1555	Clay Loam	No
96-117	Cotton	2nd Discing	Kings	Stone Land Co., Section 11E	12/2/96	1655	1815	Clay Loam	Yes
96-118	Cotton	2nd Discing	Kings	Stone Land Co., Section 11E	12/4/96	1041	1151	Clay Loam	Yes
96-119	Cotton	2nd Discing	Kings	Stone Land Co., Section 11E	12/4/96	1237	1411	Clay Loam	Yes
96-120	Cotton	3rd Discing	Kings	Stone Land Co., Section 11E	12/5/96	1047	1200	Loam	Yes
96-121	Cotton	Listing	Kings	Stone Land Co., Section 11E	12/5/96	1540	1637	Loam	Yes
*Three soil samples analyzed, multiple textures recorded, Loam, Clay Loam, & Silty Clay Loam.									

## APPENDIX D – INVENTORY OF 1997 FIELD TESTS

### Inventory of 1997 field tests using upwind-downwind sampling array

TESTID	COMMODITY	OPERATION	COUNTY	SITEDESC	TESTDAT	TEST1	TEST2	SOILTEXT1	VALID?	COMMENTS
97-001	Milk	Loafing	Tulare	Curti Dairy #2	2/6/97	1355	1655		No	
97-002	Milk	Loafing	Tulare	Curti Dairy #2	2/12/97	0952	1156		No	
97-003	Milk	Loafing	Tulare	Curti Dairy #2	2/12/97	1156	1445		No	
97-004	Milk	Loafing	Tulare	Curti Dairy #2	2/12/97	1445	1715		No	
97-005	Milk	Evening Loafing	Tulare	Curti Dairy #2	2/12/97	1715	2231		No	
97-006	Milk	Sleeping	Tulare	Curti Dairy #2	2/12/97	2231	0830		No	
97-007	Milk	Loafing	Tulare	Curti Dairy #2	2/13/97	0959	1200		No	
97-008	Milk	Loafing	Tulare	Curti Dairy #2	2/14/97	0757	1000		No	
97-009	Milk	Loafing	Tulare	Curti Dairy #2	2/14/97	1200	1355		No	
97-010	Milk	Loafing	Tulare	Curti Dairy #2	2/14/97	1355	1550		No	
97-011	Alfalfa	Ambient	Kings	River Ranch, Section 03	2/15/97	1155	1354		No	
97-012	Alfalfa	Ambient	Kings	River Ranch, Section 03	2/15/97	1338	1554		No	
97-013-->031	Caltrans Research								No	Not SJV Ag
97-032	Wheat	Harvest	Kings	Stone Land Co., Section 2E	6/17/97	1638	1813		Yes	
97-033	Wheat	Harvest	Kings	Stone Land Co., Section 2E	6/18/97	0940	1116	Loam	Yes	
97-034	Wheat	Harvest	Kings	Stone Land Co., Section 2E	6/18/97	1600	1706	Loam	Yes	
97-035	Wheat	Harvest	Kings	Stone Land Co., Section 2E	6/18/97	1706	1756	Loam	Yes	
97-036	Wheat	Harvest	Kings	Stone Land Co., Section 2E	6/18/97	1756	1923	Loam	Yes	
97-037	Wheat	Discing	Kings	Stone Land Co., Section 2E	6/19/97	1040	1155		No	Contaminated Upwind
97-038	Wheat	First Discing	Kings	Stone Land Co., Section 2E	6/19/97	1544	1737		No	Lacks Upwind PM
97-039	Wheat	First Discing	Kings	Stone Land Co., Section 2E	6/20/97	1130	1258	Sandy Loam	No	Contaminated Upwind
97-040	Wheat	First Discing	Kings	Stone Land Co., Section 2E	6/20/97	1319	1452	Sandy Loam	No	Contaminated Upwind
97-041	Wheat	Harvest	Kings	Stone Land Co., Section 14	6/21/97	1306	1413	Silty Clay Ld	Yes	
97-042	Wheat	First Discing	Kings	Stone Land Co., Section 2E	6/23/97	1241	1345		No	
97-043	Wheat	First Discing	Kings	Stone Land Co., Section 2E	6/23/97	1421	1552		No	
97-044	Wheat	First Discing	Kings	Stone Land Co., Section 2E	6/23/97	1552	1651		No	
97-045	Wheat	First Discing	Kings	Stone Land Co., Section 2E	6/24/97	0956	1137	Sandy Loam	Yes	
97-046	Wheat	Ripping	Kings	Stone Land Co., Section 2E	6/24/97	1342	1635	Sandy Loam	Yes	
97-047	Wheat	First Ripping	Kings	Stone Land Co., Section 2E	6/25/97	0941	1207	Sandy Loam	No	Lacks PM Profile
97-048	Wheat	First Ripping	Kings	Stone Land Co., Section 2E	6/25/97	1231	1410	Sandy Loam	Yes	
97-049	Wheat	Ripping	Kings	Stone Land Co., Section 2E	6/25/97	1411	1551	Sandy Loam	Yes	
97-050	Wheat	Ripping	Kings	Stone Land Co., Section 2E	6/26/97	0820	0850		Yes	
97-051	Wheat	Ripping	Kings	Stone Land Co., Section 2E	6/26/97	1000	1040		Yes	

## 12 APPENDIX E – INVENTORY OF 1998 FIELD TESTS

### Inventory of 1998 field tests using upwind-downwind sampling array

TESTID	COMMODITY	OPER_BASIC	COUNTY	SITEDESC	TESTDATE	TESTSTART	TESTEND	SOILTEXT(WETSIEVE)	VALID?	COMMENTS
98-001	Cotton	Weeding	Fresno	J and J farms, Field 10W	6/4/98	0905	1026	Clay Loam	Yes	OK
98-002	Cotton	Weeding	Fresno	J and J farms, Field 10W	6/4/98	1026	1205	Clay Loam	Yes	OK
98-003	Cotton	Weeding	Fresno	J and J farms, Field 10W	6/4/98	1231	1429	Clay Loam	Yes	OK
98-004	Cotton	Weeding	Fresno	J and J farms, Field 10W	6/4/98	1231	1429	Clay Loam	Yes	OK
98-005	Cotton	Weeding	Fresno	J and J farms, Field 10W	6/5/98	0834	0929	Clay Loam	Yes	OK
98-006	Cotton	Weeding	Fresno	J and J farms, Field 10W	6/5/98	0939	1128	Clay Loam	Yes	OK
98-007	Cotton	Weeding	Fresno	J and J farms, Field 10W	6/5/98	1133	1301	Clay Loam	Yes	OK
98-008	Cotton	Weeding	Fresno	J and J farms, Field 10W	6/5/98	1308	1442	Clay Loam	Yes	OK
98-009	Cotton	Weeding	Fresno	J and J farms, Field 10W	6/5/98	1450	1625	Clay Loam	Yes	OK
98-010	Cotton	Weeding	Fresno	J and J farms, Field 10W	6/6/98	0755	0922	Clay Loam	Yes	OK
98-011	Cotton	Weeding	Fresno	J and J farms, Field 10W	6/6/98	0932	1136	Clay Loam	Yes	OK
98-012	Almonds	Pickup Outside Near	Kern	Paramount Farms Field 310	9/11/98	0925	0955	Clay Loam	No	MET, PM NOT CO-LOCATED
98-013	Almonds	Pickup Middle	Kern	Paramount Farms Field 310	9/11/98	1028	1047	Clay Loam	No	MET, PM NOT CO-LOCATED
98-014	Almonds	Pickup Outside Far	Kern	Paramount Farms Field 310	9/11/98	1113	1130	Clay Loam	No	MET, PM NOT CO-LOCATED
98-015	Almonds	Pickup Outside Near	Kern	Paramount Farms Field 310	9/11/98	1342	1406	Clay Loam	No	MET, PM NOT CO-LOCATED
98-016	Almonds	Pickup Middle	Kern	Paramount Farms Field 310	9/11/98	1436	1453	Clay Loam	No	MET, PM NOT CO-LOCATED
98-017	Almonds	Pickup Outside Far	Kern	Paramount Farms Field 310	9/11/98	1522	1533	Clay Loam	No	MET, PM NOT CO-LOCATED
98-018	Almonds	Pickup Outside Far	Kern	Paramount Farms Field 310	9/11/98	1750	1802	Clay Loam	No	MET, PM NOT CO-LOCATED
98-019	Almonds	Pickup Middle	Kern	Paramount Farms Field 310	9/11/98	1831	1841	Clay Loam	No	MET, PM NOT CO-LOCATED
98-020	Almonds	Pickup Outside Near	Kern	Paramount Farms Field 310	9/11/98	1857	1905	Clay Loam	No	MET, PM NOT CO-LOCATED
98-021	Almonds	Pickup Outside Near	Kern	Paramount Farms Field 310	9/12/98	0829	0838	Clay	No	MET, PM NOT CO-LOCATED
98-022	Almonds	Pickup Middle	Kern	Paramount Farms Field 310	9/12/98	0944	0951	Clay	No	MET, PM NOT CO-LOCATED
98-023	Almonds	Pickup Outside Far	Kern	Paramount Farms Field 310	9/12/98	1008	1018	Clay	No	MET, PM NOT CO-LOCATED
98-024	Almonds	Pickup Outside Far	Kern	Paramount Farms Field 310	9/12/98	1220	1239	Clay Loam	No	MET, PM NOT CO-LOCATED
98-025	Almonds	Pickup Middle	Kern	Paramount Farms Field 310	9/12/98	1254	1307	Clay Loam	No	MET, PM NOT CO-LOCATED
98-026	Almonds	Pickup Outside Near	Kern	Paramount Farms Field 310	9/12/98	1318	1335	Clay Loam	No	MET, PM NOT CO-LOCATED
98-027	Almonds	Pickup Outside Far	Kern	Paramount Farms Field 310	9/12/98	1405	1414	Clay Loam	No	MET, PM NOT CO-LOCATED
98-028	Almonds	Pickup Outside Near	Kern	Paramount Farms Field 306	9/13/98	0902	0913	Sandy Loam	No	MET, PM NOT CO-LOCATED
98-029	Almonds	Pickup Middle	Kern	Paramount Farms Field 306	9/13/98	0929	0943	Sandy Loam	No	MET, PM NOT CO-LOCATED
98-030	Almonds	Pickup Outside Far	Kern	Paramount Farms Field 306	9/13/98	0959	1010	Sandy Loam	No	MET, PM NOT CO-LOCATED
98-031	Almonds	Pickup Outside Far	Kern	Paramount Farms Field 306	9/13/98	1206	1216	Sandy Loam	No	MET, PM NOT CO-LOCATED
98-032	Almonds	Pickup Middle	Kern	Paramount Farms Field 306	9/13/98	1231	1241	Sandy Loam	No	MET, PM NOT CO-LOCATED
98-033	Almonds	Pickup Outside Near	Kern	Paramount Farms Field 306	9/13/98	1251	1301	Sandy Loam	No	MET, PM NOT CO-LOCATED
98-034	Almonds	Pickup Outside Far	Kern	Paramount Farms Field 306	9/13/98	1517	1527	Sandy Loam	No	MET, PM NOT CO-LOCATED
98-035	Almonds	Pickup Middle	Kern	Paramount Farms Field 306	9/13/98	1539	1549	Sandy Loam	No	MET, PM NOT CO-LOCATED
98-036	Almonds	Pickup Outside Near	Kern	Paramount Farms Field 306	9/13/98	1601	1611	Sandy Loam	No	MET, PM NOT CO-LOCATED
98-037	Almonds	Pickup Outside Near	Kern	Paramount Farms Field 306	9/14/98	0915	0925	Sandy Loam	No	MET, PM NOT CO-LOCATED
98-038	Almonds	Pickup Middle	Kern	Paramount Farms Field 306	9/14/98	0938	0948	Sandy Loam	No	MET, PM NOT CO-LOCATED
98-039	Almonds	Pickup Outside Far	Kern	Paramount Farms Field 306	9/14/98	0957	1007	Sandy Loam	No	MET, PM NOT CO-LOCATED
98-040	Almonds	Pickup Outside Far	Kern	Paramount Farms Field 306	9/14/98	1153	1205	Sandy Loam	No	MET, PM NOT CO-LOCATED
98-041	Almonds	Pickup Middle	Kern	Paramount Farms Field 306	9/14/98	1215	1226	Sandy Loam	No	MET, PM NOT CO-LOCATED
98-042	Almonds	Pickup Outside Near	Kern	Paramount Farms Field 306	9/14/98	1240	1250	Sandy Loam	No	MET, PM NOT CO-LOCATED
98-043	Cotton	Stalk Cutting	Fresno	J and J farms, Field 10W	11/5/98	0945	1032	Clay Loam	Yes	OK
98-044	Cotton	Stalk Cutting	Fresno	J and J farms, Field 10W	11/5/98	1050	1150	Clay Loam	Yes	OK
98-045	Cotton	Discing	Fresno	J and J farms, Field 10W	11/6/98	0820	0921	Clay Loam	Yes	OK
98-046	Cotton	Discing	Fresno	J and J farms, Field 10W	11/6/98	0929	1015	Clay Loam	Yes	OK
98-047	Cotton	Discing	Fresno	J and J farms, Field 10W	11/6/98	1015	1040	Clay Loam	Yes	OK
98-048	Cotton	Discing	Fresno	J and J farms, Field 10W	11/6/98	1050	1115	Clay Loam	Yes	OK
98-049	Cotton	Discing	Fresno	J and J farms, Field 10W	11/6/98	1137	1247	Clay Loam	Yes	OK
98-050	Cotton	Discing	Fresno	J and J farms, Field 10W	11/6/98	1404	1450	Clay Loam	Yes	OK

**Contract No. 98-38825-6063**  
**November 29, 1999**

**PROGRESS REPORT**  
**Comparison of Almond Harvester PM<sub>10</sub> Dust Emissions**

A study for  
United States Department of Agriculture

Lowell L. Ashbaugh, Principal Investigator  
Crocker Nuclear Laboratory

Robert G. Flocchini, Investigator  
Department of Land, Air & Water Resources and  
Crocker Nuclear Laboratory

Britt Holmén, Chris Tsubamoto, Teresa A. James,  
Omar F. Carvacho, Mike Brown,  
Jose Mojica, Minh Cao, and Thinh Tran, Investigators  
Crocker Nuclear Laboratory

---

---

**Air Quality Group  
Crocker Nuclear Laboratory  
University of California  
Davis, CA 95616-8569**





## 14 TABLE OF CONTENTS

Table of Contents.....	i
List of Figures.....	ii
List of Tables.....	iii
Introduction.....	1
Study design.....	1
Location and test period.....	1
Test strategy.....	1
Results.....	2
Meteorology.....	2
PM <sub>10</sub> Mass.....	9
Lidar data observations.....	9
Discussion.....	13
Lidar data animations.....	15
Averaged 2D vertical scans.....	17
Conclusions.....	18

**15**

## LIST OF FIGURES

Figure 1. Mean wind speed, wind direction, and Richardson Number outside the tree canopy for each harvester test.....	3
Figure 2. Meteorology outside the tree canopy for September 10, 1999.....	7
Figure 3. Meteorology outside the tree canopy and test periods for September 11, 1999.....	7
Figure 4. Meteorology outside the tree canopy and test periods for September 12, 1999.....	8
Figure 5. Meteorology outside the tree canopy and test periods for September 13, 1999.....	8
Figure 6. Meteorology outside the tree canopy and test periods for September 14, 1999.....	9
Figure 7. Lidar configuration on solid-set irrigation field September 11, 1998.....	10
Figure 8. Diagram of lidar vertical scan configuration.....	11
Figure 9. Lidar configuration for horizontal scans.....	12
Figure 10. Lidar view at solid-set irrigated field (field 310).....	13
Figure 11. Average lidar backscatter signal during harvester operation.....	19
Figure 12. PM <sub>10</sub> concentrations downwind of harvester #1 and #2, (a) all tests, (b) Solid-set irrigation, (c) Micro-spray irrigation. ....	21
Figure 13. PM <sub>10</sub> concentrations downwind of harvester #3 and #4, (a) all tests, (b) Solid-set irrigation, (c) Micro-spray irrigation. ....	22
Figure 14. Dust concentrations for harvesters #1-#4 on both fields by harvest row. ....	23
Figure 15. Dust concentrations for all harvesters #1-#4 on solid-set irrigated field by harvest row. ....	24
Figure 16. Dust concentrations for harvesters #1-#4 on micro-sprayed field by harvest row. ....	25
Figure 17. PM <sub>10</sub> concentrations downwind of harvester #5, (a) all tests, (b) Solid-set irrigation, (c) Micro-spray irrigation, (d) near row, (e) middle row, (f) far row.....	26

## 16 LIST OF TABLES

Table 1. Mean wind speed, wind direction, and Richardson Number for each harvester test.....	4
Table 2. Integrated PM <sub>10</sub> concentrations ( $\mu\text{g}/\text{m}^3$ ) for each harvester test.....	14
Table 3. Pre-harvest windrow trash <2mm in size (grams).....	14
Table 4. PM <sub>10</sub> concentrations normalized to amount of windrow trash <2mm prior to harvest ( $\mu\text{g}/\text{m}^3/\text{g}$ ) .....	15



# 1998 Almond Harvester PM<sub>10</sub> Emission Tests

## 17 INTRODUCTION

In 1994 and 1995, UC Davis tested PM<sub>10</sub> emissions of almond shakers, sweepers, and nut pickup machines. All tests were conducted without interfering with the grower's operation to obtain data on real-world harvesting operations. These tests identified almond harvesting, specifically nut pickup, as an operation that would benefit from efforts to reduce the dust emissions. This report describes a test conducted in July 1998 to measure PM<sub>10</sub> dust emissions under controlled conditions from older and newer models of the two major manufacturers of harvesting equipment. The tests identify the extent of reduced emissions that can be expected from replacing older harvesters with newer ones. The tests also identify differences in emissions that could result from management practices of the grower.

## 18 STUDY DESIGN

### 18.1 Location and test period

The tests were conducted at Paramount Farms in Kern County on September 11-14, 1998 during the nonpareil almond harvest. The tests described here were conducted on fields 310 on September 11-12, and field 306 on September 13-14. Field 310 was irrigated with solid-set sprinklers, while field 306 was irrigated with micro-sprayers.

The tree rows on each orchard are oriented along the north/south axis. The prevailing winds were from the east during most tests, but sometimes switched to the west.

### 18.2 Test strategy

The overall test strategy was to sample PM<sub>10</sub> dust concentrations upwind and downwind for each harvester under conditions that were as identical as possible. Multiple simultaneous tests were conducted on older and newer model harvesters from Flory Industries and Weiss-McNair, Inc. and an older model Ramacher harvester to determine whether there is a difference between the older and newer designs. The harvesters will be referred to here only by code, not by manufacturer. Three sampling towers were used to collect replicate test data simultaneously. The tests were conducted on two different orchards; one with solid-set and one with micro-spray irrigation. Three replicate tests were conducted concurrently for each harvester/orchard combination, and the three replicate tests were repeated twice. The orchards were planted with two rows on nonpareil trees, then a pollinator tree, followed by two more rows of nonpareil trees. Each harvester was tested sequentially on three rows, once on the outside of the two nonpareil rows near the towers, once on the middle row between the nonpareil trees, and once on the outside of the two nonpareil trees far from the towers. After these three tests, the sampling platforms were moved three rows and the tests were repeated using another harvester.

Flory Industries and Weiss-McNair each provided one older model harvester and one new model harvester with PTO for the tests. Weiss-McNair also provided a Ramacher harvester. The Weiss-McNair harvesters were models 948H for the older model and 8900X for the newer one. The Flory harvesters were models 3100 for the older model and 480 for the newer one. The Ramacher harvester

was a model 9500. The harvesters are referred to in this report only by numbers 1–5. Harvesters 1 and 2 were the new and old models from one manufacturer, while harvesters 3 and 4 were the new and old models from another manufacturer. Harvester 5 had no new model to compare to. Paramount Farms shook the trees and swept the nuts using a single sweeper model to prepare all the rows as identically as possible. The harvesting was performed using a single tractor to power the harvesters. The older models were operated at 0.8 mph, and the two new models were operated at 1.1 mph. Each harvester was tested in a configuration that had the fan blower pointing toward the particle samplers during operation so that the dust plume was carried over the samplers as the harvester passed them.

UC Davis erected an upwind fixed tower for upwind particle and meteorological measurements, and three downwind towers for particle measurements for each test. The downwind towers were located two rows (nine meters) downwind of the nearest row harvested for each harvester, and were placed 15 meters apart in the row. For the second row harvested, the towers remained in place, but were 15 meters downwind. For the third row, the towers were 21 meters downwind. After testing each harvester on three successive rows, the towers were moved up three rows for the next harvester.

UC Davis also used lidar to measure the plume characteristics, to the extent possible, throughout the testing. During the almond harvest the lidar was positioned to scan both vertically along the downwind edge of the orchard as well as horizontally over the top of the trees to assess the maximum height of the dust plume. The lidar data demonstrate the capability of lidar to detect PM as it is transported out of the orchard and to identify the routes of PM transport that can subsequently be quantified by other means. For example, the lidar data can be used to plan the placement of filter point samplers and to evaluate the results of the point samplers in terms of the larger scale of plume spatial distribution and plume variability.

Because of the format (many multi-megabyte files) of the lidar data, it is currently best examined qualitatively as animations of successively collected two-dimensional vertical or horizontal scans. These files can be viewed using Netscape or Internet Explorer (see instructions below). Prior to discussion of the almond harvest data, a brief introduction to the lidar data scans is given.

Two meteorological towers were used to collect wind speed and direction data. One was located outside the orchard; the other was located inside. The meteorological data were examined to confirm valid test conditions.

## **19 RESULTS**

### **19.1 Meteorology**

The tree canopy creates a much different environment inside the orchard than exists outside, so the outside meteorology is not representative of the conditions experienced at the samplers. It is useful to examine the outside meteorology for overall sampling conditions, but it can not be used to calculate emission fluxes. The almond harvesters create their own winds, too, so the meteorology within the canopy is strongly affected by the harvest activities. Each time a harvester passes the sampler, it creates strong winds that are not necessarily aligned with the natural air movement in the canopy. Furthermore, the natural wind profile in the canopy is not logarithmic with height as is normally the case in the outside environment. Instead, the tree structure modifies the winds; the highest wind speeds are found close to the ground where there are few leaves and branches to slow it. The slowest winds are found at canopy height, about 3-5 meters above ground. Above the tree canopy, the wind speeds typically increase

logarithmically with height. These factors combine to make it impossible to calculate emission fluxes for the harvester tests. Instead, this report will focus on the PM<sub>10</sub> mass concentrations for each harvester and field tested.

Table 8 shows the mean and standard deviation of the wind direction, wind speed, temperature, and Richardson Number during each harvester test. These data are plotted in Figure 7. It's clear that the most stable conditions (large positive Richardson Number) occurred during periods of light winds. During a few tests, notably 22 and 25, large shifts in wind direction took place. Most of the tests occurred during winds from the northeast, though several had south and southwest winds. The second set of tests, on the micro-sprayed field, had somewhat higher wind speeds than the first set, on the solid-set irrigated field. Temperatures ranged from a low of 20 °C to a high of 35 °C and increased slightly from the start of testing to the end.

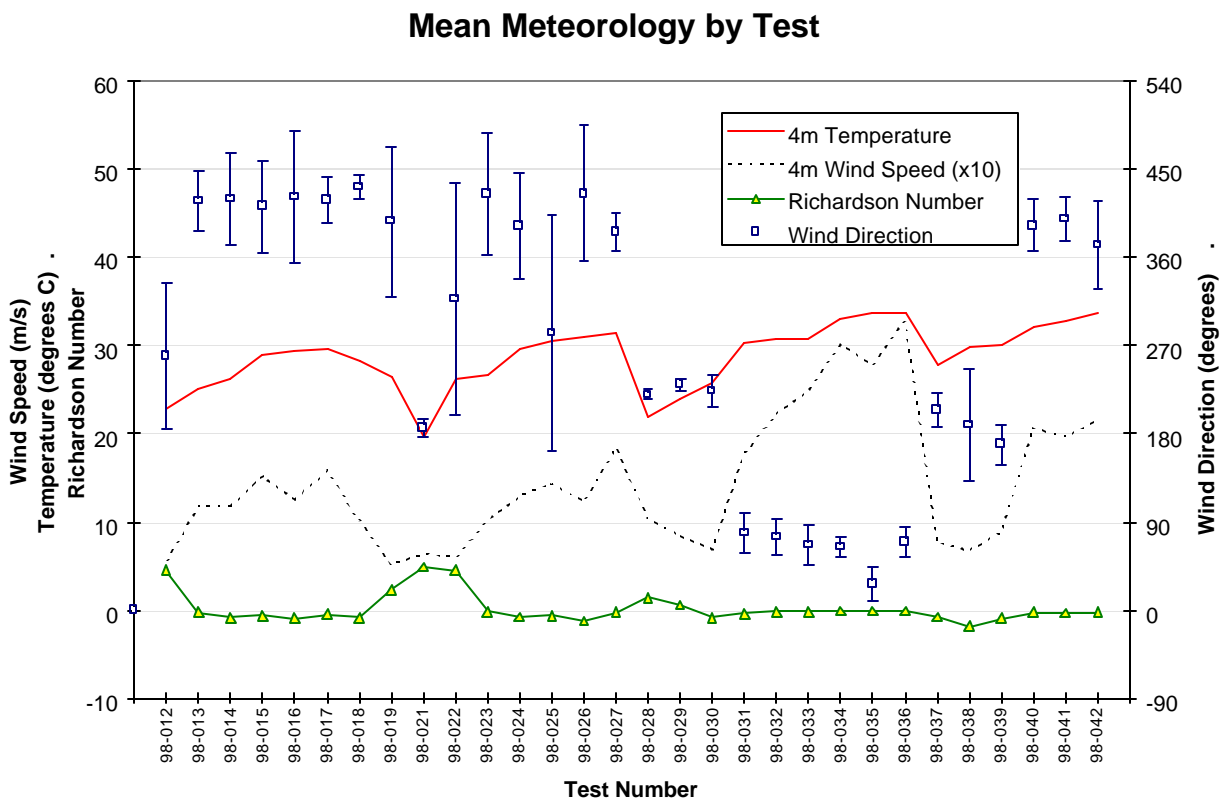


**Figure 7. Mean wind speed, wind direction, and Richardson Number outside the tree canopy for each harvester test**

The meteorological data are shown in Figure 8 through Figure 12. Each figure shows the wind speed, wind direction, and the Richardson number, a measure of atmospheric stability. In general, negative Richardson numbers indicate a turbulent atmosphere, while positive Richardson numbers indicate a stable atmosphere. These data were collected outside the tree canopy, so are shown here as an indication of overall environmental conditions.

**Table 8. Mean wind speed, wind direction, and Richardson Number for each harvester test**

Test	Date and start time	Elapsed Time	Mean wind direction at 4m	Mean wind speed at 4m	Mean Richardson Number at 4m	Mean air temperature at 4m
12	9/11/98 9:25	30	212±69	0.56±0.13	4.52±2.53	22.8±0.4
13	9/11/98 10:28	19	96±90	1.17±0.43	-0.26±0.25	25.1±0.3
14	9/11/98 11:13	17	103±91	1.18±0.35	-0.82±0.51	26.2±0.3
15	9/11/98 13:42	24	82±92	1.53±0.45	-0.61±0.69	28.9±0.4
16	9/11/98 14:36	17	104±76	1.25±0.33	-0.92±0.44	29.5±0.3
17	9/11/98 15:22	11	60±23	1.59±0.43	-0.47±0.43	29.7±0.3
18	9/11/98 17:50	12	72±11	1.01±0.25	-0.83±0.50	28.4±0.1
19	9/11/98 18:31	10	73±49	0.52±0.11	2.35±1.06	26.6±0.3
20	9/11/98 18:57	8	117±0	0.45±0.00	9.57±0.44	23.6±0.3
21	9/12/98 8:29	9	186±9	0.64±0.19	4.87±2.15	19.6±0.2
22	9/12/98 9:44	7	318±118	0.61±0.16	4.53±2.31	26.3±0.1
23	9/12/98 10:08	10	101±100	1.01±0.35	-0.18±0.25	26.7±0.2
24	9/12/98 12:20	19	108±117	1.29±0.36	-0.78±0.55	29.7±0.2
25	9/12/98 12:54	13	145±91	1.44±0.46	-0.62±0.40	30.6±0.4
26	9/12/98 13:18	17	87±39	1.23±0.39	-1.17±0.85	31.1±0.3
27	9/12/98 14:05	9	66±108	1.84±0.33	-0.28±0.11	31.6±0.1
28	9/13/98 9:02	11	220±5	1.04±0.22	1.45±0.69	22.0±0.3
29	9/13/98 9:29	14	230±7	0.84±0.21	0.56±0.49	24.1±0.3
30	9/13/98 9:59	11	224±16	0.69±0.18	-0.87±0.45	25.9±0.2
31	9/13/98 12:06	10	79±20	1.79±0.66	-0.39±0.38	30.4±0.1
32	9/13/98 12:31	10	75±18	2.22±0.38	-0.17±0.07	30.7±0.1
33	9/13/98 12:51	10	67±21	2.50±0.57	-0.13±0.05	30.8±0.2
34	9/13/98 15:17	10	64±10	3.01±0.40	-0.10±0.03	33.1±0.3
35	9/13/98 15:39	10	27±17	2.79±0.55	-0.11±0.04	33.8±0.2
36	9/13/98 16:01	10	70±15	3.28±0.41	-0.07±0.02	33.8±0.2
37	9/14/98 9:15	10	205±17	0.78±0.24	-0.77±0.52	27.9±0.3
38	9/14/98 9:38	10	189±57	0.67±0.23	-1.82±0.89	29.8±0.3
39	9/14/98 9:57	10	170±20	0.89±0.30	-0.90±0.54	30.1±0.2
40	9/14/98 11:53	12	63±90	2.07±0.53	-0.26±0.28	32.1±0.4
41	9/14/98 12:15	11	40±22	1.97±0.60	-0.29±0.21	32.8±0.2
42	9/14/98 12:40	10	193±156	2.16±0.89	-0.24±0.21	33.6±0.2

Figure 8 shows the meteorological data for September 10, 1998. This was a setup day, so no PM<sub>10</sub> tests were conducted. The meteorological data were used to confirm the expected wind direction. Unfortunately, on this day the wind was very light, though the direction was steady. The atmosphere was unstable from shortly after 9:00 a.m. until noon, then remained stable for the rest of the day. The first test day was September 11, 1998. The meteorological data and test periods are shown in Figure 42. The first test of the day, indicated as Test 12, occurred during stable air flow with light winds (<1 m/s) from the southwest. Tests 13 through 18 occurred during neutral to unstable air flow with slightly stronger winds (1-2 m/s) from the northeast. The final two tests occurred during progressively more stable calm air.

The meteorological data and test periods for September 13 are shown in Figure 44. On this day the wind shifted from the south and southwest to the northeast between 9:00 a.m. and noon, and the wind speed picked up from very light (~1m/s) to moderate (3-4 m/s) as the day progressed. Tests 28-30 were conducted during the south/southwest very light wind period. Tests 31 through 36 were conducted in the later period of stronger northeasterly winds. The atmospheric stability ranged from slightly stable to slightly unstable in the morning to neutral or slightly unstable in the afternoon.

The meteorological data and test periods for September 14 are shown in Figure 12. Only six tests were conducted on this day, all before 1:00 p.m. Tests 37-39 took place under moderately unstable very light winds (<1 m/s) from the south. Tests 40-42 occurred under near neutral light winds (1-3 m/s) from the northeast.

The meteorological data and test periods for September 12 are shown in Figure 43. Tests 21 and 22 were conducted under calm, stable atmospheric conditions, while tests 23 through 27 were conducted during neutral to slightly unstable conditions with light winds (1-2 m/s) from the northeast. These latter tests were conducted under very similar conditions.

### Meteorology During Almond Harvester Tests

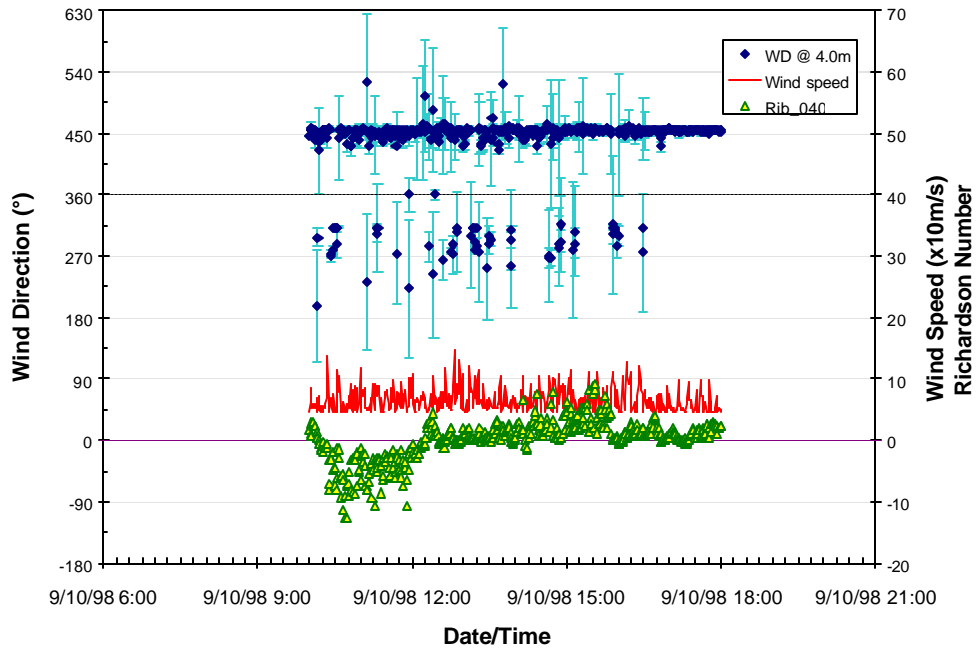


Figure 8. Meteorology outside the tree canopy for September 10, 1998

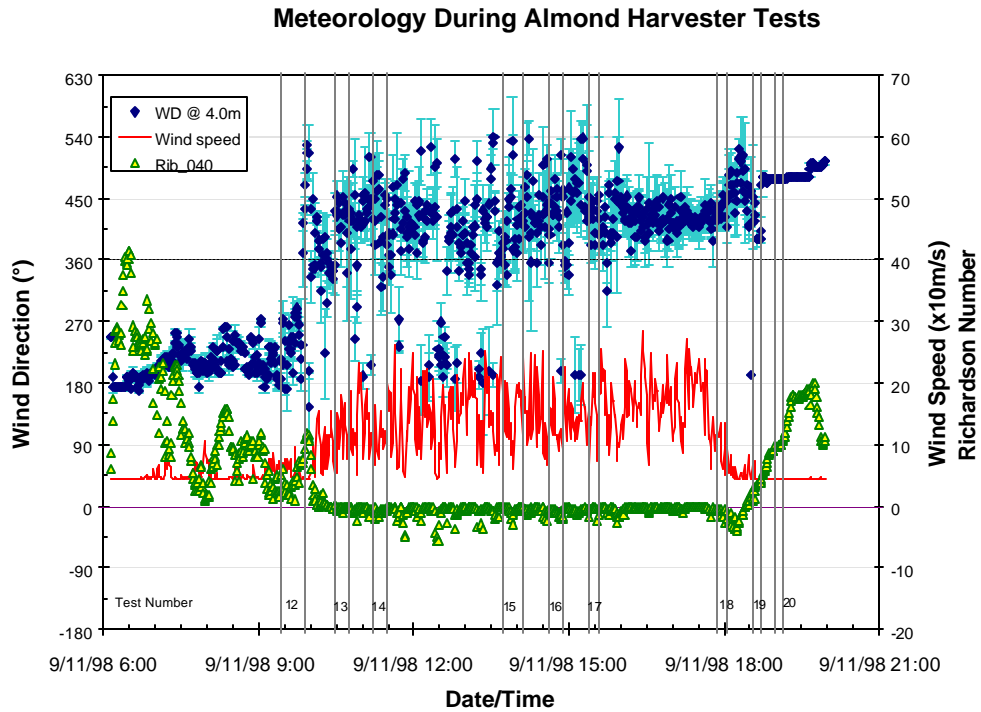


Figure 42. Meteorology outside the tree canopy and test periods for September 11, 1998

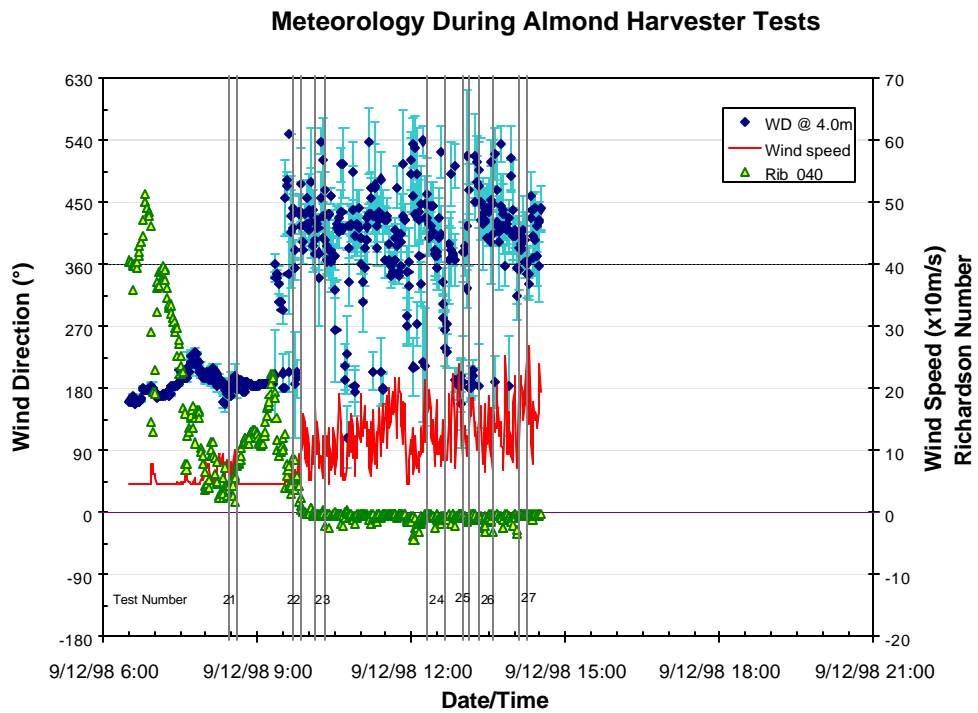


Figure 43. Meteorology outside the tree canopy and test periods for September 12, 1998

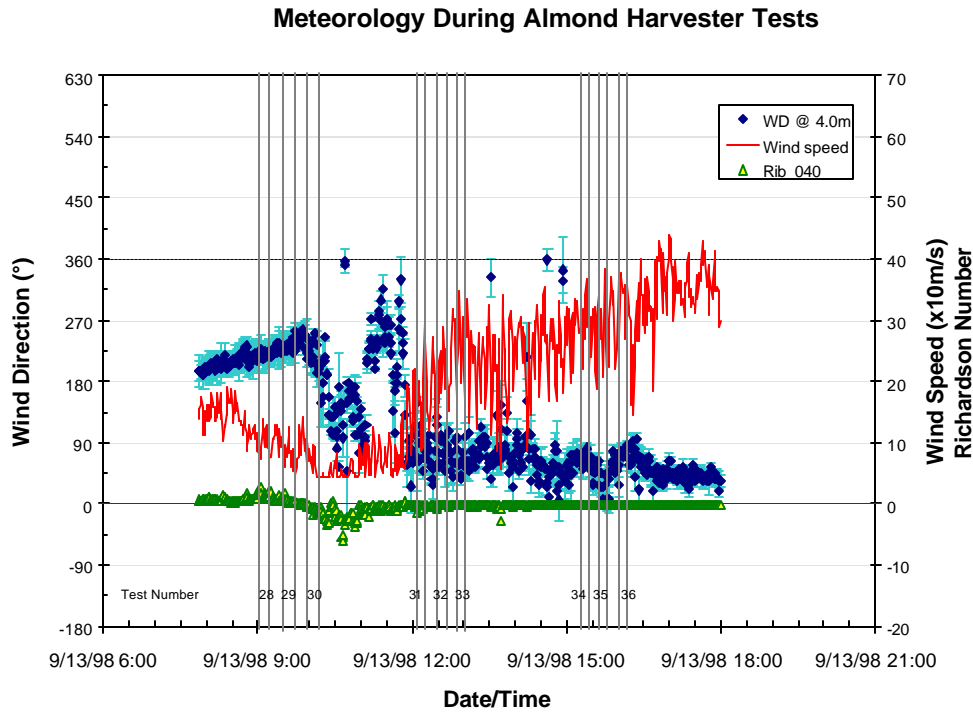
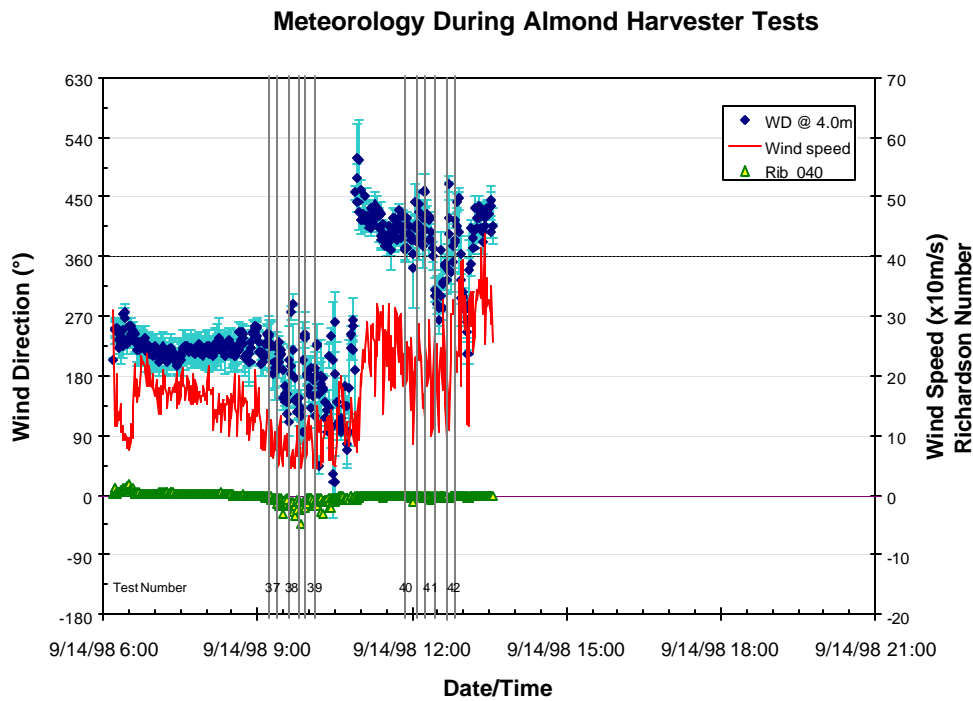


Figure 44. Meteorology outside the tree canopy and test periods for September 13, 1998



## Figure 12. Meteorology outside the tree canopy and test periods for September 14, 1998

### 19.2 PM<sub>10</sub> Mass

The PM<sub>10</sub> mass was measured at three heights on three towers for each test. A complete set of tests included one with the harvester two tree rows from the towers picking up nuts on the outside of the harvested trees, one with the harvester three rows from the towers picking up from between the two rows of harvested trees, and one with the harvester four rows from the towers picking up nuts on the outside again. In Figure 51 through Figure 56 the uncertainty bar represents the standard deviation of all measurements that were averaged for that figure.

Figure 51 shows a set of plots for harvesters 1 and 2 on both fields, and on each field separately. In Figure 51a it appears harvester 1 created higher PM<sub>10</sub> concentrations than the older harvester 2. Upon closer inspection, though, this seems to be the case only on the micro-spray irrigated field, and only at 1m above the soil surface. This may be due to the way in which dust and trash is ejected from the machine and to the field management practiced on the micro-spray irrigated field. In any case, dust ejected closer to the ground should deposit sooner than dust ejected higher up. On the solid-set irrigated field the PM<sub>10</sub> concentrations created by the newer harvester 1 were lower than those from the older harvester 2.

Figure 52 shows PM<sub>10</sub> plots for harvesters 3 and 4. On both fields, the newer harvester 3 shows lower PM<sub>10</sub> concentrations than the older model. For this harvester, too, the PM<sub>10</sub> concentrations from the micro-spray irrigated field were higher than for the solid-set irrigated field. The PM<sub>10</sub> concentration profile for the newer harvester 3 is similar to that for harvesters 1 and 2.

Figure 53 shows PM<sub>10</sub> concentrations for harvesters 1–4 on all fields for the near outside, middle, and far outside harvest rows. The outside rows are those between nonpareil trees and pollinators, while the middle row is between two rows of nonpareil trees. There is a slight decrease in PM<sub>10</sub> concentration with distance of the harvest operation from the sampling towers. Figure 54 shows the same plots for the solid-set irrigated field. There is little difference between the different harvest positions. Figure 55 shows the same plots for the micro-spray irrigated field. In this case there is a striking difference between the harvest positions. There is a clear decrease in PM<sub>10</sub> concentrations from the near outside row to the far outside row.

Figure 56 shows plots of PM<sub>10</sub> concentration from harvester 5 on both fields combined, each field separately, and for each harvest row tested. Note that the horizontal PM<sub>10</sub> scale for these plots is significantly higher than for the other harvesters. Harvester 5 produced much higher PM<sub>10</sub> concentrations than the other two harvesters.

### 19.3 Lidar data observations

The following three observations were made regarding using lidar to sample PM emissions from harvest operations in orchards:

- (1) We were able to document intermittent PM plumes extending to heights of greater than 50 meters during midday convective conditions; lidar data were collected for all five of the harvester machines being compared. The importance of holes in the orchard (due to dead or removed trees) as dust escape routes was noted during this field study. The holes seem to act as ‘chimneys’ for PM<sub>10</sub>

escape during midday vertical convective periods, allowing the dust plumes to extend visibly above the orchard to over 50 meters height (Animation 1).

- (2) Since the lidar can detect dust from any PM<sub>10</sub> source but cannot easily distinguish between plumes from different sources, it is very important to keep all other dust-producing activities on neighboring fields to a minimum during lidar sampling. At Paramount Farms, the harvest was rushed due to the poor weather conditions during 1998 (El Niño). Therefore, many different activities were taking place in close proximity to our lidar sampling area. Truck and three-wheeler traffic on the dirt roads, poling on adjacent upwind orchards and impatient traffic driving off paved roads and through the dirt fields (creating huge dust clouds!) often caused interference in the lidar data set.
- (3) The use of lidar for PM<sub>10</sub> sampling in orchards is expected to give quite different quantitative results than for samples collected using filters positioned within the canopy because of (a) different meteorological conditions inside and outside the canopy, and (b) the trees act to ‘catch’ some of the PM, resulting in lower PM<sub>10</sub> concentrations outside the orchard boundaries.

This latter conclusion, however, does not hold for nut pickup from windrows at the very edge of the orchard. For these edge windrows, the harvester’s powerful fans push the dust out of the trees allowing the lidar to monitor the dust plume. Thus, to compare the five harvesters via lidar, we conducted lidar-only tests on the windrows at the edge of fields 310 (solid-set irrigation) and 306 (micro-spray irrigation). For these tests, each harvester collected nuts from about a 100m section of the near-edge windrow and the lidar collected 2D vertical scans parallel to the edge of the orchard. (On the solid-set field the 2nd windrow was used due to the presence of an elevated berm at the field edge that caused dust interference). On the micro-spray field, the first windrow was used to compare all five harvesters. Unfortunately, the micro-spray field is next to a well-traveled paved road and the traffic created interference problems, so our data interpretation will focus on the solid-set field results for September 11, 1998.

The lidar data on the solid-set field were collected from the sampling layout shown in Figure 46. Figure 47 shows the configuration of the lidar for vertical scans, and Figure 48 shows the configuration for horizontal scans. Because of time constraints on the harvester drivers, only four harvesters were compared on windrow #2 (harvester #2 ran on windrow #1 only). The lidar was positioned ~300m north of the field and data were collected using a 2D vertical and horizontal scan sequence controlled by the lidar computer. The vertical scan plane was approximately five meters east of the edge of the orchard over a dry irrigation canal that borders the east edge of the field (see Figure 49).

Lidar vertical scans were made in quick succession at three different azimuths (90.1, 89.6, 88.6; the

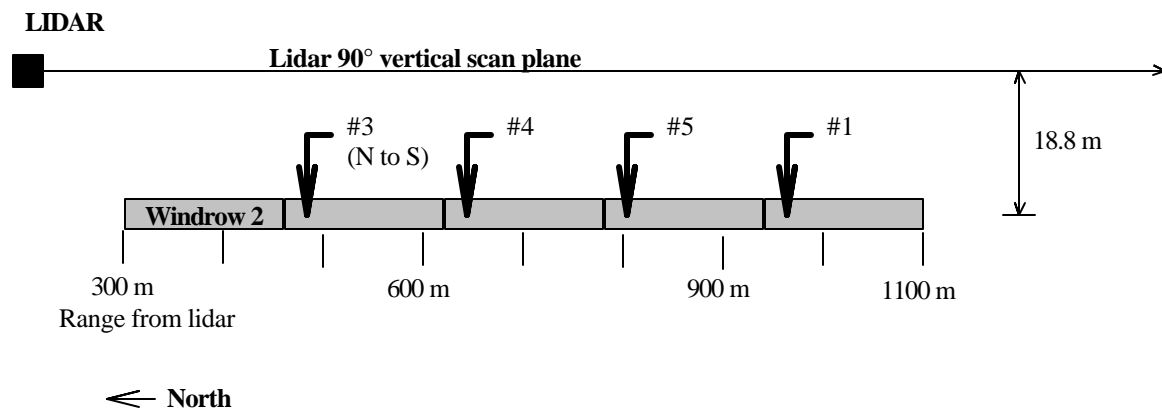


**Figure 46. Lidar configuration on solid-set irrigation field September 11, 1998**

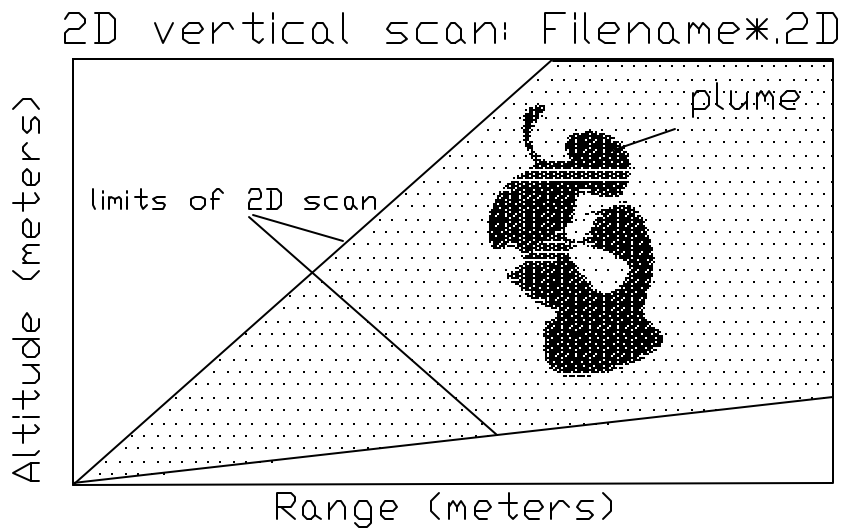
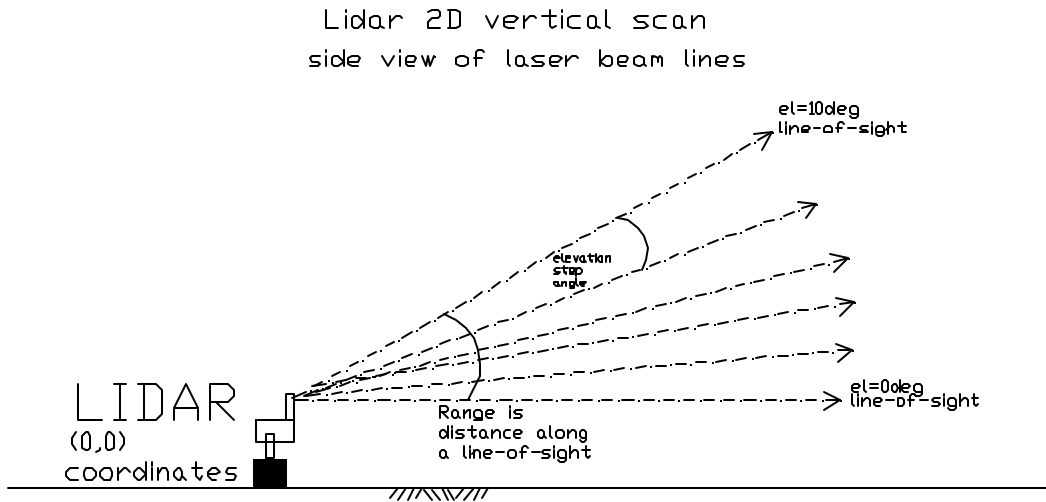


**Figure 47. Diagram of lidar vertical scan configuration**

order represents scans collected further to the east or away from the edge of the orchard) and monitor the location of the dust plume as the plume moved away from the edge of the orchard and as the harvester traveled up the windrow. Animation 2 shows the vertical scans collected only for the 90.1 degree azimuth (closest to the edge of the orchard).

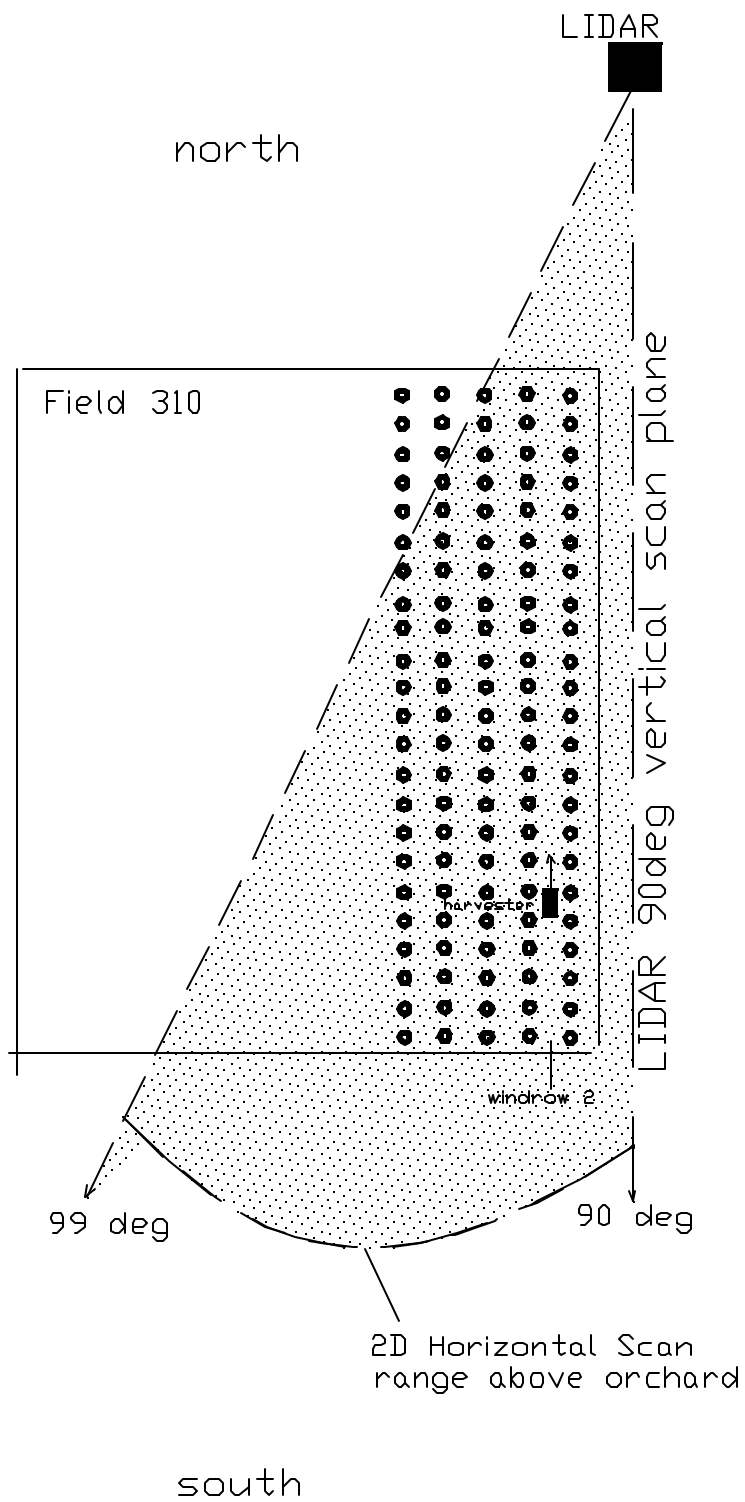


**Figure 48. Lidar configuration for horizontal scans**

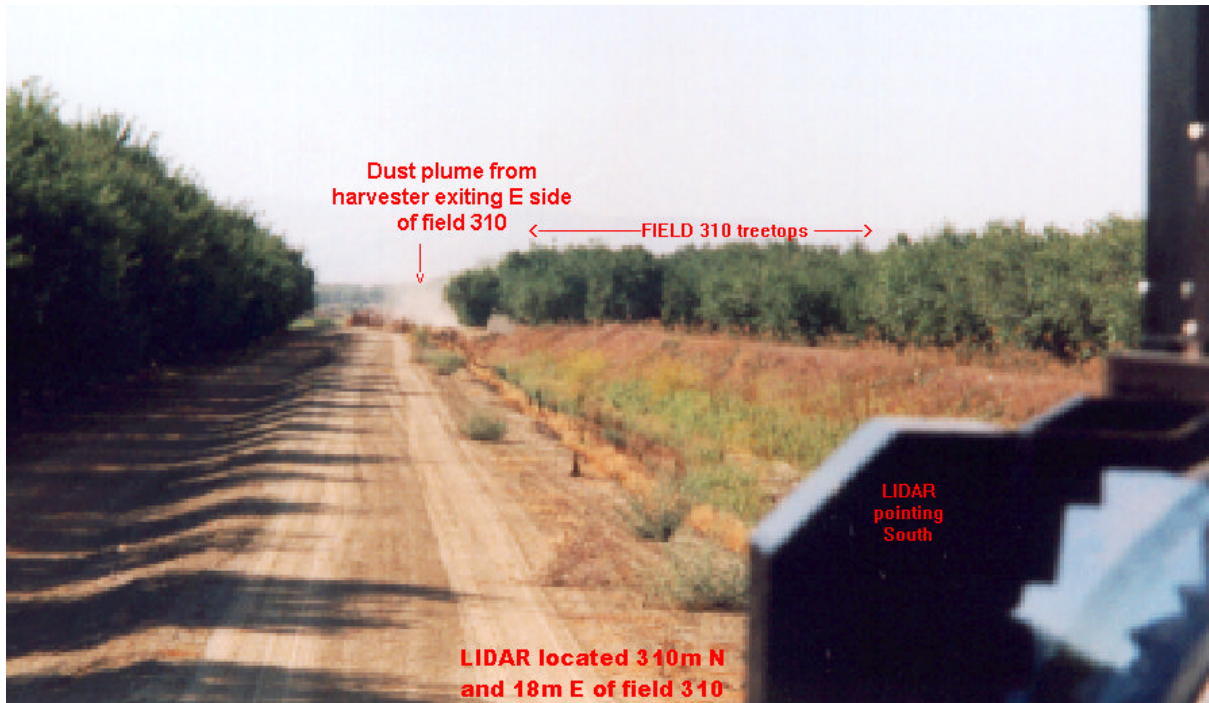


**Figure 49. Lidar view at solid-set irrigated field (field 310)**

## 20 DISCUSSION

The PM<sub>10</sub> mass measurements from each tower were averaged to obtain mean PM<sub>10</sub> concentrations by height for each harvester test. Each average vertical PM<sub>10</sub> profile was then integrated from 1m to 9m using Simpson's Rule to obtain an average PM<sub>10</sub> concentration for the dust plume. The results are shown in Table 9. The older harvester #1 generated lower PM<sub>10</sub> concentrations than the newer harvester #2 in all but one case. The older harvester #3 generated higher PM<sub>10</sub> concentrations than the newer harvester #4 in all cases. Harvester #5 generated higher concentrations than any other harvester in all cases but one.

The most appropriate way to compare the performance of the harvesters is to examine the PM<sub>10</sub> concentrations normalized to the amount of windrow trash that passed through a 2mm (tabulated in Table 10). The results of this calculation are shown in Table 11. For the solid-set irrigated field, the newer harvester #2 showed overall lower concentrations than the older harvester #1 relative to the amount of windrow trash, but it showed higher concentrations for the micro-spray irrigated field. The newer harvester #4 showed decreases over the older harvester #3 in both fields, though the decrease was larger for the solid-set irrigated field than for the micro-spray irrigated field. The overall change in PM<sub>10</sub> concentrations for both fields combined, normalized to the amount of windrow trash, ranged from +32% to -35%.

Overall, for both fields combined, both new harvesters (#2 and #4) showed very similar PM<sub>10</sub> concentrations relative to the amount of windrow trash. The newer harvester #2 showed better results on the solid-set irrigated field, while the newer harvester #4 showed better results on the micro-spray irrigated field. It is not possible to recommend one brand of harvester over the other. Harvester #5, on the other hand, showed 2-4 times the PM<sub>10</sub> concentrations, relative to the amount of windrow trash, as the other two brands.

**Table 9. Integrated PM<sub>10</sub> concentrations (µg/m<sup>3</sup>) for each harvester test**

	Harvester						
	1	2	% Difference	3	4	% Difference	5
Solid-Set	860	880	2%	2,336	671	-71%	2,953
Near	681	1,008	48%	2,465	282	-89%	3,096
Middle	158	1,186	652%	2,601	710	-73%	3,020
Far	1,782	302	-83%	1,942	827	-57%	2,957
Micro-Spray	1,537	3,314	116%	3,272	2,002	-39%	5,295
Near	1,594	2,663	67%	3,959	879	-78%	6,762
Middle	1,115	2,481	122%	3,077	2,852	-7%	5,787
Far	1,865	4,800	157%	2,761	2,174	-21%	3,338
Both fields	1,258	2,344	86%	2,916	1,730	-41%	4,195
Near	1,049	1,821	74%	3,099	573	-82%	5,125
Middle	730	1,824	150%	2,962	2,419	-18%	4,489
Far	1,071	2,424	74%	2,601	1,041	-28%	2,147

**Table 10. Pre-harvest windrow trash <2mm in size (grams)**

	Harvester						
	1	2	% Difference	3	4	% Difference	5
Solid-Set	211	370	76%	193	142	-26%	300
Near	268	435	62%	80	103	28%	410
Middle	295	474	61%	303	184	-39%	126
Far	70	203	191%	195	139	-29%	366
Micro-Spray	405	498	23%	593	579	-2%	437
Near	348	512	47%	627	521	-17%	419
Middle	423	409	-3%	663	771	16%	432
Far	446	573	28%	489	446	-9%	461
Both fields	308	434	41%	393	361	-8%	369
Near	308	473	54%	354	312	-12%	414
Middle	359	441	23%	483	477	-1%	279
Far	258	288	50%	242	202	-14%	114

**Table 11. PM<sub>10</sub> concentrations normalized to amount of windrow trash <2mm prior to harvest (µg/m<sup>3</sup>/g)**

	Harvester						
	1	2	% Difference	3	4	% Difference	5
Solid-Set	4.1	2.4	-42%	12.1	4.7	-61%	9.8
Near	2.5	2.3	-9%	30.8	2.8	-91%	7.6
Middle	0.5	2.5	368%	8.6	3.9	-55%	24.1
Far	25.6	1.5	-94%	10.0	5.9	-40%	8.1
Micro-Spray	3.8	6.7	76%	5.5	3.5	-37%	12.1
Near	4.6	5.2	13%	6.3	1.7	-73%	16.2
Middle	2.6	6.1	130%	4.6	3.7	-20%	13.4
Far	4.2	8.4	101%	5.7	4.9	-14%	7.2
Both fields	4.1	5.4	32%	7.4	4.8	-35%	11.4
Near	3.4	3.8	13%	8.8	1.8	-79%	12.4
Middle	2.0	4.1	103%	6.1	5.1	-17%	16.1
Far	7.6	8.8	160%	7.0	6.6	160%	7.6

## 20.1 Lidar data animations

Two animation files highlight the lidar results of monitoring the almond harvest operations. The lidar was positioned in the same location for both sets of data – north of the solid-set irrigated field along the levee of a wide irrigation channel that borders the east side of the field (see Figure 49).

**Animation 1 – 11SEP303ZOOM.GIF** – Horizontal scans collected at three different elevation angles over the top of the field. The horizontal sweeps were made while the harvesters were picking up nuts from the 7th windrow, or about 42 meters inside the field’s east edge, during PM test 15. The scans were made at lidar azimuth angles between 90.1 (~True South) and 99.1 ( 9° West of South) degrees and lidar elevation angles of 1.8, 2 and 2.2 degrees. These elevation angles correspond to heights above ground of approximately 31, 35 and 38 meters at a range (i.e., distance along the lidar line-of-sight) of 1000 meters. Interesting features to notice in this animation include:

- (a) Note the movement of the plumes toward the top right of the images. This direction corresponds to movement of the plumes that are rising out of the orchard towards the southwest due to the prevailing wind coming from the northeast at 1330 hr (see Figure 42, meteorology).
- (b) The harvester was moving from the south end of the field (located at a distance of ~1100m from lidar) towards the north end where the PM towers were located. The harvester movement to the north is noticeable in the lidar data in that the high signal (red) moves toward the bottom of the images with time.
- (c) The harvester was started on the second frame of the animation (file 11SEP304.2D) and the harvester was turned off during the last 6 frames of the animation. These latter frames therefore illustrate the manner in which the plume dies off. Note that the signal in these last frames is

significantly lower after the harvester was turned off. The first frame's intensity is similar to that in the last frames, therefore is fairly representative of the 'background' atmospheric conditions for the test period.

**Animation 2 – 11SEPALLup.GIF** – Vertical scans collected at 90.1° azimuth angle for elevation angles between 0 and 2°. The scans were collected while the harvesters were picking up nuts from the 2<sup>nd</sup> (or 1<sup>st</sup>) windrow, or about 18 (or 12) meters inside the field's east edge, during "lidar-only" PM tests. The animation is organized in the order the harvesters were run on windrow #2 from south to north (#1, #5, #4, #3) followed by the results for harvester #2 on windrow #1. The table at the bottom of Figure 16 indicates which lidar file numbers (appearing along the top of individual frames in the animation) correspond to the period during which the harvester was operating. File numbers outside the intervals indicated in the table represent periods either before or after harvester operation and show background atmospheric conditions and/or dissipation of the dust plumes generated by the harvesting. Interesting features to notice in this animation include:

- (a) The first harvester (#1) has a strong plume located at ranges (x-axis) > 1050 meters. This plume did not dissipate very quickly after the harvester was turned off. The range location is consistent with the harvester operating at the far south end of the field and adjacent to the dirt road at the south end. The presence of the road may have allowed the plume to escape to the south and then it was moved further south by the northerly and northeasterly winds prevailing outside the canopy. Note the movement of the plume to the left of the images at the start of the animation – this is because the harvester was traveling south to north on the windrow. After the harvester stopped (file 11SEP545.2D), the plume moved to the right in the images (i.e., to the south) because of the prevailing winds.
- (b) The animation sequence for the second harvester (#5) starts with a thin tall plume at ~900m range. The plume moves to the right (south) due to the wind and merges into a wide plume between 1000-1500m range in file 11SEP595.2D. Like harvester #1's sequence, there is strong vertical movement at ranges >1200 meters after the harvesting stopped (file 11SEP604.2D).
- (c) Harvester #4's run shows the plume starting at a closer range, about 800m, and it also moves south, broadens and rises to over 30m height. Significant rapid dissipation of the plume from this harvester is observed after file 11SEP779.2D.
- (d) Harvester #3 has its discharge on the left-hand side, therefore its lidar-only test was run with the harvester starting on the north end of its section of windrow #2, at about 450m range from the lidar. The plume is first visible in the lidar's line-of-sight at a range of ~650m and it moves quickly to the south, both because of advection by the wind, and because the dust source is moving south. The plume rises immediately to over 30m height and maintains a sharp front on its south side. The plume dissipates much more slowly than harvester #4's plume. Note, however that the mean wind speed was lower during the run with harvester #3 (see Figure 3).
- (e) Like harvester #1, harvester #2 was run on the windrow section closest to the road at the south end of the field. However, the intensity of the plume from harvester #2 is not as great. Movement of the plume northward from the 1100m range is evident at the start of the sequence; plume dissipation begins after file 11SEP455.2D.
- (f) Throughout the scan sequence of all harvesters, there is a low-elevation (i.e., between 5 and 20m height) signal at 1200-1500m range. This signal may represent dust that is "trapped" and recirculated within the open space along the drainage ditch between neighboring orchards. This

hypothesis supported by lidar data from the 2D vertical scans collected at azimuth angles farther east of the field.

Whereas the point sampler tests indicated that harvester #5 was the dirtiest, #4 was second and the other three harvesters gave similarly lower levels of  $PM_{10}$  when sampled immediately adjacent to the windrows. The lidar data seem to give different relative results between harvesters. The highest signals in the “lidar-only” tests were obtained for harvester #1. This may indicate differences in the portions of the plume sampled by the point samplers versus the lidar. For example, the lidar could not capture the plumes under the canopy that were sampled by the filters. Rather, the lidar measured the plume after it exited the orchard, where it was subject to convective and advective transport and dispersion. Any factors that affect dispersion will affect the intensity of the lidar signal, thus signal intensity alone is not a very useful comparison variable for different harvesters. We are continuing lidar data analysis to develop a quantitative measure that includes plume dimensions as well as signal intensity. Alternatively, the windrow sections sampled by each harvester during the lidar-only tests may have had different amounts of trash prior to harvesting. If so, the lidar data must be normalized to trash content as was done for the point sampler comparison.

Another complication is the fact that harvester #4 was sampled in its lidar-only test while running south to north despite the fact that its discharge is to the left. Thus, the dust generated was blown away from the lidar line-of-sight. This may explain why the observed plume from #4 dissipated so quickly. Given the problems with interferences in the lidar data due to activity on neighboring fields and because (1) meteorological conditions were not the same for each “lidar-only” test, and (2) the wind was generally blowing the dust back towards the orchard (and back over the lidar beam line), rather than in one-direction away from the source (and the lidar line-of-sight), interpretation of the lidar data is extremely complex under these adverse testing conditions.

## **20.2 Averaged 2D vertical scans**

The animation files provide a time series of images that show the movement of the dust plumes generated by the harvesters as the implement moved along the windrow. Another way of presenting the lidar data from the lidar-only test runs is to average the lidar images collected on the  $90.1^\circ$  azimuth during the time periods when each harvester was actively harvesting. In the averaged files (Figure 50), each pixel represents the average lidar backscatter signal at that specific location over the duration of an individual harvester’s run. Due to different harvester speeds, the test duration and the number of lidar files comprising a test varied between harvesters. To compare the harvesters, then, the average lidar signal is plotted in each image. The data in Figure 50 is a subset of the data in Animation 2.

The harvester number and time of day of the beginning of the run is indicated in the header of each image in Figure 50. The range location of each harvester’s operation is shown in Figure 46. Harvesters #1 and #2 were run on the windrow section at the southernmost part of field 310 (see Figure 46). Therefore, it is likely that at least part of the high signal level at ranges of 1100-1200 meters is due to traffic on the road at 1100 meters range. This road-generated signal can be seen in the averaged images from Harvester #3 and #4 at a range of approximately 1175-1200m and a height between 5-15m.

Observations we can make about differences in  $PM_{10}$  generation by the different harvesters from the averaged lidar data include:

- (1) plume size and shape differ greatly between harvesters. This may be a real phenomenon, or it may be the result of differences in plume transport and dispersion because the harvesters were sampled by the lidar at different times of day when meteorological conditions were variable.
- (2) because of changes in plume size and shape, direct comparisons of lidar signal intensity do not necessarily correlate directly with total PM<sub>10</sub> emissions. In other words, a small area of high intensity on the averaged lidar image may correlate to a lower PM<sub>10</sub> flux than a very large area of low intensity signal. This is due to the fact that PM<sub>10</sub> flux is an integral function of concentration as well as areal distribution of the particulate matter. A two-dimensional integration of the plumes in the 2D vertical lidar scans is being investigated as a useful data analysis tool for comparing the harvesters, despite the complexities imposed by meteorological variability and less than ideal lidar-only test conditions.

## **21 CONCLUSIONS**

The new harvesters #2 and #4 from either manufacturer perform comparably with regard to PM<sub>10</sub> dust production. The older harvester #1 also performs comparably to the newer ones, but the older harvester #3 produces somewhat more dust. Harvester #5 produces significantly more dust than any of the other four models. The change in PM<sub>10</sub> dust production, relative to the amount of windrow trash in the row, ranged from an increase of 76% to a decrease of 61%. On the solid-set irrigated field, which was sprinkler irrigated, both new harvesters produced 42-61% lower PM<sub>10</sub> emissions than their older counterparts. On the micro-spray irrigated field, which was irrigated by micro-spray emitters, the newer harvester #2 produced 76% more PM<sub>10</sub> dust relative to the amount of windrow trash, while the newer harvester #4 produced 37% less, than their older counterparts. Harvesters #1-#4 produced much less dust relative to the amount of windrow trash than harvester #5.

# Animation 2 figure

**Figure 50. Average lidar backscatter signal during harvester operation**

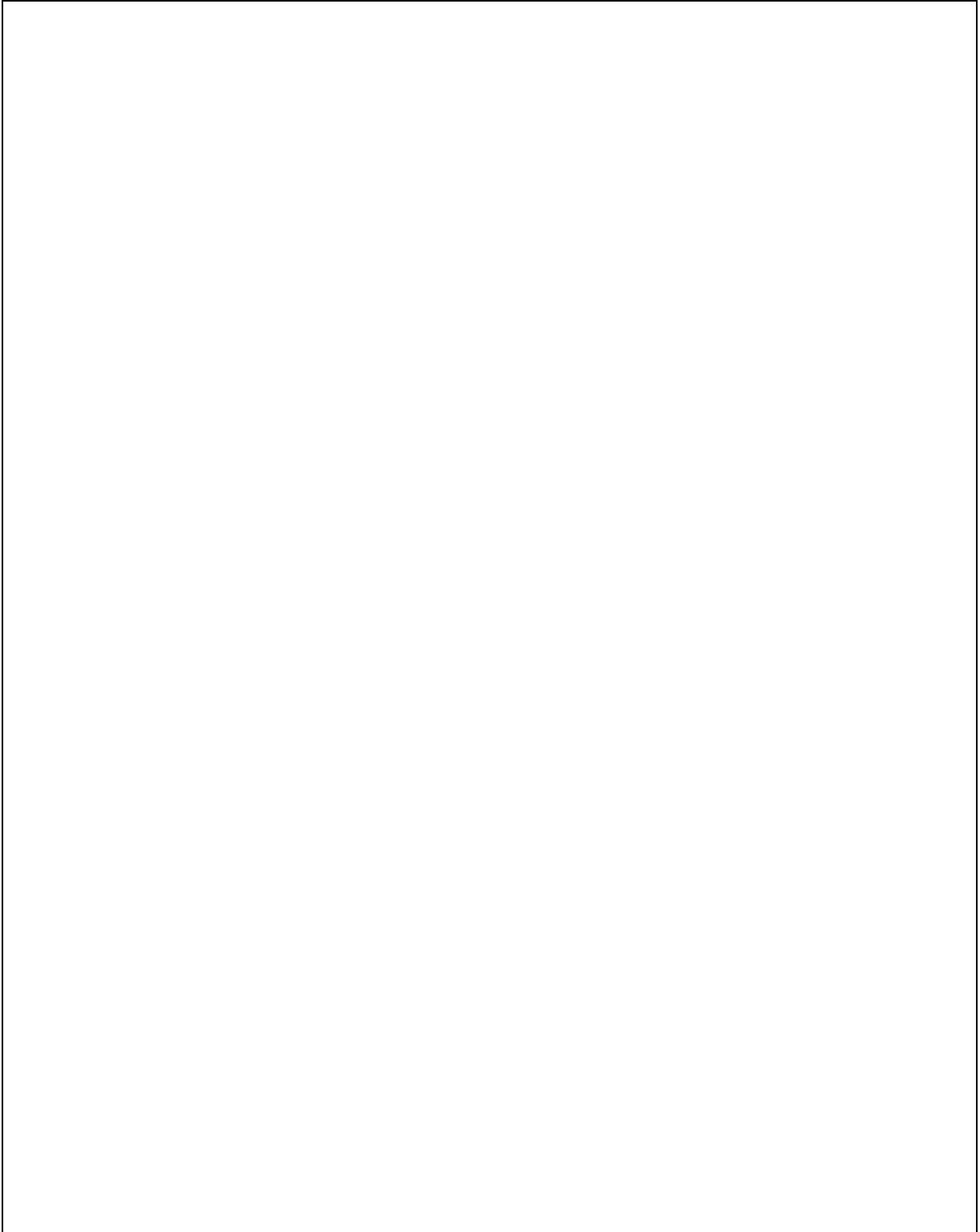


**Figure 50. Average lidar backscatter signal during harvester operation**

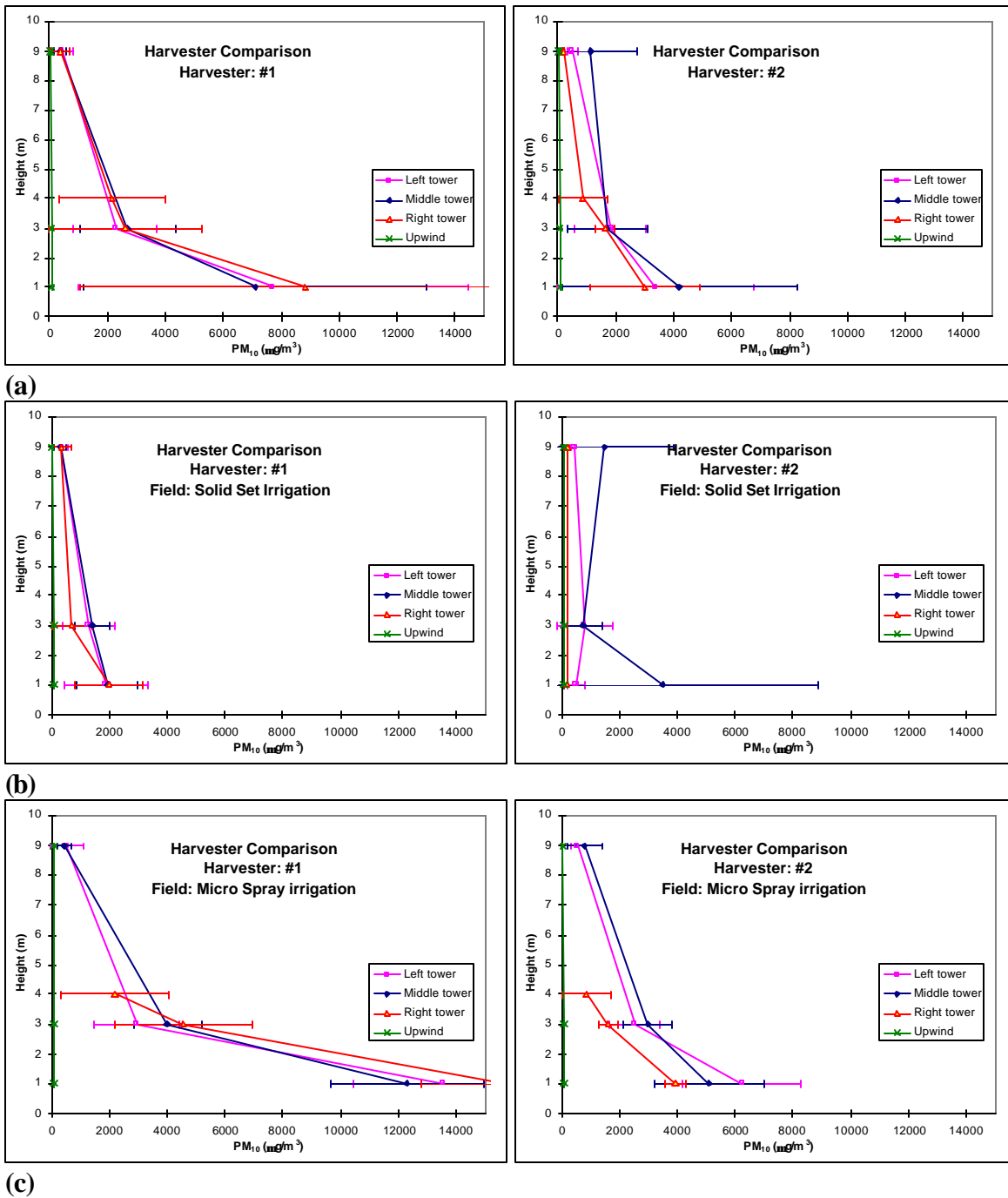


Figure 51.  $PM_{10}$  concentrations downwind of harvester #1 and #2, (a) all tests, (b) Solid-set irrigation, (c) Micro-spray irrigation.

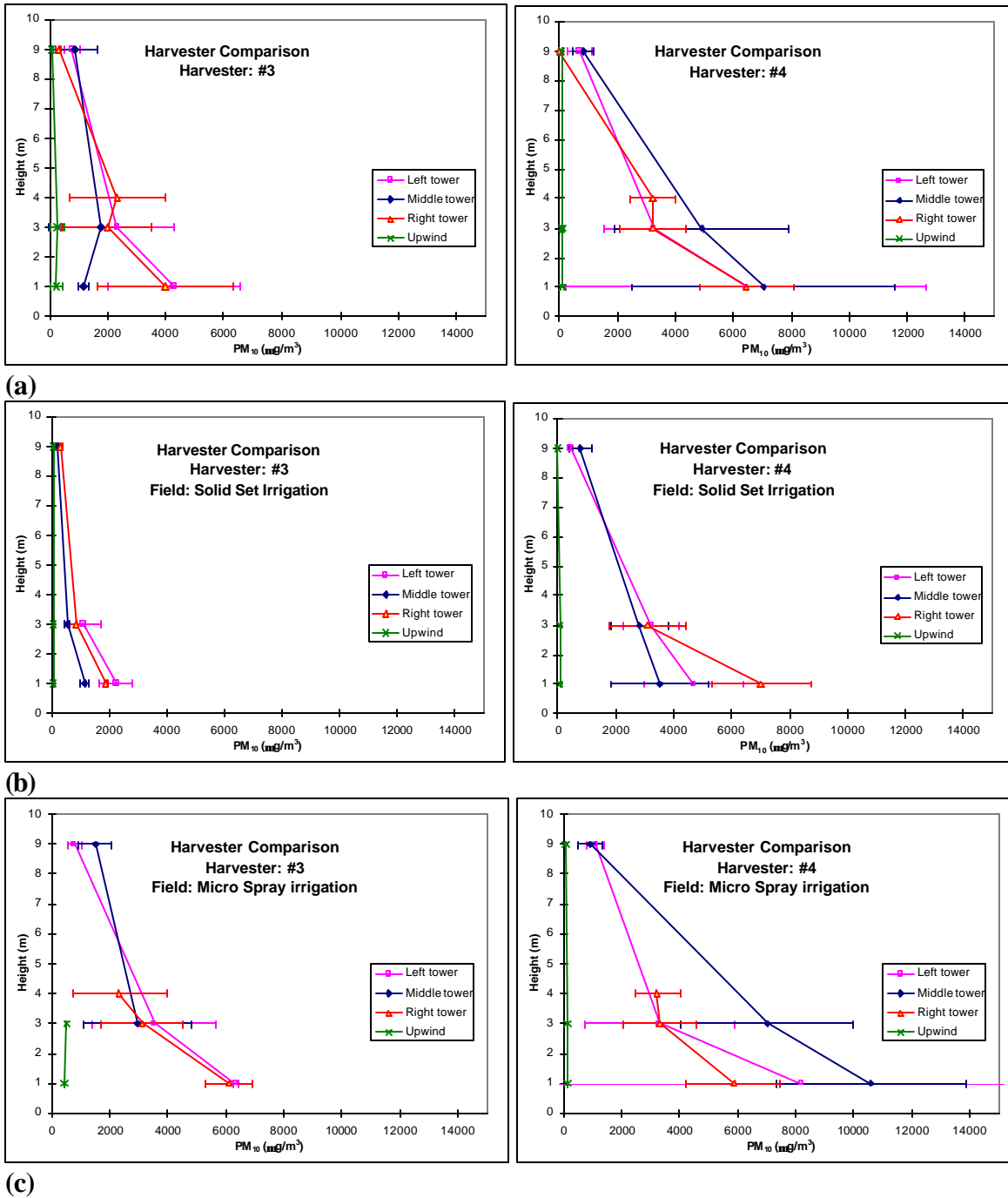


Figure 52. PM<sub>10</sub> concentrations downwind of harvester #3 and #4, (a) all tests, (b) Solid-set irrigation, (c) Micro-spray irrigation.

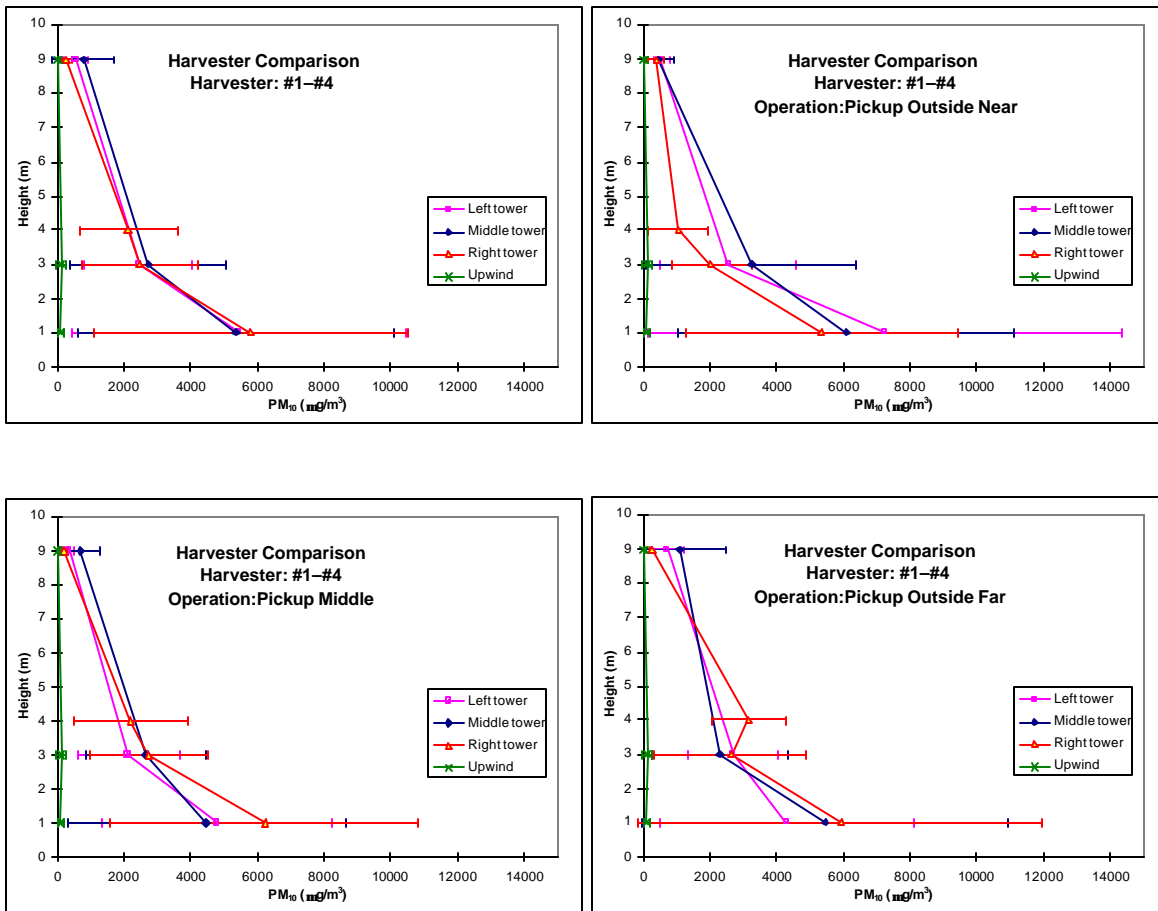
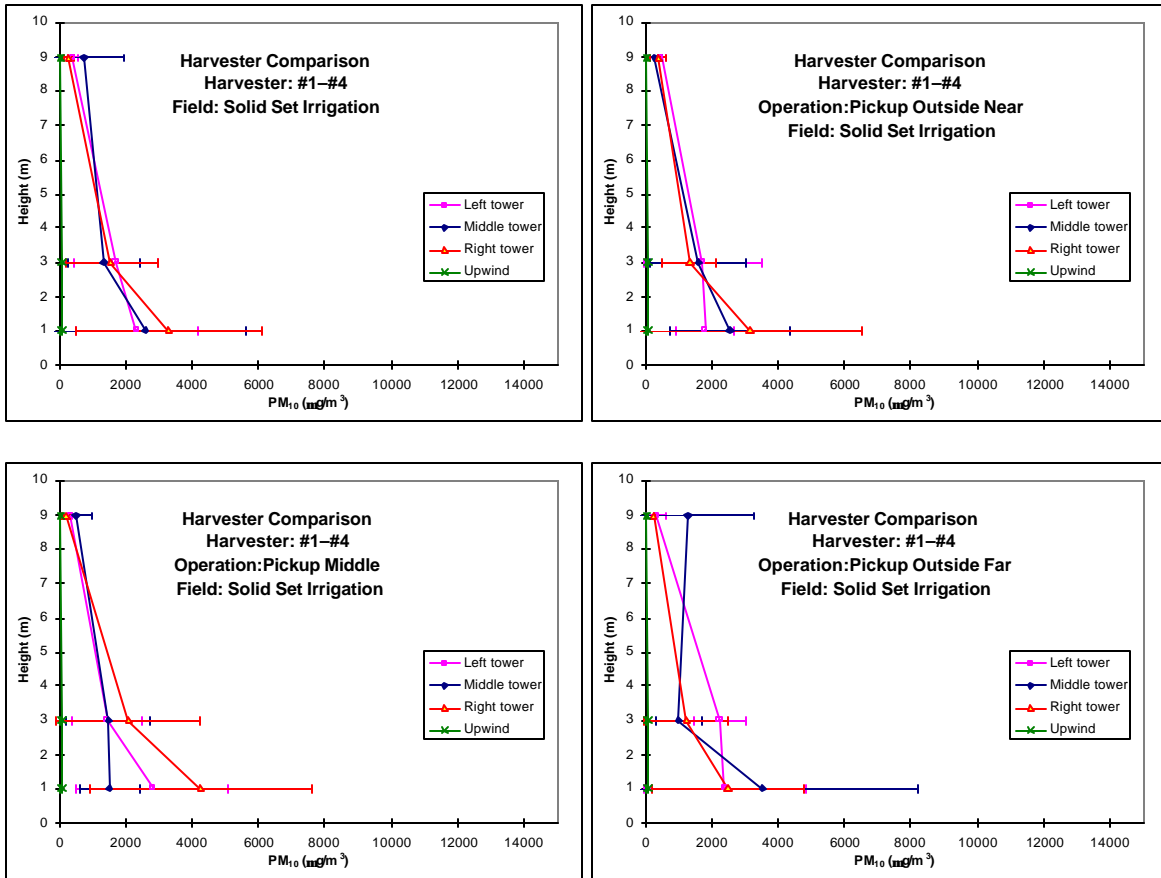


Figure 53. Dust concentrations for harvesters #1–#4 on both fields by harvest row.



**Figure 54. Dust concentrations for all harvesters #1-#4 on solid-set irrigated field by harvest row.**

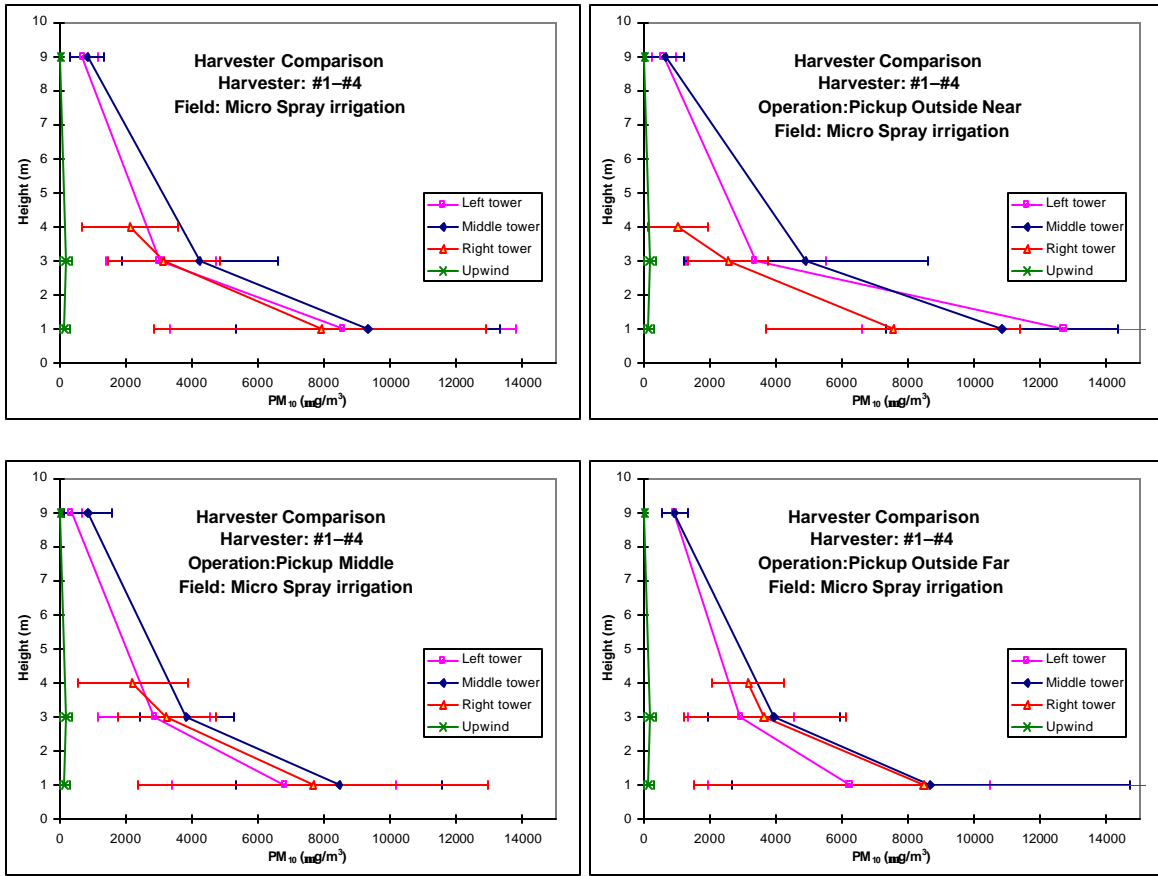


Figure 55. Dust concentrations for harvesters #1-#4 on micro-sprayed field by harvest row.

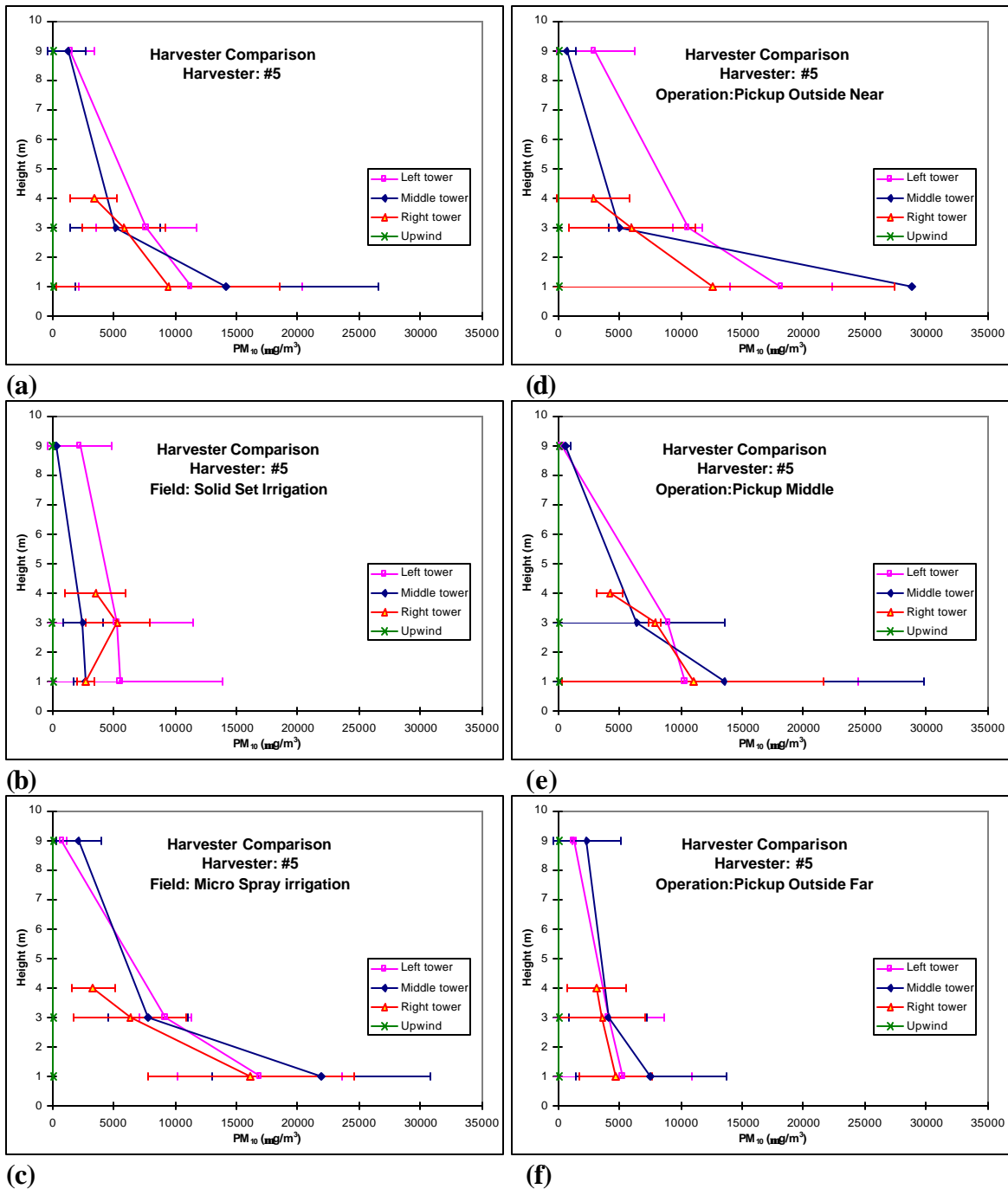


Figure 56. PM<sub>10</sub> concentrations downwind of harvester #5, (a) all tests, (b) Solid-set irrigation, (c) Micro-spray irrigation, (d) near row, (e) middle row, (f) far row.

## 22 APPENDIX A

### Simpson's Rule and Application to these data

Simpson's Rule is used to numerically integrate a function over an interval a to b. The form of the integration formula is

$$\int_a^b f(x)dx \approx \frac{\Delta x}{3} [f(x_0) + 4f(x_1) + 2f(x_2) + 4f(x_3) + \dots + 2f(x_{2n-2}) + 4f(x_{2n-1}) + f(x_{2n})]$$

For this study, the limits of integration are a = 1, the lowest measurement height, and b = 9, the highest measurement height. The PM<sub>10</sub> concentration was interpolated at each integral meter height between 1 and 9 meters, so there were eight intervals in the calculation. For some calculations, there was a measurement at 4m, due to a malfunction in the 9m sampler for one tower. The Δx, then, is 1m.

For example, Harvester #2 on the micro-sprayed field produced the following PM<sub>10</sub> measurements:

Operation	Height (m)	PM <sub>10</sub> Mass (μg/m <sup>3</sup> )			
		Upwind Tower	Left Tower	Middle Tower	Right Tower
Pickup Outside Far	9	38	373	1476	
	4				1813
	3	56	1864	3239	1998
	1	57	5290	3355	3577
Pickup Middle	9	38*		454	
	4				357
	3	56*	2166	2049	1427
	1	57*	4780	4882	3973
Pickup Outside Near	9	38*	718	414	
	4				396
	3	56*	3496	3674	1453
	1	57*	8604	7076	4270

\*The upwind were collected for an entire morning or afternoon to ensure that sufficient mass was collected for analysis.

These measurements produced the following average values:

Position	Height	PM <sub>10</sub> mass (µg/m <sup>3</sup> )
Down	1	5090
	3	2374
	4	855
	9	687
Up	1	57
	3	56
	9	38

These average values then produce the following interpolated concentrations at 1m intervals:

Height (m)	Down (µg/m <sup>3</sup> )	Up (µg/m <sup>3</sup> )	Difference (µg/m <sup>3</sup> )
1	5,090	57	5,033
2	3,732	56	3,675
3	2,374	56	2,318
4	855	53	803
5	822	50	772
6	788	47	741
7	754	44	711
8	721	41	680
9	687	38	650
Integrated result by Simpson's Rule (µg/m <sup>2</sup> )	1,586	49	1,537

## 23 APPENDIX G – DESCRIPTION OF DATABASE STRUCTURE

### Description of database structure

A test is considered to be a set of simultaneous measurements (aerosols, Ammonia gas, meteorology, source of emissions, etc.) of an emissions source. The duration of the test is normally dictated by the measurements of the closest downwind samplers, enough mass for species sensitivity without overloading. The start and end times the test is determined by the start and end times of the PM<sub>10</sub> sample collected at 3 m height closest to the source. The meteorological data is averaged for the test based on these times, as are the lidar data.

Test ID = Year (2 characters) + “-“ + Test Number (3 characters)

e.g. “99-001”, “99-002”, “99-003”, etc. or “00-001”, “00-002”, “00-003”, etc.

Oftentimes, an upwind or background measurement extends over several tests. In such cases, we use the variables StrTest and EndTest (each 3 characters) to identify which individual tests a background measurement is associated with (e.g. StrTest = “001” , EndTest = “003”)

A sampling array (2 characters) is defined as a collection of sampling locations which share a common origin as the basis for measuring distances. Typically, the array designation changes when the field or facility changes or with wind shifts. Some examples are:

Paramount Farms = P1, P2,.....

A sampling location (3 characters) is the point, in three dimensional space relative to the origin, where the sample was collected. The first character indicates the general location of the sample in the array:

U = Upwind (UP)

I = In field (IN)

D = Downwind (DN)

L = Left of array downwind axis (LT), left while facing upwind

R = Right of array downwind axis (RT), right while facing upwind

The second character specifies the sequence of use for that location, for example D1, D2, and D3 for 3 downwind samplers. The final character designates the height at which the sample was collected, following some rules to stay within the single character:

1) Use the actual height as the character when  $\leq 9$  meters.

2) Use a letter designation for the character when  $> 9$  meters in ascending order from the highest height (e.g. A = 100m , B = 50m, C = 10m)

Examples of elemental analysis site codes:



PERGAMON



Atmospheric Environment 35 (2001) 3251–3264

**ATMOSPHERIC  
ENVIRONMENT**

[www.elsevier.com/locate/atmosenv](http://www.elsevier.com/locate/atmosenv)

# Lidar-assisted measurement of PM<sub>10</sub> emissions from agricultural tilling in California's San Joaquin Valley – Part I: lidar

Britt A. Holmén\*, Teresa A. James, Lowell L. Ashbaugh, Robert G. Flocchini

*Air Quality Group, Crocker Nuclear Laboratory, University of California, Davis, CA 95616, USA*

Received 25 April 2000; accepted 31 October 2000

## Abstract

Vertical profiling with point samplers is an accepted method for quantifying the fluxes of PM<sub>10</sub> from non-point fugitive dust sources, but is limited by uncertainty in estimates of the actual height of the dust plume, especially for plumes that exceed the highest sampling height. Agricultural land preparation operations in the San Joaquin Valley were monitored using upwind–downwind vertical PM<sub>10</sub> profiles and data collected during the first successful experiment to include light detection and ranging (lidar), in 1998, were analyzed to provide modeling criteria for the 1996 and 1997 data. A series of six comprehensive PM<sub>10</sub> tests with concurrent lidar data was examined to: (a) develop a framework for analyzing upwind–downwind point PM<sub>10</sub> concentration profiles of land preparation operations (disking, listing, root cutting, and ripping) and (b) identify conditions under which the field sampling strategies affect the reproducibility of PM<sub>10</sub> concentration measurements. Lidar data were used to verify that the plume heights and shapes extrapolated from the point sampler vertical profiles adequately described the plumes. The shortcomings of the vertical profiling technique and lidar methods are discussed in the light of developing efficient robust methods for accurate PM<sub>10</sub> emissions quantification from complex non-point sources. © 2001 Elsevier Science Ltd. All rights reserved.

*Keywords:* PM<sub>10</sub>; Lidar; Plume height; Agricultural dust; Nonpoint sources

## 1. Introduction

In late summer and fall, a large fraction (>50%) of the PM<sub>10</sub> in California's San Joaquin Valley (SJV) has been attributed to primary geologic material, generally soil dust (Chow et al., 1990, 1992). This material becomes airborne by suspension of surface soils during wind erosion, agricultural activities, traffic on paved and unpaved roads, and construction activity. Late summer and fall PM<sub>10</sub> standard violations (Dolislager and Motallebi, 1999) coincide with the harvest season of many California crops (e.g., cotton, almonds, tomatoes), suggesting that agricultural activities (both harvesting and sub-

sequent land preparation) may be significant sources of PM<sub>10</sub> during this time of year. Potential efforts to control this component of PM<sub>10</sub> require accurate quantification of these sources, but little information has been available to date to estimate PM<sub>10</sub> emissions from SJV agricultural activities.

Since 1991, the University of California has collected PM<sub>10</sub> emissions data from a wide range of agricultural activities in the SJV. Current techniques use (a) upwind/downwind vertical profiles of wind speed and PM concentrations (PM<sub>2.5</sub> and PM<sub>10</sub>) to quantify PM emission factors and (b) lidar vertical scans to verify plume heights and profile shapes. The PM point sampling techniques draw on observations made by previous fugitive dust researchers using upwind/downwind arrays (Cowherd et al., 1974; Flocchini et al., 1994), exposure profiling (Cowherd et al., 1974; Cuscino et al., 1984; Flocchini et al., 1994), high-volume filtration samplers

\* Corresponding author. Tel.: +1-530-752-1213; fax: +1-530-752-4107.

*E-mail address:* baholmen@ucdavis.edu (B.A. Holmén).

(Cuscino et al., 1984; Cowherd and Kinsey, 1986); cascade impactors (Cowherd et al., 1974; Cuscino et al., 1984; Flocchini et al., 1994), and respirable dust monitors (Snyder and Blackwood, 1977; Clausnitzer and Singer, 1996, 1997).

Previous studies that quantified agricultural emissions represent a very limited number of sites, a low number of replicate samples, and few early studies quantified PM<sub>10</sub>. Instead, total suspended particulate (TSP) matter or industrial workplace respirable dust (PM<sub>4</sub>) was measured. For example, early UCD field measurements incorporated PM<sub>10</sub> samplers at a single height (3.3 m) upwind and downwind, and TSP monitors at four heights (3, 5, 7, and 9 m) downwind, of the source (Flocchini et al., 1994; Ashbaugh et al., 1996), but the lack of PM<sub>10</sub> vertical profiling to define the vertical extent of the plume was suspected to have caused underestimation of emission factors using the box model (Ashbaugh et al., 1997).

The application of lidar to PM emission factor measurements is relatively new (Holmén et al., 1998). Lidar techniques help overcome one of the major limitations of the vertical profiling methods, namely, the uncertainty in determining the dust plume height over which to integrate the modeled PM<sub>10</sub> concentrations.

In this paper, the results of a series of six comprehensive PM<sub>10</sub> tests conducted when a full complement of ancillary data (lidar, laser rangefinder) was collected are used to: (a) develop a framework for analyzing upwind–downwind point PM<sub>10</sub> concentration profiles of SJV land preparation operations (disking, listing, root cutting, and ripping) and (b) identify conditions under which the field sampling strategies affect the reproducibility of PM<sub>10</sub> concentration measurements. Results of recently developed lidar data reduction techniques are used to assess whether the shapes of the plumes measured as three-point PM<sub>10</sub> vertical profiles were representative of the average plumes recorded during the sampling period. From this assessment, a best-fit function for quantifying plume height and emissions is identified for each category of vertical profiles observed in the PM<sub>10</sub> data. The observations based on comparisons of lidar and point sampler data are used to develop an emission factor quality rating system in a companion paper (Holmén et al., 2000).

## 2. Experimental methods

### 2.1. PM<sub>10</sub> field test strategy and array design

All field measurements were made under actual field conditions. While sampling was coordinated with cooperative growers, special treatment of the fields to accommodate PM<sub>10</sub> sampling was not requested. A combination of upwind/downwind source isolation and vertical profiling methods was used to quantify

PM<sub>10</sub> emissions (Cowherd et al., 1974; Cuscino et al., 1984; Cowherd and Kinsey, 1986; Flocchini et al., 1994; James et al., 1996). The fields studied were 0.4–0.8 km<sup>2</sup> (0.25–0.5 mile<sup>2</sup>) and were planted and worked in a direction perpendicular to the predominant wind direction. Test durations were between 25 and 175 min. Valid tests were conducted between fall 1996 and winter 1998 on two farms near Firebaugh and Huron, CA. Average wind speeds at 4 m were between 1.0 and 6.5 m s<sup>-1</sup>. In all cases aerosol samples were collected using one upwind and at least one downwind vertical profile.

Aerosol samples and meteorological data were collected at the heights indicated in Table 1 and PM measurements made at the top of the tower are referred to by the nominal height of 9 m throughout this paper. Both PM<sub>10</sub> and PM<sub>2.5</sub> were collected downwind of the agricultural operation in a sampling array (Fig. 1) that was flexible enough to ensure downwind sampling relatively close to the moving source. Note that PM<sub>10</sub> was collected at three heights but PM<sub>2.5</sub> was collected only at the upper two heights due to equipment limitations. For the PM<sub>10</sub> tests examined here, the average distance between the PM samplers and the tractor/implement for the test period after correction for the angle of the operation was between 1 and 324 m (see Table 3). When the agricultural operation was far from the stationary PM tower located at the downwind edge of the field, the vertical profiles of PM<sub>10</sub> and PM<sub>2.5</sub> were sampled using a pneumatic tower mounted in a mobile unit that was driven into the field. While the PM<sub>2.5</sub> emissions data will not be discussed in this study, the ratio of PM<sub>2.5</sub> to PM<sub>10</sub> has been reported in earlier reports (Matsumura et al., 1996; James et al., 2000). Future sampling will collect PM<sub>2.5</sub> and PM<sub>10</sub> at four heights to enable PM<sub>2.5</sub> emission factor estimation.

### 2.2. PM point samplers

The Interagency Monitoring of Protected Visual Environments (IMPROVE) aerosol samplers (Eldred et al., 1988, 1990) were used to collect PM<sub>10</sub> and PM<sub>2.5</sub> on 25 mm stretched Teflon filters (3 µm Teflo®, Gelman R2P1025). These samplers have been used extensively in a nationwide monitoring program at Class 1 sites (Malm et al., 1994). Portable gasoline-powered generators placed downwind of the samplers provided power. EPA-approved Sierra Anderson inlets (Model 246b) produced the 10 µm size-cut, a cyclone was used for the PM<sub>2.5</sub> size-cut (John and Reischl, 1980). The IMPROVE samplers were modified to reduce their size and weight for placement atop the towers. The essential elements of the modified samplers from inlet to filter were identical to that of IMPROVE samplers; the differences were a shortened inlet stack (less than a meter long) and replacement of electronic solenoids with manual ones in some cases. Additionally, a calibration device used to audit

Table 1  
Aerosol and meteorological sampling equipment

Variable (units)	Sampler	Specifics	Heights (m)	Analyses (Method) <sup>a</sup>
PM <sub>10</sub> (µg m <sup>-3</sup> )	IMPROVE Module D	PM <sub>10</sub> inlet	1, 3 (8.25, 9 or 10) (highest height nominally 9 m)	Gravimetric mass (PM <sub>10</sub> concentration); Optical absorption (LIPM, HIPS); Elemental analysis (PIXE, PESA, XRF)
PM <sub>2.5</sub> (µg m <sup>-3</sup> )	IMPROVE Module A	AIHL Cyclone	3 (8.25, 9 or 10) (highest height nominally 9 m)	Gravimetric mass (PM <sub>2.5</sub> concentration); Optical absorption (LIPM, HIPS); Elemental analysis (PIXE, PESA, XRF)
Note that PM <sub>2.5</sub> was not collected at 1 m height				
<i>The following meteorological instruments were located on upwind tower</i>				
Temperature (°C)	Fenwal UUT51J1 radiation-shielded thermistor	± 0.4°C	0.5, 1, 2, 4, 7.5	Vertical temperature profile Bulk Richardson number Stability class
Wind speed (m s <sup>-1</sup> )	Met One 014A cup anemometer	0.45 m s <sup>-1</sup> threshold ± 0.11 m s <sup>-1</sup>	1, 2, 4, 7.5	Vertical wind speed profile, z <sub>0</sub> , u* used in PM flux calculation
Wind direction (deg)	Met One 024A	Vane	4	Used in PM flux calculation
Relative humidity (%)	HMP35C	Vaisala capacitive	2	Atmospheric conditions
Solar radiation (W m <sup>-2</sup> )	Pyranometer		4	Stability class

<sup>a</sup>LIPM = laser integrating plate method; HIPS = hybrid integrating plate system (Campbell et al., 1995; Bond et al., 1999); PIXE = proton-induced X-ray emission (for elements Na–Mn; Eldred et al., 1988); XRF = X-ray fluorescence (for elements Fe–Pb); PESA = proton elastic scattering (for hydrogen; Cahill et al., 1989).

flow rates directly was substituted for in situ flow measurement gauges for samples collected in 1998, and flow measurements for the 9 m samplers were made using only vacuum gauges, rather than both magnehelic and vacuum gauges, for samples collected in 1996 and 1997. These modifications were shown in laboratory testing to have no effect on the integrity of the PM<sub>10</sub> and PM<sub>2.5</sub> samples collected or on the quality of the flow measurement (unpublished data).

### 2.3. Tractor upwind distance

For some tests in 1998, a laser rangefinder (Laser Atlanta) was used to independently observe the location of the tractor during the lidar scans. The time, distance, and bearing to the tractor were recorded every 30 s to 1 min by an observer located along the edge of the field (see Fig. 1). For other tests, upwind distances reported in Table 3 were calculated from the number of implement passes, implement width, angle of operation, and the measured start and end distances upwind of the array origin.

### 2.4. Light detection and ranging (lidar)

Tests conducted since June 1997 often had corresponding light detection and ranging (lidar) data. The lidar instrument, described previously (Holmén et al.,

1998), records range-resolved elastic backscatter signals from airborne PM with high temporal (s) and spatial (5 m) resolution. The lidar 2D vertical scans were collected downwind of the tractor operation, just upwind of the downwind point sampler tower, as depicted in Fig. 1. The lidar scan plane therefore approximated a cross section of the downwind edge of the area source being sampled by the upwind/downwind point sampler profile array. The lidar scans are qualitative measures of relative PM backscatter, but provide useful information on PM plume variability over time in terms of spatial homogeneity, size, and shape.

#### 2.4.1. Lidar vertical profiles and plume heights

Vertical profiles of lidar data were obtained by averaging the lidar signal at 2 m height intervals over a specified range (distance from the lidar) interval. The range interval was selected to correspond to the location of the point sampler tower. Background vertical profiles were similarly obtained from the lidar scans collected when the tractor was either stopped or downwind of the lidar vertical scan plane.

Maximum plume heights were recorded for each 2D vertical scan collected over a point sampler test period and averaged for comparison with the point sampler estimates. These average values of test period plume heights were based on plumes occurring at all locations across the field and, unlike the lidar vertical profiles, were

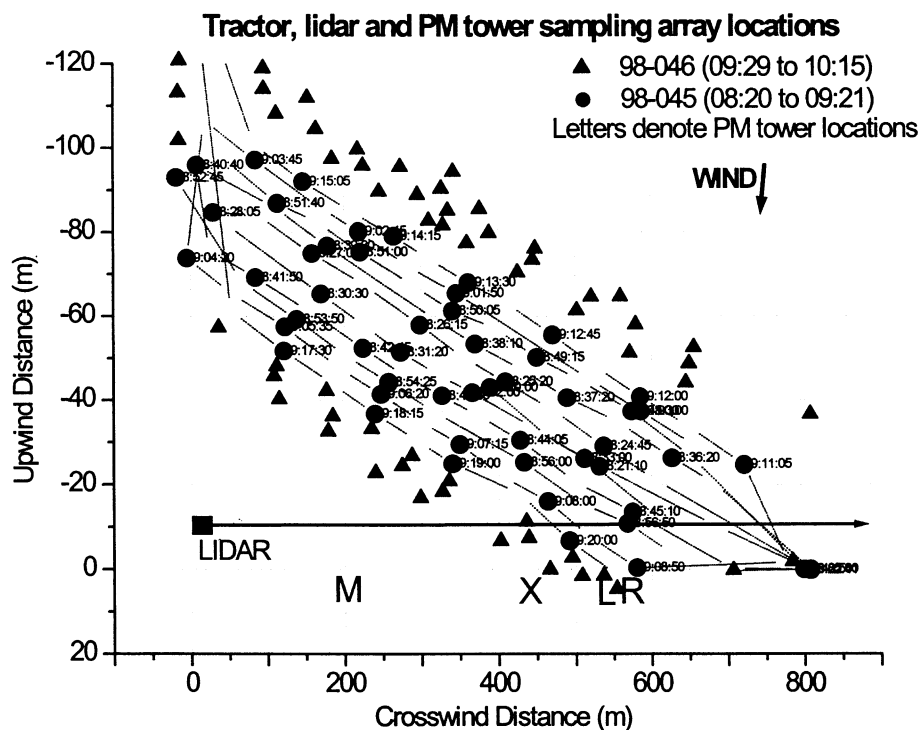


Fig. 1. Map view of tractor point source locations (circles and triangles) on field during first disking tests 98-045 and 98-046. The tractor paths (determined by laser rangefinder measurements) for the two different test periods are indicated by circles (98-045) and triangles (98-046). The times for tractor locations during 98-045 are shown. The arrow from the lidar location indicates the projection of the vertical scan plane for lidar 2D scans. Note that (0, 0) is at the SW corner of the field and (800, 0) is the SE corner of field. Locations of the point sampler towers are indicated by letters: right (R) and left (L) stationary towers, and mobile tower (M). The upwind tower was located at coordinates (793, -805). The "X" marks the location of observer collecting laser rangefinder data on tractor location.

not restricted to the ranges where the point sampler towers were located.

#### 2.4.2. Lidar measurement error

Although the lidar cannot distinguish between PM generated by different sources, the plume generated by the tractor and implement was usually easily distinguished from background PM because of the distinctive movement of the plume across the field from one lidar scan to the next. Possible sources of error in measuring the maximum extent of the plume from the lidar vertical scans include the fact that some plumes extended higher than the programmed vertical limits of the lidar scan; when plumes were very close to the lidar this problem was most severe. Another source of measurement error resulted from near field-of-view geometric optics considerations: because of the lidar's periscope arrangement, plumes within 200 m of the lidar were not fully quantified by the lidar receiver. Both of these factors could result in underestimation of the maximum plume height when the plume was close to the lidar instrument.

#### 2.5. Laboratory analyses and quality control

All PM samples were analyzed for gravimetric mass, light absorbing carbon, and elemental composition in accordance with IMPROVE protocols (Eldred et al., 1989, 1990, 1997). The elemental and carbon analyses are used chiefly for quality assurance purposes but also provide chemical characterization of these near-source aerosols for comparison with IMPROVE ambient monitoring data. The mass gain of dynamic field blanks (i.e., filters loaded into the samplers, subjected to flow measurement, but no air sampling) was used to calculate blank concentrations and minimum quantifiable limits (MQLs) for both  $PM_{10}$  and  $PM_{2.5}$  (Eldred et al., 1990). The MQLs were calculated from the standard deviation of the average of the blanks and the sampled air volumes. Uncertainties in mass concentration were calculated by propagation of the analytical errors introduced in the measurements of mass and air volume.

The hybrid integrating plate and sphere (HIPS) laser analysis technique (Campbell et al., 1995; Bond et al.,

1999) was used to provide an estimate of light absorbing carbon soot (BABS). Particle-induced X-ray emission (PIXE) and X-ray fluorescence (XRF) spectroscopy were used to determine the mass concentration of the elements of atomic mass between sodium and manganese and between iron and lead, respectively (Cahill, 1995). There is considerable overlap in the range of elements analyzed by these two methods such that independent analyses of the transition metals facilitate quality control between them (Cahill, 1995). Proton elastic scattering analysis (PESA), performed simultaneously with PIXE, provided a measure of the mass concentration of the bound hydrogen (as these analyses are performed under vacuum). Mass concentrations in air of each element were calculated from concentrations ( $\text{ng cm}^{-2}$ ) measured on a representative portion of the filter (at least 28%), the area of the sample on the filter, and the volume of air sampled. Minimum detectable limits (MDLs) were defined as 3.3 times the square root of the background counts. Analytical uncertainties were based on the propagation of counting errors and uncertainties in the measurement of the elemental mass (from reanalysis) and air volume.

#### 2.6. Reconstructed mass (RCMA) concentrations

The accumulation of a large database of measurements of  $\text{PM}_{10}$  and  $\text{PM}_{2.5}$  mass and elemental profiles through the operation of the IMPROVE particulate matter sampling and analysis network led to the development of a series of composite variables that are defined by assumptions regarding the likely atomic mass ratio of the dominant elements of an aerosol constituent (Cahill et al., 1977; Eldred et al., 1997). These assumptions have been tested against independent analyses of related measurements for the database of IMPROVE samples (Cahill et al., 1981) and for agricultural source samples (James et al., 2000). For example, the gravimetric mass has been shown to be consistently well correlated with the composite variable “RCMA” which is the reconstructed mass obtained by summing factors of the common crustal elements (Al, Si, Ca, Ti, Fe), sulfur, light absorbing elemental carbon, hydrogen and non-soil potassium to emulate an average aerosol (Cahill et al., 1989):

$$\text{RCMA} = 0.5\text{BABS} + 2.5\text{Na} + \text{SOIL} + 13.75(\text{H} - 0.25\text{S}) + 4.125\text{S} + 1.4(\text{K} - 0.6\text{Fe}), \quad (1)$$

where  $\text{SOIL} = 2.2\text{Al} + 2.49\text{Si} + 1.63\text{Ca} + 1.94\text{Ti} + 2.42\text{Fe}$ ; BABS is an estimate of the mass concentration of light absorbing carbon (Campbell et al., 1995; Bond et al., 1999), and the elemental mass concentrations are represented by their atomic symbols.

The availability of elemental data for all aerosol samples collected in this study allowed assessment of the applicability of RCMA for  $\text{PM}_{10}$  emission factor estima-

tion. Gravimetric  $\text{PM}_{10}$  and RCMA were highly correlated ( $r^2 = 0.94$ ) for the 525 samples with non-zero RCMA measured during the three analysis year sets (1996–98). Therefore, either measure of  $\text{PM}_{10}$  can be used to model the plume characteristics and estimate emission factors. However, as indicated by the slope of the linear regression between these variables (0.77 with standard error = 0.0065), emissions based on RCMA will represent a lower limit. In the samples analyzed here, the reconstructed mass (RCMA) was generally lower than gravimetric mass by an average of 13% (SD = 23%) due in part to the loss of volatile constituents in the vacuum of PIXE analysis. Other mass losses sometimes occurred due to sample handling between the two analytical procedures and where the sequential mass loss from gravimetric to elemental analyses was atypically high, the samples were considered invalid. Because the elemental analyses were sufficiently more sensitive than the gravimetric mass measurements, the calculated RCMA was above detectable limits for 13 samples (of 90 in the land preparation dataset) for which measured mass was not. Thus, RCMA was the parameter chosen for analysis of the  $\text{PM}_{10}$  mass concentration profiles. The uncertainty in the RCMA composite variable was calculated as a propagation of the uncertainties calculated for the mass concentrations of each constituent weighted by its coefficient.

#### 2.7. Plume height and uncertainty calculations

Functional fits to the vertical profiles of  $\text{PM}_{10}$  concentration were used to calculate the average heights of the plumes sampled from the land preparation operations and the most appropriate functional fits to each downwind profile type were determined based on examination of lidar vertical profiles. Three different methods – the line, block, and logarithmic profile models – were used to fit the  $\text{PM}_{10}$  vertical concentration profiles (Fig. 2). The height at which the best-fit function of the downwind concentration profile intersected the average upwind concentration was the calculated plume height,  $H$ . A fourth model, the box model, was used to describe the  $\text{PM}_{10}$  flux in cases of uniform downwind vertical concentration profiles.

##### 2.7.1. Line profile model

In the line profile model, the three downwind  $\text{PM}_{10}$  concentrations were fit to a line as a function of height. Linear vertical profiles have been used previously for PM profiles downwind of unpaved roads (Venkatram et al., 1999).

##### 2.7.2. Block profile model

The block model essentially “connects the dots” of the three PM measurements in each vertical profile. The

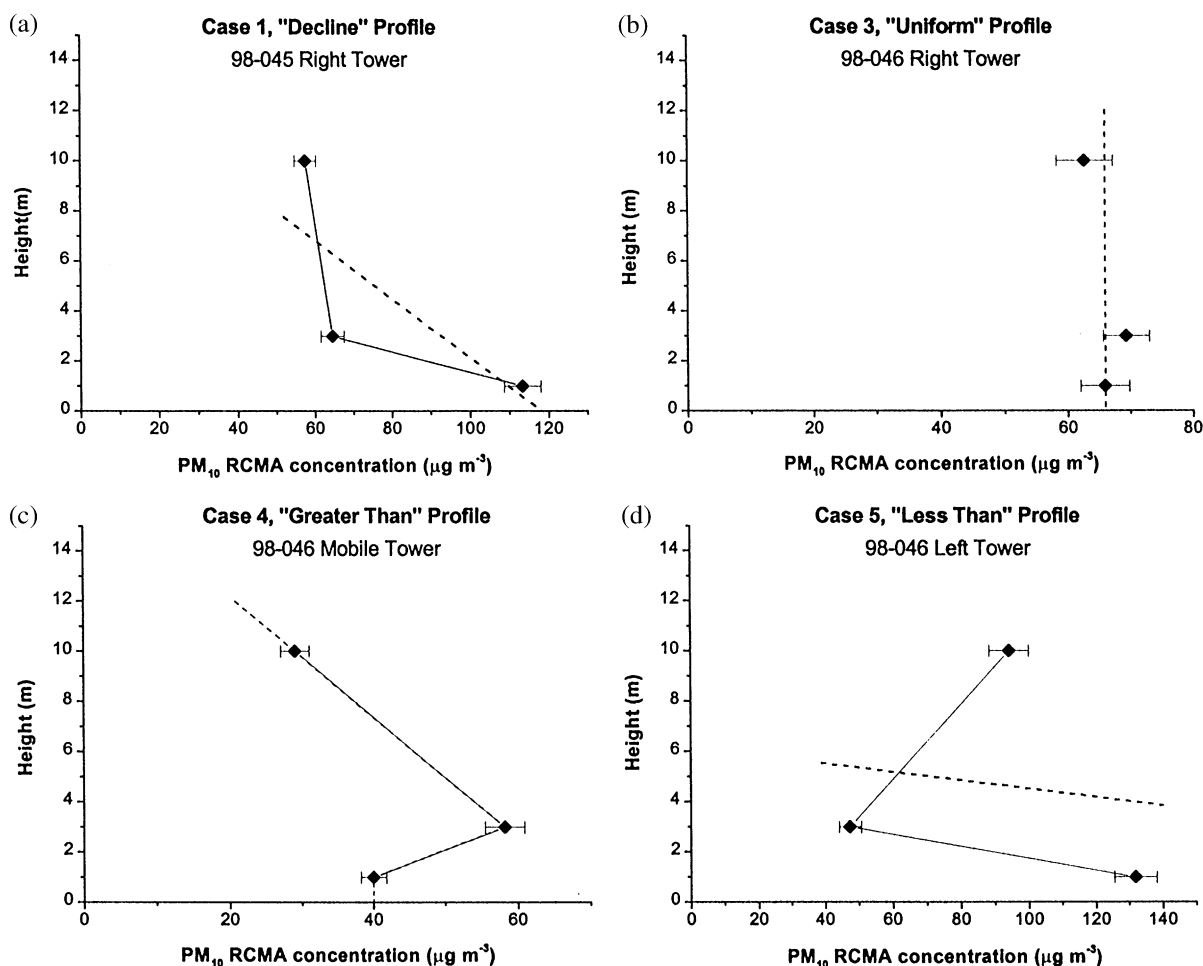


Fig. 2.  $PM_{10}$  RCMA mass concentration profile types and examples of the most appropriate function fits (dashed lines). Panels (b)–(d) were for samples collected simultaneously at three different tower locations (test 98-046). All three towers were located on the downwind edge of the field, but at different crosswind coordinates (see Fig. 1). The right (b) and left (d) stationary towers were 6 m apart from each other but were also located near the tractor turning point at the field edge. The mobile tower (c) was located 145 m from the midpoint between the other two towers. Due to differences in crosswind location, the three towers were at different downwind locations from the tractor due to the angle of the disking operation. This may explain the distinct differences in profile shapes during simultaneous sampling.

block fit assumed that the 1 m concentration was constant down to  $z_0$ , the  $PM_{10}$  concentration was linear from 1 to 3 m, and linear from 3 to 9 m. Above the highest  $PM_{10}$  measurement at 9 m, the vertical concentration profile was extrapolated linearly using the 3–9 m line until the block profile intersected the average upwind  $PM_{10}$  concentration at  $H$ .

### 2.7.3. Logarithmic profile model

Downwind  $PM_{10}$  vertical profiles were also fit with natural logarithmic decay curves as a function of height. The block and logarithmic profile methods

were previously shown to give similar results for almond and cotton harvesting operations (Ashbaugh et al., 1997).

### 2.7.4. Box model

The box model transforms the measured  $PM_{10}$  and wind speed profiles to a profile of uniform  $PM_{10}$  concentration and wind speed by defining the height,  $H_{\text{box}}$ , required to give the same total integrated  $PM_{10}$  mass flux. The box model height was determined by regressing the line-fit integrated mass fluxes for all of the profiles for which the most appropriate model was not the box

Table 2  
Downwind vertical profile classification

Profile class	Profile features	Profile shape <sup>a</sup>	Model fit characteristics	Number of test cases <sup>b</sup>
1 “decline”	Decreasing PM <sub>10</sub> mass concentration with height		Line, block, and log models give reasonable and equivalent heights and emission factors	10
2 “incline”	Increasing PM <sub>10</sub> mass concentration with height		Negative heights for line, block, and log; box model required	0
3 “uniform”	PM <sub>10</sub> concentrations equal at all three heights when measurement uncertainty is considered		Box model required otherwise heights unreasonable	4
4 “greater than”	PM <sub>10</sub> concentration at 1 m < 3 m and 3 m > 9 m		Fit dependent on relative concentrations. Block gives reasonable heights	5
5 “less than”	PM <sub>10</sub> concentration at 1 m > 3 m and 3 m < 9 m		Block fit gives unreasonable height	5

<sup>a</sup>Profile shapes assume height is on the y-axis and concentration on the x-axis.

<sup>b</sup>Number of valid land preparation tests collected during 1996–98 analysis year sets.

versus the product: (net 1 m PM<sub>10</sub> concentration × 1 m wind speed ×  $H_{\text{box}}$ ). Height in this product was empirically adjusted until a unit slope was achieved, indicating the equivalent box height (7 m) that would produce a PM<sub>10</sub> integrated mass flux equal to that measured using the functional models.

Uncertainties in the modeled plume heights were estimated using error propagation techniques (Coleman and Steele, 1989). Standard errors on the slope and intercept of the model fits to the downwind concentration profiles and the standard deviation in the upwind concentration measurements were used to propagate errors for the plume height estimate. The uncertainty calculations are shown in the appendix. The reported uncertainties do not take into account the uncertainty in individual upwind RCMA concentration measurements.

### 3. Results and discussion

#### 3.1. Vertical profile data recovery

For the three years of data examined, a total of 42 downwind and 17 upwind vertical profiles of PM<sub>10</sub> were collected for land preparation operations (disking, ripping, root cutting, and listing). There were fewer upwind profiles because the measurement times required to collect sufficient mass for gravimetric analysis were significantly longer for upwind than for downwind measurements. Average mass concentration ratios of PM<sub>2.5</sub> to PM<sub>10</sub> measured at two heights downwind of these operations ranged from 0.12 to 0.65 (James et al., 2000). Criteria were established to determine that: (1) the profile data were adequate for calculating a reliable emis-

sion factor, and (2) the measurements were made under conditions free of interference from other sources.

First, *only data sets (“tests”) comprised of both upwind and downwind profiles with valid PM<sub>10</sub> concentration measurements at three heights and concurrent meteorological data were accepted.* If either the upwind or downwind profile had any PM<sub>10</sub> RCMA concentrations below the MDL, or PM or meteorological data at one or more heights were missing, that test was considered invalid. This was the case for 15 of the 42 downwind and 2 of the 17 upwind PM<sub>10</sub> profiles. Note that the three-height requirement ruled out PM<sub>2.5</sub> emission factor calculation because PM<sub>2.5</sub> was collected at two heights only (Table 1).

Second, *the upwind profiles were scrutinized to ascertain whether or not the upwind tower was influenced by another source.* Since the upwind locations were generally 0.5–1 mile away from the downwind samplers, contamination of the upwind may not have influenced how well the measured downwind profile represented the source. However, isolation of the dust source was critical for characterizing the plume using the profiling method, so the upwind criterion was part of the test acceptance protocol. Most (11 of 15) of the complete upwind profiles were as expected for an upwind free of interference: the PM<sub>10</sub> concentrations did not vary with height when taking measurement uncertainties into account. However, for 3 cases, upwind mass concentrations at 1 m exceeded two times the 9 m upwind mass concentration, indicating the presence of an additional source upwind of the source being characterized. Since these upwind profiles were suspect, the tests associated with these upwind profiles were considered invalid. Because the majority of upwind profiles had essentially uniform PM<sub>10</sub> concen-

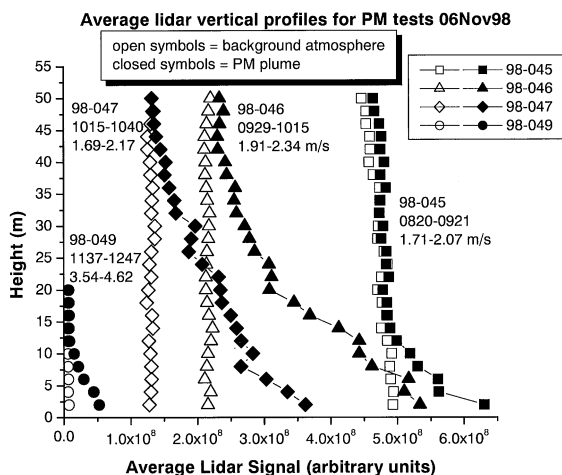


Fig. 3. Lidar vertical profiles determined by averaging lidar signal at 2 m height intervals for the range interval of the point sampler tower location (R tower for 98-045, -046, -047 and M tower for 98-049). The lidar 'sample' (closed symbols) and 'background' (open symbols) profiles are labeled by PM test ID, time period of test and range of measured wind speeds. Background vertical profiles were collected when the tractor was downwind of the lidar beam (see Fig. 1) or when the tractor was stopped and not generating  $PM_{10}$ .

trations with height, the average upwind  $PM_{10}$  RCMA mass concentration was used to calculate all emission factors reported here. Use of the average upwind value resulted in calculated emission factors that did not differ significantly from the emission factors calculated using a linear profile fit to the upwind data.

The final criterion used to evaluate profile validity was meteorological conditions. Wind speed and direction both affect the ability of the stationary tower array to adequately capture the  $PM_{10}$  plume from the moving point source (e.g., the tractor and implement). *The wind speed was considered valid if the average speed at 2 m height over the test period was between 1.0 and 6.5 m s<sup>-1</sup>.* The upper limit on wind speed was intended to minimize the sampling and quantification of wind-blown dust emissions and the lower limit is two times the quantifiable range of the cup anemometers. Wind direction was a less clear-cut test validation variable because most of the land preparation operations were conducted at an angle to the field boundaries. Thus, unlike the more regular harvest operations where a definitive wind direction cutoff could be assigned (Ashbaugh et al., 1997), wind direction was not used here as a criterion for invalidating any of the profiles in the dataset. Instead, as discussed in the companion paper (Holmén et al., 2000), the measured average wind direction and its standard deviation were used to qualify the level of confidence in the emission factors for each test.

### 3.2. Using lidar data to interpret $PM_{10}$ vertical profiles

Simultaneous collection of PM profiles, lidar scans, and tractor location data on 6 November 1998 provided a comprehensive data set that allowed the development of methods for interpreting all the PM profiles, including those collected before lidar data were available. The observations from the comprehensive data collected on this day were used to develop assessment criteria for profile model fits and plume height reasonableness, and to provide insight into the factors affecting the quality of the  $PM_{10}$  profile data.

#### 3.2.1. Downwind profile shape

Five categories of downwind profile shape are possible based on three measurement heights (Table 2, Fig. 2). Four of these types were represented in the land preparation data (Fig. 5) and three of the types were seen in profiles measured simultaneously (test 98-046, Fig. 2). Many of the measured downwind vertical profiles showed an overall decrease in  $PM_{10}$  concentration with increasing height (Case 1, see Table 2 and Fig. 2) and could be fit reasonably well with the linear model. Regions of non-linearity that occurred over limited height intervals in the test-averaged lidar vertical profiles (Fig. 3) are consistent with the Case 3–5 profile shapes for the point sampler tests. For example, the 98-047 lidar profile between 8 and 12 m resembles a Case 4 ("greater than") profile and the 98-045 and -046 lidar profiles below 6 m both resemble Case 5 ("less than") profiles. There are also height intervals in all of the measured lidar profiles that can be interpreted as Case 3 ("uniform") profiles, depending on the height-to-height measurement uncertainty.

Thus, the complex profile shapes measured with the PM towers are likely the result of sampling over a limited height range with very few samplers. In contrast, the relatively smooth test-averaged lidar vertical profiles (Fig. 3) reflect: (a) the high spatial resolution of the lidar that allowed horizontal and vertical averaging of the backscatter signal compared to the point sampler data that cannot be spatially averaged (Fig. 2), and (b) the lidar's vertical scanning capabilities that enabled measurements above the plume to background atmosphere levels. Note that the lidar beam diverges so that the beam cross section increases with range; this makes it difficult to sample at 1 m height with the lidar due to changes in the field elevation with range. Thus, while the lidar data confirm the reasonableness of the Cases 3–5 profile shapes over limited height intervals, the lidar spatial averaging and beam divergence result in more "well-behaved" lidar profiles on a test-by-test basis compared to those measured with the point samplers.

Lidar data also confirmed that the dust plumes measured over a short time interval often had higher concentrations above the ground than at the ground (data not shown). The time-averaged lidar data in Fig. 3 suggest

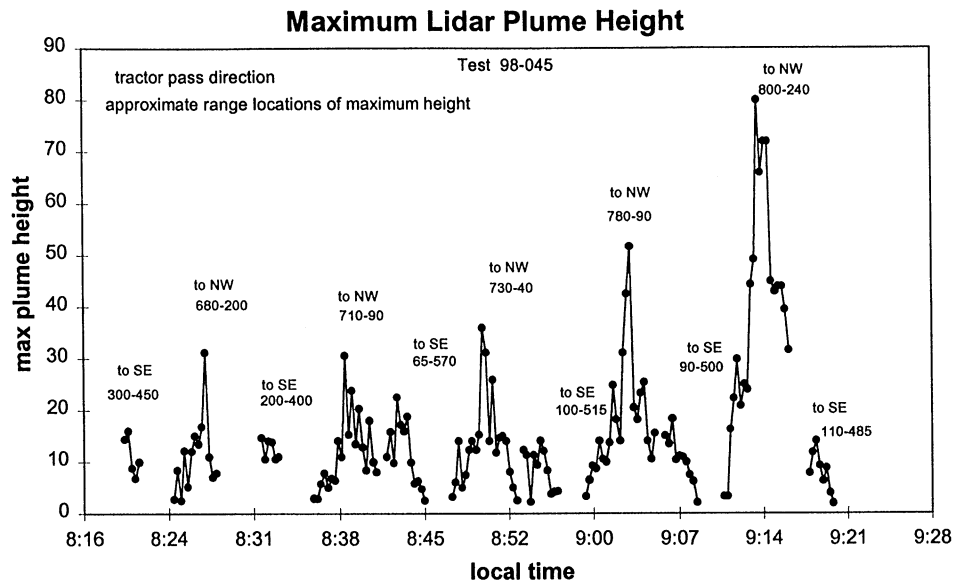


Fig. 4. Maximum plume heights recorded from the lidar 2D vertical scans during one point sampler test period (98-045, see Fig. 1). Note the variability in plume height over the course of the test as the tractor traversed the field. For each peak the direction of tractor travel and the range interval of plumes is noted. Interestingly, the plumes were higher when the tractor traveled to the NW (average wind direction for this test was  $9.6 \pm 15.7^\circ$ ). This could be due to differences in the tractor's distance from the lidar vertical scan plane because of the spiral path the tractor traveled (see Fig. 1 dotted lines).

that the Cases 4 and 5 vertical PM profiles captured actual small-scale deviations from a larger-scale overall linear decrease in concentration with increasing height. For the test conditions on 6 November 1998, the lidar data suggest that towers of up to 50 m height would have been required to adequately sample the entire plume with point samplers (Fig. 3).

### 3.2.2. Plume height

Maximum plume heights determined for individual lidar vertical scans (collected over a <30 s period) showed significant variability over the duration of a single PM test (Fig. 4), but test-to-test variability in the averaged plume heights was smaller (Fig. 5, open bars) and comparable to the heights determined by fitting the point sampler vertical profiles to the line, block, and log models (Fig. 5). The test-averaged plume heights over only those range locations where the point sampler towers were located (Fig. 3), agreed fairly well with the average heights from all ranges during a test period (Fig. 5, compare open and closed bars). This indicates that, on average, the plume monitored at a specific location on the downwind edge of the field had the same height, within measurement uncertainty, as the plume over the entire crosswind length of the tractor pass.

For the lidar vertical profiles based on data only from the tower ranges (Fig. 3), lidar field-of-view effects (see Section 2.4.2) could partly explain the significantly lower plume heights quantified for test 98-049 (Fig. 3) because

the tower was located only 180 m from the lidar during this test whereas it was over 500 m from the lidar for the other three tests. However, the agreement between the lidar height and the best-fit heights for all three point sampler models (Fig. 5) suggests that field-of-view effects were not significant for this test and the smaller plume height measured by the lidar was real. A more likely explanation for the decrease in plume height during test 98-049 was the higher wind speed during this test ( $3.5\text{--}4.6 \text{ m s}^{-1}$ ) compared to the tests earlier in the day ( $1.7\text{--}2.3 \text{ m s}^{-1}$ ). The decrease in the background lidar signal in Fig. 3 with time of day was likely due to relative humidity effects on the lidar response. The measured test period average (SD) relative humidity (%) values were 63.7 (3.2), 52.3 (1.7), 49.1 (0.8), 43.8 (0.8) for tests 98-045, 98-046, 98-047, 98-049, respectively. Thus, as relative humidity decreased, the lidar background signal decreased, as expected.

### 3.3. Best-fit emission factor model selection for individual profile types

Comparison of the lidar average plume heights and vertical profile shapes to the profiles measured with the point samplers on 6 November 1998 led to assignment of particular best-fit models to each of the four observed profile shape categories (Table 2, Fig. 2). Since plume height is a critical parameter for emission factor calculation (Holmén et al., 2000), models that gave reasonable fits to plume height were assumed to provide best

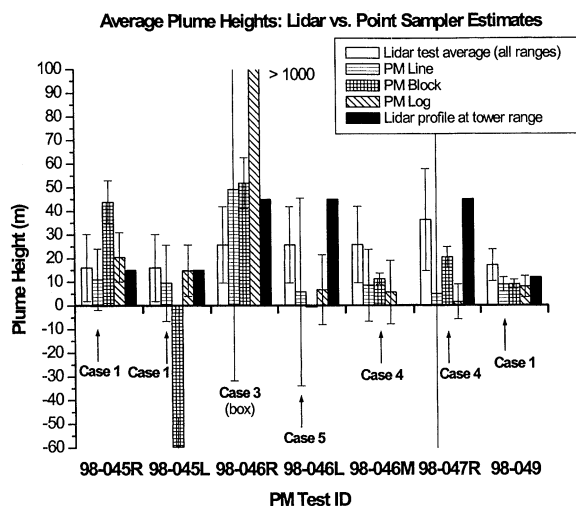


Fig. 5. Average plume heights determined by lidar (average and standard deviation of maximum plume heights recorded for each scan of PM test period, over all range locations), by three model fits to vertical exposure profiles (see text for model descriptions), and by averaging the lidar signal at 2 m height intervals at the tower profile range (see Fig. 3). Data are for the tests where lidar and point sampler data were collected simultaneously. For tests 98-046 the lidar vertical profile was not measured for the range of the mobile tower (no filled bar for 98-046 M). Error bars for lidar test average (open bar) are the standard deviation of individual scan maximum plume heights over the test period. Error bars for PM models are based on error propagation (see the appendix). Arrows indicate PM best-fit model height as determined by profile shape (Table 2).

estimates for emission factor calculation. The lidar average heights consistently showed better agreement with the line fits to the vertical profiles whereas the block and log models could give unreasonably high (i.e., 98-046R log) or low (i.e., 98-045L block) height estimates (Fig. 5). The best-fit model assignments for each profile type are described below.

*Case 1:* When the downwind concentrations were significantly higher than the upwind concentrations and the overall profile shape showed a decrease with height (Case 1), there was very good agreement between the line, block, and log model fits to the data. Therefore, the simple line model was used for plume height and emission factor calculation from Case 1 profiles.

*Case 3:* The plume heights determined by the line and block models for the Case 3 profile (98-046R) agreed fairly well with the lidar vertical profile plume height, but the log model height was unrealistically high (Fig. 5). The plume height uncertainty for the line model was also very high and both the line and block models could give negative heights for some Case 3 profiles. Because of these difficulties of fitting the uniform concentration profiles with the line, block, and log models in general, the

box model was determined to be the most representative for all Case 3 profiles. The 7 m box height determined by fitting 24 valid land preparation tests (standard error of the unit slope = 0.08) should be considered a very conservative estimate of the actual plume height.

*Case 4:* For the “greater than” profile shape tests (98-046 M and 98-047R), the block model provided height estimates closest to those measured with the lidar (Fig. 5). This observation along with the fact that the uncertainties for the heights computed by the block model were less than for the line or log models suggests that Case 4 profile shapes (“greater than”) are best fit using the block model.

*Case 5:* The most difficult profile shape to fit with the four models was Case 5 (“less than”); the block fit could be ruled out as it gave unrealistic negative heights for many Case 5 tests. Both the line and log models gave plume heights close to the average lidar values (Fig. 5), but because the log function could give unreasonably high heights if the 3 and 9 m concentrations were similar, the line fit model was selected as the best-fit model for all Case 5 profiles. Use of the linear model for all Case 5 tests was confirmed by comparing the standard errors of the two models: the line model always resulted in lower standard errors on the slope of the fit. However, the difficulty of fitting the Case 5 profile types indicates the need to further examine these results relative to other profile types with a larger data set.

#### 3.4. Downwind RCMA concentration “Replicates”

Multiple  $PM_{10}$  samples were collected at the same height and downwind array distance, but at different crosswind locations during 1997, and on 6 November 1998 similar replicates were collected at multiple heights. Because the lidar data on 6 November 1998 indicated that the test-averaged plume height measured at a single location was representative of the average height over all crosswind locations, suggesting that the tractor was a uniform moving point source, the point sampler concentrations at a given height were also expected to be similar regardless of crosswind location. However,  $PM_{10}$  concentrations at individual heights were often very different from location to location along the field edge (Table 3). The large differences between samplers that were intended to be replicates (based on their downwind array coordinate) were attributed to different test-averaged distances between the samplers and the tractor that resulted from the land preparation operations being conducted on an angle to the point sampler array. For example, during test 98-046 (Fig. 1) the mobile (M) and stationary (L and R) towers were all located on a road at the downwind edge of the field, but the average distance to the operation varied by about 30 m due to the angle of the disking operation. The average upwind tractor distances for each “replicate” sampler location varied

Table 3  
 PM<sub>10</sub> RCMA concentrations ( $\mu\text{g m}^{-3}$ ) for replicate PM<sub>10</sub> samplers at different crosswind locations but same downwind array locations, and all data collected on 6 November 1998

Test	ID	Array location <sup>a</sup> (m)			PM <sub>10</sub> RCMA ( $\mu\text{g m}^{-3}$ )			Operation direction (compass)
		UP	Y <sub>loc</sub>	Avg. UP	1 m	3 m	9 m	
97-037				152 ± 117				60/210
	<b>L</b>	20	– 81			<b>85.2 ± 3.8</b>		
	<b>D</b>	43	0			<b>610.4 ± 25.0</b>		
	R	97	94			86.0 ± 3.9		
97-046				55.9 ± 20.9				135/315
	M	75	168			250.6 ± 10.3		
	R	149	94			226.2 ± 8.5		
	D	243	0			82.7 ± 3.4		
	L	324	– 81			62.2 ± 2.5		
97-048				67 ± 15				135/315
	R	34	94			118.4 ± 4.8		
	D	128	0			241.8 ± 10.2		
	L	209	– 81			101.2 ± 4.2		
97-049				67 ± 15				135/315
	<b>R</b>	2 <sup>b</sup>	94			<b>74.2 ± 3.0</b>		
	<b>D</b>	68	0			<b>167.7 ± 6.9</b>		
	L	111	– 81			195.1 ± 8.3		
98-045				23.6 ± 4.9				100/280
	<b>R</b>	23	0		<b>113.3 ± 4.7</b>	<b>64.5 ± 3.0</b>	<b>57.5 ± 2.8</b>	
	<b>L</b>	26			<b>79.8 ± 3.3</b>	<b>43.7 ± 2.9</b>	<b>46.0 ± 4.1</b>	
98-046				23.6 ± 4.9				100/280
	<b>R</b>	30			<b>65.9 ± 3.9</b>	<b>69.3 ± 3.7</b>	<b>62.7 ± 4.5</b>	
	<b>L</b>	30			<b>131.8 ± 6.3</b>	<b>47.4 ± 3.3</b>	<b>94.2 ± 5.8</b>	
	M	63			<del>40.0</del> ± 1.8	58.2 ± 2.7	29.1 ± 2.0	
98-047				23.6 ± 4.9				100/280
	R	98			47.6 ± 3.1	78.5 ± 3.8	56.5 ± 5.1	
	L	99			87.6 ± 5.5	ND	ND	
98-048	M	123	– 466	23.6 ± 4.9	56.8 ± 3.4	164.5 ± 7.7	243 ± 10.3	100/280
98-049	M	56	– 385	23.6 ± 4.9	12.5 ± 0.9	95 ± 4.1	96.9 ± 4.0	100/280
98-050	M	34	– 394	17.4 ± 4.0	44.9 ± 2.9	74.5 ± 3.7	118 ± 5.5	100/280

<sup>a</sup>UP = average upwind distance between sampler and tractor/implement. Y<sub>loc</sub> = crosswind distance relative to array origin.

<sup>b</sup>During most of test 97-049 the R sampler was upwind of tractor. ± values indicate RCMA uncertainties based on error propagation. Samplers listed in bold were impacted by edge effects. ND = below detectable limits.

by as much as 200 m for a single test (Table 3) and may explain the data for tests, such as 97-046, where the measured PM<sub>10</sub> concentrations at a given height decreased as the upwind tractor distance increased (Table 3).

The average upwind distances (Table 3) were estimated from the upwind tractor distance measured at the array origin at the beginning of the test, the counted number of tractor tower passes during the test, and the implement width, taking the approximated operation angle into account. When rangefinder data were available (98-045, 98-046) upwind distance was estimated from the mea-

sured tractor path. It should be noted that during land preparation operations many implements work in a spiral pattern over small sections of ground as shown by the tractor path detailed in Fig. 1 (98-045, circles labeled with time). This complicated path makes assignment of test-average upwind distances difficult, especially for tests such as 98-046 where an outer ring of ground was disked during the test (Fig. 1, triangles).

Sampler-to-tractor distance did not explain all of the variability between replicates, however, because even samplers located at the same average distance from the

tractor and within 6 m of each other (98-045 to 98-047) had  $PM_{10}$  concentrations that differed by up to a factor of 2. These results probably reflect the fact that the tractor turned in the proximity of the L and R towers during these tests because the edge of the field was reached at this crosswind location (see Fig. 1). The turning of the tractor near the towers affected the  $PM_{10}$  concentrations measured at each tower differently. For example, in test 98-045, the R tower was closer than the L tower to the tractor turn location and this could explain the higher  $PM_{10}$  concentration in the R sampler at 1 m. In test 98-046, however, the situation was reversed: the L tower was closer to the tractor turn at the field edge and correspondingly, the L 1 m  $PM_{10}$  concentration was higher.

These interpretations of tractor turning or “edge effects” rely on the tractor location data that were collected throughout these tests using the laser rangefinder. Without these detailed data, identifying the reasons for the discrepancies between measurements made 6 m apart would be extremely difficult. The lack of rangefinder data prior to 1998 tests makes it impossible to explain the discrepancies in Table 3 for these tests, especially the disparate results of 97-037 where the measured D tower 3 m concentration was over 6 times that of the L and R samplers. The high variability in  $PM_{10}$  collection by the point samplers due to the tractor’s behavior near the towers indicates the need for rating the quality of individual test measurements on the basis of the presence or absence of edge effects (Holmén et al., 2000).

### 3.5. Factors influencing plume height

Interestingly, the lidar scan plume heights varied with the direction of tractor travel during one test for which this information was recorded in detail (98-045, Fig. 4). This was probably due to the relative upwind distances between the tractor and the lidar scan plane during the operation. As Fig. 1 shows, when the tractor traveled to the NW during test 98-045 (see time points, Fig. 1) it was also up to 40 m farther upwind of the lidar measurement plane due to the spiral path of the tractor. These results bring up the question of whether or not there is a maximum sampling distance for reliable determination of plume height and emission factors using 9–10 m towers. This issue is discussed in more detail in the companion paper (Holmén et al., 2000).

## 4. Conclusions

Micrometeorological mass balance methods have been successfully applied to the quantification of emissions of gases such as ammonia and methane from homogeneous area sources with well-developed upwind fetches (Denmead et al., 1998). The usefulness of these methods in

quantifying PM emissions from nonpoint sources has been restricted by difficulties in measuring the height of the plumes and the complexities associated with adequately modeling the vertical profile of PM mass concentrations (Venkatram et al., 1999). The framework developed here for analyzing PM profiles by shape class and the identification of problematic field conditions that affect the reproducibility of PM measurements relied on simultaneous collection of lidar and PM data. The lidar provided information on plume height and shape with much higher spatial and temporal resolution and range than the PM samplers and helped overcome many of the limitations experienced in previous studies. The capability of the lidar scans to extend over the top of the plumes provided independent measurements of plume height and aided evaluation of various models for estimating plume height from  $PM_{10}$  vertical concentration profiles. The lidar and laser rangefinder data also helped identify the adverse impact field edge effects had on replicate  $PM_{10}$  concentration measurements and profile interpretation.

The number of valid vertical profile tests collected without interference from other sources increased from 50% in 1996 to 64% in 1997 and 100% in 1998, indicating improvement in the field reconnaissance methods used for collecting useful  $PM_{10}$  data. However, the lack of reproducibility in PM concentrations and profile shape during a single test suggests that changes in field sampling methods are necessary to further improve emissions measurements from land preparation operations. For example, the large number of Cases 4 and 5 profiles (where concentrations did not uniformly decrease with height) suggests that many plumes were not fully characterized by the three sampling heights. The lidar data on 6 November 1998 confirmed that both local maxima and minima occurred in the overall plume profile, but showed that limited point sampler heights can bias overall plume shape interpretation for plumes that are highly irregular or very tall (i.e., greater than the highest point sampler height). Addition of another sampling height to the profiles at 5 m is expected to improve the ability to accurately characterize the more irregular Case 4 and 5 profile types. The need to represent  $PM_{10}$  mass using RCMA rather than gravimetric mass should also be reduced by the addition of a fourth height to the vertical profile because there will be a greater probability that at least three of the samples collected will have valid gravimetric masses. Addition of  $PM_{2.5}$  measurements at a third and a fourth height both upwind and downwind will enable calculation of  $PM_{2.5}$  emission factors in the future. Collection of lidar data with future tests will continue to provide independent verification of the plume parameters, such as plume height, determined from the point sampler data.

Future land preparation tests should also include collection of as much information as possible about the

tractor location relative to the towers to enable identification of sampling conditions that compromise the interpretation of the point sampler data. The angle of the implement relative to the point sampler array must be measured with greater accuracy in the future to enable calculation of the limits of the test operation. Finally, where feasible, towers should be erected to take the operation angles into account, so true replicate profiles can be collected and their measured masses compared.

### Acknowledgements

The authors thank Robert Matsumura and Christopher Tsubamoto for their hard work in designing and implementing the PM field equipment, method protocols and database structure, and Krystyna Trzepla-Nabaglo for lidar data reduction assistance. Support for this work was from USDA Special Research Grants Program grants 94-33825-0383 and 98-38825-6063 and NSF POWRE grant 99-73434.

### Appendix A. Plume height uncertainty calculation

The PM<sub>10</sub> profile as a function of height was fit to a line for all three models in order to determine the plume height,  $H$ , where the downwind concentration profile intersected the average upwind concentration (AVE):

$$H = (\text{AVE} \times \text{slopeC}) + \text{IntC} \quad (\text{for line fit and 3–9 m block concentration fit}),$$

$$\ln H = (\text{AVE} \times \text{slopeC}) + \text{IntC} \quad (\text{for log model}), \quad (\text{A.1})$$

where slopeC and IntC are the slope and intercept of the downwind PM<sub>10</sub> concentration model fits, respectively. The error on the (AVE slopeC) product term,  $S_h$ , was calculated as

$$S_h = H \left[ \left( \frac{S_{\text{up}}}{\text{AVE}} \right)^2 + \left( \frac{S_{\text{slopeC}}}{\text{slopeC}} \right)^2 \right]^{0.5}, \quad (\text{A.2})$$

where  $S_{\text{up}}$  is the standard deviation of the measured upwind concentrations, and  $S_{\text{slopeC}}$  is the standard error on the slope of the downwind profile best-fit line. This error term combined with the error on the intercept term gives the overall error on plume height:

$$S_H = [(S_h)^2 + (S_{\text{intc}})^2]^{0.5}, \quad (\text{A.3})$$

where  $S_{\text{intc}}$  is the computed standard error on the intercept of the downwind profile best-fit line. Eqs. (A.2) and (A.3) can be combined to give the expanded expression for the uncertainty in the plume height:

$$S_H = \sqrt{H^2 \left( \frac{S_{\text{up}}^2}{\text{AVE}^2} + \frac{S_{\text{slopeC}}^2}{\text{slopeC}^2} \right) + (S_{\text{intc}})^2}. \quad (\text{A.4})$$

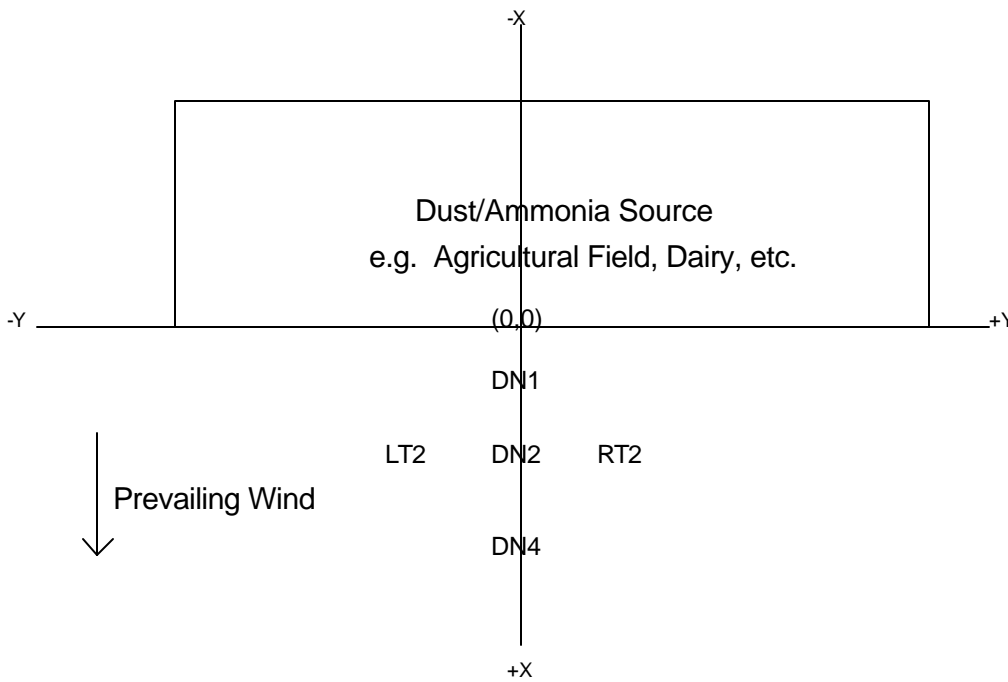
### References

- Ashbaugh, L.L., Matsumura, R., James, T., Carvacho, O., Flocchini, R., 1996. Modeling PM<sub>10</sub> dust emissions from field harvest operations. International Conference on Air Pollution from Agricultural Operations, Kansas City, KS.
- Ashbaugh, L.L., Matsumura, R., Flocchini, R., 1997. Calculation of PM<sub>10</sub> emission rates using a simple box model and a vertical profiling method. In: Emission Inventory: Planning for the Future. AWMA & EPA, Research Triangle Park, NC.
- Bond, T.C., Anderson, T.L., Campbell, D., 1999. Calibration and intercomparison of filter-based measurements of visible light absorption by aerosols. *Aerosol Science and Technology* 30, 582–600.
- Cahill, T.A., 1995. Compositional analysis of atmospheric aerosols. In: Johansson, S.A.E., Campbell, J.L., Malmqvist, K.G. (Eds.), Particle-Induced X-Ray Emission Spectrometry. Chemical Analysis Series, Vol. 133. Wiley, New York.
- Cahill, T.A., Eldred, R.A., Flocchini, R.G., Barone, J., 1977. Statistical techniques for handling PIXE data. *Nuclear Instruments and Methods* 142, 259–261.
- Cahill, T.A., Ashbaugh, L.L., Eldred, R.A., Feeney, P.J., Kusko, B.H., Flocchini, R.G., 1981. Comparisons between size-segregated resuspended soil samples and ambient aerosols in the western United States. *Atmospheric Aerosol: Source/Air Quality Relationships*, ACS Symposium Series # 167. American Chemical Society, Washington, DC, pp. 269–285.
- Cahill, T.A., Eldred, R.A., Motallebi, N., Malm, W.C., 1989. Indirect measurement of hydrocarbon aerosols across the US by nonsulfate hydrogen-remaining gravimetric mass correlations. *Aerosol Science and Technology* 10, 421–429.
- Campbell, D., Copeland, S., Cahill, T., 1995. Measurement of aerosol absorption coefficient from Teflon filters using integrating plate and integrating sphere techniques. *Aerosol Science and Technology* 22, 287–292.
- Chow, J.C., Watson, J.G., Lowenthal, D.H., Pritchett, L.C., Richards, L.W., 1990. San Joaquin Valley Air Quality Study Phase. 2: PM<sub>10</sub> Modeling and Analysis. DRI 8929.1F, Desert Research Institute, Reno, NV.
- Chow, J.C., Watson, J.G., Lowenthal, D.H., Solomon, P.A., Magliano, K.L., Ziman, S.D., Richards, L.W., 1992. PM<sub>10</sub> source apportionment in California's San Joaquin Valley. *Atmospheric Environment* 26A, 3335–3354.
- Clausnitzer, H., Singer, M.J., 1996. Respirable-dust production from agricultural operations in the Sacramento Valley, California. *Journal of Environmental Quality* 25, 877–884.
- Clausnitzer, H., Singer, M.J., 1997. Intensive land preparation emits respirable dust. *California Agriculture* 51, 27–30.
- Coleman, H.W., Steele Jr., W.G., 1989. Experimentation and Uncertainty Analysis for Engineers. Wiley, New York, 205pp.
- Cowherd Jr., C., Kinsey, J.S., 1986. Identification, assessment and control of fugitive particulate emissions. EPA/600/8-86/023, US EPA, Research Triangle Park, NC.
- Cowherd Jr., C., Axetall Jr., K., Guenther, C.M., Jutze, G.A., 1974. Development of Emission Factors for Fugitive Dust Sources. NTIS PB-238 262, Midwest Research Institute, Kansas City, MO.

- Cuscino Jr., T.A., Kinsey, J.S., Hackney, R., 1984. The Role of Agricultural Practices in Fugitive Dust Emissions. Midwest Research Institute, Kansas City, MO.
- Denmead, O.T., Harper, L.A., Freney, J.R., Griffith, D.W.T., Leuning, R., Sharpe, R.R., 1998. A mass balance method for non-intrusive measurements of surface-air trace gas exchange. *Atmospheric Environment* 32, 3679–3688.
- Dolislager, L.J., Motallebi, N., 1999. Characterization of particulate matter in California. *Journal of Air and Waste Management Association*, 49 (Special Issue on PM<sub>2.5</sub>: A Fine Particulate Standard), PM 45–56.
- Eldred, R.A., Cahill, T.A., Wilkinson, L.K., Feeney, P.J., Malm, W.C., 1989. Particulate characterization at remote sites across the U.S.: first year results of the NPS/IMPROVE network. Air and Waste Management Association 82nd Annual Meeting. Air and Waste Management Association, Anaheim, CA, pp. 89–151.3.
- Eldred, R.A., Cahill, T.A., Wilkinson, L.K., Feeney, P.J., Chow, J.C., Malm, W.C., 1990. Measurement of fine particles and their chemical components in the IMPROVE/NPS network. In: Mathai, C.V. (Ed.), *Visibility and Fine Particles*. Air and Waste Management Association, Anaheim, CA, pp. 187–196.
- Eldred, R.A., Cahill, T.A., Flocchini, R.G., 1997. Composition of PM<sub>2.5</sub> and PM<sub>10</sub> aerosols in the IMPROVE network. *Journal of Air and Waste Management Association* 47, 194–201.
- Eldred, R.A., Cahill, T.A., Pitchford, M., Malm, W.C., 1988. IMPROVE – a new remote area particulate monitoring system for visibility studies. Air Pollution Control Association 81st Annual Meeting, Dallas, TX, pp. Paper 88–54.3.
- Flocchini, R.G., Cahill, T.A., Matsumura, R.T., Carvacho, O., Lu, Z., 1994. Study of fugitive PM-10 emissions for selected agricultural practices on selected agricultural soils. SJV Grant File # 20960, University of California, Davis, CA.
- Holmén, B.A., Eichinger, W.E., Flocchini, R.G., 1998. Application of elastic lidar to PM<sub>10</sub> emissions from agricultural nonpoint sources. *Environmental Science and Technology* 32, 3068–3076.
- Holmén, B.A., James, T.A., Ashbaugh, L.L., Flocchini, R.G., 2000. Lidar-assisted measurement of PM<sub>10</sub> emissions from agricultural tilling in California's San Joaquin Valley. II: emission factors. *Atmospheric Environment* 35, 3265–3277.
- James, T.A., Matsumura, R.T., Carvacho, O.F., Ashbaugh, L.L., Flocchini, R.G., 1996. Strategies for measuring fugitive dust emissions. International Conference on Air Pollution from Agricultural Operations, 7–8 February. Midwest Plan Service, Kansas City, MO, pp. 161–168.
- James, T.A., Fan, T.W.-M., Higashi, R.M., Flocchini, R.G., 2000. Size and elemental characterization of dust from agricultural sources. Second International Conference on Air Pollution from Agricultural Operations Specialty Conference. ASAE (American Society of Agriculture Engineers), Des Moines, IA.
- John, W., Reischl, G., 1980. A cyclone for size-selective sampling of ambient air. *APCA Journal* 30, 872–876.
- Malm, W.C., Sisler, J.F., Huffman, D., Eldred, R.A., Cahill, T.A., 1994. Spatial and seasonal trends in particle concentration and optical extinction in the US. *Journal of Geophysical Research* 99 (D1), 1347–1370.
- Matsumura, R.T., Ashbaugh, L.L., James, T.A., Carvacho, O.F., Flocchini, R.G., 1996. Size distribution of PM<sub>10</sub> soil dust emissions from harvesting crops. International Conference on Air Pollution from Agricultural Operations. Midwest Plan Service, Kansas City, MO, pp. 147–153.
- Snyder, J.W., Blackwood, T.R., 1977. Source assessment: mechanical harvesting of cotton – State of the art. EPA/600/2-77-107d, US EPA, Research Triangle Park, NC.
- Venkatram, A., Fitz, D., Bumiller, D., Du, S., Boeck, M., Gan-guly, C., 1999. Using a dispersion model to estimate emission rates of particulate matter from paved roads. *Atmospheric Environment* 33, 1903–1912.

<u>Description</u>	<u>Sampling Code</u>	<u>Location</u>
Upwind 1 - 1m	U11	
Downwind 1 - 3m	D13	
Downwind 1 - 9m	D19	

Each sampling location in an array is described by a downwind and crosswind location, in meters, measured from the origin. The convention of distance away from or towards the source (positive and negative, respectively) making up the X axis and distance in a plane parallel to the source boundary to the right and left (positive and negative when facing downwind, respectively) is followed for PM, ammonia, soil, and meteorological data collection. A diagram of the coordinate system follows:



Channel codes are used to represent a set of specific measurements (sample collection and analysis) for specific specie(s). Soil samples have yet to be assigned channel codes, as the soils data is currently archived in a database independent of the aerosol, ammonia, and meteorological data.

Channel Code	Sampler	Substrate	Substrate Size	Analysis
A1	IMPROVE PM <sub>2.5</sub>	Teflon	25 mm diameter	Gravimetric Mass, Optical Absorption, XRF, PIXE, PESA
B1	IMPROVE PM <sub>2.5</sub>	Nylon with denuder	25 mm dia.	Ion Chromatography
B4	IMPROVE PM <sub>10</sub>	Nylon with denuder	25 mm dia.	Ion Chromatography
C1	IMPROVE PM <sub>2.5</sub>	Single Quartz	25 mm diameter	Thermal Reflectance Optical
D1	IMPROVE PM <sub>10</sub>	Teflon	25 mm diameter	Gravimetric Mass, Optical Absorption, XRF, PIXE, PESA
L2	STACKED FILTER UNITS	Teflon & Citric Acid coated Quartz Filter	25 mm diameter	Ion Selective Membrane
V2	BUBBLERS	1.5% H <sub>3</sub> BO <sub>3</sub>	20 ml vol.	Ion Selective Membrane
N1	WILLIAMS BADGE	PreFilter (Teflon or Zefur) + Citric Acid coated Whatman 41	37mm diameter	Ion Selective Membrane
RD	IMPROVE PM <sub>10</sub>	Teflon from Dust Resuspension	25 mm diameter	Gravimetric Mass, Optical Absorption, XRF, PIXE, PESA
RA	IMPROVE PM <sub>2.5</sub>	Teflon from Dust Resuspension	25 mm diameter	Gravimetric Mass, Optical Absorption, XRF, PIXE, PESA
M1	DRUM Stage 1	Mylar, 10-15 μm	--	PIXE
M2	DRUM Stage 2	Mylar, 5-10 μm	--	PIXE
M3	DRUM Stage 3	Mylar, 2.5-5 μm	--	PIXE
M4	DRUM Stage 4	Mylar, 1.15-2.5 μm	--	PIXE
MB	DRUM Stage 4-6	Mylar, 0.34 - 1.15 μm	--	PIXE
Q1	PM <sub>10</sub> Portable Filter Sample	Quartz	25 mm	Pyrolysis Gas Chromatography Mass Spectrometry
	Surface Samples (< 0.5" depth)	Moisture Cans	~ 300 g	Moisture Content
	Surface Samples (< 0.5" depth)	Plastic Bags	~ 1kg	Dry Sieving, Wet Sieving, Organic Carbon, Nitrogen

	Surface Samples ( $< 0.5''$ depth)	Plastic Bags	$\sim 1$ kg	SFAME, PLFA, DNA
W*	Datalogger	Anemometers Wind Vanes Temp. Probe RH Probe Pyranometer	--	Wind Speed Wind Direction Temperature Relative Humidity Solar Radiation

\*Datalogger channels are numbered to designate the program used to collect and average the data.

Mass concentrations of PM and ammonia are calculated from constituent mass in the sample and the volume of air sampled. Air flow rates are measured before and after sampling as the differential pressure created using recorded using an inline orifice and recorded by a magnehelic gauge. The gauge and orifice as a unit is calibrated to a spirometer in Davis each year and the logarithmic relationship between flow and pressure difference is recorded as a slope and intercept. These parameters are entered into the database separately for each PM or ammonia sampler, allowing for the use of multiple magnehelic devices. Additionally, a second set of calibration parameters can be accommodated in the database for each sampler. This attribute was used in calculating flows for samples collected in 1994 through 1997 such that magnehelic gauges in each sampler were calibrated to the gauge and orifice unit and the in situ gauges were used to record readings.

Each PM and ammonia sample is labeled with a four digit number designated as the media ID. Teflon filter pre-weights are stored in one database and the empty weights of vials for the bubblers and lot numbers for all samples to undergo speciated analyses are stored in another. When substrates are transferred from sampling apparatus the media Id label is transferred to the holding vessel and a label is added to indicate the Test ID, the SamLoc, and the Chan. A third permanent label replaces both original labels once data entry is complete. Error trapping is performed in the relation of the databases to produce the permanent label which contains all of the data on the first two labels as well as the array code and a data to track the sample through the data acquisition software.

Gravimetric, elemental, and ammonia masses are reported from the analytical sources on a per-sample basis. These data are combined with the sample air volumes using relational databases which rebuild a temporary database from the raw data each time they are queried by the user. Meteorological data are also related to databases of test information to calculate average values for each test in a similar manner. This allows access to original data files by multiple users simultaneously and ensures that database corrections are universally available to all users. Quality assurance protocols are followed for each analysis year set using the temporary databases and erroneous data is listed in a perpetual file that is also related with the raw data to exclude those points from all subsequent queries. Current protocols for calculating emission

factors from PM or ammonia concentrations and meteorological data query the relevant temporary files and relate them to information about site locations, soil types, crop and livestock type, and specifics about implements on a test-by-test basis. General equations described in section 3.0 are used in spreadsheets by a dynamic process that we are still fine tuning to compute emission factors using several different models and methods for normalizing data collected from disparate operations to form a comparable, consistent table. Quality ratings and estimates of emission factor errors will help considerably in elucidating the essential sources of variance in the data set, determine the correct grouping of sources, and provide data will fit into a PM-10 emissions inventory of agricultural operations.

## **24 APPENDIX H – TEXT OF ATMOSPHERIC ENVIRONMENT PAPERS**

Electronic versions of these documents are attached.



PERGAMON



Atmospheric Environment 35 (2001) 3265–3277

**ATMOSPHERIC  
ENVIRONMENT**

[www.elsevier.com/locate/atmosenv](http://www.elsevier.com/locate/atmosenv)

## Lidar-assisted measurement of PM<sub>10</sub> emissions from agricultural tilling in California's San Joaquin Valley – Part II: emission factors

Britt A. Holmén\*, Teresa A. James, Lowell L. Ashbaugh, Robert G. Flocchini

*Air Quality Group, Crocker Nuclear Laboratory, University of California, Davis, CA 95616, USA*

Received 25 April 2000; accepted 31 October 2000

### Abstract

Emission factors for agricultural operations are needed in order to develop reliable PM<sub>10</sub> emissions inventories and air quality models for air basins with significant agricultural land use. A framework was developed to analyze the PM<sub>10</sub> vertical profiles collected downwind of tilling operations in the San Joaquin Valley. The methods calculate emission factors on the basis of profile shape and assign quality ratings to each land preparation test. Uncertainties in the calculated emission factors and plume heights were used as one criterion for evaluating the relative quality of the reported emission factor. Other quality ratings were based on the magnitude of the difference in measured up- and downwind concentrations, wind direction, whether the tests were conducted near the edges of the field, and how well the proposed model fit the profile data. The emission factors from different operations were compared taking the quality of the emission factor into account. Plume heights and emission factors for 24 valid test profiles ranged from 2 to 20 m (mean = 9.8; SD = 3.6; median = 9.8) and zero to 800 mg m<sup>-2</sup> (mean = 152; SD = 240; median = 43), respectively. Key environmental properties governing PM<sub>10</sub> emission from these operations include relative humidity, soil moisture and vertical temperature gradient. Surprisingly, no discernable relationships were found between implement type or wind speed and the measured emission factors. © 2001 Elsevier Science Ltd. All rights reserved.

*Keywords:* PM<sub>10</sub>; Emission factor; Quality rating; Agricultural dust

### 1. Introduction

Methods to estimate agricultural tilling contributions to PM<sub>10</sub> inventories (U.S.E.P.A., 1995) are currently based on surface soil silt content, a parameter that cannot account for the myriad of factors affecting emissions. Because the observed late summer and fall PM<sub>10</sub> standard violations in California's San Joaquin Valley (SJV) (Dolislager and Motallebi, 1999) coincide with the harvest season of many California crops (e.g., cotton, almonds, tomatoes), agricultural activities (both harvesting and subsequent land preparation) have been identi-

fied as potentially significant sources of PM<sub>10</sub> during this time of year. Quantification of these sources and understanding of the key environmental variables controlling emissions must be achieved before efforts to control agricultural PM<sub>10</sub> can be planned.

Lidar data were used to validate the choice of emission factor best-fit model for individual PM<sub>10</sub> profiles depending on downwind vertical profile shape (Holmén et al., 2000). In this paper, the PM<sub>10</sub> data for three years of testing SJV land preparation operations (disking, listing, root cutting and ripping) are discussed in terms of a new analysis framework for PM<sub>10</sub> concentration profile measurements that estimates an emission factor, its associated uncertainty, and assigns a test quality rating. Relationships between PM<sub>10</sub> emission factors and field sampling conditions such as implement type, wind speed, relative humidity, temperature gradient and distance between the dust-generating implement/tractor and the

\* Corresponding author. Tel.: +1-530-752-1213; fax: +1-530-752-4107.

E-mail address: [baholmen@ucdavis.edu](mailto:baholmen@ucdavis.edu) (B.A. Holmén).

sampling location are examined. The quality rating system developed for individual sampling tests is partly based on interpretations of the simultaneously collected point sampler and lidar data described previously (Holmén et al., 2000). Modifications to both the sampling techniques and the modeling methods that can be employed in the future to achieve more realistic and reliable PM emission factors from nonpoint agricultural operations are discussed.

## 2. Experimental methods

### 2.1. $PM_{10}$ point sampling

A combination of upwind/downwind source isolation and vertical profiling methods was used to quantify  $PM_{10}$  emissions from land preparation operations as described in detail in the accompanying paper (Holmén et al., 2000). The tests were conducted between Fall 1996 and Winter 1998 in two counties, Kings and Fresno, under conditions (see Table 1) that varied from very hot and dry (temperature = 26–35°C; soil moisture = 1.5–2.3%; relative humidity = 20–40%), prior to the season's first precipitation, to cool and wet (temperature = 7–20°C; soil moisture = 11–20%; relative humidity = 40–90%), between winter storms. In all cases aerosol samples were collected using one upwind and at least one downwind vertical profile in a sampling array diagramed previously (see Fig. 1, Holmén et al. (2000) and Fig. 2a, Holmén et al. (1998)). For the tests examined here, the downwind samplers were located between 1 and 235 m from the limits of the operation ( $X_{loc}$ , Table 2). When the agricultural operation was far from the stationary PM tower that was located at the downwind edge of the field, the vertical profiles of  $PM_{10}$  were sampled using a mobile tower unit that was driven into the field.

Vertical  $PM_{10}$  profiles were based on three  $PM_{10}$  measurement heights – at 1, 3 and 9 (or 10 for some towers) m – using modified Interagency Monitoring of Protected Visual Environments (IMPROVE) aerosol samplers (Eldred et al., 1988, 1990) that collected  $PM_{10}$  on 25 mm stretched Teflon filters (3  $\mu$ m Teflo<sup>®</sup>, Gelman R2P1025). EPA-approved Sierra Anderson inlets (Model 246b) produced the 10  $\mu$ m size-cut, flow rates were regulated with critical orifices, and the essential elements of the modified samplers from inlet to filter were identical to those of IMPROVE samplers (see Holmén et al., 2000).

### 2.2. Soil moisture

Surface soil samples (upper 6 cm) were collected from at least two locations on each field for laboratory determination of soil moisture, particle size distribution and  $PM_{10}$  potential index (Carvacho et al., 1996a). Soil moisture was measured by determining the mass differ-

ence of tared aluminum moisture cans before and after heating at 105°C for 12 h overnight to remove moisture (ASTM, 1992). Soil samples were collected and analyzed per field per operation, unless meteorological conditions changed noticeably. Soil samples were not available for tests 96-103 and 96-104.

All of the tests were conducted on soils with sandy loam, clay loam or loam textures. For example, the Westhaven loam, Panoche clay loam and Kimberlina fine sandy loam of Kings County (Arroues and Anderson, 1986) are represented in the samples collected. Investigations of how soil texture influences  $PM_{10}$  emissions potential from these agricultural soils has been reported previously (Carvacho et al., 1996a, b, 2000). While soil silt content has been reported to be a key variable for emissions estimation (i.e., AP-42), soil texture is not examined as an environmental variable here because of the narrow range of textures in the soil samples with accompanying valid  $PM_{10}$  profiles and the fact that the Fresno County soils have not been mapped. A forthcoming paper will summarize soil texture and  $PM_{10}$  emissions based on laboratory tests using a resuspension apparatus.

### 2.3. Meteorological parameters

Measurements of air temperature, wind speed and direction, relative humidity and solar radiation were recorded at the upwind towers using Campbell Scientific CR10 data loggers to download data averages every 5 or 1 min (the averaging time was decreased to 1 minute in 1998 tests). Vertical profiles of temperature and wind speed were monitored for determining atmospheric stability and PM emission fluxes. In one-third of the sampling periods presented here, simultaneous meteorological measurements of the same parameters were made at three heights (1, 2 and 3 m) using a 3 m tripod downwind of the operation for quality assurance.

### 2.4. Implement and field characteristics

Specific information about the agricultural operation was recorded to enable comparisons between crop and implement types, soil conditions, irrigation techniques, and to allow development of predictive relationships between  $PM_{10}$  emissions and field or implement conditions. Typical parameters measured included: implement type, make, model and dimensions (i.e., overall width; height/soil depth); number of implement passes per test; tractor type; operation speed; compass direction of operation; and distance of the operation from the PM samplers. Upwind distances reported in Table 2 ( $X_{loc}$ ) represent the average distance between the PM samplers and the tractor/implement over the test period after correction for the angle of the operation. For some tests in 1998, a laser rangefinder (Laser Atlanta) was used to

Table 1  
Average meteorological and field parameters for PM<sub>10</sub> tests

TestID	Date	Crop	Op	Wind DIR <sup>a</sup>	RH (%)	SR (W m <sup>-2</sup> )	Bulk Ri	Temperature (°C)			Wind speed (m s <sup>-1</sup> )			Soil Moist (%)		
								1 m	2 m	4 m	7.5 m	1 m	2 m		4 m	7.5 m
<i>Case 1: "decline" – all three concentrations decrease with increasing height</i>																
96-103	11/16/96	Cotton	Root cut	139.21*	53.93	583.39	0.60	14.96	14.11	13.84	13.52	1.79	2.12	2.63	2.83	N/A
96-104	11/16/96	Cotton	Root cut	141.97*	46.58	371.90	0.26	16.95	16.12	16.08	15.79	2.08	2.54	3.36	3.67	N/A
96-117	12/02/96	Cotton	Disk	347.01	79.82	0.18	–	7.26	7.35	8.31	8.90	0.90	1.27	2.00	2.16	18.15
97-046	06/24/97	Wheat	Rip	358.26	22.49	893.47	0.19	33.11	31.08	31.28	30.92	3.04	3.44	3.88	4.11	2.32
97-050	06/26/97	Wheat	Rip	317.45	40.45	586.59	0.36	25.21	23.71	24.17	23.94	1.99	2.11	2.40	2.45	2.21
97-051	06/26/97	Wheat	Rip	331.62	36.92	806.50	0.41	27.72	25.62	26.32	26.07	2.01	2.17	2.48	2.49	2.21
98-045R	11/06/98	Cotton	Disk	11.43	63.68	352.44	1.16	11.62	11.29	11.19	11.06	1.71	1.91	1.68	2.07	12.95
98-048	11/06/98	Cotton	Disk	312.12	46.45	381.61	0.45	16.04	14.85	14.63	14.37	2.71	3.08	3.45	3.59	12.95
98-049	11/06/98	Cotton	Disk	312.12	43.67	382.21	0.20	17.21	16.38	16.11	15.80	3.54	3.96	4.44	4.62	11.50
98-050	11/06/98	Cotton	Disk	309.50	41.17	246.51	0.16	18.30	17.65	17.43	17.13	3.69	4.20	4.71	4.93	11.50
<i>Case 3: "uniform" – all three concentrations ~ equal when uncertainties are considered</i>																
96-118	12/04/96	Cotton	Disk	134.18*	72.44	566.62	0.51	11.16	10.14	10.04	9.90	2.52	2.79	3.14	3.24	18.00
96-119	12/04/96	Cotton	Disk	119.96*	59.78	454.29	0.39	13.35	12.43	12.43	12.26	2.48	2.70	3.00	3.13	16.25
96-119M	12/04/96	Cotton	Disk	119.96*	59.78	454.29	0.39	13.35	12.43	12.43	12.26	2.48	2.70	3.00	3.13	16.25
98-046R	11/06/98	Cotton	Disk	338.75	52.26	480.94	1.22	14.33	13.13	13.02	12.79	1.91	2.11	2.19	2.34	12.95
<i>Case 4: "greater than" – &gt; – concentration at 3 m is greater than both 1 and 9 m</i>																
96-120	12/05/96	Cotton	Disk	140.27*	80.04	72.52	–	11.30	10.97	11.44	11.49	4.10	4.65	5.50	5.92	16.65
97-045	06/24/97	Wheat	Disk	324.31	30.72	874.89	0.52	27.86	26.19	26.29	25.96	2.68	2.95	3.34	3.50	2.32
97-048	06/25/97	Wheat	Rip	347.78	23.34	799.46	0.26	34.39	32.37	32.44	32.11	2.60	2.93	3.30	3.43	2.21
98-046M	11/06/98	Cotton	Disk	338.75	52.26	480.94	1.22	14.33	13.13	13.02	12.79	1.91	2.11	2.19	2.34	12.95
98-047	11/06/98	Cotton	Disk	317.60	49.13	483.60	2.50	15.68	14.18	13.96	13.71	1.69	1.93	2.04	2.17	12.95
<i>Case 5: "less than" – &lt; – concentration at 3 m is less than both 1 and 9 m</i>																
96-114	11/27/96	Cotton	Root cut	58.24	91.77	479.03	1.37	10.60	9.93	10.08	10.03	1.23	1.26	1.37	1.43	19.80
96-121	12/05/96	Cotton	List	123.85*	91.49	16.51	–	12.01	11.73	12.09	12.11	1.65	2.02	2.39	2.59	16.65
97-049	06/25/97	Wheat	Rip	358.83	21.62	915.05	0.17	35.49	33.70	33.66	33.35	3.02	3.44	3.91	4.13	2.21
98-045L	11/06/98	Cotton	Disk	11.43	63.68	352.44	1.16	11.62	11.29	11.19	11.06	1.71	1.91	1.68	2.07	12.95
98-046L	11/06/98	Cotton	Disk	338.75	52.26	480.94	1.22	14.33	13.13	13.02	12.79	1.91	2.11	2.19	2.34	12.95

<sup>a</sup>Best wind direction was 360 for all tests except those marked with an asterisk where the best wind direction was 180.

Table 2  
Point sampler test data, emissions model results and test quality ratings<sup>a</sup>

Test ID	Date	Time	Op	$X_{\text{PM}_{10}}$ ( $\mu\text{g m}^{-3}$ )			BCMA ( $\mu\text{g m}^{-3}$ )			Plume height (m)			Emission factor ( $\text{mg m}^{-2}$ )			Test ratings <sup>b</sup>								
				9 m	3 m	1 m	Upwind	9 m	3 m	1 m	Line	Block	Log	Line	Block	Log	Ben	Case	$Q_{\text{up}}$	$Q_{\text{dir}}$	EFU Total (%)			
<i>Case 1: "Avalanche" - all three concentrations decrease with decreasing height</i>																								
96-103	11/16/96	1008-1050	Root cut	176	0	38	97.5	25.3	26.8	55.2	165.1	8.7	10.9	9.3	30	25	23	40	1	A	40.8	+	12	B
									(2.5)	(5.1)	(6.2)	(1.5)	(2.3)	(3.1)	(3.6)	(3.1)	(2.9)				(15.4)	+	8	A
96-104	11/16/96	1349-1358	Root cut	72	0	44.7	58.1	25.3	30.8	63.6	81.3	10.7	11.2	13.6	36	34	31	33	1	A	38.0	+	8	A
									(2.0)	(3.7)	(2.6)	(0.5)	(2.8)	(2.4)	(2.7)	(2.4)	(2.3)				(8.0)	+	9	A
96-117	12/02/96	1655-1815	Disk	25	0	59.3	86.3	11.46	26.2	52.1	83	11.2	14	17.1	91	94	92	65	1	A	13.0	-	9	A
									(2.0)	(2.7)	(3.6)	(5.5)	(2.6)	(3.5)	(8.5)	(7.8)	(7.3)				(21.1)	-	5	A
97-046	06/24/97	1342-1635	Rep	75	55.8	214	284.3	55.91	56.4	250.6	299.9	10	10	11	765	770	623	853	1	A	1.7	+	5	A
									(2.3)	(10.3)	(12.0)	(3.5)	(3.5)	(5.3)	(3.6)	(3.2)	(3.1)				(7.9)	+	5	A
97-050	06/26/97	0820-0950	Rep	233	42.8	216	327.8	48.07	60.8	161.1	205.9	10.7	10.9	13.1	112	110	97	130	1	A	42.5	+	5	A
									(2.5)	(6.8)	(8.2)	(2.6)	(2.2)	(3.7)	(5.3)	(4.3)	(4.3)				(7.8)	+	3	A
97-051	06/26/97	1000-1040	Rep	234	191.5	558	849.9	48.07	253.1	434.8	598.5	14.7	18.1	40.1	776	840	1109	651	1	A	26.4	+	3	A
									(11.0)	(18.0)	(24.1)	(6.5)	(3.7)	(8.2)	(27)	(27)	(31)				(8.6)	+	146	B
98-045R	11/06/98	0820-0921	Disk	23	62	65.6	143.9	23.56	57.5	64.5	113.3	11.1	43.9	20.5	50	117	55	58	1	A	11.4	-	8	B
									(4.88)	(5.0)	(4.7)	(3.0)	(9.1)	(10.5)	(7.9)	(16.9)	(8.9)				(16.5)	-	8	B
98-048	11/06/98	1050-1115	Disk	123	0	174	348.5	23.56	56.8	164.5	342.3	11.1	12.2	15.6	58.9	57	54	64	1	A	47.9	-	8	B
									(3.4)	(7.7)	(10.3)	(3.9)	(2.5)	(3.4)	(4.7)	(4.3)	(3.5)				(10.2)	-	8	B
98-049	11/06/98	1137-1247	Disk	56	0	116	117.9	23.56	12.5	95	96.9	9.0	9.1	8.0	93.5	100.4	73	107	1	A	47.9	+	9	B
									(4.88)	(0.9)	(4.1)	(4.0)	(1.9)	(4.5)	(8.5)	(8.9)	(8.1)				(10.2)	+	9	B
98-050	11/06/98	1404-1450	Disk	34	0	52.7	80.2	17.37	48.9	74.5	114.8	12.2	16.5	22.4	74.2	80	81	74	1	A	90.5	+	8	B
									(4.04)	(2.9)	(5.7)	(7.3)	(3.8)	(5.8)	(6.3)	(5.8)	(5.5)				(16.5)	+	8	B
<i>Case 3: "background" - all three concentrations ~ equal when uncertainties are considered</i>																								
96-118	12/04/96	1041-1151	Disk	60	83.9	68.4	75.6	33.72	50.1	53.6	51.5	-17.8	-18.4	0.01	NC	NC	0.00	9.2	3	A	45.8	-	8	B
									(2.18)	(3.0)	(2.9)	(2.4)	(1.7)	(1.9)	NC	NC	(-0.14)				(8.1)	-	8	B
96-119	12/04/96	1237-1411	Disk	185	63	50.4	48.7	33.72	26.9	37.3	35.4	-2.5	-5.1	0.5	NC	NC	(-0.03)	0.6	3	B	60.0	+	17	B
									(2.18)	(2.2)	(2.1)	(1.9)	(2.8)	(1.7)	NC	NC	(-0.2)				(11.2)	+	17	B
96-119M	12/04/96	1237-1411	Disk	77	56.8	57.1	58.7	33.72	40.4	46.6	43.9	16.5	17.5	26.2	6.6	7.5	6.5	3.6	3	A	60.0	+	5	A
									(2.18)	(2.0)	(2.2)	(2.2)	(42.6)	(1.1)	(18.7)	(8.8)	(0.7)				(11.2)	+	5	A
98-046R	11/06/98	0929-1015	Disk	30	52.1	86.4	78	23.56	62.7	69.3	63.9	42.2	51.9	593.1	164	180	592.4	35	3	A	31.2	-	3	A
									(20.94)	(4.5)	(5.7)	(3.9)	(10.5)	(11.4)	(8.0)	(8.7)	(24.4)				(15.1)	-	3	A
<i>Case 4: "greater than" - &gt; - concentration at 3 m is greater than both 1 and 9 m</i>																								
96-120	12/05/96	1047-1200	Disk	70	45.8	39.8	36.2	30.64	29.2	32.4	24.5	4.9	6.3	3.9	-5.4	-0.5	-2.9	-5.6	4	D	36.7	-	240	E
									(4.32)	(1.7)	(2.1)	(1.6)	(0.9)	(10.0)	(-1.1)	(-1.2)	(-1.1)				(5.1)	-	240	E
97-045	06/24/97	0956-1137	Disk	87	82.2	54	380.6	53.91	92.5	483.1	325.9	9.4	10.7	7.5	352	430	271	230	4	A	35.7	+	17	B
									(20.94)	(3.7)	(18.5)	(12.4)	(9.1)	(4.0)	(10.2)	(63.0)	(72.6)	(62.6)			(29.6)	+	17	B
97-048	06/25/97	1231-1410	Rep	128	100.1	289	348.7	67	101.1	241.8	221.6	9.6	9.5	10.8	306	331	268	299	4	A	12.2	+	5	A
									(15.01)	(4.2)	(10.2)	(8.9)	(6.0)	(2.1)	(9.2)	(17.1)	(14.9)				(7.0)	+	5	A
98-046M	11/06/98	0929-1015	Disk	63	0	36.5	48	23.56	29.1	58.2	40	8.5	11.3	5.6	21.5	28	18	14	4	A	21.2	-	10	A
									(4.88)	(2.0)	(2.7)	(1.8)	(15.2)	(2.4)	(13.4)	(2.8)	(3.9)				(15.1)	-	10	A
98-047	11/06/98	1015-1040	Disk	98	0	0	0	23.56	56.5	78.5	47.6	5.0	20.5	1.6	30	32.4	-2.8	7.6	4	A	42.4	+	9	A
									(4.88)	(5.1)	(5.8)	(3.1)	(18.9)	(4.3)	(7.4)	(18.0)	(2.9)				(21.0)	+	9	A
<i>Case 5: "less than" - &lt; - concentration at 3 m is less than both 1 and 9 m</i>																								
96-114	11/27/96	0855-1100	Root cut	45	89	72.1	97.7	27.78	55.5	52.4	63.7	14.8	-4	110.7	18.5	NC	55	15	5	A	98.3	+	76	D
									(2.25)	(2.9)	(3.2)	(3.0)	(5.3)	(18.1)	(14.1)	NC	(41.5)				(44.2)	+	76	D
96-121	12/05/96	1540-1637	Lat	30	45.3	30.6	42.4	30.64	39.3	29.1	32.7	2.5	3.9	2.0	-0.3	0.1	-0.7	1.1	5	C	56.1	+	167	E
									(4.32)	(2.3)	(2.1)	(1.9)	(15.6)	(0.6)	(6.1)	(-0.5)	(0.6)				(9.1)	+	167	E
97-049	06/25/97	1411-1551	Rep	68	226.1	218	477.7	67	239	167.7	298.3	7.5	-5.5	10.6	577	NC	502	696	5	A	1.2	-	6	A
									(15.01)	(10.3)	(6.9)	(14.9)	(17.8)	(1.2)	(12.1)	(36.1)	(27.8)				(11.8)	-	6	A
98-045L	11/06/98	0820-0921	Disk	26	0	0	104.3	23.56	46	43.7	79.2	9.6	-9.5	14.8	24.4	NC	27	36	5	A	11.4	-	148	B
									(4.88)	(4.1)	(2.9)	(3.3)	(16.2)	(12.3)	(10.9)	(41.2)	(39.3)				(16.5)	-	148	B
98-046L	11/06/98	0929-1015	Disk	30	0	0	142.6	44.88	94.2	47.4	131.8	5.8	-0.6	6.7	117	NC	61	89	5	A	21.2	-	18	B
									(4.88)	(5.8)	(5.3)	(6.3)	(39.7)	(0.1)	(14.8)	(20.6)	(10.5)				(15.1)	-	18	B

<sup>a</sup>Values in parentheses are uncertainties; NC = not calculated (unreasonable value).

<sup>b</sup> $Q_{\text{up}}$  = upwind qualifier;  $Q_{\text{dir}}$  = cases 5 linear fit qualifier;  $Q_{\text{sd}}$  = average wind direction (SD) used to evaluate wind direction quality; EFU = relative emission factor uncertainty = (calculated uncertainty/emission factor)\*100. Bold  $Q_{\text{sd}}$  values highlight wind direction quality criteria violation and reduced test confidence.

independently observe the location of the tractor during the lidar scans. The time, distance and bearing to the tractor were recorded every 30 s to 1 min by an observer located along the edge of the field (see Holmén et al., 2000, Fig. 1).

### 2.5. Lidar

Lidar data collected concurrently with the point sampler tests were used to understand plume behavior for plumes that exceeded the 10 m tower height, and to confirm that test-averaged plumes sampled at one crosswind location on the field were representative of the operation at all crosswind locations (Holmén et al., 2000).

### 2.6. Emission factor calculations

PM<sub>10</sub> emission factors for agricultural operations such as tilling and harvesting are logically quantified on the basis of the area of land worked because the source being quantified is the field where the operation takes place, not the moving tractor/implement. Vertical profiles of wind speed and PM<sub>10</sub> concentration were used to calculate emission factors for the land preparation operations. As discussed in the companion paper, because gravimetric mass was consistently well correlated with the “reconstructed mass” composite variable (RCMA) and the elemental analyses were sufficiently more sensitive than the gravimetric measurements (Holmén et al., 2000), all emission factors were calculated from PM<sub>10</sub> RCMA concentrations. The composite variable RCMA was calculated using a relationship based on the ratios of the common crustal elements (Al, Si, Ca, Ti, Fe), sulfur, light absorbing elemental carbon, hydrogen and nonsoil potassium in an average aerosol (see Holmén et al., 2000, Eq. (1) and references therein). When the RCMA mass concentration was below the MDL at any of the three sampling heights, emission factors were not calculated for that test.

Each downwind PM<sub>10</sub> profile was classified according to its shape into one of five types (see Table 2, Holmén et al., 2000):

- Case 1 – decreasing PM<sub>10</sub> with height (“decline”);
- Case 2 – increasing PM<sub>10</sub> with height (“incline”);
- Case 3 – uniform PM<sub>10</sub> with height (“uniform”);
- Case 4 – 3 m concentration highest (“greater than”);
- Case 5 – 3 m concentration lowest (“less than”).

Three different methods – the line, block and logarithmic profile models – were used to fit the PM<sub>10</sub> RCMA vertical concentration profiles as described previously (Holmén et al., 2000). A fourth model, the box model, was used to describe the PM<sub>10</sub> flux in cases of uniform downwind vertical concentration profiles. The choice of the appropriate model for each downwind concentration

profile type was based on analysis of simultaneous lidar and PM<sub>10</sub> vertical profile data (Holmén et al., 2000).

For each model, a horizontal PM<sub>10</sub> flux was calculated as the product of the net (i.e., downwind – upwind) PM<sub>10</sub> concentration (mg m<sup>-3</sup>),  $C(h)$ , and the average horizontal wind speed (m s<sup>-1</sup>),  $U(h)$ , at 10 equally spaced height intervals (m),  $dh$ , between the roughness length,  $z_0$ , and the top of the plume,  $H$ . The roughness length was determined by fitting the wind speed data to a logarithmic profile. The plume height was defined by the intersection of the downwind profiles with the average upwind concentration (Holmén et al., 2000). The flux was integrated over the height of the plume using Simpson’s Rule, and normalized by the time of the test,  $t$ , the upwind width of soil worked during the test period,  $w$ , and the angle between the measured wind direction and the direction perpendicular to the field edge,  $\theta$ , to compute the PM<sub>10</sub> emission factor (mg m<sup>-2</sup>):

$$E = \int_{z_0}^H \frac{U(h)C(h)t \cos \theta}{w} dh. \quad (1)$$

Uncertainties in the calculated emission factors were estimated using error propagation techniques (Coleman and Steele, 1989) for the line, block and logarithmic fit models. The PM<sub>10</sub> RCMA measurement uncertainties and the test period wind speed standard deviation at each measurement height were used to estimate the uncertainty in the horizontal flux at each of the 10 model heights. Details regarding the uncertainty calculations are in the appendix.

### 2.7. Emission factor confidence rating

Each calculated emission factor was assigned an overall test rating based on five qualifiers that attempt to assess the ability of the emission factor estimate to quantify the actual nonpoint source emissions. The overall test ratings ranged from A to E and were designed to account for a decreased reliability in the computed emission factor when: (1) the upwind concentrations were equal to or exceeded the downwind concentrations at any height ( $Q_{up}$ ); (2) the wind direction deviated from ideal ( $Q_{wd}$ ); (3) the test suffered from multiple passes due to edge effects ( $Q_{edge}$ ); (4) the fit to Case 5 profiles was poor ( $Q_{fit}$ ); or (5) emission factor relative uncertainty (EFU) was high. Each of these qualifiers is described in Table 3 and was based on observations made for all tests (see Section 3.2).

## 3. Results and discussion

### 3.1. Best-fit emission factors for individual profile types

Comparison of the average plume heights and vertical profile shapes determined by lidar to the profiles

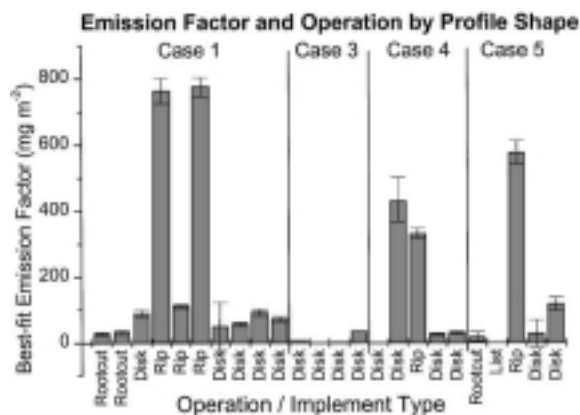


Fig. 1. Best-fit emission factors did not vary directly with type of operation. The tests are in order by profile shape class as tabulated in Table 2. Error bars for Case 1, 4 and 5 profile types represent two times the best-fit emission factor uncertainties reported in Table 2 (shaded values).

measured with the point samplers on 6 November 1998 led to assignment of particular best-fit models to the  $PM_{10}$  profiles for each of the four observed profile shape categories (Holmén et al., 2000). Although there were some tests that were difficult to categorize, overall the model selected for each category tended to have the lowest calculated uncertainties for both plume height and emission factor.

The calculated emission factors (and uncertainties) for all models are shown in Table 2 for comparison; the shaded values represent the best-fit model plume height and emission factor values for each profile type. As the test results indicate, there was general agreement in the emission factors computed by the different functional fits to the profiles for an individual test when all four models could be calculated (Cases 1, 4 and 5). Thus, the magnitude of the computed emission factors was not biased by the selection of the best-fit model.

The five highest best-fit emission factors ( $330$ – $776 \text{ mg m}^{-2}$ ) were seen for Case 1, 4 and 5 profiles collected on hot dry summer days for ripping and disking (Fig. 1, Tables 1 and 2). Similar field conditions, however, also resulted in a much lower ripping emission factor of  $112 \text{ mg m}^{-2}$  (test 97–050), thus complicating interpretation between different tests. When the downwind concentrations were uniform with height (Case 3) emissions were generally low but downwind  $PM_{10}$  values were significantly higher than upwind concentrations. The low emission factors were not due to the use of the box model, however, because the box model emission factors showed fairly good agreement (within a factor of 2) with the emission factors calculated by the other models for the other profile types (Table 2). Interestingly, the lowest 5 emission factors were measured in winter when temper-

atures were cooler and soil moisture was relatively high (Tables 1 and 2), suggesting that environmental conditions greatly influence emission rates.

### 3.2. Test quality ratings

The emission factors in Table 2 represent a wide range of values, but were collected under disparate sampling conditions. In order to compare the test results and identify the key factors controlling emissions, an individual measurement confidence must be assigned to each test. Five qualifying factors identified for this purpose are defined in Table 3 and justified below.

#### 3.2.1. Upwind qualifier, $Q_{up}$

Individual upwind  $PM_{10}$  concentrations were compared directly to the corresponding downwind concentrations at the same height for each test profile in order to qualify the calculated emission factor based on the relative upwind–downwind concentration values. The rationale for  $Q_{up}$  was that profiles where upwind and downwind concentrations were similar indicate either that: (1) the downwind measurements were not significantly different from background and therefore the emissions from the operation were small and more difficult to accurately quantify, or (2) the upwind profile was influenced by another source, but not so obviously as to warrant omission of the test. The latter scenario would reduce the confidence that the computed emission factor accurately describes the source of interest.

Tests were not omitted on the basis of having individual upwind concentrations higher than those at downwind in order to prevent biasing the emission factor estimates to the high end. For example, there were test conditions, especially in late winter, when soil moisture was high, emissions were significantly lower than at other times, and upwind concentrations at a *single* height would be close to or greater than the measured downwind value. Such a test would be qualified with a “B” rating on the basis of the upwind qualifier scale outlined in Table 3. A special case occurred, however, if the single height where the upwind and downwind concentrations were equal was the highest sampling height. Because this occurrence indicates that the highest sampler was close to the top of the plume, the two special case tests (96–103; 98–049) received an “A” value for  $Q_{up}$ , rather than a “B”. The fact that the modeled plume heights for these tests were  $\sim 9 \text{ m}$  adds credibility to the definition of this special case.

Note that all but three tests had  $Q_{up}$  ratings of “A” indicating that most of the downwind  $PM_{10}$  concentrations were significantly above background values. Of the three tests with poor  $Q_{up}$  ratings, two tests (96–120, 96–121) were collected under relatively unstable atmospheric conditions as indicated by negative bulk Richardson numbers (Table 1). Test 96–120 (Case 4) was particularly

Table 3  
Emission factor confidence ratings summary

Qualifier	Criteria/rationale	Scale
1. $Q_{up}$ , upwind conc	Number of upwind $PM_{10}$ RCMA concentrations that exceed downwind concentration at the same height  <i>Special case:</i> If only the 9 m downwind < upwind, test rating = “A” under the assumption that highest sample was above plume	A = 0 exceed, or special case B = 1 exceeds C = 2 exceeds D = 3 exceeds
2. $Q_{wd}$ , wind direction	(a) Test wind direction $SD > 25^\circ$  (b) (test wind direction)-(best wind direction) $> 45^\circ$  Note: best wind direction = $90^\circ$ to downwind edge of sampling array	Reduce letter rating (assigned on the basis of $Q_{up}$ ) by 1 scale (i.e., A $\rightarrow$ B, B $\rightarrow$ C) if <i>either</i> (a) or (b) is true 2 scales (i.e., A $\rightarrow$ C, B $\rightarrow$ D) if <i>both</i> (a) and (b) are true
3. $Q_{edge}$ , edge effects	$X_{loc} \sim 0$ any time during test If test included passes at the field edge immediately upwind of the tower, test deserved lower quality rating (negative $Q_{edge}$ )	- = edge effects present + = no edge effects
4. $Q_{fit}$ , Case 5 fit	Assesses how well linear model described fit $[PM]_{9m} - [PM]_{3m} > \frac{1}{2}[PM]_{1m} - [PM]_{9m}$ $[PM]_{9m} - [PM]_{3m} < \frac{1}{2}[PM]_{1m} - [PM]_{9m}$	- = poor linear fit + = better linear fit
5. EFU, relative emission factor uncertainty	Accounts for unidentified qualifying factors $\left[ \frac{\text{emission factor uncertainty}}{\text{emission factor}} \right] > 20\%$	Reduce letter rating by one scale (i.e., A $\rightarrow$ B, B $\rightarrow$ C) if true

difficult to model because all the downwind concentrations were similar to upwind values. Consequently, to indicate reduced confidence in the emission factor computed for this test it received a “D”  $Q_{up}$  rating.

### 3.2.2. Criteria for wind direction, $Q_{wd}$

Confidence in the calculated emission factor was also reduced when: (1) the wind direction was highly variable over the test period, or (2) the mean wind direction was very different from the ideal wind direction (defined as the direction perpendicular to the downwind edge of the *sampling array*). Both of these conditions would reduce the ability of the point samplers to capture the entire plume in a reproducible manner. An emission factor was assigned a lower confidence rating when the standard deviation in the mean wind direction over the test period was greater than  $\pm 25^\circ$  or if the wind direction deviated from the ideal wind direction by more than  $\pm 45^\circ$  (Table 3). When either of these conditions occurred, the overall test rating was reduced by one level (i.e., an “A” rating would decrease to a “B” level), and, if both conditions occurred, the overall test rating was reduced by

two levels (i.e., “A” to “C”). Nine tests were collected when wind direction data met one or both of the above criteria; these tests are indicated by the bold  $Q_{wd}$  values in Table 2.

### 3.2.3. Qualifier for edge effects, $Q_{edge}$

Because tractor turning near towers located at the edge of the fields was shown to affect the  $PM_{10}$  measurements (Holmén et al., 2000), individual tests were assigned a negative  $Q_{edge}$  rating (Tables 2 and 3) if the PM profile was collected near the downwind edge of an operation that was conducted at an angle such that tractor turning could have adversely affected the test. A (-)  $Q_{edge}$  rating indicated a reduced confidence that the emission factor was representative of the operation. The  $Q_{edge}$  rating was used to modify the  $Q_{up}$  rating only if  $Q_{edge}$  was negative (e.g., an “A” test based on  $Q_{up}$  was demoted to an “A -” if edge effects were suspected during sample collection). Ten tests, encompassing all of the observed profile shapes, were identified as influenced by edge effects (Table 2).

Emission factors calculated from towers affected by edge effects were expected to be significantly different from each other; this was seen for the two adjacent profiles collected during a single test (98-046) that was impacted by edge effects: the L tower emission factor ( $117 \pm 21 \text{ mg m}^{-2}$ ) was three times higher than that for the R tower ( $35 \text{ mg m}^{-2}$ ) (Table 2). The large variation in emission factors calculated from measurements taken within 6 m of one another illustrates the difficulty in interpreting data impacted by these field edge effects.

### 3.2.4. Qualifier for case 5 fit, $Q_{\text{fit}}$

Each profile exhibiting a Case 5 shape (“less than”) was assigned a qualifier for the goodness-of-fit of the data to the linear model ( $Q_{\text{fit}}$ ). The quality of the line fit to Case 5 profiles depended on the extent to which the  $\text{PM}_{10}$  concentration measured at the 3 m height was less than that which would be predicted by a linear fit to the measured 1 and 9 m concentrations. The  $Q_{\text{fit}}$  qualifier (Table 3) depended on the difference in measured RCMA concentrations: if the 9 and 3 m concentrations were more similar than the 1 and 9 m concentrations, then the line fit was considered to give reasonable emission estimates for Case 5 profiles. Use of the linear model was more problematic when the 1 and 9 m concentrations were similar because then the linear fit essentially ignored either the 1 or 9 m concentration and resulted in plume heights that were unrealistically low (e.g., 98-046L (9 m not fit) and 96-121 (1 m not fit)). The low plume heights resulted in correspondingly low emission factors in these cases and therefore these tests received lower confidence ratings because it was suspected that the difficulty of fitting the three-point  $\text{PM}_{10}$  profile data was biasing the emission factor low. For test 98-046L, lidar vertical scan data indicated a plume height of approximately 45 m (see Holmén et al., 2000, Fig. 3) confirming that the modeled plume height was unreasonably low.

### 3.2.5. Relative emission factor uncertainty, EFU

Relative emission factor uncertainties (EFU) were computed as the ratio of the propagated emission factor uncertainty (see the appendix) divided by the emission factor, expressed as a percentage. The emission factor errors were expected to increase when the measured data did not fit the appropriate model and when external factors such as edge effects and highly variable meteorological conditions occurred during a test period. This was generally the case for the tests summarized in Table 2, with the notable exception of tests 98-045R and 98-045L, which both had very high EFU values ( $\sim 145\%$ ), but had high quality ratings (i.e., high confidence) for the other quality factors. The linear fits to both of these tests were not significantly poor compared to other tests, so the high relative uncertainties probably indicate that some other as yet unidentified factor affected these profiles to explain the low confidence in the computed emission

factors. For test 98-045R, the high EFU was probably due to the fact that the 3 and 9 m concentrations were nearly equal; this tended to reduce the ability of all the models to fit the measured profile (Table 2).

The five tests where the uncertainty in the computed emission factor exceeded 20% of the emission factor value had their test quality rating reduced by one level. EFU was used as a final factor in quality rating because there were tests that had high EFU values but none of the other identified confidence criteria indicated a problem with the test. This suggests that there remain other unidentified qualifying factors that affect confidence in the modeled emission factors.

### 3.3. Maximum sampling distance

The question of whether or not there was a maximum distance between the tractor and samplers beyond which the profile technique was incapable of reliably quantifying an emission factor was examined. If the data collected by point samplers at farther downwind distances from the tractor had higher EFU values, the possibility of a limited reliable sampling range could be inferred. This did not appear to be the case because there was no systematic relationship between the distance from the tractor and either the relative emission factor error (Fig. 2) or the error on the plume height. The highest EFU values occurred at intermediate average upwind distances between 30 and 100 m from the towers and predominately for Case 5 test profiles.

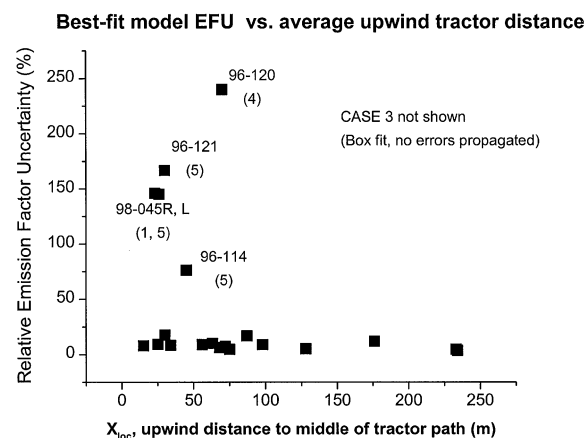


Fig. 2. Relative error in calculated emission factor (EFU) as a function of the average tractor-to-sampler distance over the test period. Note that for most test profiles, the relative error was less than 50%. The tests with high relative errors were usually Case 5 profiles. Case 4 profile 96-120, had a negative emission factor close to zero ( $-0.5 \text{ mg m}^{-2}$ ) with a high error ( $-1.2$ ) and was difficult to fit because two of its three downwind concentrations were below the average upwind value.

While it is likely that some physical limits exist regarding the proximity of the samplers to the point source in order to obtain interpretable relationships between field conditions and plume characteristics such as height, the land preparation data (Table 2, Fig. 2) suggest that downwind distances up to 250 m could be reliably sampled using the vertical profiling technique with a relative error of less than 20% as long as the profile shape was not Case 5. However, while relative errors were low, there is no way to know how accurate the reported emission factor values are. The high EFU profiles resulted from different factors, including: (a) downwind concentration values close to background (96-120, 96-121), (b) highly variable or non-ideal wind direction (96-114, 96-121), (c) edge effects (98-045R, L) and (d) highly exaggerated Case 5 profile shapes (96-121). This latter effect is probably due, as the lidar vertical profiles showed (Holmén et al., 2000), to the limited sampling height of the towers that capture only part of the entire vertical extent of the plume under some test conditions.

#### 3.4. Replicate emission factors

The mobile tower could be positioned well inside the field boundaries and easily repositioned to follow the operation up the field and achieve similar upwind distances to the tractor ( $X_{loc}$ ) between tests. Such “duplicate” profiles resulted in similar emission factor estimates when the averaged activity of the tractor was the same relative to each sampling location. This is evidenced by the agreement between the emission factors calculated from mobile tower profiles collected in tests 98-049 ( $93.5 \pm 8.5 \text{ mg m}^{-2}$ ) and 98-050 ( $74.2 \pm 6.3 \text{ mg m}^{-2}$ ) at slightly different crosswind locations (585 and 594 m, respectively) but similar distances downwind of the tractor (56 and 34 m, respectively) and well away from the downwind field edge. The repeatability in these tests was enhanced compared to those reported earlier (see Table 3, Holmén et al., 2000) due to the more consistent activity of the source when working the central areas of the field, where the absence of tractor turning eliminated edge effects. The east–west implement angle (i.e., perpendicular to field crosswind edges) also produced more consistent results for these tests compared to 98-045 to 98-047, despite the fact that the tractor still worked the field in spiral sections.

Whether the emission factors measured at the edges of the field should be weighted similarly to the values obtained by monitoring the more repeatable and representative tractor activities in the midpoints of the field requires further investigation. Of concern is biasing the average emission factor high because of the presence of the stationary sampling array (at the field edge) that, despite efforts to have minimal impact on the agricultural operation, inevitably did have some effect on the tractor's path and therefore on emissions estimates due to the multipass “edge” phenomenon.

#### 3.5. Factors influencing plume height and emissions

Emission factor comparisons among these nonpoint sources must take into account differences in soil conditions, tractor/implement speed, sampler location relative to the tractor/implement and meteorological conditions between sampling tests. All of these factors can influence the measured  $\text{PM}_{10}$  concentrations, the shape of the vertical profile, and therefore, the calculated emission factor. Some of the relationships expected based on atmospheric dispersion theory include higher plume heights when sampling was conducted farther from the tractor or when the vertical temperature profile indicated convective conditions. Lower plumes were expected when wind speeds were high and low emissions were expected when the soil was relatively moist. The land preparation data (lidar plus point measurements) support most of these expectations, as outlined below, but questions arise as to how well the point samplers alone are capable of identifying the expected relationships due to their limited height range and the long averaging times required to collect measurable mass.

##### 3.5.1. Plume height

The relationship between maximum plume height and upwind tractor distance determined from the lidar and laser rangefinder data (Fig. 3a) indicates a trend of higher plume heights for scans collected when the tractor was farther upwind of the lidar scan plane, as expected for a plume dispersing from a ground source. The correlation was not very strong, probably because no correction was made for the time lag between emission of the plume at the higher upwind coordinates and the time of measurement of the plume at the lidar scan location. A stronger correlation would take the instantaneous wind speeds into account, but this analysis is beyond the scope of the present work.

The relationship between the plume heights estimated from the point sampler profiles and upwind distance was not as strong as that indicated by the lidar scan data (Fig. 3b). This is probably the result of: (1) the difficulty of assigning reliable upwind distances to data collected before the tractor location was monitored closely and (2) meteorological variability over the long point sampler test durations. Better definition of this relationship may require determination of the minimum and maximum upwind distances of the tractor during the tests relative to the location of each profile tower. The angle of the implement relative to the point sampler array must also be measured with greater accuracy in the future to enable calculation of the limits of the test operation. Improved estimates of plume height will also be possible if another sampling height is added to the vertical profiles because this will improve the interpretation and analysis of plume shape and best model fit.

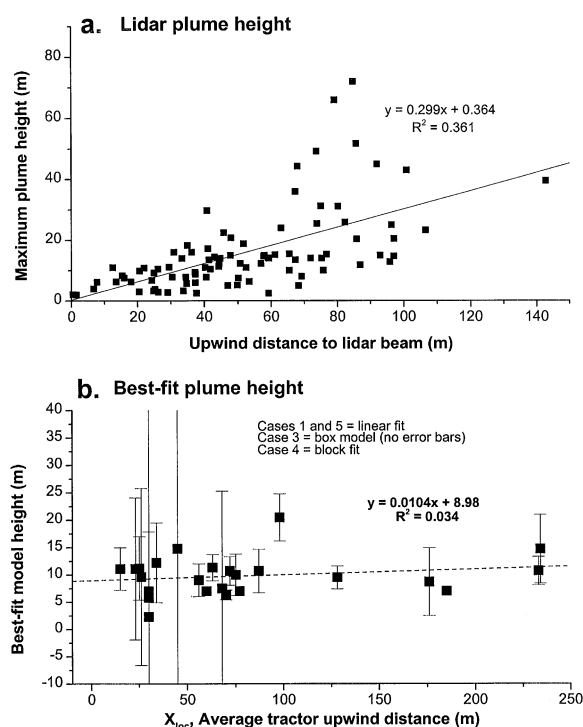


Fig. 3. (a) Lidar maximum plume height measured from individual lidar 2D scans versus upwind tractor distance determined by laser rangefinder for PM test 98-045; (b) calculated best-fit model plume height did not correlate well with test-averaged downwind distance for samples collected using point samplers. The poor correlation most likely reflects the difficulty of back-calculating average tractor upwind distances for tests conducted in 1996 and 1997 before careful measurements of relative tractor location were recorded.

### 3.5.2. Environmental conditions and emission factors

The calculated emission factors for land preparation activities (Table 2): (a) showed no correlation with wind speed over the range of wind speeds tested ( $1\text{--}5.5\text{ m s}^{-1}$ ); (b) increased with decreasing relative humidity; (c) were generally lower when soil moisture was higher and (d) generally increased with increasing vertical temperature differential (Fig. 4).

These dependencies of emissions from land preparation activities on environmental conditions such as temperature and relative humidity have been documented before (Clausnitzer and Singer, 1996, 1997; Kantamaneni et al., 1996) and illustrate the necessity of incorporating local meteorological conditions into the development of predictive  $\text{PM}_{10}$  emission factor models. This calls for the development of an empirically derived functional form of the emission or the activity factors used to calculate  $\text{PM}_{10}$  inventories. The two distinct populations of emission factors below and above 40% relative humidity (Fig. 4b) and below and above 10% soil moisture (Fig. 4c)

suggest that relative humidity and soil moisture are important parameters requiring further investigation. As stated above, relationships between emission factors and soil properties other than moisture were not examined because soil texture data were not available for any of the 1998 tests examined here.

The range of soil types for the 24 tests that had valid PM data is too narrow for us to draw any conclusions with respect to soil properties other than moisture content. A forthcoming paper from our laboratory will examine how laboratory resuspension and soil texture experiments can be used for emissions estimation. The main focus of the present paper is on developing a method for analyzing field data for emission factors that quantifies the measurement uncertainty. Soil texture should not be a source of measurement uncertainty; rather it is more likely that soil texture will be a key environmental variable, like relative humidity or temperature differential, that can be correlated with the measured emission factor.

### 3.5.3. Implement characteristics and emissions

Differences in  $\text{PM}_{10}$  emission factors from two operations, disking and ripping, for which a representative number of repeated measurements were made, were used to examine the importance of implement type. The average emission factor for ripping operations,  $507 \pm 292\text{ mg m}^{-2}$ , was significantly larger than that for disking,  $91.2 \pm 104\text{ mg m}^{-2}$ . However, direct comparison of implement-average emissions is not reliable because differences in environmental conditions (e.g., relative humidity and wind direction variability) between individual tests appear to have a larger impact on measured emissions than does implement type. Variability in measured emissions due to environmental factors is highlighted by three Case 1 ripping tests collected on 24–26 June 1997 (see Table 2). The emission factors for two tests (97-046,  $765 \pm 36\text{ mg m}^{-2}$  and 97-051,  $776 \pm 27\text{ mg m}^{-2}$ ) were similar and significantly higher than disking tests conducted under similar relative humidity conditions (98-050,  $74.2 \pm 6.3\text{ mg m}^{-2}$ ) but the emissions from the third ripping test, 97-050,  $112 \pm 5.3\text{ mg m}^{-2}$ , were much lower and similar to emissions measured for disking (see Fig. 1). The much higher deviation of wind direction from the ideal direction, the higher relative humidity and lower solar radiation during this third ripping test likely explain these results and highlights the complexity of comparing emission tests with different implements unless all other environmental factors are held constant.

Emission factors measured for different crops such as cotton and wheat that are harvested at different times of the year are also difficult to compare because emissions-related environmental conditions vary significantly with season. For example, wheat land preparation is conducted in summer when conditions are hot and dry and soil moisture is quite low, but conditions for cotton land

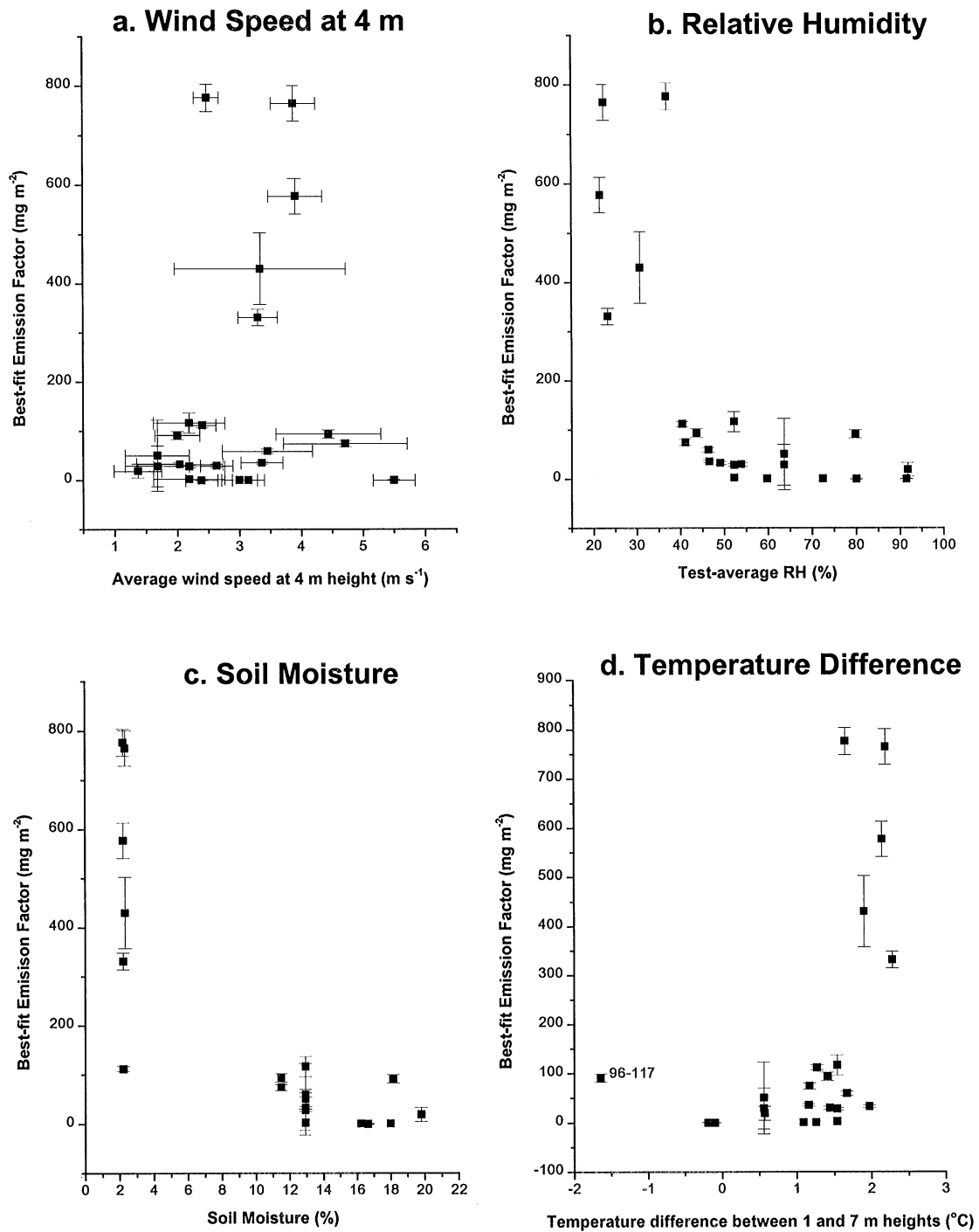


Fig. 4. Best-fit emission factors as a function of meteorological conditions for all tests in Table 2. (a) wind speed ( $\text{m s}^{-1}$ ) at 4 m height, (b) relative humidity (%), (c) soil moisture (%), (d) air temperature gradient calculated as the temperature difference between 1 and 7.5 m heights ( $^{\circ}\text{C}$ ). Error bars on wind speed are based on two times the average standard deviation of the wind speeds recorded every 1 or 5 min over the test duration. Emission factor error bars are 2 times the emission factor uncertainties reported in Table 2.

preparation, in the late fall, are cold and moist. Despite the fact that land preparation operations on these two crops use similar implements, measured emissions were very different due to seasonal effects. Thus, it seems prudent to develop empirical emission factor models that take these seasonal environmental variables into account. For example, correcting AP-42 emission factors for monthly variations in soil moisture will result in more realistic emissions estimates than assuming no relationship between emissions and soil moisture (ARB, 1997).

#### 3.5.4. Comparison to AP-42

Agricultural land preparation emission factors are generally estimated using EPA's guidance document, AP-42, based on the soil's silt content and a default silt content of 18%. For California soils and PM<sub>10</sub> emissions, the default emission factor is therefore 4.02 lb acre<sup>-1</sup> (ARB, 1997). The emission factors measured in this field study range from zero (96-120 and 96-121) to 6.9 lb acre<sup>-1</sup> (97-051) a range that encompasses the default AP-42 value. Despite the apparent agreement, it is important to note that a very high (44%) soil silt content (< 75 µm, dry sieve) would be required to predict the highest emission factor measured in this study using the AP-42 methodology and that AP-42 would over predict emissions for the majority of the tests examined here (mean = 1.4 lb acre<sup>-1</sup>, SD = 2.1). Clearly, AP-42 is not accounting for the myriad of environmental factors that affect emissions. A more robust estimation procedure should account for the seasonal factors discussed above.

## 4. Conclusions and future work

Quality ratings for the individual emission factors calculated from each PM<sub>10</sub> profile demonstrated the sensitivity of the measurements to the following factors, listed in order of decreasing importance: (1) whether downwind concentrations exceeded upwind concentrations; (2) the variability in wind direction over the test period; (3) whether or not the profile was affected by tractor turning effects at the edge of the field; (4) for Case 5 profiles, how well the linear model fit the measured profile and (5) other unidentified factors that resulted in high computed emission factor relative uncertainty (EFU) values.

The resolving power of the vertical profile method was clearly reduced when the emissions were small and measured downwind PM<sub>10</sub> concentrations were close to background concentrations. Continuing efforts to calibrate the lidar instrument to quantify PM<sub>10</sub> using this much more sensitive and highly resolved tool will improve the quality of emissions estimates for less dusty conditions. Because of the need to use RCMA to improve the sensitivity of the method in the reported analyses, emission factors presented here are conservative estimates of the total PM<sub>10</sub> emissions by mass.

Because emission factors computed from different models showed good agreement for individual tests where multiple models could be reasonably applied, the methods developed here are independent of model choice and can be used to identify the key variables controlling emissions for a wide range of conditions. For the 24 valid tests reported here, environmental conditions such as soil moisture and relative humidity had a greater influence on PM<sub>10</sub> emissions than crop, implement type or choice of vertical profile model. Emission factors were inversely proportional to relative humidity and soil moisture and positively correlated with the ground-level temperature gradient. These environmental variables should be examined in more detail to develop predictive PM<sub>10</sub> emission factor expressions based on a combination of environmental conditions and agricultural operation parameters. Soil texture properties were not examined here but should also be the focus of future investigations.

The results of the field tests presented here represent a large collection of PM<sub>10</sub> emissions measurements from tillage operations. Variability in measured emissions was large (0–800 mg m<sup>-2</sup>; mean = 152, SD = 240, median = 43) and most likely due to the wide range of environmental conditions under which samples were collected. Data reliability will be enhanced by the addition of a fourth sampling height to the profile, avoiding field edge effects, and restricting sampling to periods of reliable and steady wind direction.

One focus of future efforts should be to collect more replicate PM<sub>10</sub> samples from a single operation, so environmental effects are held constant and the inherent sampling variability can be determined. This was attempted in tests 98-045 and 98-046, but was not successful because different spatial relationships between the towers and the operation resulted in different profile types and calculated emission factors that varied by a factor of 2–4. Additional field tests should also be conducted on a wider range of soil types for the same types of operations studied here in order to elucidate the key relationship between soil properties and emissions.

## Acknowledgements

The authors thank Robert Matsumura, Christopher Tsubamoto and Omar Carvacho for data collection and analysis assistance. Support for this work was from USDA Special Research Grants Program grants 94-33825-0383 and 98-38825-6063 and NSF POWRE grant 99-73434.

## Appendix A. Emission factor uncertainty calculation

The error on the computed horizontal flux at height  $i$ , SFh <sub>$i$</sub> , depends on: (1)  $F_{hi}$  – the calculated horizontal flux

at model height  $i$ ; (2)  $S_{ci}$  – the uncertainty in measured  $PM_{10}$  concentration at the measurement height closest to height  $i$ ; (3)  $S_{ui}$  – the measured standard deviation on wind speed at the height closest to  $i$ ; (4) the modeled concentration at height  $i$ ,  $C_i$  and (5) the modeled wind speed at height  $i$ ,  $U_i$ :

$$SFh_i = F_{hi} \left[ \left( \frac{S_{ci}}{C_i} \right)^2 + \left( \frac{S_{ui}}{U_i} \right)^2 \right]^{0.5}. \quad (A.1)$$

In Eq. (A.1) for each modeled height value of  $i$  greater than 1.5 m, the measured analytical uncertainties for the measurement height closest to, but less than  $i$  were assigned to the variables  $S_{ci}$  and  $S_{ui}$ .

The  $F_{hi}$  values at each of the 10 model heights were summed to calculate the total horizontal flux, FH. Therefore, the error on the total horizontal flux was calculated as

$$S_{FH} = [(SFh_1)^2 + (SFh_2)^2 + (SFh_3)^2 + \dots + (SFh_9)^2 + (SFh_{10})^2]^{0.5}. \quad (A.2)$$

Finally, because the emission factor,  $E$ , is a product of the total horizontal flux, the cosine of wind direction and the duration and operation distance of the test (see Eq. (1)), the overall uncertainty in the emission factor,  $S_E$ , can be expressed as

$$S_E = E \left[ \left( \frac{S_{FH}}{FH} \right)^2 + \left( \frac{S_\theta}{\theta} \right)^2 + \left( \frac{S_t}{t} \right)^2 + \left( \frac{S_w}{w} \right)^2 \right]^{0.5}. \quad (A.3)$$

Note that height is not explicitly represented in Eq. (A.3) because it is imbedded in the horizontal flux term that was summed over the 10 model heights. Errors on the duration of the test ( $t$ ) and the operation distance ( $w$ ) were assumed to be small and were ignored. This leaves the following expanded form of the emission factor uncertainty:

$$S_E = E \sqrt{\frac{[(SFh_1)^2 + \dots + (SFh_{10})^2]}{FH^2} + \left( \frac{S_\theta}{\theta} \right)^2}. \quad (A.4)$$

The reported uncertainties (Table 2) do not take into account the analytical uncertainties in individual upwind RCMA concentration measurements or whether the downwind concentrations were close to the upwind values. The latter consideration was evaluated for each test using an upwind qualifier as described in the text.

## References

- ARB, 1997. Emission Inventory Procedural Manual Volume III: Methods for Assessing Area Source Emissions. California Environmental Protection Agency Air Resources Board, Sacramento, CA.
- Arroues, K.D., Anderson, C.H.J., 1986. Soil Survey of Kings County California. Soil Conservation Service, USDA.
- ASTM, 1992. Standard Test Method for Laboratory Determination of Water (Moisture) Content of Soil and Rock. American Society for Testing and Materials.
- Carvacho, O.F., Ashbaugh, L.L., Flocchini, R.G., 1996a. Characteristics of the UC Davis dust resuspension test chamber. Proceedings of the 15th Annual Conference, The American Association for Aerosol Research, 14–18 October, Orlando, FL.
- Carvacho, O.F., Ashbaugh, L.L., Matsumura, R.T., Southard, R.J., Flocchini, R.G., 1996b. Measurement of  $PM_{10}$  potential from agricultural soils using a dust resuspension test chamber. International Conference on Air Pollution from Agricultural Operations, 7–8 February. Midwest Plan Service, Kansas City, MO, pp. 87–92.
- Carvacho, O.F., Ashbaugh, L.L., Brown, M.S., Flocchini, R.G., 2000. Comparison of  $PM_{10}$  emission potential using the UC Davis dust resuspension test chamber and the soil texture of San Joaquin Valley soils. Proceedings of the Second International Conference on Air Pollution from Agricultural Operations. American Society of Agricultural Engineers, Des Moines, IA.
- Clausnitzer, H., Singer, M.J., 1996. Respirable-dust production from agricultural operations in the Sacramento Valley, California. *Journal of Environmental Quality* 25, 877–884.
- Clausnitzer, H., Singer, M.J., 1997. Intensive land preparation emits respirable dust. *California Agriculture* 51, 27–30.
- Coleman, H.W., Steele Jr., W.G., 1989. Experimentation and Uncertainty Analysis for Engineers. Wiley, New York, 205pp.
- Dolislager, L.J., Motallebi, N., 1999. Characterization of particulate matter in California, (Special Issue on  $PM_{2.5}$ : A Fine Particulate Standard). *Journal of Air and Waste Management Association* 49, PM 45–56.
- Eldred, R.A., Cahill, T.A., Pitchford, M., Malm, W.C., 1988. IMPROVE – a new remote area particulate monitoring system for visibility studies. Air Pollution Control Association 81st Annual Meeting, Dallas, TX, pp. Paper 88–54.3.
- Eldred, R.A., Cahill, T.A., Wilkinson, L.K., Feeney, P.J., Chow, J.C., Malm, W.C., 1990. Measurement of fine particles and their chemical components in the IMPROVE/NPS network. In: Mathai, C.V. (Ed.), *Visibility and Fine Particles*. Air & Waste Management Association, Pittsburgh, PA, pp. 187–196.
- Holmén, B.A., Eichinger, W.E., Flocchini, R.G., 1998. Application of elastic lidar to  $PM_{10}$  emissions from agricultural nonpoint sources. *Environmental Science and Technology* 32, 3068–3076.
- Holmén, B.A., James, T.A., Ashbaugh, L.L., Flocchini, R.G., 2000. Lidar-assisted measurement of  $PM_{10}$  emissions from agricultural tilling in California's San Joaquin Valley. I: Lidar. *Atmospheric Environment* 35, 3251–3264.
- Kantamaneni, A.G., Bamesberger, L., Allwine, E., Westberg, H., Lamb, B., Claiborn, C., 1996. The measurement of roadway  $PM_{10}$  emission rates using atmospheric tracer ratio techniques. *Atmospheric Environment* 30, 4209–4223.
- U.S.E.P.A., 1995. Compilation of Air Pollution Emission Factors. AP-42, United States Environmental Protection Agency, Research Triangle Park, NC.